Novel Target Discovery and Validation in Renal Cell Carcinoma

Sebastian Trainor

MB BCh BAO, MRCP Ireland

Submitted in accordance with the requirements for the degree of
Doctor of Philosophy

The University of Leeds
School of Medicine

November, 2018

The candidate confirms that the work submitted is his own and that appropriate credit has been given where reference has been made to the work of others.

Acknowledgements

I would firstly like to thank my supervisors, Professor Roz Banks, Dr Naveen Vasudev, Professor David Beech and Professor Peter Selby, for the guidance, encouragement, support and advice they have provided throughout my time in the laboratory. I have been extremely fortunate to have had such knowledgeable supervisors who have cared so much about my work.

I would especially like to thank the Tony Bramall Charitable Trust for the funding, without which this research would not have been possible. I feel very fortunate to have been able to meet Mr and Mrs Bramall on numerous occasions and to have been able to update them on my work throughout this project.

I would also like to thank all the members of the Banks and Beech labs at the University of Leeds who have helped me throughout this process and have been a continuous support to me. I must mention in particular my gratitude to Michelle Hutchinson, Karen Dunn, Roisean Ferguson, Nick Hornigold and Norma Lister for their help and guidance. I want to particularly thank Dr Alexandre Zougman for your patient support and guidance throughout my time in the lab. I have met some amazing people and have made life-long friends. The rest of you are too numerous to mention by name, but you all know who you are.

I must mention my amazing wife, Ciara, for her continued support, encouragement and patience. My two boys, Oran and Finn, were born during this research time, which at times has added to the challenges of completing this research. If it were not for Ciara's endless commitment to our family this thesis would not have been possible.

I would again like to reiterate my extreme gratitude particularly to Professor Banks and Dr Vasudev for investing such an enormous amount of time in me. At times I did not think this thesis was achievable but your constant encouragement gave me the determination to keep going.

Abstract

Renal cell carcinoma (RCC) is the 7th most common cancer in the UK. Almost one third of patients will have locally advanced or metastatic disease at presentation and a similar proportion will relapse despite undergoing surgery with a curative intent. More effective treatments are now available, although resistance is typically observed within months of starting treatment and median survival remains in the order of two years, highlighting the need for continued progress

The aim of this work was the discovery and further investigation of novel therapeutic targets in ccRCC through proteomic approaches. Two potential emerging targets were further investigated in ccRCC. Spleen tyrosine kinase (SYK) was identified to be alternatively spliced in ccRCC compared to normal tissue. SYK inhibition with R406 caused cell death at concentrations >1 μM. Transient Receptor Potential Canonical (TRPC) channels 1, 4 and 5 expression was variable at an mRNA level in primary ccRCC and normal kidney tissue but the lack of antibodies to accurately detect the TRPC proteins using Western blot limited detection at a protein level. The activation and inhibition of these channels *in-vitro* was explored in the A498 RCC cell line.

A comprehensive proteomic analysis of ccRCC tissue compared with normal kidney tissue, selected on the basis of underlying genomic changes was undertaken. Integration of the data led to the identification of a number of potential novel therapeutic targets. Cyclooxygenase-1 (COX-1) and proteasome subunit type beta-9 (PSMB9), were taken forward and their upregulation in ccRCC at a protein level were demonstrated. Inhibition of COX-q was shown to cause RCC cell line death.

The genetics of RCC at a descriptive level is comprehensive, but has not yet led to advances in treatment options. This work has demonstrated a valid approach to the integration of genomic and proteomic data that may be adopted in future studies.

Contents

List of Tables

List of Figures

Abbreviations

ACN	Acetonitrile
AJCC	American Joint Committee on Cancer
ATCC	American Tissue Culture Collection
AUC	Area Under the Curve
BCA	Bicinchoninic Acid
BSA	Bovine Serum Albumin
CA	Cryo-ablation
CAIX	Carbonic Anhydrase IX
CBB	Coomassie Brilliant Blue
ccRCC	Clear cell renal cell carcinoma
COX-1	Cyclooxygenase-1
CK	Cytokeratin
CSS	Cancer-Specific Survival
Da	Dalton
DDA	Data Dependent Acquisition
DAI	Data Independent Acquisition
DMEM	Dulbecco's Modified Eagle's Medium
DTT	Dithiothreitol
EA	Englerin A
ER	Endoplasmic Reticulum
ESR	Erythrocyte Sedimentation Rate
FCS	Foetal Calf Serum
FISH	Fluoresence in-situ Hybridisation
HBSS	Hank's Buffered Salt Solution
β-HCG	Human Chorionic Gonadotrophin
HIF	Hypoxia Inducible Factor
IFN	Interferon
Ig	Immunoglobulin
ICH	Immunohistochemistry
IFC	Integrated Fluidic Circuits
IL-2	Interleukin-2
IPA	Ingenuity® Pathway Analysis
ISUP	International Society of Urological Pathology
KPS	Karnofsky Performance Status

LC-MS/MS	Liquid-Chromatography-Tandem Mass Spectrometry
LDH	Lactate Dehydrogenase
LFQ	Label Free Quantification
MHC	Major Histocompatibility Complex
mRNA	Messenger Ribonucleic Acid
MS	Mass Spectrometry
NCI	National Cancer Insttiute
OS	Overall Survival
PBS	Phosphate Buffered Saline
PCR	Polymerase Chain Reaction
PDGF	Platelet Derived Growth Factor
PFS	Progression-Free Survival
pI	Isoelectric point
PSMB9	Proteasome Subunit Beta-type 9
PTM	Post-Translational Modification
RCC	Renal Cell Carcinoma
RFA	Radiofrequency Ablation
ROC	Receiver Operator Characteristic
RTB	Research Tissue Bank
RPMI	Roswell Park Memorial Institute
SDS-PAGE	Sodium Dodecyl Sulphate-Polyacrylamide Gel Electrophoresis
SOP	Standard Operating Procedure
STAGE	Stop And Go Extraction
STrap	Suspension Trapping
SWATH-MS	Sequential Window Acquisition of all Theoretical Fragment Ion Spectra Mass Spectrometry
SYK	Spleen Tyrosine Kinase
TBE	Tris-Borate-ETDA
TBS	Tris-Buffered Saline
TNM	Tumour Node Metastasis
TRPC	Transient Receptor Potential Canonical
UICC	Union for International Cancer Control
VHL	Von Hippel Lindau
VEGF	Vascular Endothelial Growth Factor
W/T	Wild type

Publications to which this work has contributed

CHEUNG, S. Y., HENROT, M., AL-SAAD, M., BAUMANN, M., MULLER, H., UNGER, A., RUBAIY, H. N., MATHAR, I., DINKEL, K., NUSSBAUMER, P., KLEBL, B., FREICHEL, M., RODE, B., **TRAINOR, S**., CLAPCOTE, S. J., CHRISTMANN, M., WALDMANN, H., ABBAS, S. K., BEECH, D. J. & VASUDEV, N. S. 2018. TRPC4/TRPC5 channels mediate adverse reaction to the cancer cell cytotoxic agent (-)-Englerin A. *Oncotarget,* 9**,** 29634-29643.

KARIMZADEH, M., JANDAGHI, P., PAPADAKIS, A. I., **TRAINOR, S.,** RUNG, J., GONZALEZ-PORTA, M., SCELO, G., VASUDEV, N. S., BRAZMA, A., HUANG, S., BANKS, R. E., LATHROP, M., NAJAFABADI, H. S. & RIAZALHOSSEINI, Y. 2018. Aberration hubs in protein interaction networks highlight actionable targets in cancer. *Oncotarget,* 9**,** 25166-25180.

Chapter 1 Introduction

1.1 Renal Cell Carcinoma

Renal cancer is the 7th most common cancer in the UK, accounting for 3% of all new cancer cases (2016). There were more than 12,000 new cases diagnosed in the UK in 2015, with a male to female incidence ratio of approximately 3:2 (Cancer Research UK). The incidence of kidney cancer in the UK has increased by 85% since the early 1990s and is projected to rise by a further 26% in the next 20 years (Smittenaar et al., 2016). The most common type of kidney cancer is renal cell carcinoma RCC) (90%), of which the three major subtypes include clear cell RCC (ccRCC) (75%), papillary RCC (15-20%) and chromophobe RCC (~5%) (Ricketts et al., 2018).

Patients may present with local or systemic symptoms or both. A classic triad of flank pain, macroscopic haematuria and a palpable abdominal mass is described (Rini et al., 2009), although is now rarely seen (Cairns, 2010). Systemic symptoms may be related to sites of metastatic disease but may also be non-specific, such as weight loss, and general malaise. Patients may present due to the paraneoplastic syndromes associated with RCC including hypercalcaemia, hypertension, polycythaemia and anaemia (Palapattu et al., 2002). With the increasing use of routine abdominal imaging, it is reported that over 50% of cases are now detected incidentally (Rabjerg et al., 2014) (Cairns, 2010). Furthermore, given the often insidious nature of these tumours, in the UK almost 25% of cases are diagnosed following an emergency presentation, often with late stage disease (Cancer Research UK) (Shaw, 2016).

Risk factors for the development of renal cancer include obesity, cigarette smoking, hypertension, family history and chronic kidney disease requiring dialysis (Chow et al., 2010). It is estimated that 4% of renal tumours are related to known hereditary syndromes including Von Hippel-Lindau (VHL) disease (Lonser et al., 2003) (Latif et al., 1993), Tuberous Sclerosis and Birt-Hogg-Dube syndrome (Linehan et al., 2003).

1.1.1 Stage and Grade

The European Society of Medical Oncology (ESMO) and the European Association of Urology (EAU) has produced clinical practice guidelines for the diagnosis, treatment and follow-up of RCC (Escudier et al., 2016) (European Association of Urology, 2018). These highlight the pathological factors that should be reported in routine practice, including the histological subtype, the International Society of Urological Pathology (ISUP) nucleolar grade (clear cell and papillary RCC subtypes only) (Table 1.1) (Delahunt et al., 2013) and the presence of necrosis, microvascular invasion, and rhabdoid and sarcomatoid differentiation. These, coupled with accurate staging as defined by the American Joint Committee on Cancer (AJCC) / Union for International Cancer Control (UICC) Tumour-Node-Metastasis (TNM) system (Table 1.2 and Table 1.3) (Paner et al., 2018) help provide important prognostic information and guide appropriate treatment options.

The International Society of Urological Pathology (ISUP) nucleolar grading system has replaced the previously widely used four-tiered system described by Fuhrman *et al.* (Fuhrman et al., 1982). In the Fuhrman grading system the first three grades were based on the nuclear features and the final grade was based upon the presence of nuclear pleomorphism. As the identification and classification of RCC subtypes has improved, concerns were raised around the fact that this system considered RCC as a single tumour type and the subjective and poorly defined nature of the assessment for nucleolar prominence and pleomorphism (Delahunt et al., 2013). The ISUP grading system has better objectivity and a stronger association with patient outcome (Dagher et al., 2017).

Table 1.1 – Grading system for renal cell carcinoma as proposed by the International Society of Urological Pathologists (ISUP)

ISUP Grade	Definition
1	Nucleoli are inconspicuous or absent at x400 magnification
2	Nucleoli are clearly visible at x400 magnification but are inconspicuous or absent at x100 magnification
3	Nucleoli are prominent and are easily visualised at x100 magnification
4	Presence of giant tumour cells and/or marked nuclear pleomorphism with clumping of chromatin or sarcomatoid differentiation or rhabdoid differentiation

The AJCC TNM staging system (8th edition) is widely recognised and is validated as a key prognostic parameter (Table 1.2) (Amin et al., 2017). The T in this staging system denotes the size and extent of the primary tumour, N denotes the extent of the nodal spread and M denotes the presence of metastatic disease. The patient can be assigned to one of four stages depending on the TNM classification (Table 1.3).

1.1.2 Prognosis

RCCs are characterised by their highly variable natural history. Almost one third of patients will have locally advanced or metastatic disease at presentation (Gupta et al., 2008) and approximately 10–28% of patients that undergo curative resection or ablation will experience a recurrence of their cancer (Kim et al., 2012) (Cairns, 2010). It is evident that patients with symptomatic presentations have a worse survival than those diagnosed incidentally (Palsdottir et al., 2012) (Kawata et al., 2008). The TNM staging system is a validated method for determining patient survival with 5-year survival being similar for males and females and ranging from approximately 83% at 5 years for stage I disease and 6% for stage IV disease (Cancer Research UK).

In the setting of localised or metastatic disease, there are a number of algorithms that have been developed to provide prognostic information. They are all based on clinical and pathological data. In the setting of resected localised disease, they have been developed to identify those patients with a high post-operative risk of recurrence so as to guide the intensity of surveillance protocols and to help counsel patients on the risks of recurrence. The first of these algorithms is the stage, size, grade and necrosis (SSIGN) score. It was developed and introduced by the Mayo Clinic and incorporates the pathological T stage, regional lymph node status, tumour size, nuclear grade and the presence of histological tumour necrosis, to assign patients to three risk groups based on either cancer-specific survival (Frank et al., 2002) or metastasis-free survival (Leibovich et al., 2003). A second algorithm commonly used is the University of California Los Angeles Integrated Staging System (UISS) which places patients into three risk groups based upon their TNM stage, Fuhrman grade and Eastern Cooperative Oncology Group (ECOG) performance status (Zisman et al., 2001). In the metastatic setting there are several algorithms utilised for the stratification of individual patient risk so as to assist in prognostication and help guide

Table 1.2 - Tumour, Node Metastasis (TNM) staging system for RCC (8th edition)

Primary Tumour (T)	
Tx	Primary tumour cannot be assessed
T0	No evidence of primary tumour
T1	**Tumour < 7 cm or less in greatest dimension, limited to the kidney**
T1a	Tumour 4 cm or less
T1b	Tumour more than 4 cm but less or equal to 7 cm
T2	**Tumour > 7 cm in greatest dimension, limited to the kidney**
T2a	Tumour more than 7 cm but less than or equal to 10cm
T2b	Tumour more than 10 cm
T3	**Tumour extends into major veins or perinephric tissues but not into the ipsilateral adrenal gland and not beyond Gerota fascia**
T3a	Tumour extends into the renal vein or its segmental branches, or invades the pelvicalyceal system or perirenal and/or renal sinus fat (peripelvic) fat but not beyond Gerota fascia
T3b	Tumour extends into vena cava below diaphragm
T3c	Tumour extends into vena cava above the diaphragm or invades the wall of the vena cava
T4	Tumour invades beyond Gerota's fascia (including contiguous extension into the ipsilateral adrenal gland)
Regional Lymph Nodes (N)	
Nx	Regional lymph nodes cannot be assessed
N0	No regional lymph nodal metastases
N1	Metastases in regional lymph nodes
Metastases (M)	
M0	No distant metastases
M1	Distant metastases

Table 1.3 - Staging of RCC

Stage	**TNM Stage**		
Stage I	T1	N0	M0
Stage II	T2	N0	M0
Stage III	T1	N1	M0
	T2	N1	M0
	T3	N0	M0
	T3	N1	M0
Stage IV	T4	N0	M0
	T4	N1	M0
	Any T	Any N	M1

treatment options. These include the International Metastatic RCC Database Consortium (IMDC) model (Heng et al., 2009) and the Memorial Sloan Kettering Cancer Centre (MSKCC) model (Motzer et al., 2002). The MSKCC model was initially

developed when cytokine treatment was the gold standard It is based upon the five criteria, Karnofsky performance status (KPS), lactate dehydrogenase (LDH), haemoglobin, corrected calcium and time from diagnosis to start of treatment. The more contemporary IMDC model is based upon KPS, haemoglobin, corrected calcium, time from diagnosis to start of treatment and serum platelet and neutrophil count.

Unfortunately, despite their wide adoption in the clinic, such models based on standard clinico-pathological factors alone, fail to fully account for tumour heterogeneity and the unpredictable biological behaviour of RCC. This has led to attempts at investigating biomolecular signatures, in particular using genomic, transcriptomic, and proteomic profiling of tumour samples to generate prognostic models. Currently, the most promising of these approaches is the use of gene expression arrays in the setting of resected localised disease. For example, the gene expression assay panel 'ClearCode34' (Brooks et al., 2014), for use in ccRCC was demonstrated to show superiority to the UISS and SSIGN models and, subsequently, in the setting of metastatic disease, it improved the predictive power of the IMDC model (de Velasco et al., 2017). More recently, a 16-gene signature has been developed, with external validation using samples from patients recruited to the S-TRAC trial of adjuvant sunitinib (Rini et al., 2018) (Rini et al., 2015). The assay was able to sub-stratify patients deemed at intermediate- or high-risk according to the Leibovich score and now warrants further evaluation in a prospective setting.

1.1.3 Genetics and Biology

The genetic landscape of ccRCC has been extensively characterised through a number of large-scale sequencing studies (Cancer Genome Atlas Research, 2013) (Sato et al., 2013) (Dalgliesh et al., 2010) (Scelo et al., 2014) (Pena-Llopis et al., 2012) (Ricketts et al., 2014) (Ricketts et al., 2018). The dominant genetic event in sporadic ccRCC is the loss of VHL activity. The *VHL* gene, located on the short arm of chromosome 3 (3p25-26) encodes a regulatory protein (pVHL), which controls a large variety of cellular processes (Frew and Moch, 2015). One of these processes includes targeting hypoxia inducible factors (HIF) for ubiquitinisation and proteasomal degradation (Latif et al., 1993) (Gossage et al., 2015). HIF is responsible for a cells adaptation to hypoxia. If not inactivated through the action of VHL, it acts as a transcription factor for a number of proteins including vascular endothelial growth factor (VEGF) and platelet derived growth factor (PDGF), which in turn leads

to angiogenesis, cell growth and cell survival. In studies of *VHL*, loss of heterozygosity is observed in approximately 98% of sporadic cases, 73% have somatic *VHL* mutations and 30% have gene methylation (Scelo et al., 2014, Young et al., 2009) (Sato et al., 2013) (Gossage et al., 2015). 2-4% of RCC are caused by germline mutations in *VHL* (Latif et al., 1993) and less than 5% of tumours do not have *VHL* involvement (Young et al., 2009).

Other frequently mutated genes include *polybromo1 (PBRM1), SET domain-containing protein 2 (SETD2)* and *BRCA1-associated protein 1 (BAP1)* at frequencies of 40%, 19% and 15% respectively (Scelo et al., 2014) (Varela et al., 2011). Like *VHL*, they are all located on chromosome 3p. *PBRM1* encodes BAF180, a SWI/SNF chromatin remodelling complex protein, which is involved in the arrest of the cell cycle in response to hypoxia. *BAP1* encodes a ubiquitin carboxy-terminal hydrolase (Benusiglio et al., 2015) and, notably, mutations in *BAP1* tend to be mutually exclusive to *PBRM1* mutations. *SETD2* functions as a histone H3 lysine 36 methyltransferase and it is notable therefore that all three TSGs can be classified as histone and chromatin regulators. Beyond this, a long 'tail' of low frequency (<5%) events are observed, the protein products of which are implicated in multiple diverse pathways (Cancer Genome Atlas Research, 2013, Scelo et al., 2014).

Whilst descriptive studies such as these are helpful in improving our understanding of the genetics and evolution of ccRCCs, the exploitation of such knowledge to inform clinical practice and improve patient outcomes is yet to be achieved. The exception to this perhaps is the development of VEGF targeted TKIs based on the biology of *VHL*, although this work predates the more recent large-scale next-generation sequencing studies revealing recurrent mutations in genes such as *BAP1, SETD2 and PBRM1*. Mutations in each of these genes have been reported to be associated with higher grade tumours and / or poorer outcomes but these associations are not always consistent. In the largest study to date, representing a pooled analysis of 1049 patients with ccRCC, mutations in *BAP1* were associated with tumour grade, tumour size and decreased CSS ($q = 0.004$) in a multivariable model, however this was lost when the SSIGN score was included. *SETD2* mutations were associated with decreased relapse-free survival in multivariable models, including models with SSIGN score (Manley et al., 2016). Thus, such mutations appear to be of relevance in driving tumour biology, although may serve only as surrogates for pathological features such tumour grade and size.

Beyond the impact of single gene mutations, recent elegant work using multi-region sampling of a series of ccRCCs has been used to track the evolution of these cancers. The study led the authors to propose genetic subclassification of ccRCC into seven types, incorporating clonality and chromosomal complexity, and which appear to correlate with clinical phenotype (Turajlic et al., 2018). However, 37 of the 101 tumours examined were not able to be classified and this remains hypothesis generating at present.

In summary, the genetics of RCC at a descriptive level is now well understood but the application of this knowledge in the clinic to guide prognosis, predict response to existing therapies or to generate novel therapeutic strategies remains to be achieved and is a research priority in this disease.

1.1.4 Current Treatment Strategies

The mainstay of management of localised, stage I - III, RCC is definitive surgery, which may be in the form of a total nephrectomy or nephron-sparing surgery depending on the size and position of the tumour (Escudier et al., 2016) (European Association of Urology, 2018). In the setting of a localised, small cortical tumour, management may entail either surveillance, surgery or an ablative approach with radiofrequency ablation (RFA) or cryo-ablation (CA), particularly if the patient is frail, is deemed to be of a high surgical mortality risk, has poor renal function, multiple co-morbidities or has multiple bilateral tumours (Stakhovskyi et al., 2011) (Wah, 2017).

RCC is considered a chemotherapy, radiotherapy and hormone therapy resistant tumour. In a large review of 72 cytotoxic agents, involving 3502 patients with metastatic disease, objective responses were demonstrated in only 5.6% of patients (Yagoda et al., 1993) (Yagoda et al., 1995). Until the advent of newer, targeted therapy, the immunomodulatory cytokine therapies interferon alfa (IFN-α) and interleukin-2 (IL-2), were the most effective treatments available, with low objective response rates of 12% (Motzer et al., 1996, Wirth, 1993) and 14% (Fyfe et al., 1995) respectively. High dose IL-2 (HD IL-2) still has a role in the management of a group of highly selected patients with advanced disease due to its ability to induce a durable complete response (Chow et al., 2016) (Chow et al., 2018). HD IL-2 carries with it

significant toxicity and must be administered in a centre with a high level of expertise in dealing with the complications and that are equipped with intensive care support.

Inhibitors of the vascular endothelial growth factor (VEGF) signalling pathway remain the mainstay of currently licensed treatments in the UK for the management of advanced RCC. Treatment options in this group include sunitinib, pazopanib, tivozanib, axitinib and cabozantinib (Table 1.4). They are all multi-targeted tyrosine kinase inhibitors (TKI) with activity against the vascular endothelial growth factor receptor (VEGFR) along with several other receptors including the platelet-derived growth factor receptor (PDGFR) and the stem cell factor receptor, KIT (Jonasch et al., 2014). They have similar side-effect profiles including hypertension, diarrhoea, fatigue, hand and foot skin reactions, nausea, cardiac events and bleeding. These toxicities can be marked, often requiring dose reductions or withdrawal of the drug.

Details of the most relevant trials are shown in Table 1.5. The first TKI (sorafenib) was used in clinic in 2005 on the basis of the phase III TARGET trial comparing sorafenib with placebo in 903 patients with advanced ccRCC resistant to pre-treatment with cytokines. Whilst crossover was permitted following a planned interim analysis, overall survival identified that sorafenib reduced the risk of death but median OS was not reached in the sorafenib arm. 10% of the sorafenib arm and 8% of the placebo arm discontinued the drug due to adverse events and 13% of patients in the sorafenib arm needed dose reductions due to toxicity compared to 3% in the placebo arm (Escudier et al., 2007) (Escudier et al., 2009). In 2006, sunitinib emerged as a new standard of care, based on a phase III trial of sunitinib versus IFN-α for the treatment of 750 patients with previously untreated metastatic renal cell carcinoma with a clear cell component. Sunitinib improved the median PFS from 5 to 11 months and had a higher objective response rate of 31 vs. 6% ($p<0.001$). Toxicities led to a dose reduction in 32% of the sunitinib group (Motzer et al., 2007) (Motzer et al., 2009). Pazopanib later became available, based on the result of a randomised controlled trial (RCT) of pazopanib versus placebo in both treatment naïve and cytokine pre-treated patients (n=435). Pazopanib improved the median PFS from 4.2 months to 9.2 months in the overall study population. The overall response rate was 30% with pazopanib versus 3% with placebo. Adverse events were again highly prevalent, with 33% of patients experiencing grade 3 or 4 toxicity with pazopanib (Sternberg et al., 2010).

Table 1.4 – Currently licensed treatment options in the UK for advanced RCC

Treatment	Target	Approved line of therapy
Sunitinib	VEGFR-1, -2, -3 PDGFR-α, -β KIT	First line
Pazopanib	VEGFR-1, -2, -3 PDGFR-α, -β c-Kit	First line
Tivozanib	VEGFR-1, -2, -3 c-Kit	First line
Axitinib	VEGFR-1, -2, -3	After failure of first line sunitinib or a cytokine
Cabozantinib	c-MET VEGFR GAS6 receptor RET TYRO3 MER KIT TRKB FLT3 TIE-2	• First line for intermediate- or poor-risk metastatic disease as defined by the IMDC model • Second line after VEGF targeted therapy
Lenvatinib	VEGFR-1, -2, -3 FGFR-1, -2, -3, -4 PDGFR-α KIT RET	Second line along with everolimus (one previous VEGF targeted therapy)
Everolimus	mTOR	Second line following progression during or after VEGF targeted therapy
Nivolumab	PD-1	For previously treated advanced RCC
Interleukin-2	Immune mediated	Decision of treating centre

The large TIVO-1 phase III trial (n=517 patients) comparing tivozanib with sorafenib in untreated patients or those who had progressed on a cytokine demonstrated an improvement in PFS with tivozanib of 11.9 versus 9.1 months in the sorafenib arm. There was a trend towards a longer survival on the sorafenib arm, although this was confounded by the large amount of cross-over in patients initially randomised to sorafenib (Motzer et al., 2013). Cabozantinib is an example of an oral multi-tyrosine kinase inhibitor that targets MET, VEGFR and AXL. Upregulation of the MET proto-oncogene is observed RCC, in particular the papillary subtype but can also occur in ccRCC, where it has been shown that VHL inactivation (Nakaigawa et al., 2006) and hypoxia (Pennacchietti et al., 2003) can lead to MET upregulation and the resultant activation of downstream signalling cascades including the mitogen activated kinase

(MAPK) and the PI3K-AKT-mTOR pathways, which in turn lead to cell proliferation and cell survival (Smyth et al., 2014). The phase 3 METEOR trial compared cabozantinib with everolimus in 658 patients with advanced or metastatic ccRCC who progressed after previous VEGR therapy. Cabozantinib demonstrated an improved median OS (7.4 versus 3.9 months) (Choueiri et al., 2016). This is an important trial as it is the only TKI to demonstrate an improvement in OS and PFS after previous VEGFR inhibiting drugs. Cabozantinib was also investigated in the first line setting against sunitinib in the phase II CABOSUN trial (Choueiri et al., 2017a) (Choueiri et al., 2018a). This investigated patients with intermediate- or poor-risk disease as defined by IMDC criteria and included 157 patients. PFS was improved significantly in the cabozantinib arm (8.6 versus 5.3 months) leading to its approval in the first-line setting.

Another class of drug licenced for use in the second line setting in the UK for advanced RCC is the mTOR inhibitor, everolimus. This was approved based on the phase III trial of everolimus versus placebo for patients (n=410) whose disease had progressed on prior anti-VEGF therapy. The study demonstrated an improved PFS in the everolimus arm (4 vs. 1.9 months). Significant toxicities with everolimus included non-infectious pneumonitis. 10% of patients receiving everolimus discontinued the drug and 34% needed dose reductions due to toxicity (Motzer et al., 2008) (Motzer et al., 2010). It is evident, however, that as a single agent, the use of everolimus in clinical practice is now limited, based on data from METEOR and other trials demonstrating its relative inferiority. The combination of lenvatinib and everolimus has been shown to improve median PFS in patients pre-treated with a tyrosine kinase inhibitor, versus everolimus alone, although this was based on a small phase II trial, with approximately 50 patients per arm (14.6 months compared with 5.5 months) (Motzer et al., 2015b).

More recently, positive trials using immune checkpoint inhibitors, targeting cytotoxic T lymphocyte antigen 4 (CTLA-4), programmed cell death 1 (PD-1), and its ligand PD-L1 (Jonasch et al., 2014, Pardoll, 2012) have been published. CTLA-4 is expressed by activated CD4 and CD8 cells and negatively regulates T cells. PD-L1 is a ligand for PD-1, a T cell receptor that negatively regulates the immune response. This is particularly relevant in kidney cancer with the finding that PD-L1 is expressed in 16-66% of RCCs (Harshman et al., 2014). An example of a monoclonal antibody

against CTLA-4 is ipilimumab, and examples of monoclonal antibodies against PD-L1 are atezolizumab, and against PD-1, nivolumab and pembrolizumab.

Single agent nivolumab was demonstrated to improve median OS compared to everolimus in the CheckMate 025 trial in the setting of prior anti-angiogenic treatment. This trial included 821 patients and also demonstrated fewer grade 3 or 4 adverse events in the nivolumab arm. In the first line setting the landmark trial of nivolumab plus ipilimumab versus sunitinib in previously untreated advanced ccRCC recruited 1096 patients (Motzer et al., 2018b), at a median follow-up of 25.2 months, the median OS was not reached for the experimental arm versus 26 months for the sunitinib arm. The objective response rate was much greater for the experimental arm at 42% versus 27% and the complete response rate was 9% versus 1%. These results represent a notable step forward in the treatment of and outlook for patients with advanced RCC and further follow-up data is awaited. It must be noted however that treatment related adverse events leading to discontinuation occurred in 22% and 12% of patients, highlighting the toxicity profile of combination immunotherapy. Although both ESMO and EAU guidelines now recommend nivolumab plus ipilimumab as front-line therapy for patients with intermediate- and poor-risk disease, the European Medicines Agency has recently declined approval based on a lack of data clarifying the contribution of ipilimumab to the observed results.

More recently there are several large ongoing trials investigating the combination of immune checkpoint inhibition combined with tyrosine kinase inhibition (Einstein and McDermott, 2017). Such trials in the first line setting include the CLEAR trial comparing lenvatinib in combination with everolimus or pembrolizumab, compared to sunitinib, the CheckMate 9ER trial comparing the combination of cabozantinib and nivolumab versus sunitinib, and the KEYNOTE-426 trial comparing pembrolizumab and axitinib versus sunitinib. The IMmotion151 was recently reported which compared atezolizumab in combination with bevacizumab (a monoclonal antibody against VEGF) with single-agent sunitinib, in the first line setting (Motzer et al., 2018a). Median PFS was improved in the experimental arm by 2.8 months (11.2 versus 8.4 months) and OS data are awaited. The treatment-related grade 3-4 adverse events were lower with the combination arm compared to the sunitinib alone arm.

In 2004 it was demonstrated that cytoreductive nephrectomy prior to IFN-α improved median overall survival (OS) by 5.8 months (Flanigan et al., 2004). It is not known whether this also applies in the era of drugs targeting the VEGF signalling pathway. An attempt at answering this question was provided in the randomised controlled phase III trial, CARMENA (Mejean et al., 2018). A total of 450 patients with metastatic ccRCC were randomly assigned to nephrectomy followed by sunitinib versus sunitinib alone. Patients were stratified according to the MSKCC prognostic model and the primary endpoint was overall survival (OS). The trial concluded that sunitinib alone was not inferior to the nephrectomy-sunitinib group, with OS 18.4 months versus 13.9 months respectively. Whilst this is an informative trial, it must be noted that it was designed to show non-inferiority of sunitinib and in the 226 patients assigned to the nephrectomy arm, 16 did not undergo surgery and 40 did not receive sunitinib. The nephrectomy arm had a higher proportion of T3/4 tumours and lower nodal burden. Furthermore, with the ever-evolving treatment landscape, the relevance of the study to future practice is questionable.

At this time, there is no evidence to support adjuvant treatment for resected renal cell carcinoma. The ASSURE trial, which assigned patients with unfavourable renal cancer to one year of sorafenib, sunitinib or placebo, has shown comparable median disease-free survival for all arms in an interim analysis, although the median 5 year overall survival has not yet been reached (Haas N, 2015). The European SORCE trial, which is looking at 1 versus 3 years of sorafenib versus placebo, has completed recruitment and the results are awaited. However, given the negative signal observed across such studies to date, it seems unlikely that this class of drug will prove useful in the adjuvant setting.

Overall, whilst these studies show that there are many treatment options available for patients with advanced and metastatic RCC, it is evident that not all patients will respond (approximately 20% of patients have disease refractory to VEGF targeted treatment (Heng et al., 2012)), they are toxic and there are no predictive biomarkers in use to guide choice of agent. Whilst checkpoint inhibitors show promise in affording some patients durable disease control, many patients do not benefit and the majority of patients will succumb to their disease. Clearly, progress in understanding the molecular pathogenesis of RCC is leading to the development of new treatments, resulting in improvements in outcome for some of these patients, but resistance is typically observed within months of starting treatment and median survival remains

in the order of two years. This survival benefit comes at the expense of significant toxicities in a considerable number of those treated, negatively impacting on patients' quality of life, frequently requiring dose interruptions or reductions, and can on occasion be life-threatening. Although there has been an improvement in treatments and outcome for patients with metastatic RCC over recent years, there remains a great need for continued progress.

Table 1.5 –Trials of systemic agents investigated in advanced RCC

Date published	Study Acronym	Arms and numbers of patients		Setting	Primary Endpoints	Median OS (HR, 95% CI, *p* value)	Median PFS (HR, 95% CI)	References
		Experimental	Control					
2007	TARGET	Sorafenib (400 mg PO BD) (n=451)	Placebo (n=452)	Pre-treatment with cytokine therapy. ccRCC. Crossover permitted from 2005	OS	17.8 versus 15.2 months (0.88, 0.74-1.04 , 0.146) (after crossover)	5.5 versus 2.8 months (0.44, 0.35-0.55, <0.001)	(Escudier et al., 2007, Escudier et al., 2009)
2007		Sunitinib (50 mg PO OD for 4 weeks followed by 2 weeks without treatment) (n=375)	Interferon α (9 MU SC three times weekly) (n=375)	Previously untreated. Clear cell component required.	PFS	26.4 versus 21.8 months (0.82, 0.67-1.00, 0.051)	11 versus 5 months (0.42, 0.32-0.54, <0.001)	(Motzer et al., 2007) (Motzer et al., 2009)
2010		Pazopanib (800 mg PO OD) (n=290)	Placebo (n=145)	Treatment naïve and cytokine pre-treated RCC	PFS	22.9 versus 20.5 months (0.91, 0.71-1.16, Not sig) (after crossover)	9.2 versus 4.2 months (0.46, 0.34-0.62, <0.0001)	(Sternberg et al., 2010)
2010	RECORD-1	Everolimus (10 mg PO OD) (n=272)	Placebo (n=138)	Metastatic RCC	PFS	14.8 versus 14.4 months (0.87, 0.65-1.15, 0.162) Crossover allowed	4.9 versus 1.9 months (0.33, 0.25-0.43, <0.001)	(Motzer et al., 2008) (Motzer et al., 2010)

Date published	Study Acronym	Arms and numbers of patients		Setting	Primary Endpoints	Median OS (HR, 95% CI, *p* value)	Median PFS (HR, 95% CI)	References
		Experimental	Control					
2013		Tivozanib (1.5 mg PO OD for 3 weeks followed by one week without treatment) (n=260)	Sorafenib (400 mg PO BD) (n=257)	Clear cell component required. 1 or more prior therapies permitted. Post nephrectomy.	PFS	28.8 versus 29.3 months (1.25, 0.95-1.62, 0.105)	11.9 versus 9.1 months (0.80, 0.64-0.99, 0.042)	(Motzer et al., 2013)
2015	CheckMate 025	Nivolumab (3 mg/kg IV) 2 weekly (n=410)	Everolimus (10 mg PO OD) (n=411)	Previous treatment with one or two anti-angiogenic treatments	OS	25.0 versus 19.6 months (0.73, 0.57-0.93, 0.002)	4.6 versus 4.4 months (0.88, 0.75-1.03, 0.11)	(Motzer et al., 2015a)
2016	METEOR	Cabozantinib (60 mg PO OD) (n=330)	Everolimus (10 mg PO OD) (n=328)	Clear cell subtype only, at least one previous VEGFR TKI	PFS	21.4 versus 16.5 months (0.66, 0.53-0.83, 0.00026)	7.4 versus 3.9 months (0.51, 0.41-0.62, 0.0001)	(Choueiri et al., 2016)
2016	CABOSUN	Cabozantinib (60 mg PO OD) (n=79)	Sunitinib (50 mg PO OD for 4 weeks followed by 2 weeks without treatment) (n=78)	Advanced RCC with a clear cell component	PFS	26.6 versus 21.2 (0.8, 0.53-1.21) not powered for OS differences	8.6 versus 5.3 months (0.48, 0.31-0.74, 0.0008)	(Choueiri et al., 2017a) (Choueiri et al., 2018a)

Date published	Study Acronym	Arms and numbers of patients		Setting	Primary Endpoints	Median OS (HR, 95% CI, *p* value)	Median PFS (HR, 95% CI)	References
		Experimental	Control					
2018	CheckMate 214	Ipilimumab (1 mg/kg IV) x 4 doses and Nivolumab (1 mg/kg IV) – both 3 weekly then single agent nivolumab 2 weekly (n=547)	Sunitinib (50 mg PO OD for 4 weeks followed by 2 weeks without treatment) (n=535)	Previously untreated. Clear cell component required	ORR, PFS and OS	Not reached versus 26.0 months (	11.6 versus 8.4 months (0.82, 0.64 – 1.05, 0.03) 99.1% CI used	(Motzer et al., 2018b)
2018	IMmotion 151	Atezolizumab (1200 mg IV) and Bevacizumab (15 mg/kg IV), both given 3 weekly (n=454)	Sunitinib (50 mg PO OD for 4 weeks followed by 2 weeks without treatment) (n=461)	Previously untreated	PFS and OS	Not reached	11.2 versus 8.4 months (0.83, 0.70-0.96)	(Motzer et al., 2018a)

1.2 Novel and Emerging Therapeutic Targets in RCC

1.2.1 What Makes An Ideal Therapeutic Target?

A therapeutic drug target is a protein, peptide or nucleic acid with proven function in the pathophysiology of a disease that can be modulated by a drug, for example a small molecular weight compound, antibody or recombinant protein (Gashaw et al., 2011). Identification of potential therapeutic targets typically begins with descriptive studies on DNA, RNA or protein expression in the chosen disease type compared with normal tissue. Information on somatic mutations and other genetic alterations may also provide a starting point for target discovery (Gashaw et al., 2011). The success rates for drug development projects in phase II clinical trials are below 20%, with 56% of failures due to lack of efficacy (Arrowsmith and Miller, 2013), for this reason it is essential to consider what defines a 'good' novel therapeutic target prior to investing further time and resources into its investigation. Some of the key desirable physical and structural properties are essential and include involvement and proven function in the pathophysiology of disease under physiological conditions (Gashaw et al., 2011) (Bakheet and Doig, 2009), the exhibition of differential expression in diseased versus normal tissue, the availability of antibodies for confirmatory studies and the ability to be 'druggable'. Not all drug-target binding and interaction results in therapeutic benefit. Structural knowledge of the novel target is helpful to predict high affinity, site-specific binding. (Bakheet and Doig, 2009). Other key properties to be considered include the presence of signal peptide, low pI, level of evidence implicating the protein-associated pathway, confirmation on tissue samples by immunohistochemistry (IHC), biological plausibility, protein properties and localisation, repurposing possibilities and whether there is a high unmet clinical need.

1.2.2 Therapeutic targets currently being explored in RCC

Novel therapeutic targets continue to be explored across RCC subtypes. In particular, agents that may augment the response rate and activity of checkpoint inhibitors are being urgently sought. RCC is known to harbour derangements in its metabolic pathways (Weiss, 2018). These include the finding of increased enzymes such as hexokinase-1 (HK-1), pyruvate kinase (PK-2) and lactate dehydrogenase A (LDH-A), suggesting increased glycolysis (Perroud et al., 2009), increased utilisation of fatty acids (Ganti et al., 2012), and evidence of tryptophan suppression, which can lead to immunosuppression if depleted (Lee et al., 2002). Glutamine utilisation is

increased in ccRCC compared with normal kidney tissue (Hakimi et al., 2016). Glutaminase inhibitors such as CB-839 have been shown to have activity in patients with RCC and appear to act synergistically with cabozantinib and everolimus (Tannir et al., 2018). Arginase inhibitors such as CB-1158, hypothesised to overcome the immunosuppressive activity of arginase, are also in early clinical trials and predicted to be active in RCC (Zea et al., 2005). Based on the concept of synthetic lethality, the activity of WEE1 inhibitors in patients with SETD2 deficient tumours is being explored (NCT03284385) (Pfister et al., 2015). There are a number of other treatment targets currently being investigated including zinc fingers and homeoboxes 2 (ZHX2). It is reported that this protein accumulates in the absence of functioning VHL, and it is slowed to interact with DNA to exert a downstream proliferative effect (Zhang et al., 2018).

1.2.3 Transient Receptor Potential Canonical (TRPC) channels

The transient receptor potential receptor canonical (TRPC) channels are an interesting potential therapeutic target in RCC that will be explored further in this study. They have been implicated in the development and biology of cancer, in particular RCC, and thus may form a novel therapeutic target (Chen et al., 2014, Veliceasa et al., 2007).

The TRPC channels belong to a super-family of transmembrane proteins that function as non-selective cation-permeable channels (Richter et al., 2014, Bon and Beech, 2013). They are linked to various processes such as angiogenesis, cancer and sensing including touch, taste and smell (Benemei et al., 2015, Damann et al., 2008, Bon and Beech, 2013). There are 7 members of the TRPC family, with all except TRPC2 expressed in humans (Damann et al., 2008). Based on their functional properties, TRPC 1, 4 and 5 are considered to form a subgroup, as are TRPC 3, 6 and 7 (Phelan et al., 2013). TRPC channels are present in almost all cells, including both excitable and non-excitable tissues (Abramowitz and Birnbaumer, 2009). TRPC 1, 4 and 5 exist as tetramers. They may assemble as homo- or hetero-tetramers and can functionally overlap making them more complex to study (Bon and Beech, 2013, Abramowitz and Birnbaumer, 2009). This section of work will focus on the TRPC 1, 4 and 5 subgroup due to the discovery of a potent modulator that will be discussed later.

There are several members of the TRPC family that may be implicated in cancer, thus explaining the observation of their altered expression in tumour compared with normal tissue (Prevarskaya et al., 2007b). For example, at an mRNA level, TRPC1 expression is increased in ductal breast cancer compared with the adjacent normal tissue (Dhennin-Duthille et al., 2011), silencing of TRPC1 and 4 in the ovarian cancer-derived cell line (SVOC3) (Zeng et al., 2013) and silencing of TRPC1 in non-small cell lung cancer (NSCLC) cell lines inhibited cell proliferation (Chen et al., 2014). The use of isoform-specific blocking antibodies of TRPC1 and 4 both had an antiproliferative effect on the A549 NSCLC cell line (Jiang et al., 2013). TRPC1 silencing and inhibition reduced cell invasiveness cellular mobility in the nasopharyngeal carcinoma cell line, CNE2 (He et al., 2012). These examples may suggest a role in the development of these cancer types. On the other hand, the normal renal epithelial cell line, HNK, demonstrates a four-fold higher TRPC4 expression compared with RCC cell lines at an mRNA level (Veliceasa et al., 2007) and TRPC1 is reduced in androgen-resistant prostate cancer cells compared with androgen-sensitive cells (Prevarskaya et al., 2007a). TRPC 1, 4 and 5 expression has not been characterised in RCC

1.2.3.1 (-)Englerin A (EA)

In 2009, Ratnayake et al. carried out an extensive study of natural product extracts using the NCI60 cell panel to identify those with anti-cancer activity (Ratnayake et al., 2009). The NCI60 is a panel of 60 cell lines representing cancers from leukaemia, colon, lung, CNS, melanoma, ovarian, renal, prostate and breast (Shoemaker, 2006). A natural product extract from the plant Phyllanthus Engleri, named (-)englerin A (EA), was found to selectively inhibit the growth of five out of the eight renal cancer cell lines with a remarkably low GI_{50} (concentration required for 50% of maximum inhibition of cell growth) of less than 20 nM (**Table 1.6**) (Ratnayake et al., 2009). In comparison, another study has shown that the normal kidney cell line (HK-2) was relatively insensitive to EA (EC_{50} >10 μM) (Sourbier et al., 2013).

Initially, the mechanism of action of EA was thought to be related to the binding to and activation of protein kinase C-θ (PKC-θ) producing an insulin-resistant phenotype whilst promoting a glucose-dependent state, thereby effectively starving the cells (Sourbier et al., 2013). More recently, it was discovered that the A498 renal cancer cell line, which was one of the most sensitive to be tested, did not express PKC-θ,

Table 1.6 – Table showing GI50 values for EA on various renal cancer cell lines in the NCI60 panel,

adapted from (Ratnayake et al., 2009).

Renal Cell Line	GI_{50} for (-)Englerin A (nM)
786-0	<10
A498	<10
UO-31	<10
ACHN	<10
RXF-393	11
SN12C	87
TK-10	15500
CAKI-1	15500

questioning the validity of the earlier finding (Akbulut et al., 2015). Instead, the work of Professor David Beech and his team (University of Leeds) led to the discovery that EA was a highly selective and very potent activator of the TRPC 4 and 5 channels. The activation of the channels trigger a massive influx of sodium into the cell and rapid cell death is observed (Ludlow et al., 2017). The finding that TRPC4 expression is necessary, and sufficient for EA induced growth inhibition has since been independently verified by others (Carson et al., 2015).

1.2.3.2 Other known TRPC channel agonists

There are few known modulators of TRPC 4 and 5 activity, which has hindered the advancement of research into these channels. Of the modulators that are known, TRPC4 is activated by lead (Pb^{2+}) (Sukumar and Beech, 2010) and both TRPC4 and 5 are activated by micromolar concentrations of lanthanum and gadolinium (Jung et al., 2003). Rosiglitazone, one of the thiazolidinedione class of drugs, is a known small molecule activator of the TRPC5 channel at concentrations greater than 10μM (Bon and Beech, 2013, Majeed et al., 2011). Rosiglitazone is a drug that was previously licenced in type 2 diabetes but its use was suspended across Europe after the discovery that it led to an increased risk of cardiovascular events (2010) (Chen et al.,

2012) (Nissen and Wolski, 2007), although it is still available in the U.S. It belongs to the thiazolidinedione class of compounds, which act as an agonist of peroxisome-proliferator–activated receptor γ (PPAR-γ). The agonist effect is not seen in other drugs and compounds within the same class (Majeed et al., 2011). The plasma concentrations of rosiglitazone in humans reach 1-3 μM following administration of a single 8 mg dose (Majeed et al., 2011). Riluzole is a second drug that is also known to activate the TRPC5 channel and the TRPC1/5 heteromer (Richter et al., 2014). It is licenced as a treatment to extend life for patients with amyotrophic lateral sclerosis (ALS), a form of motor neurone disease (MND) (National Institute for Health and Care Excellence (NICE), 2001). The plasma concentration in patients receiving 100 mg per day is approximately 2 μM (Mohammadi et al., 2002).

The drug discovery and development process is expensive, estimated at $2.6 billion per drug, (DiMasi et al., 2016) and can take many years (Paul et al., 2010). Theoretically, the concept of repurposing drugs that have already been approved for other indications is an appealing one. The extensive pharmacokinetic, bioavailability, dosing and toxicity data that will already have been obtained for these drugs gives this approach an advantage of potentially bypassing some of this process, thereby reducing the time and costs involved (Sleire et al., 2017). If rosiglitazone is found to be an effective drug for use in RCC, its known cardiac toxicity may hinder its use, although in the setting of advanced cancer, the risk-benefit ratio may be deemed more acceptable.

1.2.4 Spleen Tyrosine Kinase (SYK)

Spleen tyrosine kinase (SYK) is a second protein that will be further explored in this study. It was first highlighted as a potential novel therapeutic target in a study undertaken as part of an ongoing collaboration with McGill University in Canada (Karimzadeh et al., 2018).

SYK is a non-receptor type protein tyrosine kinase (PTK) initially discovered in bovine thymus and porcine spleen (Kobayashi et al., 1990, Taniguchi et al., 1991, Zioncheck et al., 1986, Zioncheck et al., 1988) that maps to chromosome 9q22 in humans (Sada et al., 2001). It is widely expressed in cells throughout the body, in particular almost all cells of a haematopoietic lineage (Yanagi et al., 1995) (Chan et al., 1994) (Yamada et al., 1993) (Benhamou et al., 1993) (Harrison et al., 1994) and has a number of functions which can be broadly classified as immunoreceptor and non-

immunoreceptor related. It is activated by a large variety of immune response receptors, cytokines, integrins, thrombin and G protein coupled receptors (Futterer et al., 1998).

1.2.4.1 Immunoreceptor related functions

Immunoreceptors do not possess intrinsic protein kinase activity (Latour et al., 1998), instead they are closely associated to transmembrane proteins that have a cytoplasmic immunoreceptor tyrosine-based activation motif (ITAM). Upon activation of the immunoreceptor, tyrosine residues in the ITAM are phosphorylated, primarily by Src tyrosine kinase family members, and subsequently recruit SYK through interaction with the tandem SH2 domains. SYK in turn activates downstream signal pathways within the haematopoietic cell (Mocsai et al., 2010, Mocsai et al., 2004) (Turner et al., 2000).

1.2.4.2 Non-immunoreceptor related functions

Whilst initially thought to have a role limited to coupling immunoreceptor signalling with downstream effects, the development of SYK knock-out mouse models highlighted additional non-immunoreceptor related functions. Abnormal communications between the lymphatic and blood circulatory systems and a haemorrhagic phenotype was observed in the embryos of SYK deficient mouse models, emphasising its role in vascular development (Turner et al., 1995). Expression was later confirmed in endothelial cells (Yanagi et al., 2001a). Mice that had been lethally irradiated and reconstituted with SYK deficient foetal liver lacked mature B cells, emphasising SYK's crucial role in the development of these cells (Turner et al., 1995). SYK also functions to mediate diverse biological functions such as osteoclast maturation (Mocsai et al., 2004) and cellular adhesion (Mocsai et al., 2010). It also has a diverse role in autoimmune functions not limited to immunoreceptor signalling (Mocsai et al., 2010, Yanagi et al., 2001b).

1.2.4.3 SYK isoforms

There are four transcripts of SYK that give rise to two isoforms through alternative splicing (Futterer et al., 1998). The longer isoform, SYK(L), measures 72 kDa, while the other, less abundant, shorter isoform, SYK(S), measures 69 kDa. SYK(S) lacks a 23 amino acid insert in the linker domain B (Turner et al., 2000) (Figure 1.1). The full significance and biological reasons for the two isoforms are not fully known. It is

clear that they have different functional roles. The 23 amino acid insert contains tyrosine 290, which has been shown to be a site of SYK autophosphorylation and subsequent activation in vitro (Furlong et al., 1997), although this was not the case in the RBL-2H3 (basophilic leukaemia cell line) or BI-141 (murine T-cell hybridoma cells) cell lines, where lack of the linker domain in SYK(S) has been linked with an inability to bind to the ITAM's, and thus to participate in immunoreceptor signalling (Latour et al., 1998). The 23 amino acid insert was also found to have a nuclear translocation signal explaining the lack of SYK(S) in the nucleus of breast cancer cell lines (Wang et al., 2003). It is likely the two SYK isoforms have different roles in different cell types.

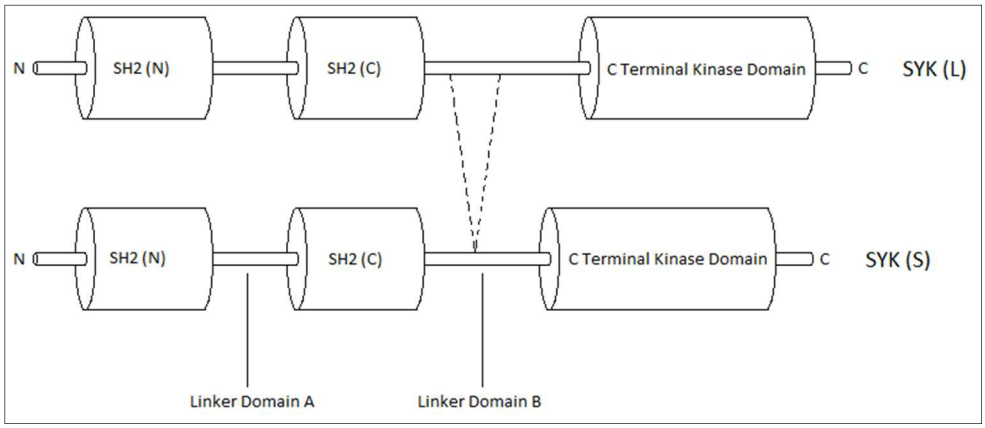

Figure 1.1 Schematic diagram showing the structure of the SYK isoform.

The SYK (S) isoform is missing a 23 amino acid insertion the linker domain B as shown (amino acids 283 – 305). Adapted from reference - (Turner et al., 2000)

1.2.4.4 Justification for examining SYK as a therapeutic target in RCC

In an ongoing collaboration in conjunction with the McGill University in Canada, a novel integrated bioinformatics analysis of the data emerging from the International Cancer Genome Consortium (ICGC) Cancer Genomics of the Kidney (CAGEKID) database was performed. Data from the CAGEKID project was analysed for an association between the proteome and genes that were either mutated or differentially expressed at an mRNA level. Proteins that interacted extensively with these genes were identified and examined as potentially representing key players in the biology of ccRCC. The identification of VEGF and several other proteins, already known to have a role in RCC supported this novel approach. SYK was identified as a potential key regulatory factor in RCC, it was alternatively spliced at the RNA level

in 24/44 ccRCC samples (54.5%) compared to matched normal kidney samples. The longer isoform of SYK was more abundant in tumour samples compared to normal kidney samples ($p<0.008$) (Figure 1.2).

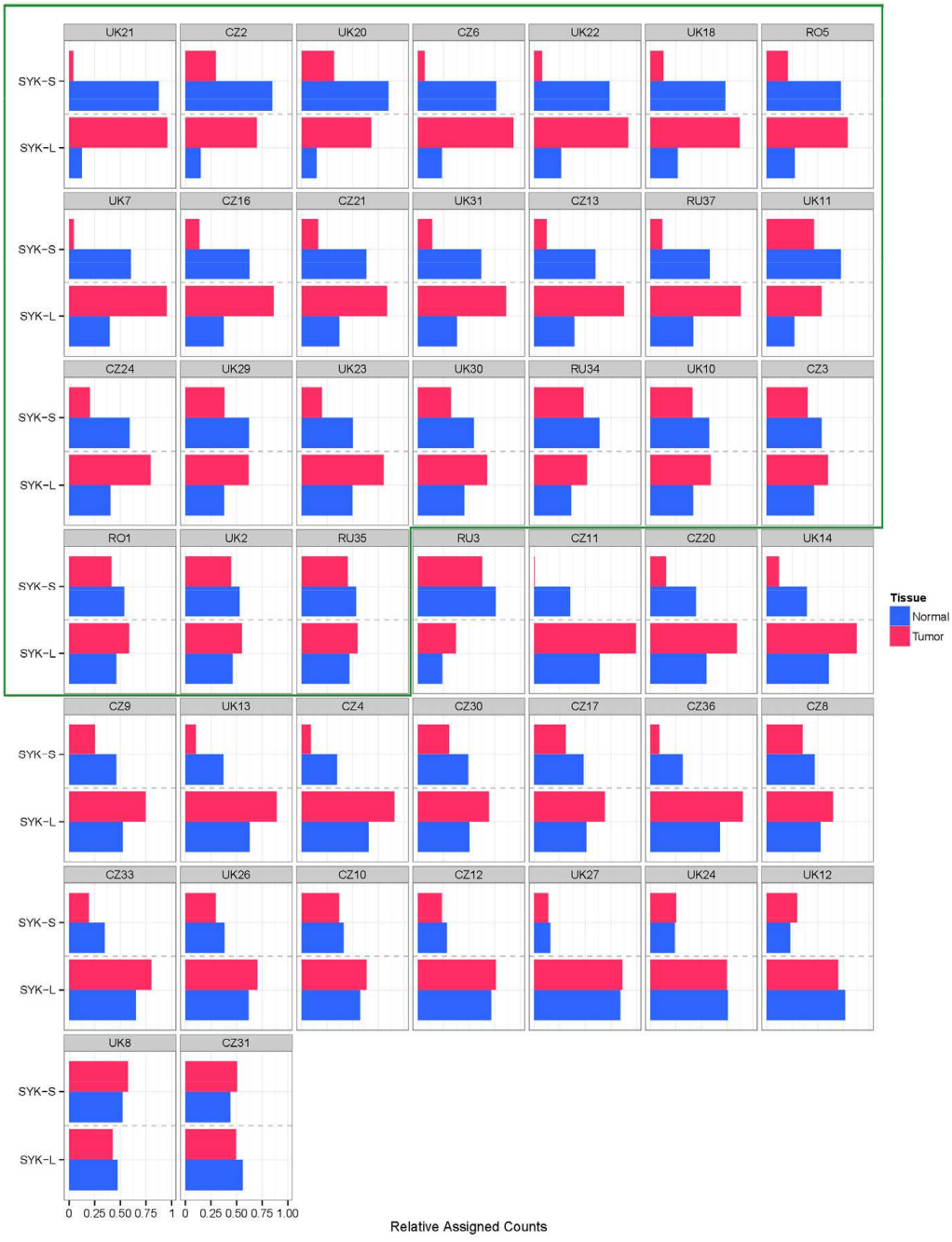

Figure 1.2- Pooled relative abundance of RNA levels for the SYK(L) and SYK(S) isoforms in matched tumour and adjacent normal kidney tissue.

Relative abundance of the mRNA levels for each SYK (L) and SYK (S) isoform in samples from 44 patients are shown. The patient identifier is at the top of each box. The blue bar represents normal tissue and the red bar matched RCC tissue (This figure is taken from (Karimzadeh et al., 2018))

Subsequent RNA interference work was undertaken which revealed that silencing SYK using shRNA reduced the ability of the 786-0 RCC cell line to form colonies, supporting the potential for SYK inhibition as a novel therapeutic strategy in RCC **(**Figure 1.3). This, together with the fact that inhibitors of SYK are already in clinical use in other indications, supported its further examination as a potential RCC therapeutic target in this work.

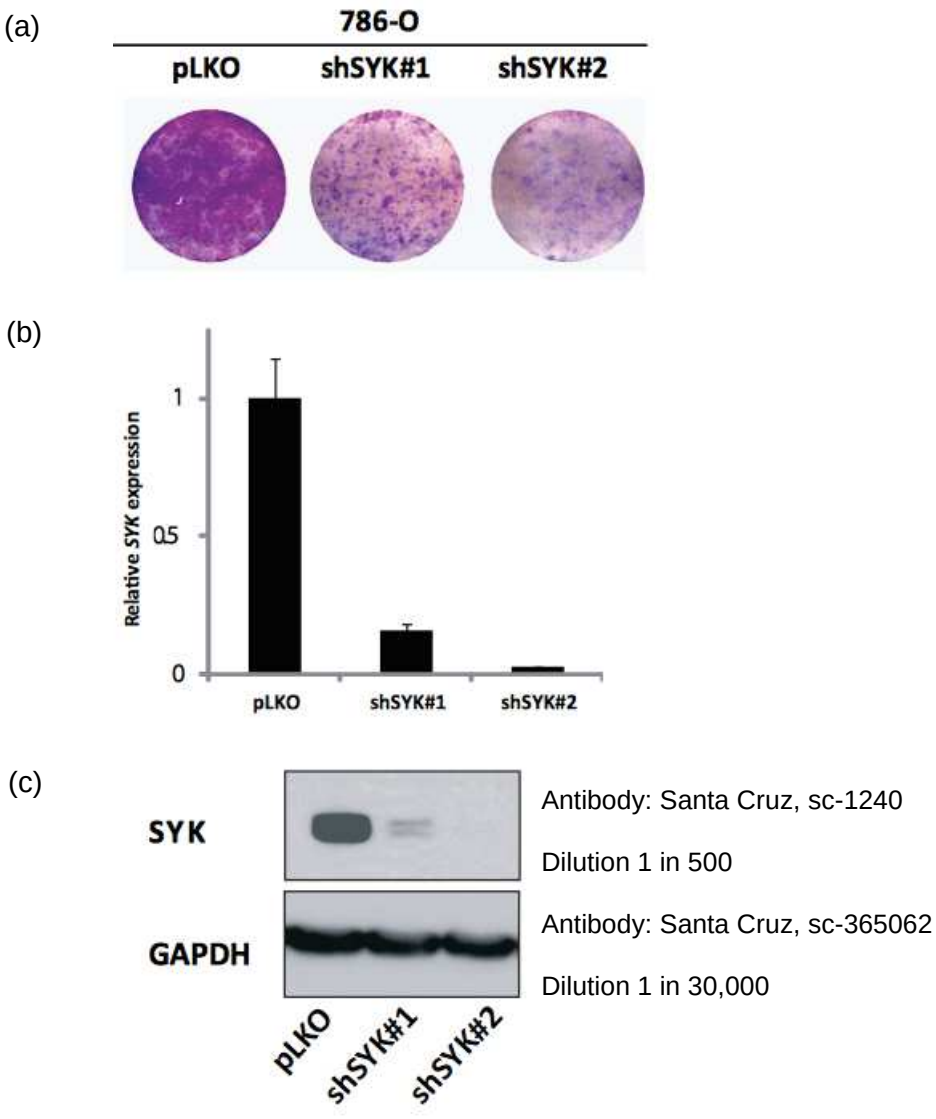

Figure 1.3 Inhibition of SYK impairs the colony formation of the 786-0 renal cancer cell line.
The modulation of SYK was examined using RNA interference (a) Silencing of SYK (shRNA♯1 and shRNA♯2) reduces the colony formation of 786-0 compared with a negative control (pLKO). (b) Confirmation of SYK expression levels determined by qRT PCR relative to the negative control. (c) Western blotting to confirm SYK knockdown efficacy. (This figure is taken from (Karimzadeh et al., 2018))

1.2.4.5 SYK expression in cancer

SYK can act as either a promoter or a suppressor of different cancer types (Krisenko and Geahlen, 2015) and this becomes more complex when the different isoforms are considered. It is hypothesised that SYK activation results in activation of various signalling cascades leading to a number of complex cellular responses including cell differentiation and cell survival (Coopman and Mueller, 2006). Amongst its many diverse roles, SYK is involved in cellular adhesion (Mocsai et al., 2010), B cell maturation (Turner et al., 1995, Mocsai et al., 2010), and the relay of signals from a large number of immunoreceptors in haematopoietic cells (Turner et al., 2000). Not all the previous work has identified between the two SYK isoforms.

Breast Cancer

SYK is expressed in normal human breast tissue and is lost in invasive breast carcinoma tissue. It is absent in highly tumourigenic breast cancer cell lines. Transfection of SYK into the SYK negative MDA-MB-435BAG breast cancer cell line reduced its tumour growth and metastasis formation in athymic mice (Coopman et al., 2000). SYK was found to be downregulated by mRNA expression in 28% (25/90 paired breast cancer and normal breast tissue samples and when downregulated was associated with poor prognosis and distant metastasis (Toyama et al., 2003). Interestingly SYK is encoded on chromosome 9 and allelic loss of chromosome 9q22 has been reported in primary breast cancer and is associated with lymph node metastasis (Minobe et al., 1998). Subsequently, it was demonstrated that the two SYK isoforms were differentially expressed in breast cancer cells. Western blot analysis of 16 paired tumour and normal breast tissue samples, SYK(S) was observed in 50% (8/16) of tumour samples (Wang et al., 2003). Overexpression of SYK(L) in breast cancer cell lines reduced cell invasion but did not effect cell migration. The manipulation of SYK(S) expression did not have an effect on cell invasion (Wang et al., 2003). Cellular imaging and Western blot analysis of cellular fractionations has demonstrated that both isoforms are found within the cytoplasm but only SYK(L) is found within the nucleus. Subsequent analysis of breast cancer cells led to the discovery of a nuclear translocation signal located within the 23 amino acid insert in linker domain B of SYK(L), thus explaining the cellular localisation of the two isoforms (Wang et al., 2003). This is complicated by the finding that in immune cells the nuclear translocation signal was separate to the 23 amino acid insert in DT40 lymphoma cell line (Zhou et al., 2006). The loss of SYK was observed

to be progressive through tumour progression from normal tissue through DCIS to invasive carcinoma using *in-situ* hybridisation (Moroni et al., 2004)

Haematological Malignancies

In cancers of a haematological origin there is a contradicting mix of SYK expression. In pro-B cell acute lymphoblastic leukaemia (ALL) (Goodman et al., 2001) and classical Hodgkin disease (Marafioti et al., 2004) SYK is observed to be down regulated, whilst it is upregulated in anaplastic large cell lymphoma (ALCL) expressing anaplastic lymphoma kinase (ALK) (Thompson et al., 2005). Conversely, SYK has also been observed to act as an oncogenic driver. There are subsets of B cell lymphomas, chronic lymphocytic leukaemia (CLL) and several other haematological malignancies that overexpress SYK and these cancers rely on SYK for survival (Buchner et al., 2009, Friedberg et al., 2010).

Hepatocellular carcinoma (HCC)

In HCC SYK was explored in seven established cell line models along with an immortalised normal liver cell line, LO2. SYL(L) was observed in the normal liver cell line and 86% (6/7) of the HCC cell lines. SYK(S) was observed in the two HCC cell lines with the highest metastatic potential. This work was carried out using qRT-PCR and confirmed with immunoblotting. In further work, SYK(L) was found to be significantly downregulated and SYK(S) upregulated in primary HCC compared with matched normal tissue and normal tissue without cirrhosis. SYK(S) was rarely found in non-tumour samples 1.3% (2/152). Using the HCC cell line, SMMC7721, two observations were noted, SYK(L) loss and SYK(S) gain were associated with increased cell growth and metastasis, confirmed by RNA interference. SYK(L) presence was associated with a more favourable outcome through better tumour differentiation, the absence of intrahepatic tumour nodules and less metastatic potential. SYK(S) expression was associated with a poorer outcome and a more aggressive tumour and higher metastatic potential (Hong et al., 2014). The cellular location of the two SYK isoforms concurs with the findings in breast cancer where SYK(L) was found in the nucleus and cytoplasm but SYK(S) was only found in the cytoplasm (Hong et al., 2014). These findings suggest that SYK(L) acts on the nucleus to suppress the oncogenic properties of select cancer types and SYK(S) has a cancer promoting role in the cytoplasm. Loss of SYK(L) and presence of SYK(S) were the most powerful indicators of time to recurrence and overall survival (Yanagi et al., 2001b)

Other cancers

The loss of SYK(L) was associated with increased cell growth and metastatic potential in pancreatic cancer (Layton et al., 2009). SYK mRNA is present in retinoblastoma cells but not in normal retinal cells (Zhang et al., 2012), indicating it may be a direct or indirect result of RB1 loss as this was the only known cancer gene mutated in a study of 4 cases of retinoblastoma. A subset of small-cell lung cancer (SCLC) overexpress SYK and SYK knockdown using siRNA decreases proliferation rate and increases cell death in the H69 and H146 SYK expressing small cell lung cancer cell lines (Udyavar et al., 2013).

In ovarian cancer a positive correlation by qPCR was observed between increased SYK(L) expression and higher cancer grade (Prinos et al., 2011). Knockdown of SYK(L) reduced colony formation of the SLOV3 ovarian cancer cell line (Prinos et al., 2011). In cell line models of malignant melanoma and normal melanocytes, SYK was found to be downregulated in melanoma cells compared to melanocytes and was progressively lost in the transition from normal tissue to invasive malignancy (Hoeller et al., 2005). SYK was found to be present in the nucleus of 42.4% (106/260) of gastric cancer cases. Nuclear SYK expression was associated with T1 tumours and the absence of lymph node metastases a better 5-year survival (92% vs. 67%, $p<0.01$) (Nakashima et al., 2006).

1.2.4.6 SYK inhibitors

There has been a great interest in the development of SYK inhibitors (Geahlen, 2014). SYK inhibitors that are currently being investigated in clinical trials include R788 (fostamatinib), an oral prodrug of R406 (tamatinib) (Braselmann et al., 2006). It inhibits SYK in an ATP-competitive manner and has shown promise in several phase I/II clinical trials of rheumatoid arthritis (Weinblatt et al., 2008), immune thrombocytopenic purpura (ITP) (Podolanczuk et al., 2009), and, of more relevance to the current work, several lymphomas including DLBCL and CLL (Friedberg et al., 2010). The toxicities included neutropenia, GI disturbances and hypertension and were reported to be manageable (Friedberg et al., 2010). Other SYK inhibitors include entospletinib, which showed benefit in a phase II clinical trial in humans in CLL (Sharman et al., 2015). It is reported to have better selectivity for SYK. No SYK inhibitors have been investigated in the treatment of RCC.

In keeping with the action of SYK to couple the activation of immunoreceptors to downstream signalling pathways, there are subsets of B cell lymphomas, chronic lymphocytic leukaemia (CLL) and several other haematological malignancies that rely on SYK for survival (Buchner et al., 2009, Friedberg et al., 2010). This explains the current investigation of SYK inhibitors in clinical trials in these cancers. A phase I/II trial of fostamatinib in recurrent B-cell non-Hodgkin lymphoma (B-NHL) has been reported. For the subsets of B-NHL, there were objective response rates of 22% (5/23) for diffuse large B-cell lymphoma, 10% (2/21) for follicular lymphoma, and 55% (6/11) for other types of B-NHL, including chronic lymphocytic leukaemia (CLL)

1.3 Proteomic Approaches to Therapeutic Target Discovery

This thesis was mainly focussed on the proteomic analysis of ccRCC and thus involved the utilisation of several proteomic technologies and techniques ranging from sample preparation and separation, to data analysis. Although these are detailed in Chapter 2, Materials and Methods, the preparation of tissue lysates for mass spectrometry analysis and the three main technologies, tandem mass spectrometry coupled with liquid chromatography (LC-MS/MS), sequential window acquisition of all theoretical fragment ion spectra mass spectrometry (SWATH-MS), and antibody arrays, will be discussed here along with their benefits and limitations.

A key requirement to enable accurate proteomic profiling is the adoption of an optimal sample processing technique. Detergent use is essential in the solubilisation of hydrophobic proteins, but these detergents are typically not compatible with mass spectrometry and must be eliminated prior to analysis. Detergent contamination of a mass spectrometer is costly and time consuming. Many sample preparation techniques, such as the filter aided sample preparation (FASP) involve multiple steps and can have varying performance (Wisniewski et al., 2009). The suspension trapping (STrap) sample preparation method, developed and validated in this laboratory, enables highly reproducible and rapid SDS based protein extraction, followed by a tryptic digest and peptide clean up and was thus employed for this study (Zougman et al., 2014).

The peptide sample is separated using liquid chromatography and is eluted into the mass spectrometer. Following this there are three main processes. Firstly the sample is ionised, it then undergoes MS1 where the abundance and mass to charge (m/z) ratio is determined for the ions. In the final process, MS2, a subset of the detected ions are subjected to fragmentation and the abundance and m/z ratio is again determined for each fragment. LC-MS/MS is the most commonly available mass spectrometry technology to analyse complex protein mixtures. This method is also known as 'discovery' or 'shotgun' proteomics. In the MS2 step, the most abundant ions are individually selected and fragmented. This MS method is characterised by data dependent acquisition (DDA), the mass spectra obtained are compared to a theoretical protein sequence database (MaxQuant) through which the proteins are identified. Adaptations to this method of MS is possible, for example using stable isotope labelling and isobaric tags, and allow the targeted identification of specific peptides. There may be limitations in the ability to analyse low abundance proteins, but it is the more widely available mass spectrometry method. A second analysis technique is data independent acquisition (DIA), for example, SWATH-MS, which has been developed to complement other MS techniques such as tandem MS. Unlike LC-MS/MS, many ions are fragmented in the MS2 step at once, producing a complex fragmentation spectra that requires a large amount of computational analysis to map each peptide using spectral libraries. It is currently less widely available but is reported to be more reproducible and sensitive (Guo et al., 2015b). Both techniques have the ability to rapidly identify thousands of proteins per sample and both will be utilised in parallel in Chapter 4 (Hu et al., 2016).

Antibody arrays have the advantage of requiring small amounts of sample and having a high level of reproducibility and sensitivity but are somewhat limited due to the lack of available reagents, lack of accuracy and dynamic range. The ability to detect protein abundance, different structural variations and post-translational modifications means it can be used to complement the mass spectrometry analysis (Haab, 2005).

1.4 Integrating Proteomics and Genomics in Therapeutic Target Discovery

A number of studies in other cancer types have recently attempted to address this deficiency in knowledge through the integration of both proteomic and genomic data from the same samples in large bioinformatic analyses (Zhang et al., 2014) (Mertins

et al., 2016) (Zhang et al., 2016). This potential benefit is demonstrated in several examples, firstly, in the identification of TOMM34 as a therapeutic target in colorectal cancer (CRC) (Zhang et al., 2014). More recently, a peptide vaccine against TOMM34 and a second protein, RNF43, has been reported in a phase one trial in patients with CRC that were intolerant or refractory to standard chemotherapy, with stable disease over the course of the trial in 6 patients (25%) (Taniguchi et al., 2017). HDAC1 was identified to be upregulated in a subset of high-grade serous ovarian cancer (Zhang et al., 2016). Its pharmacological inhibition in addition to conventional chemotherapy has been explored in a phase II study in patients with previously treated ovarian cancer, with results suggesting a clinical benefit (Dizon et al., 2012). PAK1 was identified as a potential therapeutic target in breast cancer (Mertins et al., 2016). Pharmacological inhibition of PAK1 *in-vitro* has been shown to inhibit breast cancer cell growth (Fajardo et al., 2015) and more recently inhibition of the Rac1-PAK1 pathway has been shown to restore tamoxifen sensitivity in a breast cancer cell line (Gonzalez et al., 2017). Although these proteins had been identified to be dysregulated prior to the completion of these three proteogenomic studies, they still highlight the potential benefits of this approach for the identification of novel therapeutic targets and provide a promising platform that may be applied to ccRCC in order to develop rational novel therapies.

The integration of proteomic and genomic information has the potential to help understand the functional effect of genome variation, in particular may provide further knowledge into the somatic gene mutations, such as those in PBRM1, SETD2 and BAP1.

1.5 Hypothesis and Aims

The underlying hypothesis of this project is that identifying differentially expressed proteins in ccRCC compared to normal kidney using proteomic technologies, and integrating the findings with the results emerging from our group's parallel ongoing genomic studies, is a useful strategy for novel therapeutic target discovery.

To achieve my overall aim of identifying novel therapeutic targets in ccRCC, I have designed several integrated and complementary sub-studies with specific aims as follows:

- To use the emerging targets, TRPC channels, as an exemplar with known drug modulators to design and implement in vitro strategies and models to both validate TRPC as a relevant target in RCC and to also subsequently explore any further emerging targets from my own proteomic studies.
- To explore the initial findings of changes in SYK isoform at the mRNA levels from the groups ongoing genomic collaborations in terms of representing a novel potential therapeutic target in RCC.
- To undertake a detailed proteomic analysis of ccRCC tissue compared with normal kidney, selected on the basis of underlying genomic changes, to understand the impacts of mutations in key genes on protein expression in ccRCC and identify potential novel therapeutics either for generic use or dependent on genetic profile.

Chapter 2 Materials and Methods

All solutions were prepared using ultrapure water (ELGA DV25, 15 MΩ). Formulations of the various solutions are detailed in Appendix 1. Unless otherwise specified, all laboratory chemicals were purchased from Sigma or AnalaR. Tissue culture plasticware was obtained from Corning. All suppliers' details are listed in Appendix 2.

2.1 Cell lines and tissue samples

2.1.1 Established cell lines

To investigate the presence of the proteins highlighted within this study, a number of established RCC cell lines and other human derived established cell lines were utilised. These cell lines were stored in the vapour phase of liquid nitrogen within the laboratory and were retrieved for culture when necessary. The source, characteristics and growth media used for these cell lines are detailed in Table 2.1. All cell lines were routinely mycoplasma tested whilst in culture in line with laboratory protocols.

Table 2.1 – Source and characteristics of RCC cell lines.

W/T denotes wild-type and ATCC and NCI denote the American Tissue Culture Collection and National Cancer Institute respectively.

Cell line	Characteristics	Source	Media
A498 (HTB44)	ccRCC from primary tumour. VHL mutant.	ATCC (Giard et al., 1973)	MEM Eagle (Sigma)
HTB45 (A704)	ccRCC from primary tumour. VHL mutant.	ATCC (Giard et al., 1973)	MEM Eagle (Sigma)
HTB46 (Caki-1)	ccRCC from metastatic site (skin). VHL W/T.	ATCC (Fogh et al., 1977)	McCoys 5a
HTB47 (Caki-2)	ccRCC from primary tumour. VHL mutant.	ATCC (Fogh et al., 1977)	McCoys 5a
HTB49 (SW839)	ccRCC from primary tumour. VHL W/T.	ATCC	50 / 50, RPMI 1640 / DMEM
CRL1933 (769-P)	ccRCC from primary tumour. VHL mutant.	ATCC	RPMI 1640
ACHN	Papillary RCC. Pleural effusion. VHL W/T.	ATCC	MEM Eagle or RPMI 1640
TK10	Primary tumour. VHL W/T.	NCI (Bear et al., 1987)	RPMI 1640
SN12C	Primary tumour. VHL W/T.	NCI (Naito et al., 1986)	MEM Eagle or RPMI 1640
SN12K	Mouse kidney subcapsular implant from human origin. VHL W/T.	NCI (Naito et al., 1986)	MEM Eagle or RPMI 1640
UMRC2	ccRCC. Primary tumour. VHL mutant.	HPA? (Grossman et al., 1985)	MEM Eagle
UO-31	RCC, unknown subtype. VHL W/T.	NCI	
HEK293	Human embryonic kidney cells	ATCC	DMEM (Gibco)
786-0 (CRL1932)	ccRCC. Primary tumour. VHL mutant.	NCI	DMEM (Gibco) or RPMI 1640
HUVEC	Human umbilical vein endothelial cells	ATCC (Jimenez et al., 2013)	F-12K Medium
Raji cells	Burkitts lymphoma B cells	ATCC (Karpova et al., 2005)	RPM! 1640

2.1.2 Cell culture

Cell lines were routinely grown in media supplemented with 10% (v/v) heat-inactivated foetal calf serum (HI-FCS) (Biosera) and 2 mM GlutaMAX-1 (Gibco) in a humidified environment at 37°C in 5% CO_2. Corning untreated cell culture flasks with

vented caps were used. For a T75 flask, cells were passaged by incubating with 5 ml PBS (Oxoid)/0.1% (w/v) EDTA (Sigma-Aldrich) for 5 minutes. Following removal of this solution, the adherent cells were incubated in 0.7 ml trypsin-versene (Gibco) for 3-5 minutes at 37ºC. Upon detachment, the trypsin was inactivated by adding FCS-containing media and the cell suspension was centrifuged at 350 g for 4 minutes. The volumes of solutions were scaled proportionately for other sized flasks. The cell pellet was resuspended and either re-plated or used for further experiments. Cells were routinely harvested at 85-90% confluence. A method used for the establishment of primary cell cultures is described in Chapter 3.

2.1.3 Cryopreservation

For storage of cell stocks, flasks of cells at 85-90% confluency were detached as detailed above and washed once with growth medium. The cell suspension was pelleted by centrifuging at 350 g for 4 minutes, then resuspended in a solution of HI-FCS (Biosera) with 10% (v/v) DMSO (Sigma-Aldrich). 1 ml aliquots were transferred into cryovials (Thermo Scientific) and placed at -80ºC in a freezing container (Biocision CoolCell FTS30) to allow controlled rate cooling. After 24 hours the cells were transferred to the vapour phase of liquid nitrogen for long-term storage. When needed, cells were retrieved, gently thawed in a water bath (37°C), and then washed with pre-warmed media before re-pelleting by centrifuging at 350 g for 4 minutes, resuspending in culture media and placing in a culture flask for culture as above.

2.1.4 Human tissue collection and storage

Tissue samples were processed according to a strict standard operating procedure (SOP) in the Leeds Multidisciplinary Research Tissue Bank (RTB). With approval from the local Research Ethics Committee (REC) and following informed patient consent, tissue was routinely collected from patients undergoing surgery for suspected RCC in St James's University Hospital, Leeds. Tissue samples were routinely collected from operating theatres immediately following nephrectomy and processed by Mrs J. Brown and Mr N. Gahir. Samples of tumour and distant normal kidney measuring approximately 5 mm x 5 mm x 10 mm were obtained and immediately transferred to the laboratory in ice-cold RPMI 1640 (Gibco) before dissection into smaller blocks, snap-freezing and storage in the vapour phase of

liquid nitrogen. Tissue samples from the RTB were accessed for use throughout this study.

2.1.5 Frozen tissue sectioning

Frozen tissue blocks were sectioned using a Leica CM3050 S Cryostat according to local SOP. Care was taken to ensure the tissue blocks remained in the frozen state throughout the process. Frozen tissue blocks and the cryostat chucks were placed in the cryostat chamber for at least 5 minutes prior to manipulation to adjust to chamber temperature. Ultrapure water was used to adhere the frozen tissue block to the cryostat chuck. For immunohistochemical staining of tissue sections, sections were cut at 5 μm and placed on a 'Superfrost Plus' microscope slide (VWR International) before short-term storage at -80^{o}C until use. For the proteomic study, tissue sections of varying thickness tissue were cut (Chapter 4). Care was taken to avoid cross-contamination by thorough cleaning of the cryostat between samples.

2.2 General protein methods

2.2.1 Protein extraction

2.2.1.1 Protein extraction from cells

Whole cell lysates were prepared as required for the various Western blotting studies analysing specific proteins. Culture media was removed from flasks of cell monolayers once 85-90% confluent. After rapid washing three times with ice cold PBS (pH 7.3 +/- 0.2) and once with ice-cold isotonic (0.25 M) sucrose, draining thoroughly after each rinse using a pipette, 1 ml of lysis buffer (Laemmli buffer) was added to each flask and the flask placed flat on wet ice. After 2 minutes cells were scraped off using a cell scraper and the lysate transferred to an eppendorf where it was incubated for a further 15 minutes on ice. During this time, the DNA was disrupted by sonicating intermittently for 3 seconds at a time, checking for residual cellular particles but avoiding foaming and overheating of the sample (Soniprep 150, MSE, London, UK). Following centrifugation at 10,000g for 10 minutes at 4°C, the supernatant was alliquotted, total protein quantified and stored at -80°C.

2.2.1.2 Protein extraction from tissue

Lysates from normal kidney and ccRCC tissue were used to investigate protein expression throughout this study. The protein extraction method used for the proteomic study in Chapter 4 is described later in this section. Prior investigations within the laboratory had determined that 10 μm sections equivalent to 1 cm x 3 cm surface area lysed with 400 μl of lysis buffer yield an average of 1000 μg total protein (250-2000 μg). Frozen tissue blocks stored in the RTB were selected and sections equivalent to the above placed in a 1.5 ml eppendorf. Flanking sections of 5 μm were also cut and were counterstained with haematoxylin and eosin for later review for evidence of necrosis, inflammation and viable tumour cells. For protein extraction, 300 μl of lysis buffer (Laemmli buffer) was added to each tube followed by incubation on wet ice for 15 minutes with occasional vortexing. Following this, DNA was disrupted by sonicating for 3 seconds at a time whilst checking for residual tissue particles, but avoiding foaming and overheating of the sample (Soniprep 150, MSE, London, UK). The solution was centrifuged at 10,000 g for 10 minutes at 4°C, following which the supernatant was alliquotted, total protein quantified and stored at -80°C.

2.2.2 Protein Assays

Protein concentrations of whole cell lysates or tissue lysates in Laemmli buffer were determined using a modified Bradford assay which is compatible with the β-mercaptoethanol and bromophenol blue present. The protein concentration of tissue lysates prepared using modified RIPA buffer for the proteomic study (Chapter 4), were determined using the Bicinchoninic acid (BCA) assay (Thermo Fisher). Prior to Western blotting, equal protein loading was confirmed by analysing densitometry of Coomassie Blue stained gels) as described in 2.2.4.

2.2.2.1 Modified Bradford Assay

5 μl of protein lysate (or standards) were added to 10 μl of PBS, 10 μl of 0.1M HCl and 75 μl of ultrapure water. A standard curve was created using standards in the range of 0-5mg/ml with 5 mg/ml BSA diluted in PBS and an internal control of BSA (2 mg/ml) was used for quality control across assays. Bio-Rad Protein Assay Dye Reagent Concentrate (Bio-Rad) was diluted 1 part to 4 parts water immediately prior

to use and 3.5 ml was added to each standard, control and test sample tube. Each sample was run in duplicate. The samples were mixed, immediately added to a disposable cuvette and absorbance (595 nm) was measured using an Ultraspec III spectrophotometer (GE Healthcare). Results were analysed against the standard curve using the Prism statistical package (GraphPad).

2.2.2.2 Bicinchoninic acid (BCA) assay

The assay was carried out according to the manufacturer's guidelines in 96 well plates. Nine protein standards ranging from 0 - 2 mg/ml were prepared using bovine serum albumin (BSA). 25 µl of each standard and unknown was pipetted into a microplate (96 well) in duplicate. Working reagent (supplied with kit) was added and the plate mixed for 30 seconds. After covering and incubating at 37 °C for 30 minutes, the plate was allowed to cool to room temperature and the absorbance of each well was measured at 562 nm using a MultiSkan EX spectrophotometer (Thermo). The Prism statistical package (GraphPad) was used to plot the standard curve and the protein concentration of each unknown sample was determined according to this.

2.2.3 Protein electrophoresis

2.2.3.1 Preparing 10% polyacrylamide gels

Glass plates and spacers of 1mm thickness and plastic sheet spacers were assembled in a minigel casting box (10 gels). . Resolving gel solution was made by mixing adding 26.4 ml of stock acrylamide (National Diagnostics, Hull, UK) 10 ml of resolving buffer (Appendix 1), 800 µl of 10% w/v SDS and 38.8 ml of water, and after addition of 4 ml of ammonium persulphate (15 mg/ml) and 40 µl of TEMED (tetramethylethylenediamine), the solution was immediately pipetted into the gel casting box to a level approximately 1 cm from the top of the gels. 400 µl of water-saturated isobutanol was carefully pipetted on top of each gel and the gels allowed to polymerise for an hour. After pouring off the isobutanol and rinsing the tops of the gels with water, a 4% stacking gel was added to each, consisting of a solution of 5 ml acrylamide, 10 ml of stacking buffer (Appendix 1), 400 µl of 10% SDS, 22.4 ml of water, 2 ml of ammonium persulphate and 60 µl of TEMED. Combs (10 wells) were carefully inserted into the top of each gel and gels allowed to polymerise for a further hour, before being used immediately or stored until use at 2-8°C for up to 2 weeks.

2.2.3.2 One dimensional SDS-polyacrylamide gel electrophoresis (1D SDS-PAGE)

Protein samples were separated prior to Western blotting or quantification with Coomassie blue stain by 1D SDS-PAGE using 10% gels (Section 2.2.3.1) or Criterion TGX precast 8-16% gradient gels with 18 wells (Bio-Rad). Tissue or cell lysates were adjusted to required concentrations using 1x Laemmli sample buffer, the proteins denatured by heating to 95°C for 3 minutes, and 10-2525 µl as appropriate was loaded into each well. A dual stained molecular weight protein standard (10 µl) was used in one well (Precision Plus Protein™ Dual Colour Standard, Bio-Rad). The proteins were resolved by electrophoresis in a Bio-Rad electrophoresis tank at 120 V (in-house gels) or 200 V (Criterion precast gels) using Tris-glycine running buffer (25mM Tris, 192 mM glycine, 0.1% w/v SDS), until protein separation was achieved as indicated by migration of the bromophenol blue dye front off the bottom of the gel (40-90 minutes).

2.2.4 Coomassie blue staining of gels

Coomassie blue staining of resolved gels was used for visualisation of the protein bands and checking equal protein loading measuring the density of the bands. Immediately following electrophoresis, the gels were fixed by immersing in Coomassie fix (40% v/v methanol, 7% v/v acetic acid, 53% v/v H_2O) for 30 minutes. Following this, the gels were placed in Coomassie Blue staining solution, which was prepared by diluting 1 part methanol with 4 parts Brilliant Blue G Colloidal Concentrate (Sigma), for 2 hours with gentle rocking at room temperature. To destain, gels were washed for 1 minute in Destain I (25% v/v methanol, 10% v/v acetic acid, 65% v/v H_2O), then Destain II (25% v/v methanol, 75% v/v H_2O) until the gels were sufficiently destained to allow visualisation of protein bands. Gels were scanned using an ImageScanner III (GE Healthcare) and densitometric analysis was performed using ImageQuant software (GE Healthcare).

2.2.5 Western blotting

Western blotting was employed for confirmation of protein identity and semi-quantitative determination of protein expression. Following separation by 1D SDS-PAGE, proteins were transferred onto Hybond™-C Super nitrocellulose membrane

(Amersham Biosciences). Gels were placed in contact with a nitrocellulose membrane and sandwiched either side between a layer of sponge and a thick sheet of Whatman filter paper. The blotting sandwich was submerged in Towbin's transfer buffer (Appendix 1) and transfer was carried out in a Mini Transfer Blot Cell (BioRad) at 100 V for 60 minutes or a Criterion Blotter (BioRad) at 100 V for 30 minutes. The complete transfer and quality of the transfer of protein was confirmed visually by placing the membrane in Ponceau S stain (Sigma) for 5 minutes at room temperature, then briefly washing with Ultrapure water until visualisation was achieved.

After blocking membranes in 10% (w/v) non-fat dried milk (Marvel) in TBS/0.1% (v/v) Tween-20 (Sigma) (TBS-T) for 60 minutes at room temperature whilst gently rocking, membranes were incubated in primary antibody diluted in 1% (w/v) non-fat dried milk (Marvel) in TBS-T for 2 hours, at room temperature. After washing again in TBS-T (4 x 5 minutes), the membrane was incubated in the appropriate secondary antibody (anti-mouse or anti-rabbit IgG horseradish peroxidase (HRP)-conjugated EnVision+ reagent) (Dako) diluted 1:200 in 5% (w/v) non-fat dried milk (Marvel) in TBS-T for 60 minutes at room temperature. Following this membranes were washed again in TBS-T (4 x 5 minutes) before being incubated in Supersignal® West Dura extended duration substrate (Thermo Scientific) as per manufacturers guidelines, for 5 minutes. The blots were developed and visualised on Kodak BioMax film (Sigma) using an X-Ray Film Processor (Konica Minolta). A list of the antibodies used in this study and their optimised working concentrations are listed in Table 2.2.

Table 2.2 – Primary antibodies used in this study

Antibody	Clonality	Host	Source
TRPC1 (clone 1F1)	Monoclonal	Mouse	NeuroMab
TRPC4 (clone N77/15)	Monoclonal	Mouse	NeuroMab
TRPC5 (clone N67/15)	Monoclonal	Mouse	NeuroMab
Syk clone 4D10) (sc-1240)	Monoclonal	Mouse	Santa Cruz
Anti-proteasome 20S LMP2 antibody (PSMB9) (ab3328)	Polyclonal	Rabbit	Abcam
Cox-1 (clone CX111) (cay160110)	Monoclonal	Mouse	Cayman Chemical
Cox-2 (clone CX229) (cay160112)	Monoclonal	Mouse	Cayman Chemical

2.2.6 Immunoprecipitation

Immunoprecipitation using the TRPC1 antibody on A498 cells was performed in an attempt to identify a band observed with this antibody in Western blotting using this cell line (Chapter 3). After reaching 85-90% confluence in a T150 flask, growth media was carefully removed from the flask and the monolayer was gently washed twice in ice cold PBS. The cell monolayer was then scraped, transferred to a 1.5 ml eppendorf and pelleted by centrifuging at 350 g for 4 minutes. The cell pellet was lysed in a modified RIPA buffer at room temperature for 15 minutes. Following centrifugation at 10,000 g for 5 minutes, the supernatant was removed and divided into two eppendorfs and the TRPC1 antibody (4 μg/ml) was added to one and an equal concentration of species-matched normal IgG, was added to the other. These were incubated on a spinner for 1 hour at room temperature. Magnetic protein G-coupled Dynabeads® (Life Technologies, Paisley, UK) were prepared by washing in the modified RIPA buffer, and added to the protein-antibody mix at 20 μl per 100 μl of lysate followed by incubation on a spinner for a further 30 minutes. The DynaMag™ magnet was used to separate the magnetic beads from the buffer and the bead pellet was washed once in modified RIPA buffer. The magnetic beads were again captured using the DynaMag™ magnet and the supernatant was processed for mass spectrometry analysis as detailed in Section 2.7.5

2.3 Cell growth and viability assessment

2.3.1 Cell growth analysis using Incucyte® equipment

The IncuCyte® live-cell analysis system which is located inside an incubator at 37°C, 5% CO_2 was used to view and analyse cell growth upon exposure to various compounds. Cells were seeded onto 24 well plates in the appropriate growth media at a predetermined seeding density to achieve 80-90% confluence at the end of the experiment. The cells were allowed to settle for 24 hours in a cell culture incubator at 37°C, 95% air/5% CO_2, before adding the investigative compound into the growth media. The analysis system was preset to image each well in four areas hourly until the end of the experiment. These images were analysed using the Incucyte® software to determine the cell confluence over time without removing the plate from the incubator.

2.3.2 Cell viability assay (WST-1)

Twenty-four hours after seeding each cell type at the seeding densities shown in Table 2.3, the growth medium was removed from each well and 100 μl of the required concentration of drug in growth medium was added to each well and cells incubated at 37°C in 95% air/5% CO_2. Englerin A is poorly water-soluble so was stored solubilised in 100% DMSO (v/v) (stock concentration 5 μM). Pluronic acid was used as a dispersing agent. The concentration of pluronic acid was kept at 0.01% (v/v) and DMSO concentrations did not exceed 0.15% (v/v) and results were compared with cells treated with vehicle controls only. After 6 hr, 10 μl of WST-1 was added to each well and gently mixed for 30 seconds. The plate was incubated for a further 30 minutes at 37°C, 95% air/5% CO_2. The absorbance was measured at 440 nm and 630 nm (background) using a MultiSkan EX spectrophotometer (Thermo). The Prism statistical package (GraphPad) was used to determine the cell viability (expressed relative to the vehicle control). This same method was used for the measurement of cell viability after exposure to the SYK inhibitor R406, except that the cells were exposed to the drug for 72 hours.

Table 2.3 – Details of seeding densities and plates used for cell viability measurement using WST-1

Cell line	Seeding density (cells/well)	Time to cell viability experimentation	Plate type (96 well microplate)
A498	5000	30 hours	Clear-bottomed Nunc plates
HUVEC	7500	30 hours	Clear-bottomed Nunc plates
HEK-293	15,000	30 hours	Clear-bottomed poly-D-lysine-coated plates
786-0	1000	96 hours	Clear-bottomed Nunc plates
CRL1933	2000	96 hours	Clear-bottomed Nunc plates
TK10	1500	96 hours	Clear-bottomed Nunc plates

2.4 Immunohistochemistry

2.4.1 Haematoxylin and eosin (H&E) staining of frozen tissue sections

Frozen sections were removed from the freezer and fixed in acetone for 1 minute before being left to air dry for 5 minutes. The sections were then stained in Meyer's haematoxylin (3 minutes) and rinsed in running tap water (1 minute). The haematoxylin pigment was blued by immersing in Scott's water (1 minute), followed by a further rinse in running tap water (1 minute) and staining in eosin (1.5 minutes). The slides were rinsed again in running tap water (30 seconds), before being dehydrated through increasing concentrations of ethanol (50%, 75% and 100%; 3 minutes each), and cleared in xylene (4 x 3 minutes). Coverslips were mounted onto the slides with DPX Mountant (Sigma) and the sections reviewed by a pathologist (Dr Pat Harnden).

2.4.2 Immunohistochemical staining of frozen tissue sections

Immediately prior to immunohistochemical staining, sections were removed from the -80°C freezer, washed twice in TBS (5 minutes each), then fixed in 4% (w/v) paraformaldehyde solution for 10 minutes followed by three washes in TBS (5 minutes each). The slides were next mounted onto Shandon cover plates with TBS, and loaded into the Sequenza tray (Thermo Fisher). Endogenous peroxidase was blocked for 15 minutes using Bloxall™ blocking solution (Vector Laboratories). Following a wash with TBS (5 minutes), the sections were blocked with 100 µl of 10% (w/v) casein in TBS for 30 minutes at room temperature. Primary antibody was diluted in antibody diluent (Life Technologies), and 100 µl was applied to the slides at room temperature for 1 hour. Slides were then washed twice in TBS followed by incubation with 100 µl of the appropriate secondary antibody for 30 minutes at room temperature. After a further 2 washes in TBS (5 minutes) the slides were further incubated with ImmPACT™ DAB Peroxidase substrate (Vector Laboratories) for 10 minutes. The reaction was stopped by placing the slides in gentle running tap water for 1 minute. Counterstaining was performed by immersing the slides in Meyer's haematoxylin for 20 seconds, followed by a rinse in tap water for 1 minute, Scott's water (1 minute) and then tap water (1 minute). Slides were then dehydrated in increasing concentrations of ethanol (50%, 75% and 100%) (3 minutes each), then

cleared in 4 changes of xylene (4 x 3 minutes). Coverslips were mounted onto the slides with DPX Mountant (Sigma).

Table 2.4 – Antibodies used in immunohistochemical staining of tissue sections

Antibody	Species	Working concentration	Source
Cox-1 (clone CX111) (cay160110)	Mouse (monoclonal)	5 μg/ml	Cayman Chemical
Cox-2 (clone CX229) (cay160112)	Mouse (monoclonal)	5 μg/ml	Cayman Chemical

2.5 RT-qPCR of tissue samples for gene expression analysis

The TaqMan® real time PCR assays (Thermo Fisher) were chosen to investigate TRPC 1, 4 and 5 gene expression in ccRCC and normal kidney samples through RT-qPCR. These were used in accordance with manufacturer's instructions. Both primary tissue and the A498 and CRL1933 ccRCC cell lines were used (Chapter 3).

2.5.1 RNA extraction

Cell lines at 80-90% confluence in a T75 tissue culture flask were harvested and resuspended as described in Section 2.1.2 and pelleted by centrifuging at 350 g for 4 minutes. The Qiagen RNeasy Mini Kit was used to purify RNA from these samples, in accordance with the manufacturer's guidelines. Essentially, cells were lysed using proprietary extraction buffers and the lysate was added to the silica membrane RAeasy spin column along with ethanol to create conditions that promote selective binding of total RNA to the RNeasy membrane with contaminants being washed away using serial centrifugations followed by elution of the RNA in RNase-free water. The approximate concentration of total RNA was determined using the NanoDrop 8000 equipment (Thermo Fisher) prior to the reverse transcription step.

2.5.2 qPCR using Biomark HD system (Fluidigm)

This system was used due to the low yields of RNA obtained from tumour samples. Flex Six™ gene expression integrated fluidic circuits (IFCs) were obtained for use on the Biomark HD system (Fluidigm), which allows automated qPCR reactions in nanolitre volumes. The circuits were used according to the manufacturer's guidelines and all analyses were run in duplicate. Initially reverse transcription was performed (all in duplicate) in 96 well plates: 1 μl of RT Master Mix (Fluidigm), 3 μl of RNase-free water and 1 μl of total RNA were mixed and 4 μl was loaded per well. This plate was placed into a Nexus thermo cycler L/R/G and reverse transcription performed by running at 25°C for 5 minutes, 42°C for 30 minutes and then 85°C for 5 minutes. Next a pre-amplification step was performed by combining 1 μl of Preamp Master Mix (Fluidigm) with 1.25 μl of a pooled Taqman® assay mix, 1.5 μl nuclease-free water and 1.25 μl of the template cDNA. 3.75 μl of this mixture was loaded into each well in a 96 well plate and heated to 95°C for 2 minutes before completing 14 cycles (95°C for 15 seconds followed by 60°C for 4 minutes). Once completed, 20 μl of 1X Tris-EDTA (TE) buffer was added to each well. The Flex Six™ IFCs were next primed in the HX loader (Fluidigm). 2 μl of each TaqMan® assay was combined with 2 μl of 2X Assay Loading Reagent and 3 μl of this was loaded onto the Flex Six™ IFC. 1.8 μl of the pre-amplified cDNA was combined with 0.2 μl 20X Gene Expression Sample Loading Reagent and 2 μl 2X Taqman Universal Master Mix. 3 μl of this mixture was loaded onto the IFC. Once all samples were loaded as required, the IFCs were loaded into the Biomark HD and run at 30°C for 25 minutes, 60°C for 70 minutes, 50°C for 2 minutes then 95°C for 10 minutes. Next the cycler was heated to 95°C for 15 seconds followed by 60°C for 60 seconds for 40 cycles. The results were analysed using the integral software.

2.5.3 DNA gel electrophoresis

Agarose gels were made by heating agarose in TBE (Tris-Borate-EDTA) buffer at a concentration of 2% (w/v) and GelRed® Nucleic Acid gel Gel Stain (Biotium) was added to the mixture (1:10,000). Slab gels were poured and allowed to cool to room temperature to set. 6X DNA loading buffer (30% (v/v) glycerol, 0.25% (w/v)

bromophenol blue) was made in-house. cDNA template/DNA loading buffer was loaded per well into the gel alongside a DNA ladder, and electrophoresed at 100 V for 2 hours immersed in 1X TBE. The bands were visualised in a GelDoc System (BioRad) using the UV illuminator.

2.6 Measurement of intracellular calcium

A498 cells were seeded at approximately $2x10^4$ cells per well (96 well microplate) and incubated at 37°C, in 95% air/5% CO_2, for 24 hr prior to experimentation. On the day of experiment, growth medium was replaced with standard bath solution (SBS) containing 2 μM fura-2-AM (Life Technologies) and 0.01% v/v pluronic acid. Loading was carried out in low light conditions and plates were wrapped in aluminium foil while incubating for 1 hr at 37°C. Cells were washed twice with SBS and left for 30 minutes at room temp bathed in SBS. Plates were placed in the FlexStationII (Molecular Devices), a bench-top scanning fluorimeter, at room temperature. This allowed for integrated fluid transfer whilst taking fluorescence measurements. Upon addition of the appropriate concentration of (–) englerin A at 60 sec (Chapter 3), fluorescence was read at 340nm (bound) and 380nm (unbound) and plotted as a ratio of 340:380.

2.7 Tissue sample preparation for proteomic analysis

Details of the tissues selected and study design are included in Chapter 4.

2.7.1 Protein extraction from tissue

Frozen tissue sections were cut as described in Section 2.1.5 aiming for a protein yield of 1000 μg as detailed in 2.2.1.2. The sections were then stored frozen in a 1.5 ml eppendorf each until extraction. SDS lysis buffer solution was used for protein lysis. 250 μl of the lysis buffer (5% SDS in 50 mM Tris-HCl, pH 7.6) was added to each eppendorf containing the frozen tissue sections at room temperature followed by gentle vortexing. DNA was disrupted by intermittent sonicating for 3 seconds at a time whilst checking for residual tissue particles but avoiding foaming and

overheating of the sample (Soniprep 150, MSE, London, UK). Disulphide bonds were next reduced by adding dithiothreitol (DTT) (stock 1 M) (Sigma Aldrich) to a final concentration of 25 mM. After heating to 95°C for 5 minutes, protein concentration was determined using the BCA assay. Prior to protein clean-up and digestion, iodoacetamide (stock 1 M) (Sigma Aldrich) was added to a final concentration of 125 mM to alkylate cysteines thereby preventing refolding of proteins, and the sample was left in the dark for 30 minutes.

2.7.2 Tryptic digestion of protein lysates (STrap technique)

STrap tips were prepared by adding 10 plugs of quartz filter paper to a 200 µl pipette tip (Zougman et al., 2014). Following tissue lysis as above, 175 µl of Strapping buffer (90% aqueous methanol containing a final concentration of 100 mM Tris-HCl, pH 7.1) was added to each STrap tip. Each SDS lysate was acidified by adding 12.5% phosphoric acid to a final concentration of 1.25% and then added to the top quartile of the strapping buffer contained in the STrap tip. The STrap tip was next placed in a 2 ml tube and centrifuged at 4000g for 30 seconds. A further 80 µl of the Strapping buffer was added to the STrap tip and centrifuged at 4000g for 30 seconds followed by addition of 40 µl of 40 mM ammonium bicarbonate solution and centrifugation at 4000g for 30 seconds. The tip was next removed from the tube and 30 µl of ammonium bicarbonate containing 2 µg of trypsin (Sequencing Grade Modified Trypsin, Promega) was added to the tip. This solution was pushed through the stack within the tip using a 10 ml syringe with an adaptor. After incubating for 1 hour at 47°C, 60 µl of 40 mM ammonium bicarbonate was added to the STrap tip and the digested peptides were eluted from the quartz stack by centrifuging at 4000g for 30 seconds.

2.7.3 Peptide clean up using Stop And Go Extraction (STAGE) Tips

Peptides generated using the STrap digestion method were next cleaned up prior to mass spectrometric analysis (Rappsilber et al., 2007). Tips were prepared by adding 4 plugs of C18 octadecyl discs (Empore™) to a 200 µl pipette tip. The C18 plugs were wetted using 50 µl methanol, which was pushed through using a syringe. The plugs were next acidified by adding 50 µl 0.25% formic acid to the tip and centrifuged

at 4000g for 15 seconds, before addition of 5 µl of 10% v/v trifluoroacetic acid to each tube (final concentration 0.5% v/v). The lysates were loaded into the STAGE tips and centrifuged at 4000 g for 30 seconds. The sample was next desalted by centrifuging 50 µl of 0.25% formic acid through the tip. The tips were placed in a further 1.5ml eppendorf and the peptides were eluted by adding 50 µl of elution buffer (60% v/v acetonitrile with 0.2% v/v formic acid) and centrifuging at 4000g for 30 seconds. The sample was heated at 90°C for 10 minutes in a fume hood to concentrate to a final volume of 10 µl.

2.7.4 Preparation of sample for transfer to Switzerland for SWATH-MS

Peptide concentration of each lysate was estimated using the NanoDrop 8000 system (Thermo Fisher). 5 µg of each sample was pipetted into individually labelled eppendorf tubes. The tubes were loaded into the rotary evaporator and run until dry. The tubes were sent to Switzerland for further analysis by SWATH-MS (Guo et al., 2015b)

2.7.5 Mass spectrometry

The digested peptide samples were randomised and analysed using an EASY-nLC 1000 ultra high pressure chromatography system linked to an LTQ Orbitrap Velos mass spectrometer (LC-MS/MS) by Dr Alexandre Zougman. Samples were injected (2 injections per sample) directly onto an in-house prepared 20 cm reversed phase fused-silica capillary emitter column of inner diameter 75 µm, packed with 3.5µm Kromasil C_{18} media.

The total acquisition time was 150 minutes, the major part of the gradient being 3–25% ACN in 0.1% formic acid at the flow rate of 0.25 µl/minutes. Survey MS scans were acquired in the orbitrap with the resolution set to 60,000. Up to the 20 most intense ions per scan were fragmented and analysed in the linear trap. The acquired data from duplicate MS runs for each sample were combined and label-free mass spectrometry data analysis was performed using MaxQuant (v1.5.2.8).[59] Proteins were identified using the Andromeda peptide search engine integrated into the MaxQuant environment and the Uniprot human database with the false discovery rate (FDR) for proteins and peptides set to 0.01 (Cox et al., 2009).(Cox et al., 2011)

Carbamidomethylation of cysteine was set as a fixed modification, with protein N-terminal acetylation and oxidation of methionine as variable modifications, enzyme: trypsin/P, maximum number of missed cleavages: 3. Differential expression between samples was assessed using label-free quantification (LFQ) intensity as a readout.

2.7.6 DNA extraction for confirmation of genetic mutations

Given the heterogeneity of RCC, the main genetic mutations in *VHL, PBRM1, BAP1* and *SETD2* were reconfirmed in parallel sections taken at the same time as sections for proteomic analysis and using similar amounts of tissue. Sections were placed in 1.5 ml eppendorfs and DNA extracted using the QIAamp DNA Mini Kit (Qiagen). In brief, tissue was initially lysed as directed by the manufacturers guidelines and RNase added to eliminate RNA. After addition of ethanol the sample was applied to the QIAamp Spin Column and centrifuged at 6000g for 1 minute. After further clean-up steps the DNA was eluted into a clean DNase-free microcentrifuge tube and stored at -20°C. The quantity of DNA was determined using the NanoDrop 8000 system (Thermo Fisher) and the DNA was then used for confirmation of the known genetic mutations. This was performed by Dr Claire Taylor from the Genomics Facility, University of Leeds.

2.8 Data analysis

Statistical analysis was performed using R (R Core Development Team, 2010), SPSS (Version 22, IBM) and Prism (Version 7, GraphPad) statistical packages. All analysis using R was performed by Mrs Michelle Hutchinson, a senior statistician within this group.

In the integrated proteomic and genomic study, principal component analysis and hierarchical clustering were used as multivariate methods of exploratory data analysis to visualise for groupings within the data. The differential expression (LFQ intensity) of each protein between genetically defined groups was assessed using non-parametric statistical tests. Initially a Kruskal Wallis test was used to determine if there were statistically significant differences and if identified, a post-hoc pairwise comparison Wilcoxen rank-sum (Mann Whitney U) test was applied. The false

discovery rate was calculated using the q-value method (Storey, 2002). When analysing for differences in global protein expression between ccRCC and normal kidney sample groups globally, a Wilcoxon rank-sum (Mann Whitney U) test was applied. Heat maps were generated by determining the z-score for each protein, the colour coding depicting the relevant score. A preliminary bioinformatics analysis was performed by Dr Lara Fuelner using Ingenuity® Pathway Analysis software.

Parametric tests such as Student's T-test and ANOVA were used as indicated throughout this study for analysis of cell growth and viability patterns.

Chapter 3 Exploration of TRPC 1, 4 and 5 and SYK as novel therapeutic targets in ccRCC

3.1 Introduction

The main aim of this chapter was to begin to establish the validity of the transient receptor potential canonical (TRPC) channels 1, 4 and 5 and spleen tyrosine kinase (SYK) as novel therapeutic targets in RCC. The strategy adopted was carefully designed to allow subsequent exploration of further emerging novel targets throughout this thesis.

Within this laboratory, the investigation of protein expression patterns in primary tissue samples is possible through utilisation of the attached Leeds Multidisciplinary Research Tissue Bank (RTB), which contains several hundred annotated frozen tissue samples from both RCC and matched normal kidney. The TRPC 1, 4 and 5, and SYK protein expression patterns were investigated in paired RCC and normal kidney samples from the same patient. Identification of established cell line models that were representative of the protein expression in primary tissue was sought. It is acknowledged that established cell lines have the advantage of being readily available and having the ability to be grown in bulk relatively quickly, but may not retain the exact characteristics of their ancestor cells (Pfaller and Gstraunthaler, 1998). To address this, significant efforts were made to develop a reproducible method for the generation and growth of primary RCC cultures (Perego et al., 2005). Finally pharmacological modulators of the proteins were investigated with a plan to proceed to *in-vivo* work if successful (Figure 3.1).

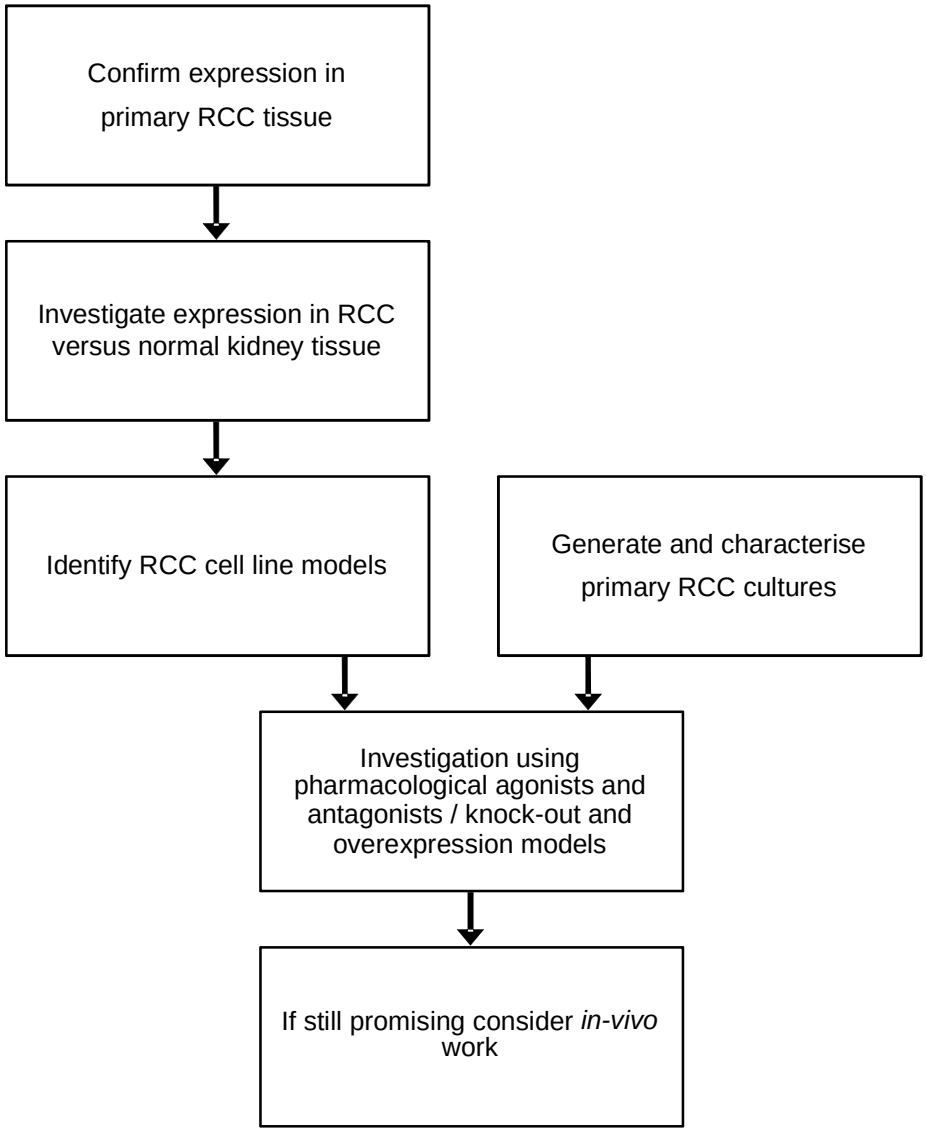

Figure 3.1 – The approach adopted in the investigation of novel therapeutic targets in ccRCC.

3.2 Transient Receptor Potential Canonical (TRPC) channels 1, 4 and 5

The TRPC 1, 4 and 5 channels are intriguing targets that have been hypothesised as being implicated in a number of malignancies including RCC (Veliceasa et al., 2007). Further research into these channels was hindered by the lack of potent modulators until the pioneering work by Professor David Beech's group discovered that the natural product extract, englerin A (EA), very potently and selectively activated the TRPC 1, 4 and 5 channels (Akbulut et al., 2015). This same compound was already known to selectively inhibit the growth of RCC cell lines in the NCI60 cell panel at

concentrations of less than 10 nM (Ratnayake et al., 2009). This section of work aims to complement this work through further exploration of the TRPC 1, 4 and 5 channels in primary RCC tissue.

The aim of this section of work was to further investigate the TRPC1, 4 and 5 channels as novel therapeutic targets in ccRCC, through:

1) Investigation of TRPC1, 4 and 5 channel expression in primary RCC tissue
2) Confirmation of the selective and potent nature of EA on RCC cell death
3) Investigation of other pharmacological TRPC channel agonists
4) Investigation of TRPC channel inhibition in ccRCC using a small molecule inhibitor (Pico145)
5) The generation of primary RCC cultures as a tool to assist in the further investigation of these channels

3.2.1 TRPC 1, 4 and 5 gene expression in ccRCC

Up to this point, investigations into TRPC1, 4 and 5 expression and the modulation of these channels were solely based upon observations using established RCC cell lines, which, as previously discussed, may not replicate the primary tissue or cell of origin. To begin this work, TRPC1, 4 and 5 gene and protein expression were investigated in primary ccRCC and matched normal kidney samples.

3.2.1.1 Selection of a suitable endogenous control for RT-PCR

To be suitable as an endogenous control gene, it must be stable in experimental samples and must not be influenced by biological, physiological, experimental or pathological conditions. Equal amplification efficiency of the endogenous control and target genes are also essential to allow determination of target gene expression (Jung et al., 2007). Whilst beta-actin and GAPDH are widely utilised endogenous controls, their stable expression in RCC and paired normal renal tissue was questioned based on several studies (Jung et al., 2007) (Dupasquier et al., 2014). Instead peptidylprolyl isomerase A (PPIA) was selected on the basis of three comparative explorative studies (Jung et al., 2007) (Dupasquier et al., 2014) (Ma et al., 2012). Features pertaining to the suitability of this gene include its ubiquitous nature within many cell types (Bergsma et al., 1991) (Koletsky et al., 1986) (Ryffel et al., 1991) (Schmid et al., 2003).

3.2.1.2 Amplification efficiencies of the PCR assays

The Taqman® Gene Expression assays (Thermo Fisher Scientific) were chosen for real-time PCR analysis of TRPC 1, 4 and 5 gene expression. To confirm the reliability of these assays, and the suitability of the selected endogenous control, the amplification efficiency of each assay was determined by analysing dilutions (range of 4 logs) of the target cDNA template by real time PCR. RNA was extracted from the A498 cell line. The gradient of the line plotted between the Ct value and the log10 RNA concentration was calculated and the efficiency of the reaction was determined using the equation [(10(-1/slope) – 1) x 100]; a slope of -3.32 indicates an efficiency of 100% (https://www.thermofisher.com/uk/en/home/brands/thermo-scientific/molecular-biology/molecular-biology-learning-center/molecular-biology-resource-library/thermo-scientific-web-tools/qpcr-efficiency-calculator.html).

The amplification efficiencies for the TRPC 1, 4 and PPIA assays were determined to be 88%, 115% and 89% respectively (Figure 3.2). The optimal C_t value range for the Fluidigm Biomark PCR system is stated to be between 5.5 and 23 (personal correspondence from Fluidigm). The C_t value for TRPC4 at 0.25 ng was not detectable. For TRPC5, the C_t values were only detectable when large quantities of cDNA were used, however these loads produced C_t values that were outside the recommended range of the PCR equipment used (C_t value range 25-27). The Taqman® assays are marketed as being almost 100% efficient.

The amplification efficiencies demonstrated in this study are acceptable for TRPC1 and TRPC4, confirming their suitability for this study, and further to this, their similar efficiency to PPIA confirmed it as a suitable endogenous control for further work. The results for TRPC5 either suggest lack of TRPC5 in this cell line, or inefficiency of the TRPC5 assay, leaving concerns over its later interpretation. This same experiment was repeated using the UMRC2 RCC cell line with similar findings, including for TRPC5 (C_t value range 24-26).

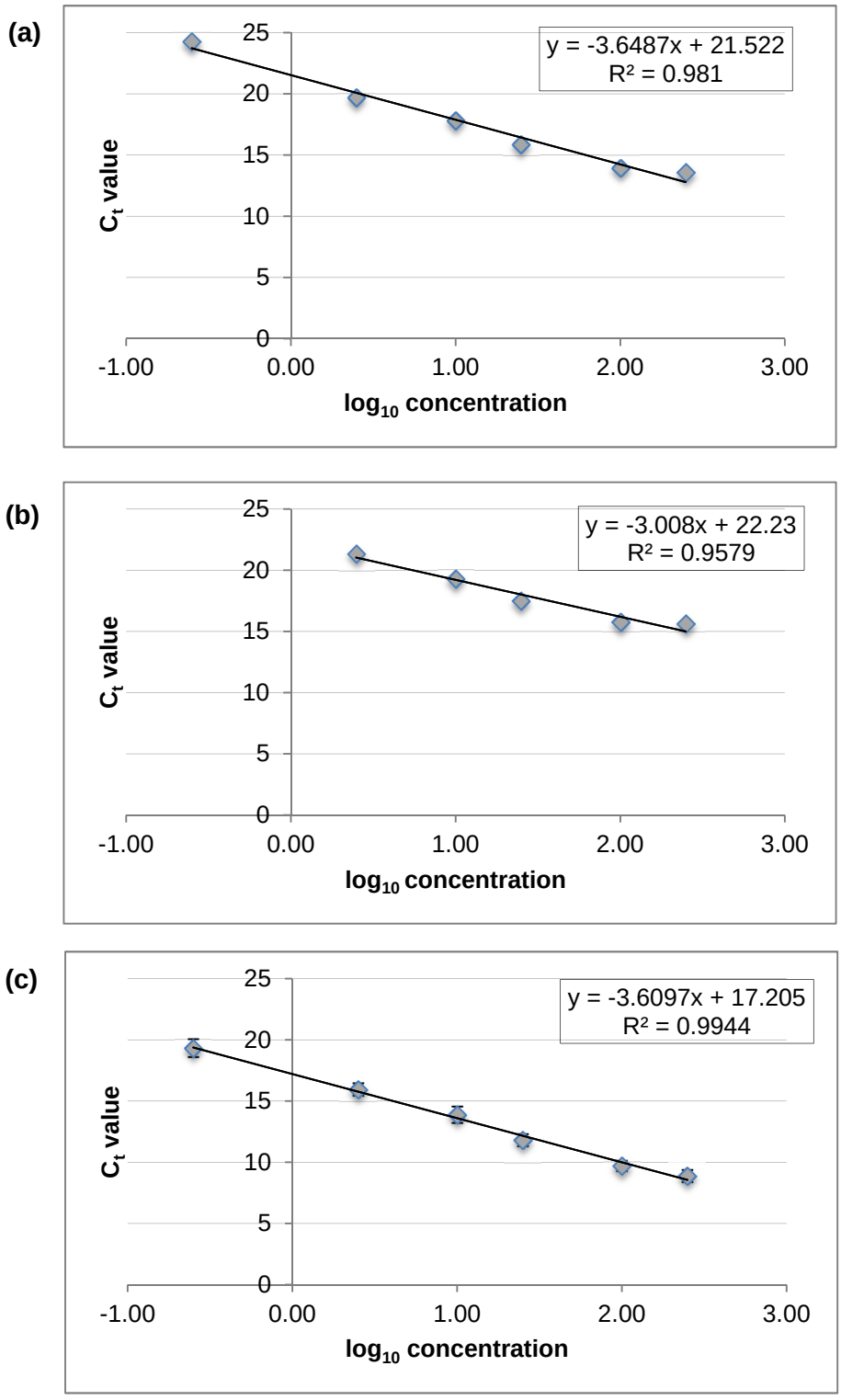

Figure 3.2 – Determination of the amplification efficiencies of the Taqman® Assays for (a) TRPC1 (b) TRPC4 (c) PPIA.
The C slope method, with minimum 5 concentrations (0.25-250 ng) covering a 4 log range, was utilised. The slope of each line and R^2 value was calculated for each assay as shown in the figure. The A498 cell line was chosen as a positive control across the real-time PCR analyses based on previous Western blot analyses. All samples were run in duplicate (error bars indicate SD).

3.2.1.3 TRPC 1, 4 and 5 gene expression in ccRCC

RNA yields from ccRCC samples, unlike normal kidney samples, were observed to be low despite strictly adhering to the manufacturers guidelines. This was felt to be related to a high lipid content interfering with the extraction and clean-up process. Despite this, the yields allowed PCR to be carried out on the Fluidigm Biomark PCR system (this includes a pre-amplification step).

Eight frozen ccRCC and matched normal kidney tissue samples were selected for investigation of TRPC 1, 4 and 5 gene expression using RT- PCR (Table 3.1).

Table 3.1 ccRCC samples used in this study to investigate TRPC 1, 4 and 5 expression.

The TNM 7th edition was used to stage these tumours.

Sample ID	Gender	Laterality	Other details	Max size mm	Grade	T	N	M	Stage	Microvascular Invasion	Necrosis
R344	F	L		39	2	1a	0	0	I	Not recorded	Not recorded
R377	F	L		65	4	3a	0	0	III	Y	Y
R389	F	R		82	4	3a	0	0	III	N	Y
R398	F	R	Rhabdoid Cells	88	4	3a	0	0	III	Y	Y
R404	F	L		105	4	3a	0	0	III	Y	N
R405	F	L		50	3	1b	0	0	I	N	N
R420	M	L	Focal sarcomatoid differentiation	80	4	3a	0	0	III	Not recorded	Y
R426	M	L		43	3	1b	0	0	I	N	N

The results demonstrate a statistically significant upregulation of TRPC1 in three of the eight RCC samples (R344, R389 and R420) compared with normal kidney. There was a statistically significant upregulation of TRPC4 in four of the eight ccRCC samples (R344, R404, R405 and R420) compared with their normal counterpart investigated in this experiment. Furthermore, there was a statistically significant downregulation of TRPC4 in two of the eight samples (R377 and R389) compared with their matched normal counterpart (Figure 3.3).

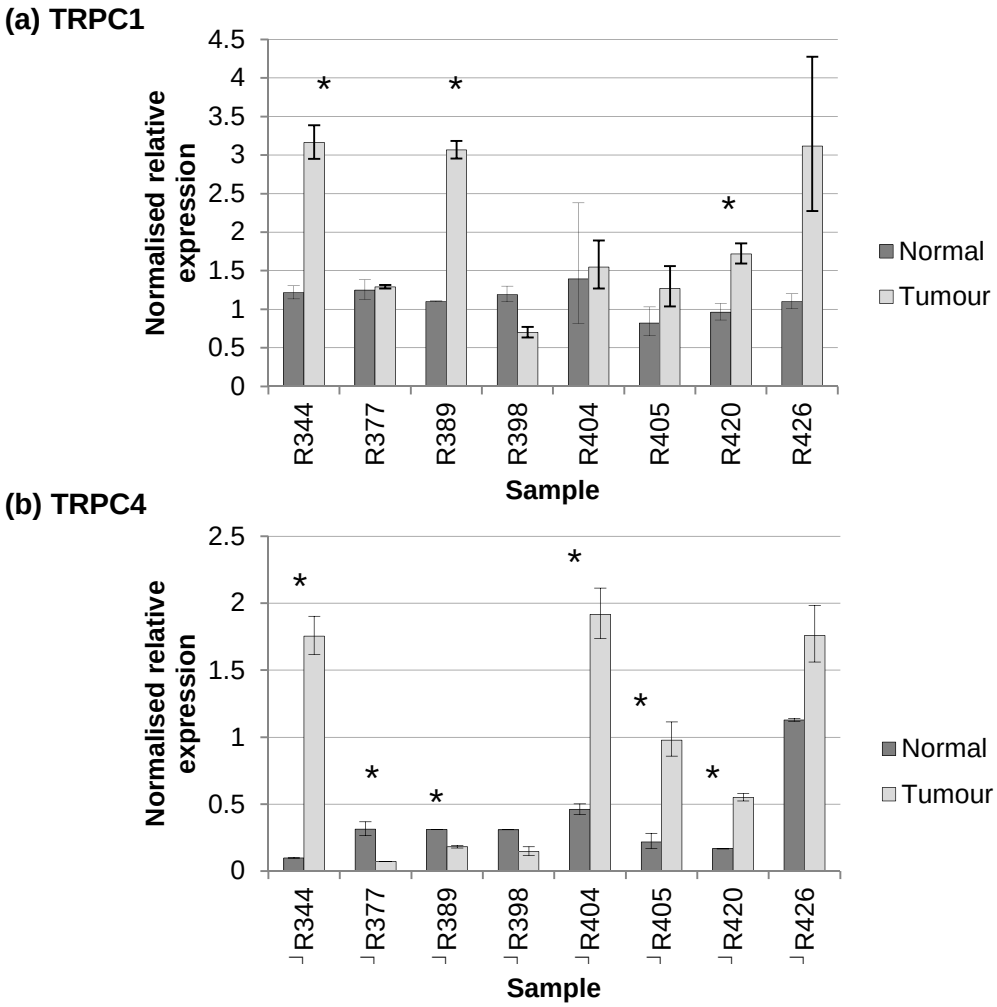

Figure 3.3 – (a) TRPC1 and (b) TRPC4 gene expression in primary ccRCC compared with paired normal kidney.
A statistically significant difference in expression between the normal kidney and ccRCC samples are indicated by * (*p*-value <0.05. Students T test). Each experimental sample was run in duplicate within each experiment (N=2). The error bars represent the standard deviation.

TRPC5 was only detected in one tumour sample (R405) (data not shown). All detectable C_t values except that of R344 Normal and R405 Normal for TRPC5

exceeded the recommended upper limit recommended for accurate interpretation using this PCR system. Given this and the previous inability to determine the amplification efficiencies, these results were deemed uninterpretable.

There were no obvious correlations discovered between the expression levels of each channel and known clinical and pathological characteristics of the tumours such as grade and stage. There was no statistical difference in TRPC1 expression between all normal kidney samples using one-way ANOVA.

To confirm the specificity of the Taqman® gene expression assays, the PCR products for the paired tissue sample R344 were further evaluated by DNA gel electrophoresis on a 2% agarose gel (Figure 3.4). A single band of the predicted length was observed for each gene of interest and the endogenous control PPIA. There were no bands in the negative control samples for each assay (not shown). This provided confidence in the gene expression assays and results obtained. Interestingly there was a single band seen for TRPC5 at the predicted length, suggesting that it did amplify, but at a value determined as uninterpretable by the qRT-PCR system used

3.2.2 TRPC 1, 4 and 5 protein expression in ccRCC

Seven ccRCC and matched normal kidney samples from the RTB were selected for investigation of TRPC1, TRPC4 and TRPC5 protein expression using Western blotting (WB), following optimisation of conditions and antibodies. A lack of reliable antibodies for Western blot analysis of the TRPC 1, 4 and 5 channels limited these studies, although primary tissue samples had not been previously investigated.

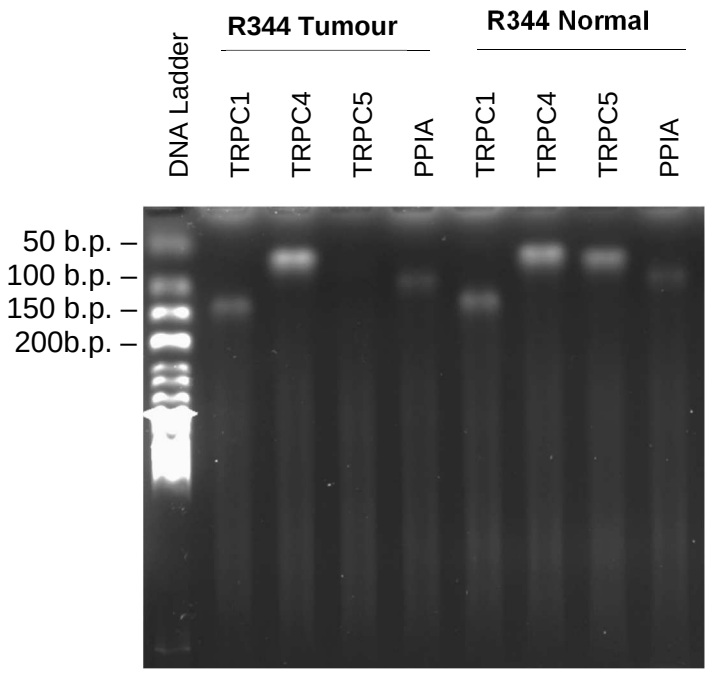

Figure 3.4 – Agarose gel electrophoresis to visualise the PCR products of TRPC1, TRPC4, TRPC5
The endogenous control PPIA is also included (sample R344 Normal and Tumour). The base pair size is expected at 137 b.p., 72 b.p., 75 b.p. and 97 b.p. for TRPC1, 4 5 and PPIA respectively. No bands were visualised for the negative controls for each Taqman® assay (not shown).

It is recognised that there are no consistent, reliable endogenous housekeeping protein for the confirmation of equal loading of polyacrylamide gels following electrophoresis when comparing across tumour and normal pairs. To confirm this two equally loaded gels, each with three paired ccRCC and normal kidney lysates and an RCC cell line were run in parallel. The first gel was blotted for β-actin and the second gel stained with Coomassie blue and densitometry readings were taken for each band. The ccRCC bands demonstrated upregulation of β-actin compared to their normal kidney counterpart consistently across the three paired samples despite the Coomassie stained gel suggesting equal loading (Figure 3.5). This is in keeping with findings previously reported by this group (Ferguson et al., 2005). Consequently, it was decided that equal loading would be confirmed through the use of Coomassie blue staining of an identically loaded parallel gel for each Western blot in this study.

(a)

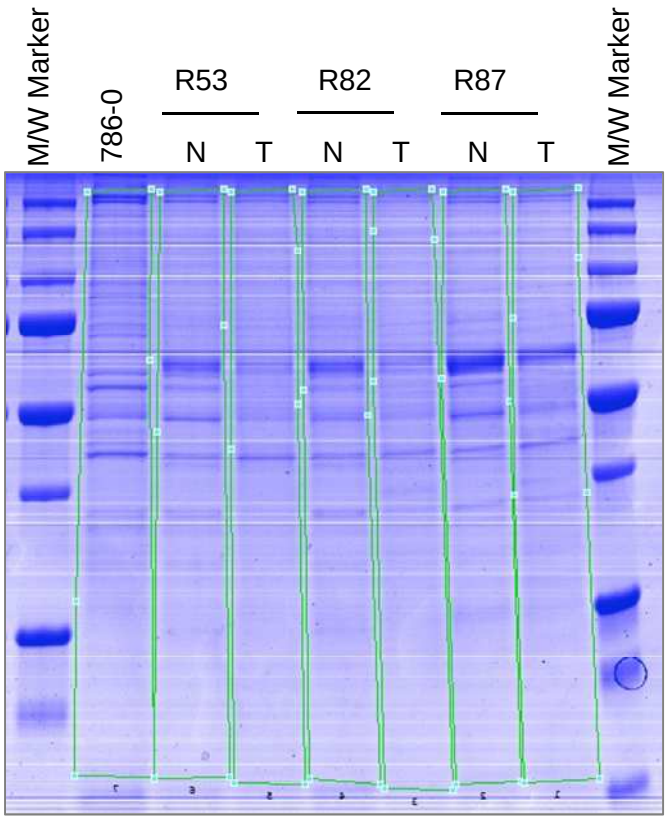

(b)

ample ID	Densitometry reading	Densitometry relative to 786-0
786-0	1983.9	1.0
53N	1355.36	0.7
53T	1649.2	0.8
82N	1349.76	0.7
82T	1675.79	0.8
87N	1546.59	0.8
87T	1541.58	0.8

(c)

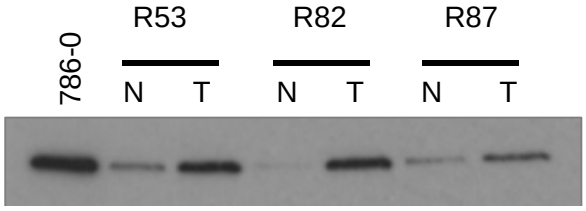

Figure 3.5 - β-actin was not a suitable loading control for Western blot analysis of RCC and paired normal samples.
(a) Coomassie blue staining of a gel loaded with three RCC (T) and normal kidney (N) samples as shown in the figure. (b) Densitometry readings for the gel shown in (a) with relative density to the RCC cell line. (c) Western blot of a parallel equally loaded gel for β-actin.

3.2.2.1 TRPC1

TRPC1 protein expression was investigated across a range of ccRCC and matched normal kidney samples and the established RCC cell lines 786-0 and A498. The two cell lines were included to allow a comparison with previously performed WB analyses using the same antibodies that were previously included in a Masters thesis, which demonstrated a band at approximately 100 kDa, with another fainter band at a lower weight (Figure 3.6). A major limitation of cutting the blot, especially when one molecular weight marker remains, includes the inability comment on lower weight bands and the inability to more accurately judge the relative size of neighbouring bands. The datasheet for the antibody demonstrated a Western blot of adult rat brain with a large smeared band between 98 and 64 kDa

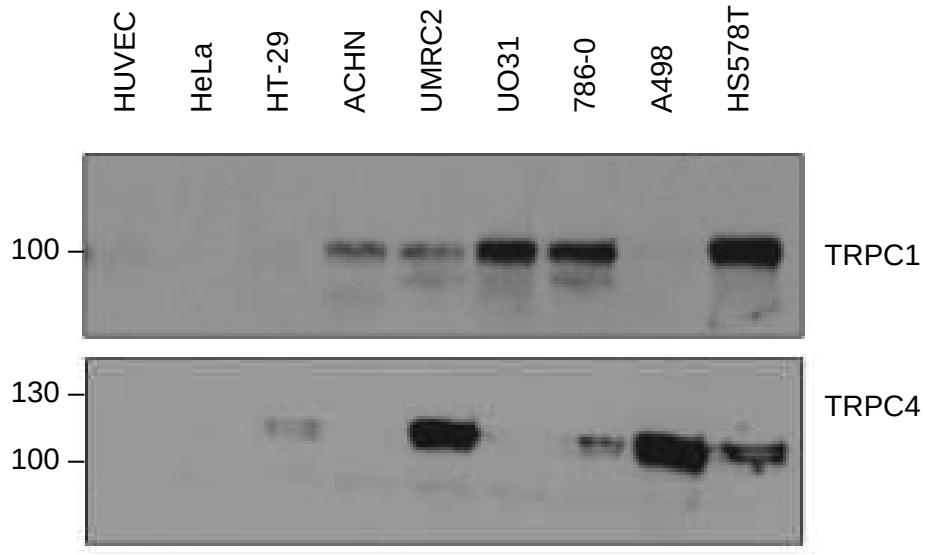

Figure 3.6 - Western blots analysing total TRPC1 and 4 protein expression in a range of cell lines.
Courtesy of Dr Melanie Ludlow. TRPC1 and TRPC4 protein expression patterns, using the antibodies utilised in this study, are shown across a range of cell lines.

TRPC1 protein has been identified to exist as two isoforms weighing 91 and 88 kDa produced by alternative splicing (www.uniprot.corg) (The UniProt Consortium, 2017). Western blot for TRPC1 that did not include a positive control cell line (Figure 3.7) revealed a band between 31 and 36.5 kDa, which was upregulated in all RCC

samples compared with the paired normal kidney counterpart. The molecular weight of this band did not correlate with any known isoforms of TRPC1. This may represent a protein that cross-reacts with the TRPC1 antibody or it may possibly represent a degradation product of TRPC1. To confirm this finding and to include a positive control cell line and expose the blot for longer, this WB was repeated. The dominant band again correlated with the previous blot but several other bands were present. Comparison with the blot shown in Figure 3.6 demonstrated a band at approximately 100 kDa with the same pattern of intensity in the A498 and 786-0 cell lines.

Immunoprecipitation was performed using this TRPC1 antibody in an attempt to resolve the identity of the protein(s) in the dominant band. The immunoprecipitate was analysed using mass spectrometry with Mouse IgG1 as a control antibody. A total of 555 proteins were identified (peptide count >/=2). Of these, 112 were not detected in the Mouse IgG1 control antibody. TRPC1 was not identified, nor were any proteins with any homology for TRPC1.Therefore the identity of this protein remains uncertain and since this was not a focus of this thesis, further work was not conducted.

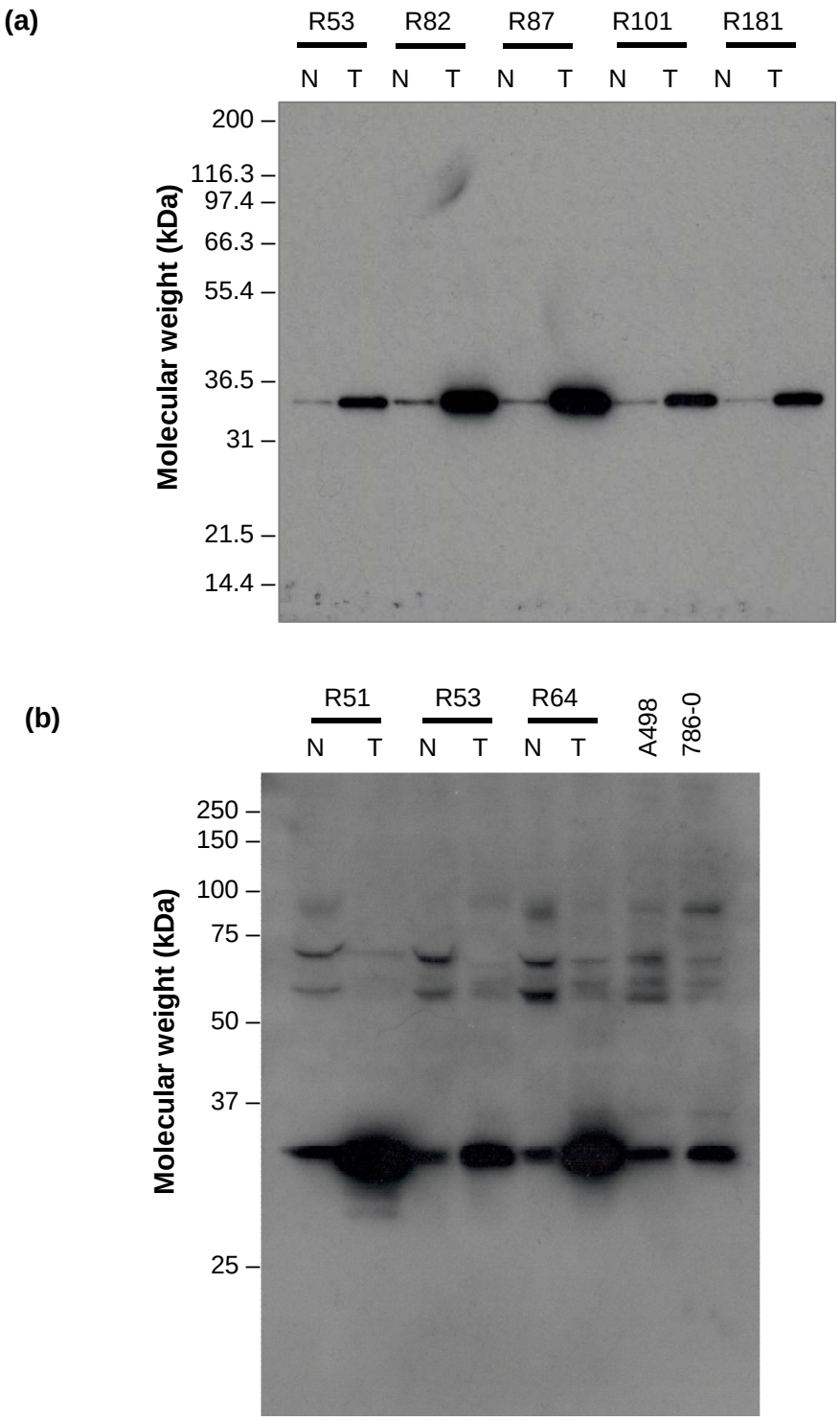

Figure 3.7 – Western blot analysis of TRPC1 protein expression in ccRCC.
(a) TRPC1 expression was explored across five ccRCC (T) and matched normal kidney (N) samples (b) a second gel of three paired samples and the RCC cell lines 786-0 and A498 was exposed for longer to look for background bands that may represent TRPC1 at the expected molecular weights. 30 μg of protein was loaded per well. Normalisation of loading was confirmed with densitometry readings of an equally loaded gel stained with Coomassie blue. No bands were seen with a no primary antibody control. The expected molecular weight for the TRPC1 isoforms are 91 and 88 kDa.

3.2.2.2 TRPC4

The expression of TRPC4 protein was next similarly investigated. There are a number of bands seen across the whole gel, with one band observed at approximately 100 kDa, and two bands between 50 kDa and 37 kDa (Figure 3.8). The band at 100 kDa was present in all samples, and possibly represents one of a number of TRPC4 isoforms (113, 112, 103, 96, 95, 92 kDa), however, no significant difference was seen between RCC and paired normal kidney samples. The higher of the two molecular weight bands, between 50 and 37 kDa were present in all samples including the cell lines and appeared to be slightly upregulated in each tumour sample compared with matched normal kidney sample. The lower molecular weight band between 50 and 37 kDa was present in all normal samples, however was only detected in one tumour sample (R53).

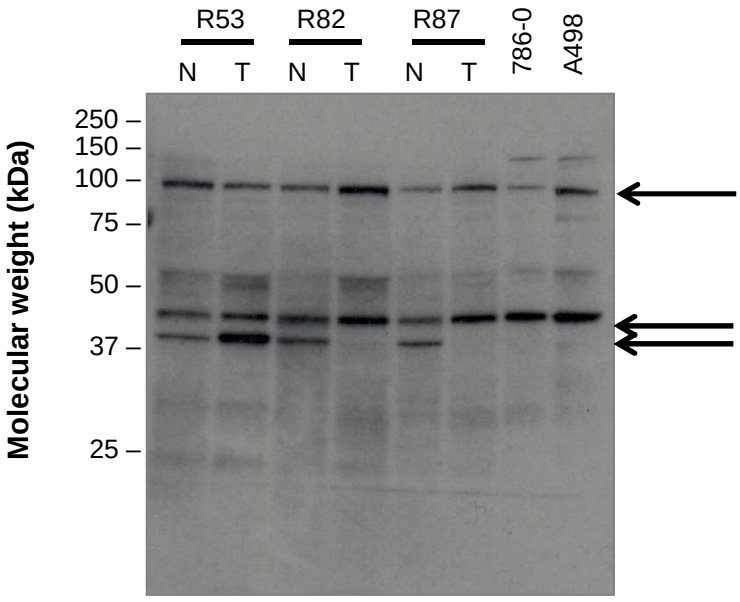

Figure 3.8 – Western blot analysis of TRPC4 protein expression in ccRCC. Western blot analysis for TRPC4 in three RCC samples, each with matched normal kidney samples, and the RCC cell lines 786-0 and A498 is shown. 30 μg of protein was loaded per well. A parallel gel was run and stained with Coomassie blue to confirm equal loading (not shown). No bands were seen with a no primary antibody control.

3.2.2.3 TRPC5

Western blot analysis was performed across a selection of RCC tumour and normal paired samples (not shown). A non-specific pattern of multiple bands was seen across the blot, with no bands at the expected molecular weight of 111 kDa.

The Western blot findings did not give confidence in the suitability of the antibodies to accurately identify the TRPC proteins investigated in this section of work. Whilst comparison with the Western blots shown in Figure 3.6 identified a similar pattern of band in the A498 and 786-0 cell lines, the blot had been cut, therefore further comment on the other bands are not possible. Further work into optimising the Western blotting using these antibodies was not successful and Western blot analysis using other antibodies had previously been undertaken by this lab, with no better antibody identified. For this reason, studies to confirm expression of the target in RCC tissues at the protein level were not taken forward.

Considering the striking results demonstrating the potent and selective nature of EA in killing RCC cells *in-vitro* (Ratnayake et al., 2009), the next section of work set out to confirm these results and explore the effect of EA on several non-cancer cell lines.

3.2.3 Exploration of the effects of Englerin A on various cell lines

The work to this point has established that TRPC1 and TRPC4 are expressed in ccRCC tissue at an mRNA level, but with no consistent pattern between tumour and matched normal samples. The A498 RCC cell line was chosen to begin this exploratory work. Alongside, HEK293 (derived from a human embryonic kidney) and HUVEC (derived from the endothelium of veins from the umbilical cord) cell lines were selected as non-RCC comparisons (Graham et al., 1977) (Jaffe et al., 1973).

3.2.3.1 A498 cell line

Englerin A (EA) has been shown to cause rapid RCC cell line death at nanomolar concentrations (Ratnayake et al., 2009, Sulzmaier et al., 2012). This was first confirmed in the A498 cell line. The optimal seeding density of each cell line used was first established, so as to reach 70-80% confluency at 30 hours to ensure the cells were in an exponential growth phase at the time of experimentation. In keeping with previously published work, cells were seeded and cell media containing englerin

A added 24 hours later. After 6 hours, cell viability was measured using the WST-1 cell viability assay (Figure 3.9). EA is shown to have a potent cell death effect in the A498 cell line. The EC50 (effective concentration of drug to cause half maximum response) was 60.2 nM.

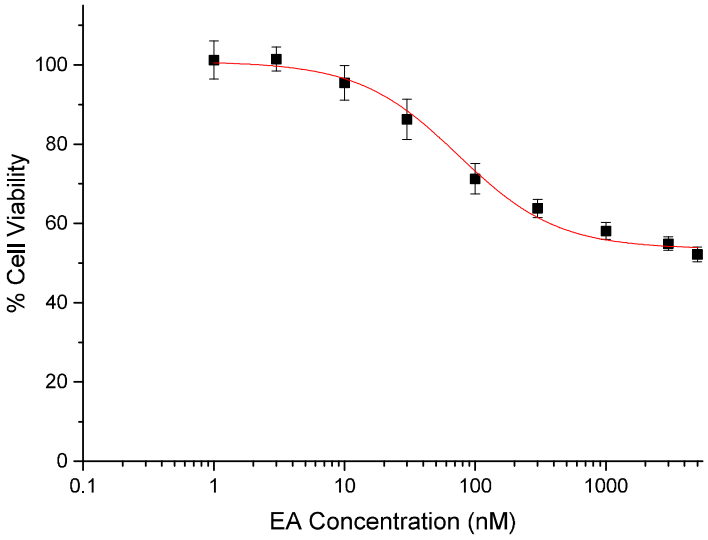

Figure 3.9 - EA reduced cell viability in the A498 RCC cell line.
A498 cells were exposed to EA at the respective concentrations for 6 hours. Cell viability was measured using the WST-1 assay. The measurement of the WST-1 absorbance is displayed as % cell viability where 100% cell viability indicates cells with the same metabolic activity as those in the untreated cells and 0% cell viability indicates cells with zero metabolic activity. The graph represents four experiments each with three replicates per condition. The error bars represent the standard error of the mean.

3.2.3.2 HEK293 cell line

The human embryonic kidney 293 (HEK293) cell line was chosen as a non-cancer cell line. The exact origin of this cell line is unclear, although it is known that it expresses the markers of renal progenitor cells, neuronal cells and adrenal gland cells (Stepanenko and Dmitrenko, 2015). The optimal seeding density was determined at 15,000 cells per well in a 96 well plate. After 24 hours, the cells were exposed to Englerin A for 6 hours and subsequent cell viability assessed using the WST-1 assay. No cell death was seen across a range of concentrations (1 nM to 5 μM) of EA in the HEK293 cells (Figure 3.10).

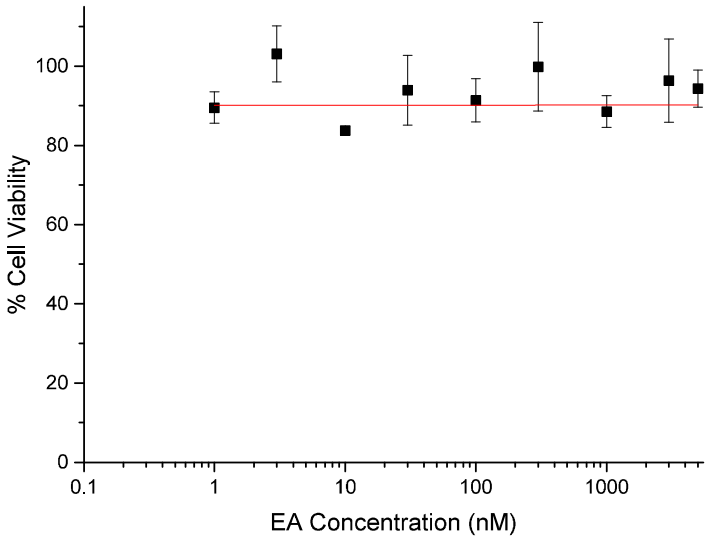

Figure 3.10 – EA does not reduce cell viability in the HEK293 cell line.
HEK293 cells were exposed to EA at the respective concentrations for 6 hours. Cell viability was measured using the WST-1 assay. The measurement of the WST-1 absorbance is displayed as % cell viability where 100% cell viability indicates cells with the same metabolic activity as those in the untreated cells and 0% cell viability indicates cells with zero metabolic activity. The graph represents two experiments, each with three replicates per condition (N=2). The error bars represent the standard error of the mean.

3.2.3.3 HUVEC cell line

The HUVEC (human umbilical vein endothelial cell line) was selected as a second cell line of a non-cancer origin. An optimal seeding density of 7,500 cells per well in a 96 well plate was determined. There was no cell death upon exposure to EA (1 nM to 5 μM), further demonstrating the apparent selectivity of EA for RCC (Figure 3.11).

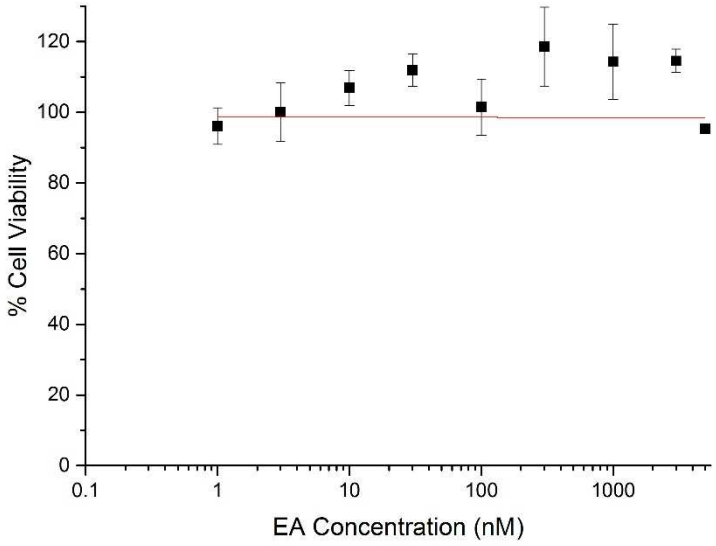

Figure 3.11 – Englerin A does not cause cell death in HUVEC cells.
EA did not cause any HUVEC cell death at a range of concentrations from 1 nM to 50 μM upon exposure for 6 hours. Cell viability was measured using the WST-1 assay. The measurement of the WST-1 absorbance is displayed as % cell viability where 100% cell viability indicates cells with the same metabolic activity as those in the negative control and 0% cell viability indicates cells with zero metabolic activity (equivalent to the absence of all cells). This graph is based on two experiments, each with three replicated per condition (N=2). The error bars represent the standard error of the mean.

3.2.3.4 Exploration of the effects of Englerin A on intracellular calcium

In keeping with the action of EA as an agonist of the non-selective cation permeable TRPC channels, the effect of EA on intracellular calcium was next explored. EA (1 μM) caused a rapid surge of calcium into the cell immediately upon exposure to EA (Figure 3.12).

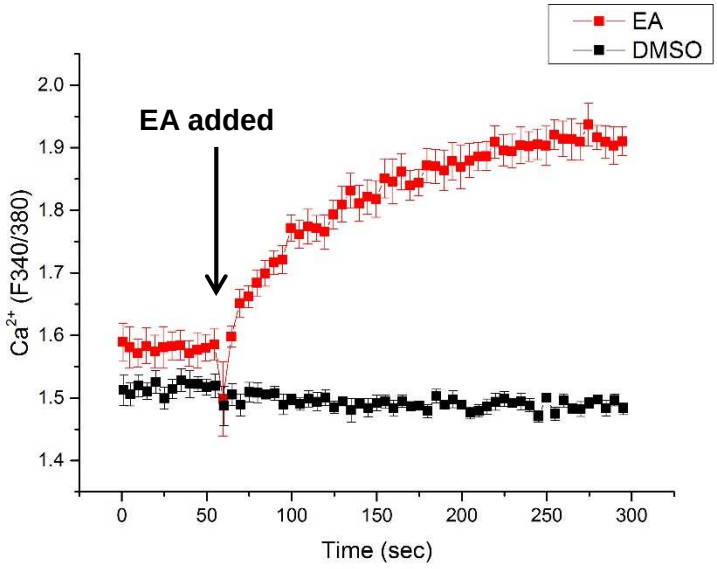

Figure 3.12 – Measurement of intracellular calcium changes upon exposure to EA.
EA (1 μM) was added to the A498 cells at the time point 60 seconds using the FlexStationII. Intracellular calcium was measured using the ratiometric calcium indicator dye, Fura-2. A surge of calcium is seen to enter the cell. The black line represents the DMSO negative control. There is no change in intracellular calcium in the vehicle control (DMSO). This graph represents one experiment with three replicates per condition (N=1) and is representative of the two independent repeats.

3.2.3.5 Investigation of the effect of the addition of the Na+/K+-ATPase inhibitor Ouabain to EA

Whilst this work was ongoing it was hypothesised that cytotoxicity was also the result of sodium influx (Ludlow et al., 2017). It was hypothesised that the sodium/potassium ATPase (Na^+/K^+-ATPase) pump was working to counteract the influx in sodium caused by EA, thus explaining the incomplete cell death (40%) even at the highest doses of EA. Ouabain, a Na^+/K^+-ATPase inhibitor, was demonstrated to increase the potency and cell death seen upon exposure to EA at a concentration that did not reduce cell viability on its own (10 nM). This finding was significant and warranted further investigation at this point as ouabain may work synergistically with EA in patients with RCC. In preparation for potential work using primary RCC cells, this finding was confirmed in A498 cells (Figure 3.13). Ouabain at 10 nM did not cause any cell death at 6 hours. EA (1 μM) induced approximately 40% cell death. The addition of ouabain (10nM) to EA (1 μM) enhanced the cell death effect to approximately 60%. There was no statistically significant difference in % cell viability

with the exposure to ouabain alone. The reduced cell viability seen with EA and ouabain and EA alone was statistically significant as shown in the figure.

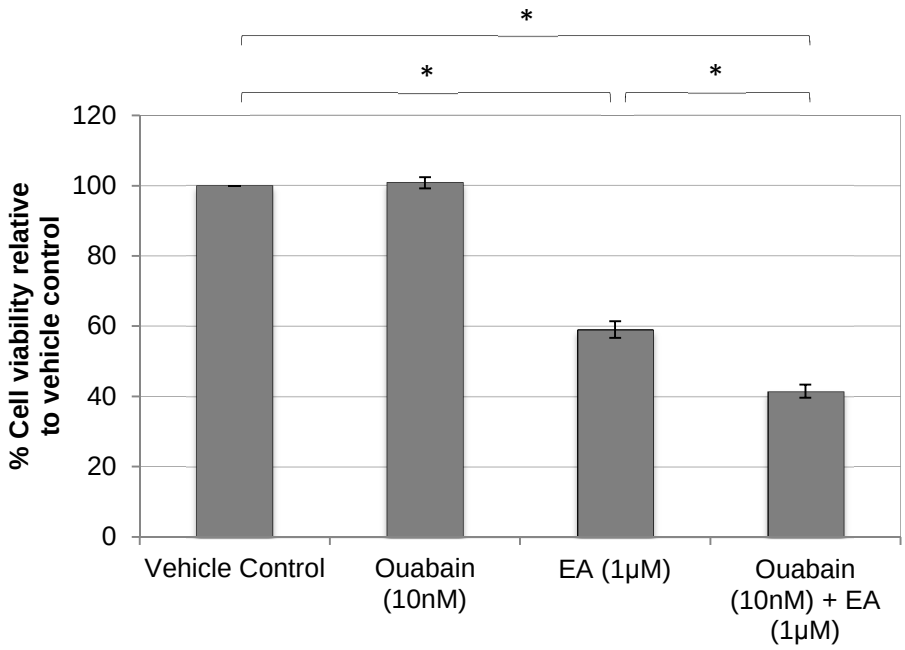

Figure 3.13 – Ouabain enhances EA induced cell death in the A498 RCC cell line.
A498 cells were exposed to 1 μM EA 6 hours. Cell viability was measured using the WST-1 assay. The measurement of the WST-1 absorbance is displayed as % cell viability where 100% cell viability indicates cells with the same metabolic activity as those in the untreated cells and 0% cell viability indicates cells with zero metabolic activity. The bars represent the standard error of the mean. Statistical analysis performed using a two-way ANOVA for multiple comparisons (* = p<0.00001). This figure represents 7 experiments each with 3 replicates per condition (N=7)

3.2.3.6 Exploration of the effect of EA on the growth of the A498 cell line

It was noted that EA did not cause 100% cell death in the A498 RCC cell line, even despite more prolonged exposure to the compound. To explore this further and to support the findings in Figure 3.13, the growth of the A498 cell line was investigated over a 72 hour period following addition of EA using the Incucyte ® system, which measures cell confluence at predetermined regular intervals over a 72 hour period.

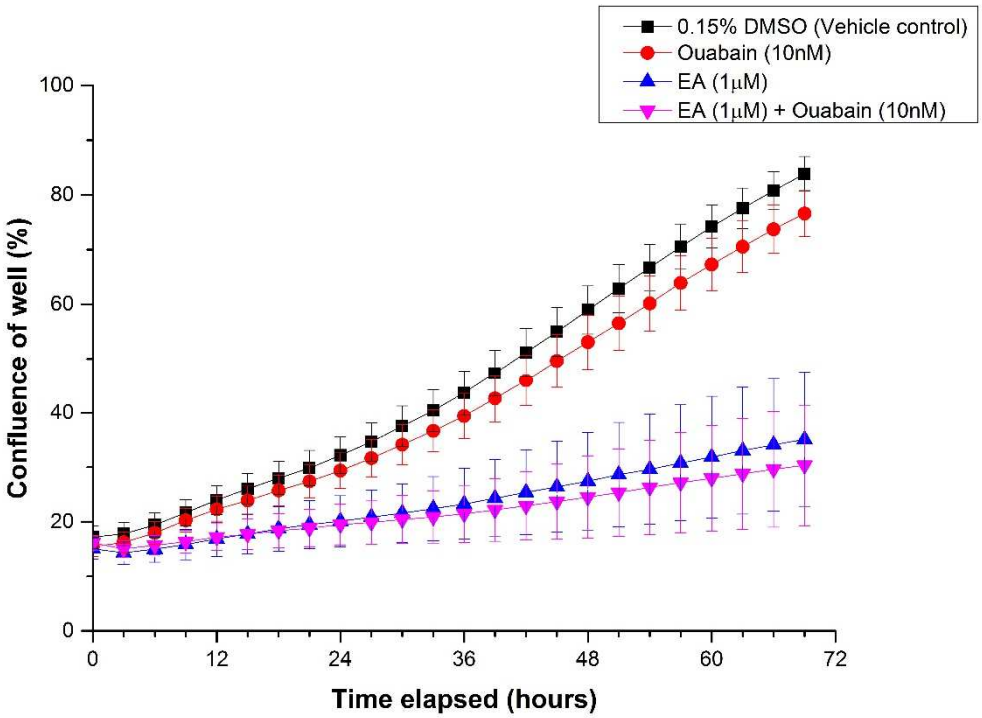

Figure 3.14 – EA reduced A498 RCC cell growth over a 72 hour period.
A498 cells were seeded onto 24 well plates to obtain a confluence of approximately 20% at 24 hours (10,000 cells per well). The cells were exposed to EA (1 μM) and Ouabain (10nM) as shown in the diagram and the confluence of the wells was recorded every 3 hours for 72 hours using the Incucyte ® system. This graph represents two experiments, each with two repeats (N=2).

EA was demonstrated to reduce the growth rate of the A498 cell line ($p<0.05$), although ouabain did not enhance this effect ($p=0.981$). There was no statistical difference between the cell growth rate of the vehicle control and 10 nM Ouabain ($p=0.950$) (Figure 3.14). In the same experiment, although not shown, the vehicle control (0.15% DMSO) had no effect on cell growth compared to growth media alone.

These results confirmed the potent and apparent highly selective nature of EA causing reduced cell viability of the A498 established RCC cell line but not the two non-cancer cell lines, HUVEC and HEK293. The activity of other alternative pharmacological TRPC agonists were next investigated.

3.2.4 Investigation of other pharmacological TRPC agonists

As previously discussed, the TRPC 1, 4 and 5 channels are known to be modulated by lead (Pb^{2+}) (Sukumar and Beech, 2010), lanthanum and gadolinium (Jung et al., 2003). These were not further explored here as they were not felt to represent viable future treatment options. This section of work introduces the concept of repurposing of drugs already licenced for other indications. The drugs rosiglitazone and riluzole, which are known to modulate the TRPC channels were further explored.

3.2.4.1 Rosiglitazone

The drug rosiglitazone is known to act as an agonist of the TRPC 1 and 5 channels. A498 cells were exposed to rosiglitazone at a number of concentrations up to 100 μM and cell viability was recorded at 6 hours. Unlike EA, significant cell death were not seen at low concentrations. The only statistically significant reduction in cell viability was observed at 100 μM (Figure 3.15).

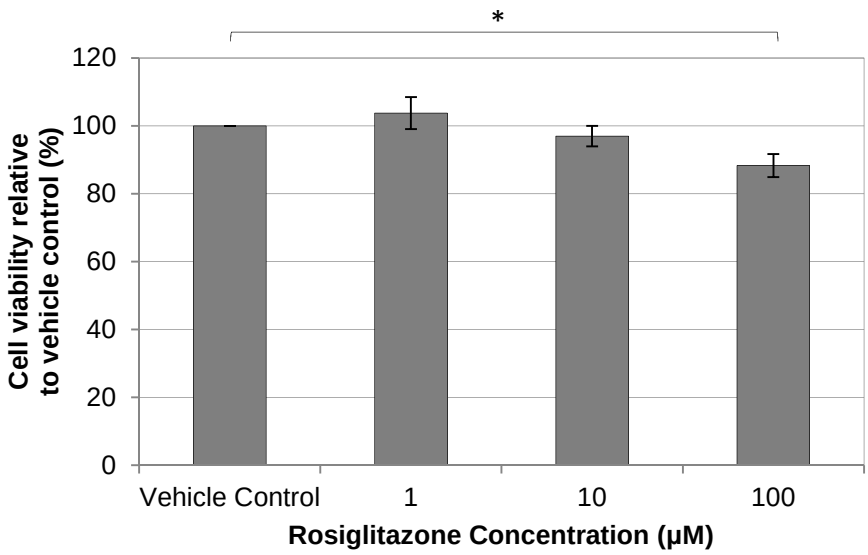

Figure 3.15 – Investigation of the effect of rosiglitazone on A498 cell viability. A498 cells were exposed to rosiglitazone for 6 hours. Cell viability was measured using the WST-1 assay. The measurement of the WST-1 absorbance is displayed as % cell viability where 100% cell viability indicates cells with the same metabolic activity as those in the no drug control and 0% cell viability indicates cells with zero metabolic activity. This graph is based on four separate experiments, each with three replicates per condition (N=4). The error bars represent the standard error of the mean. There was a statistically significant difference as indicated by * ($p = 0.009$)

3.2.4.2 Riluzole

Riluzole is also known to activate the TRPC 1 and 5 channels. A498 cells were exposed to riluzole at a range of concentrations up to 100 μM for 6 hours. There were no statistically significant reductions in cell viability observed (Figure 3.16).

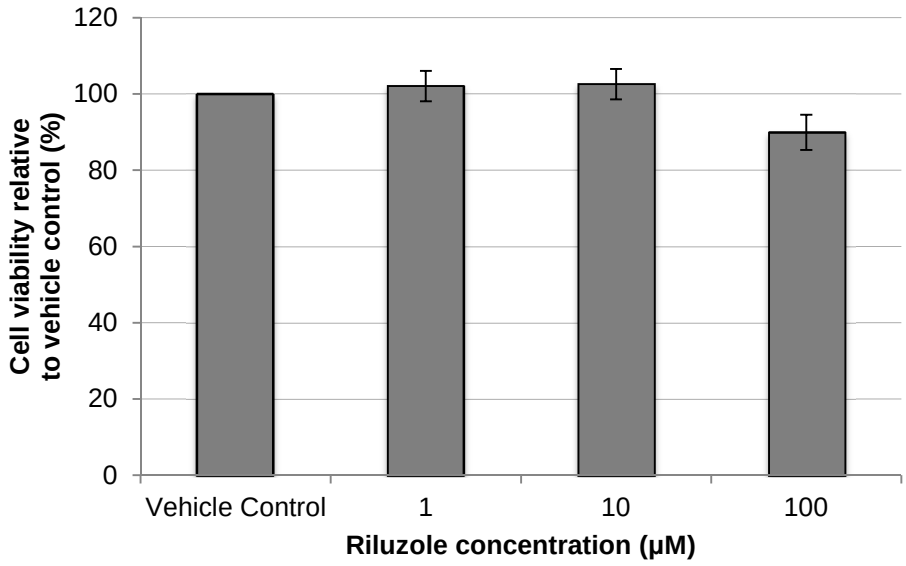

Figure 3.16– Investigation of the effect of riluzole on A498 cell viability
A498 cells were exposed to riluzole for 6 hours. Riluzole is known to activate the TRPC1 and 5 channels similar to EA. This graph is based on three experiments with three repeats each (N=3). The error bars represent the standard error of the mean. There was no statistical difference between each concentration of drug as analysed using ANOVA for paired samples.

3.2.5 Exploration of TRPC channel inhibition in RCC cell lines

The lack of highly selective and potent modulators of the TRPC channels has limited investigation of their biological function. During this work a highly potent and selective small molecule inhibitor of TRPC1, TRPC4 and TRPC5 was described by the David Beech group. This compound, named Pico145, was found to inhibit EA (10 nM) evoked calcium entry with an IC_{50} of 0.349nM for TRPC4, and 1.32nM for TRPC5 (Rubaiy et al., 2017b). Inhibition of the TRPC1, 4 and 5 channels has not been previously investigated in RCC. The effects of the inhibition of the TRPC channels were next investigated using Pico145 on the A498 cell line. Based on the previously determined IC_{50} values, three concentrations (1, 5 and 10 nM) of this compound were chosen for further investigation.

The growth patterns of the A498 RCC cell line were investigated using the Incucyte® system. This demonstrated no difference when the A498 cell line was exposed to the Pico145 compared to cell lines exposed to the vehicle control (0.15% DMSO) (Figure 3.17). Statistical analysis of the final time-point using a one way ANOVA for multiple group comparisons indicated there was no statistical difference between the conditions.

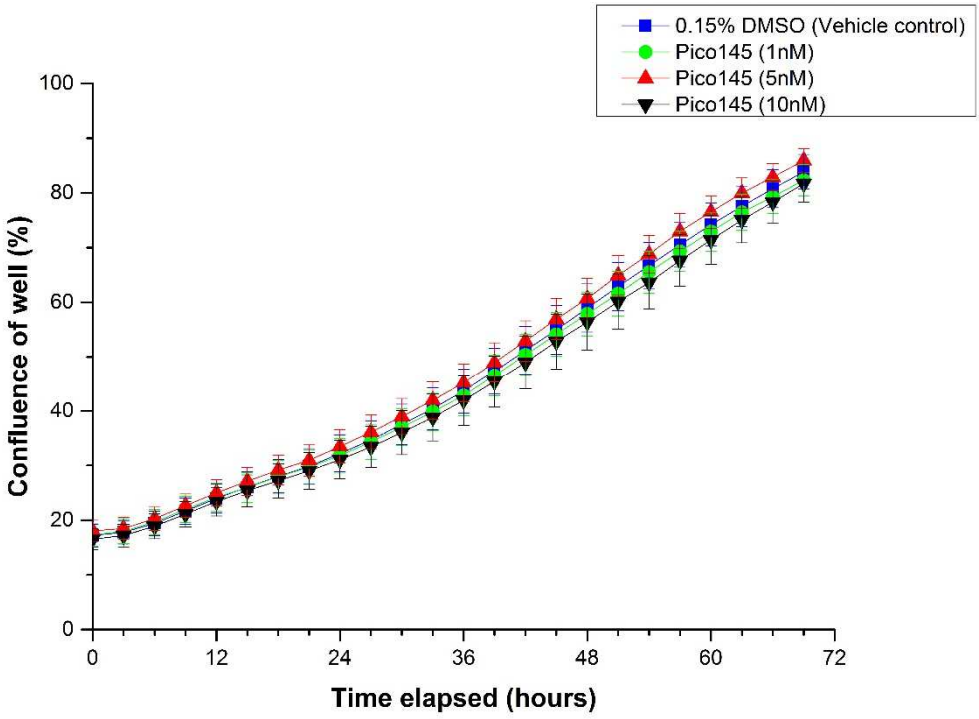

Figure 3.17 – Pico145 did not alter the growth rate of the A498 cell line.
A498 cells were seeded onto 24 well plates to obtain 20% confluence at 24 hours (10,000 cells per well). The selective TRPC 1, 4 and 5 inhibitor was applied to the cells and confluence was measured every 3 hours for 72 hours using the Incucyte ® equipment. There was no statistical difference identified between the groups at the last time-point using a one-way ANOVA (p=0.724). This graph represents two experiments, each with two replicates per condition (N=2). The error bars represent the standard error of the mean. A positive control (EA) was included in this experiment but not shown here.

The growth of the A498 RCC cell line was next investigated when exposed to EA in combination with Pico145.

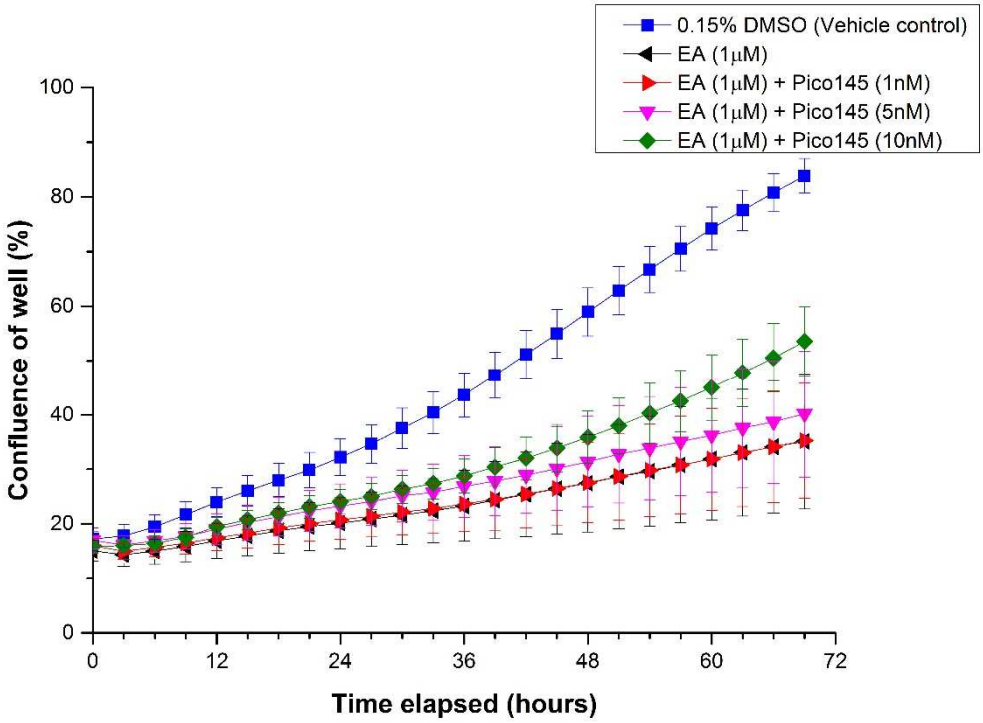

Figure 3.18 – Pico145 partially rescues the A498 RCC cell line from the effects of EA.
A498 cells were seeded into 24 well plates to obtain 20% confluence at 24 hours (10,000 cells per well) The cells were exposed to EA and Pico145 as indicated. Cell confluence was measured every 3 hours for 72 hours using the Incucyte ® equipment. This represents two experiments, each with 6 and 4 replicates per condition respectively (N=2). The error bars represent the standard error of the mean.

This experiment demonstrated that EA inhibited cell growth, which was statistically significant at the final time point (72 hours). Pico145 in combination with EA reduced the inhibition of cell growth at concentrations of 5 nM and 10 nM, but not at 1 nM (Figure 3.18).

This concluded the investigations into TRPC 1, 4 and 5 in RCC. The expression at an RNA level is variable and due to lack of suitable antibodies, expression at a protein level using Western blot is not possible. The potent and selective nature of action of EA has been confirmed and the inhibition of the TRPC channels does not cause RCC cell death.

3.3 Spleen Tyrosine Kinase (SYK)

SYK was chosen to investigate as a novel therapeutic target as it fulfilled the essential characteristics sought - SYK had proven function in the pathophysiology of a number of types of human cancer under physiological conditions, the differential expression of SYK had been highlighted at an mRNA level between RCC and matched normal tissue, and finally, SYK inhibitors were available and were being actively investigated in several clinical trials. Approval was being sought for a SYK inhibitor (fostamatinib) in idiopathic thrombocytopenic purpura in the UK (NICE guidance GID-TA10387).

This section of work set out to:

1) Examine the relative expression of the two isoforms of SYK in RCC versus normal kidney tissue at a protein level
2) Identify any representative ccRCC cell line models that may be utilised for further work
3) Explore the effect of small molecule inhibitors of SYK on RCC cell line models

3.3.1 Western blotting analysis of primary tissue samples for SYK

Initially the expression of SYK was investigated at a protein level in primary RCC and matched normal kidney tissue. The 786-0 RCC cell line was used as a positive control based on preliminary work (Karimzadeh et al., 2018). Following initial optimisation experiments (data not shown), four paired tissue samples were selected from the RTB and Western blot analysis was performed (Figure 3.19).

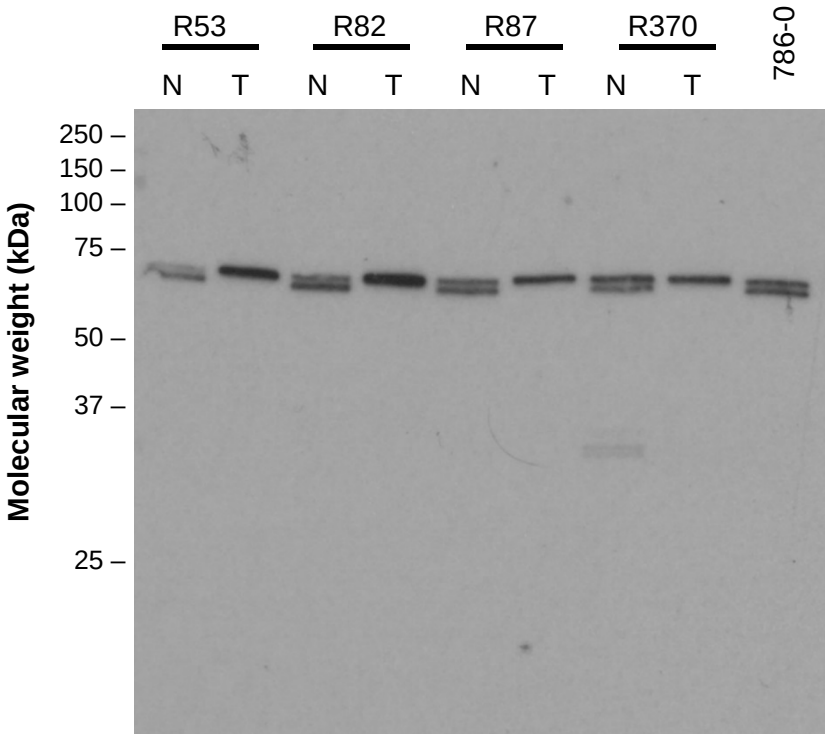

Figure 3.19 - Western blot analysis of paired tumour and normal tissue lysates probed for SYK.
Four paired ccRCC and adjacent normal kidney samples were blotted with the Santa Cruz anti-SYK (sc-1240) antibody. 5 μg of lysate was loaded per lane. The positive control is a 786-0 cell lysate. A parallel gel was stained with Coomassie blue stain to confirm equal loading. No bands were seen with a no primary antibody control.

Similar to the positive control, two bands were seen in the normal kidney samples. These bands were at a molecular weight consistent with the known SYK isoforms (72 and 70 kDa). Only the longer isoform, SYK(L), was present in the ccRCC samples consistent with the findings at the mRNA level. This pattern was also observed across all four paired samples.

3.3.2 SYK protein expression in RCC cell lines

The expression of SYK was next investigated across a range of RCC cell lines with the aim to identify a representative model. The 786-0 RCC cell line was again chosen as a positive control. There were two bands present, with a molecular weight consistent with both isoforms of SYK, in four of the twelve RCC cell lines (786-0, A498, HTB49, TK10). There were no bands observed across the other cell lines (Figure 3.20).

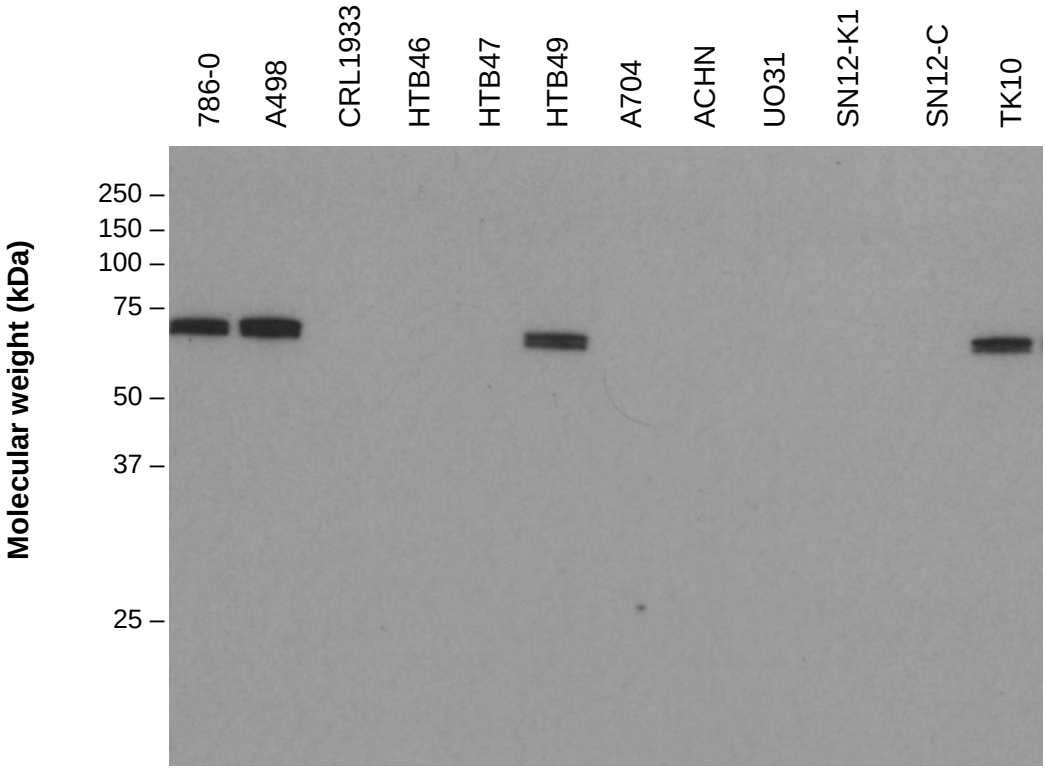

Figure 3.20 - Western blot analysis of a range of RCC cell line lysates for SYK. 20 µg of protein was loaded per well. A parallel gel was stained with Coomassie blue stain to confirm equal loading. No bands were seen with a no primary antibody control.

This demonstrated that, out of the 12 cell lines investigated, none of them were representative of the primary ccRCC tumours as shown in Figure 3.19. Thus, no available established cell line model was available for further investigation of the potential for SYK as a therapeutic target in RCC. On this basis it was decided that attempts to generate primary cultures derived from freshly excised renal tumours would be investigated to attempt to provide such a model.

3.3.3 Investigation of the effect of SYK inhibition on the 786-0 RCC cell line

Preliminary work undertaken by our collaborative group in McGill University, Canada, indicated that there was cell death when RCC cell lines (786-0, ACHN, UOK-171, HTB46 and HTB47) were exposed to the SYK inhibitor PRT062607 for 72 hours. The 786-0 RCC cell line was chosen for investigation of SYK inhibition using R406, the

active compound of the oral prodrug fostamatinib. Fostamatinib is currently awaiting review by the National Institute for Health and Care Excellence (NICE) for the management of immune thrombocytopenic purpura, and is therefore the most advanced of the SYK inhibitors in terms of licensing and approval within the UK. For this reason R406 was chosen for this work. Cell viability was measured using the WST-1 cell viability assay. An optimal seeding density of 2500 cells per well in a 96 well plate was determined to allow cell viability to be measured at 72 hours following exposure to R406. It was noted that the cell viability, was reduced (approx. 90%) at the lowest concentrations investigated compared with untreated cells, but further reduced above 0.1 μM of SYK inhibitor (Figure 3.21).

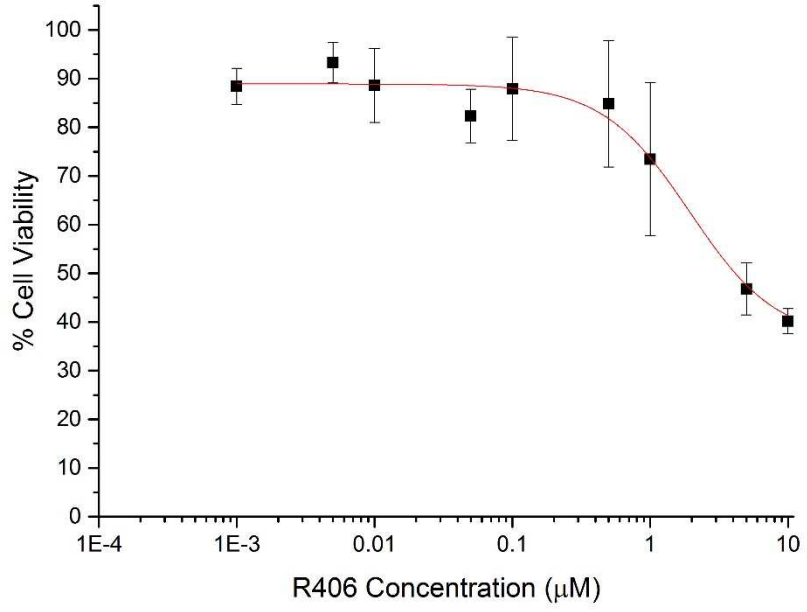

Figure 3.21 – Investigation of the effect of the SYK inhibitor, R406, on the 786-0 RCC cell line.

786-0 cells were exposed to R406 at the respective concentrations for 72 hours. Cell viability was measured using the WST-1 assay. The measurement of the WST-1 absorbance is displayed as % cell viability where 100% cell viability indicates cells with the same metabolic activity as those in the untreated cells and 0% cell viability indicates cells with zero metabolic activity. The graph represents three experiments, each with three replicates per condition (N=3). The error bars represent the standard error of the mean.

3.4 Generation of primary cultures

Established cell lines are commonly used in the laboratory. Whilst these have successfully been at the forefront of research, for example, in vaccine and antibody production, investigation of drug metabolism and effectiveness, novel therapeutic target discovery and study of gene function (Kaur and Dufour, 2012), they may not retain the exact characteristics of their ancestor cell (Pfaller and Gstraunthaler, 1998), thus raising the question of how representative they are of the primary cell of origin. In a study of genomic derangements in RCC which studied a panel of 21 RCC cell lines and 90 primary RCC tissue samples, it was noted that the RCC cell lines exhibited many more genomic derangements than the genome of the primary RCC samples (Beroukhim et al., 2009). Primary cell cultures have the theoretical advantage of providing a more representative experimental model (Perego et al., 2005) and in RCC and normal kidney, have been demonstrated to retain the proteomic profile and genomic alterations of their corresponding tissues in short term culture (less than three passages) (Perego et al., 2005) (Cifola et al., 2011). However, culture can be difficult to establish (Turin et al., 2014) and is associated with the problems of early senescence and cell contamination with other cells such as fibroblasts.

The aim of this section of work was to generate a method to establish primary RCC and normal kidney cultures to aid in the subsequent validation of the novel therapeutic targets investigated within this chapter. This area was felt to be particularly important to explore, especially given the lack of a representative cell line model for the validation of the novel therapeutic target, SYK. A plan for careful characterisation of these primary cultures was developed using immunohistochemistry and targeted genomic analysis, thereby providing confidence in their identity. The aim was to perform experiments at the second passage so as to retain as much of the original characteristics of the ancestor cell, and avoid dedifferentiation of the cells. A proportion of the cells would be cryopreserved after the first passage. The histopathological diagnosis (Table 3.3) was not known at the time of tissue culture but was later recorded.

3.5 Description of method utilised

As described in the materials and methods, tissue was routinely collected from consenting patients undergoing surgery for suspected RCC. Immediately following surgery samples of tumour and matched normal kidney measuring approximately 5 x 5 x 10 mm were obtained from the pathology specimen. These were transferred to the laboratory in ice cold RPMI 1640 for further processing.

The basic technique involved cutting the specimen into small pieces (<1 mm^3) using two scalpels and placing these on a culture plate with a minimal covering of growth media (RPMI 1640 supplemented with 10% foetal calf serum, 1% glutamine and 1% penicillin and streptomycin). Cell outgrowth was awaited. No cell growth was seen in the normal kidney explants and a fungal infection became a problem at day 5 in the tumour sample. There was concern that the samples were becoming necrotic during the time in the culture plate, therefore the method was changed to using tissue disaggregation.

Following receipt of the tissue in the laboratory, each tissue sample was cut up finely using two scalpels in a tissue culture hood. The connective tissue was digested using a mixture of 1 mg/ml type 1 collagenase and 1 mg/ml type 2 collagenase in phosphate buffered saline (PBS) supplemented with magnesium chloride and calcium chloride. Following incubation for 30 minutes in a water bath the solution was filtered through a 100 μm cell strainer and washed with growth media (DMEM/F12) containing foetal calf serum (FCS) to deactivate the collagenase. The solution was washed twice in Hanks Balanced Salt Solution (HBSS) and resuspended in 1 ml growth media (RPMI 1640 supplemented with 10% FCS, 1% glutamine and 1% penicillin and streptomycin. This solution was placed in a T25 culture flask and an additional 4 mls of growth media was added after 4 hours to allow for cell adherence.

Throughout this section of work, this tissue digestion technique was adapted to try to achieve cell growth (Table 3.2 and Table 3.3). A detailed literature review was undertaken and the various utilised techniques were taken into account. Overall, the steps could be grouped into three main stages, namely tissue collection, preparation and cell culture (Figure 3.23). This formed the basis of the variations made to the evolution of the methods used here (Table 3.1).

The problem of fungal infections was encountered in early attempts. This was likely related to contamination outside the operating theatre, in particular whilst dissecting the sample on the bench top in the pathology laboratory, which was unavoidable. The addition of anti-fungal treatment to the growth media was helpful and necessary in controlling this.

Normal primary kidney cultures were easier to grow (Figure 3.22), which is in agreement with the literature (Perego et al., 2005) and fibroblast outgrowth was not found to be a significant problem in the successful cultured samples, again in concordance with the literature (Perego et al., 2005). The normal kidney cells were observed to grow diffusely throughout the flask, whereas the RCC cells tended to grow in small clumps that eventually began to coalesce.

There was a greater success rate in terms of initiation of cell growth *in-vitro* and in sustaining this growth prior to first passage, with the commercially available Renal Epithelial Cell Medium 2. This was most likely as a result of various growth factors and supplements within this growth media including 5% foetal calf serum, epidermal growth factor (EGF), insulin, epinephrine, hydrocortisone, transferrin and tri-iodo-L-thyronine. Despite this, there were major difficulties in encouraging continued growth beyond the first passage, despite attempts at using various dissociation reagents and cell seeding densities.

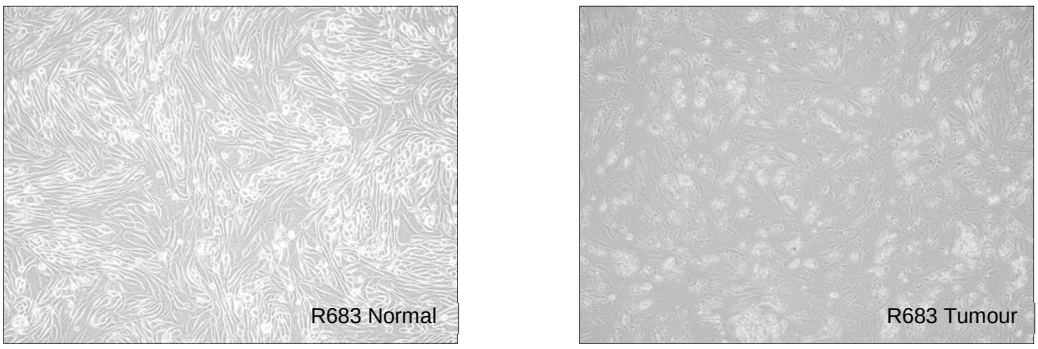

Figure 3.22 Light microscope images of sample number R683 normal kidney and RCC tumour primary cultures prior to the first passage.

In summary, successful culture of primary cells was not successful beyond the first passage despite the adaptations made throughout this work. For that reason, the pursuit of primary cultures was stopped at this point.

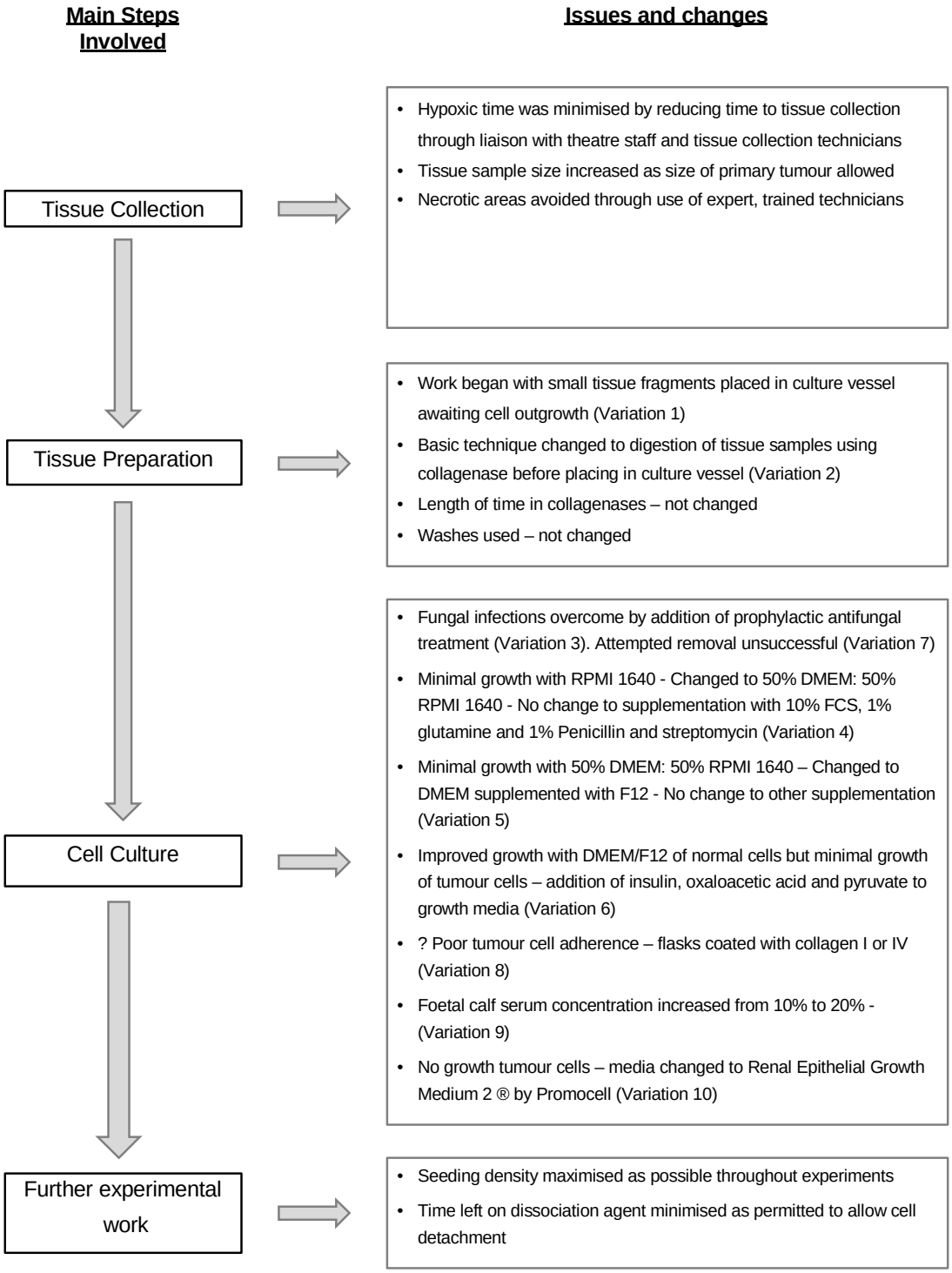

Figure 3.23 – Steps involved in the generation of primary RCC and normal kidney cultures.

Table 3.2 – Variations to the steps involved in the generation of primary RCC and normal kidney cultures.

This table details the variations explored to generate primary RCC and normal kidney cultures.

Variation Number	Notes
1	Basic method - In this method the tissue did not undergo disaggregation, instead, under the tissue was cut into small pieces and was placed in a culture flask containing RPMI 1640 supplemented with 10% foetal calf serum, 1% glutamine and 1% penicillin and streptomycin.
2	A tissue digestion step (disaggregation) using collagenase was introduced, followed by wash in HSBB and incubation in RPMI 1640 supplemented with 10% foetal calf serum, 1% glutamine and 1% penicillin and streptomycin.
3	(2) + addition of prophylactic anti-fungal treatment
4	(3) + change in growth media to 50% RPMI 1640: 50% DMEM supplemented with 10% foetal calf serum, 1% glutamine and 1% penicillin and streptomycin
5	(3) + change in growth medium to DMEM supplemented with Ham's F12 nutrient mixture, 10% foetal calf serum, 1% glutamine and 1% penicillin and streptomycin
6	(5) + addition of insulin, oxaloacetic acid and pyruvate to growth medium
7	(6) + removal prophylactic anti-fungal treatment from media
8	(5) + coating culture flasks with collagen I or IV
9	(5) + increase the FCS supplementation from 10% to 20%
10	(5) + change growth medium to Renal Epithelial Growth Medium 2 ® by PromoCell

Table 3.3 – Tissue samples processed to establish primary renal cell and normal kidney cultures.

The pathological characteristics of each sample along with the variation used (Table 3.2) and the outcome is detailed.

	Sample ID	Normal/ Tumour	Subtype	ISUP grade	T stage	Necrosis present	TNM Stage	Leibovich score	Growth in culture	No of passages reached	Variation	Notes
1	635N	Normal							NO	-	1	No growth
2	635T	Tumour	Clear cell	3	3b	N	III	5	NO	-	1	No growth. Fungal infection at day 5
3	638N	Normal							NO	-	2	No growth. Fungal infection at day 15
4	641N	Normal							YES	P1	3	
5	641T	Tumour	Papillary type 2	3	2b	Y	II		NO	-	3	No growth at day 20
6	644N	Normal							NO	-	3	Bacterial infection day 3
7	644T	Tumour	Oncocytoma	-	-	-		-	NO	-	3	No growth day 20
8	646N	Normal							NO	-	3	No growth day 20
9	646T	Tumour	Clear cell with rhabdoid change	4	3a	Y	III	9	NO	-	3	No growth day 20
10	648N	Normal							YES	P1	4	
11	648T	Tumour	Chromophobe		2a	N	II		NO	-	4	No growth day 20
12	649N	Normal							YES	P1	5	
13	649T	Tumour	Papillary type NOS	3	2a		II	5	YES	P1	5	

	Sample ID	Normal/ Tumour	Subtype	ISUP grade	T stage	Necrosis present	TNM Stage	Leibovich score	Growth in culture	No of passages reached	Variation	Notes
14	650N	Normal							YES	P1	5	
15	650T	Tumour	Clear cell	3	3a	N	III	5	YES	P1	5	
16	656N	Normal							NO	-	5	No growth at day 20
17	656T	Tumour	Clear cell	3	1b	Y	I	4	NO	-	5	No growth at day 20
18	657N	Normal							YES	P1	5	
19	657T	Tumour	Clear cell	3	3a	N	III	5	NO	-	5	No growth at day 20
20	658N	Normal							YES	P1	6	
21	658T	Tumour	TCC						NO	-	6	No growth at day 20
22	659N	Normal							NO	-	6	No growth at day 20
23	659T	Tumour	Clear cell	3	1b	N	I	3	NO	-	6	No growth at day 20
24	660N	Normal							NO	-	7	No growth at day 20
25	660T	Tumour	Clear cell	3	1a	N	I	1	NO	-	7	No growth at day 20
26	661N	Normal							NO	-	7	No growth at day 20
27	661T	Tumour	Papillary type NOS	3	1b	N	I	3	NO	-	7	Fungal infection at day 19
28	662N	Normal							NO	-	8	No growth at day 20
29	662T	Tumour	Clear cell	4	1a	N	I	3	NO	-	8	No growth at day 20
30	664N	Normal							YES	P1	8	
31	664T	Tumour	Chromophobe		1a	N	I		NO	-	8	No growth at day 20
32	665N	Normal							YES	P1	9	

	Sample ID	Normal/ Tumour	Subtype	ISUP grade	T stage	Necrosis present	TNM Stage	Leibovich score	Growth in culture	No of passages reached	Variation	Notes
33	665T	Tumour	Chromophobe		3a	N	III		NO	-	9	Fibroblastic like growth – did not grow on passage
34	666N	Normal							NO	-	9	No growth
35	666T	Tumour	Clear cell	3	3a	N	III	5	NO	-	9	Fibroblastic growth pattern – did not grow on passage
36	667N	Normal							YES	P1	8,9	
37	667T	Tumour	Oncocytic variant of papillary carcinoma with rhabdoid change	3	1a	Y	I		NO	-	8,9	Viable cells although no growth
38	669T	Tumour	Papillary type NOS	3	2b	Y	II		NO	-	8,9	No growth
39	670N	Normal							YES	P1	8,9	
40	670T	Tumour	Clear cell with rhabdoid change and suspicious for sarcomatoid	4	3a	Y	III	11	NO	-	8,9	No growth

	Sample ID	Normal/ Tumour	Subtype	ISUP grade	T stage	Necrosis present	TNM Stage	Leibovich score	Growth in culture	No of passages reached	Variation	Notes
41	671T	Tumour	Papillary type 2 (Metastasis)				IV		NO	-	9	No growth, cells initially looked viable
42	672N	Normal							YES	P1	10	
43	672T	Tumour	Clear cell with rhabdoid change	4	2a	Y	II	7	NO	-	10	Growth initially, although did not grow following passage
44	673N	Normal							YES	P1	10	
45	673T	Tumour	Clear cell	2	1a	N	I	0	NO	-	10	No growth
	675N	Normal							YES	P1	10	
46	675T	Tumour	Clear cell	2	1b		I	2	NO	-		Cells looked viable but did not grow
47	680T	Tumour	Papillary mixed type	3	3a	N	III		NO	-	10	No growth. Small tumour sample size
48	681N	Normal							YES	P1	10	
49	681T	Tumour	Clear cell with rhabdoid change	4	2b	Y	II	8	YES	P1	10	
50	682N	Normal							YES	P1	10	

	Sample ID	Normal/ Tumour	Subtype	ISUP grade	T stage	Necrosis present	TNM Stage	Leibovich score	Growth in culture	No of passages reached	Variation	Notes
51	682T	Tumour	Clear cell with rhabdoid and sarcomatoid change	4	3a	Y	III	9	YES	P1	10	
52	683N	Normal							YES	P1	10	
53	683T	Tumour	Clear cell	3	3a	Y	III	6	YES	P1	10	
54	684N	Normal							YES	P1	10	
55	684T	Tumour	Clear cell	3	1b	Y	I	4	YES	P1	10	

3.6 Discussion

The investigation of the role and function of the TRPC channel proteins has been slow, mostly hindered by the lack of potent and highly selective modulators. More recently the discovery of englerin A and the synthesis of Pico145 is allowing further analysis of the effect of the activation and inhibition of these channels both *in-vitro* and *in-vivo.* This work has contributed to the study of TRPC channel expression and *in-vitro* modulation in RCC. It has allowed the design of an *in-vitro* strategy and model to explore any further emerging targets throughout this thesis.

3.6.1 TRPC 1, 4 and 5 expression in RCC

This study has characterised TRPC 1, 4 and 5 expression in RCC, which had not been published elsewhere at that time. At an mRNA level, compared to the matched normal kidney samples, TRPC1 was observed to be upregulated in 37.5% (3/8) of the samples studied and TRPC4 was observed to be upregulated in 50% (4/8) of the samples studied. TRPC4 was also found to be down regulated in 25% (2/8) of the samples studied relative to normal kidney. This pattern of expression for TRPC1 and TRPC4 was not found to correlate with any of the clinic-pathological features of the tumours. The TRPC5 gene expression assay produced C_t values that were above the acceptable range for the qRT-PCR system used.

Since this work was completed, gene expression data for all the TRP genes, including TRPC 1, 4 and 5 has been published for 14 different types of human cancer from the International Cancer Genome Consortium data (Park et al., 2016). This included 496 RCC of the clear cell subtype with 72 matched normal kidney samples. The median RCC to normal kidney ratio for TRPC1, TRPC4 and TRPC5 were 1.318, 2.278 and 0.230 respectively (Park et al., 2016). If this same descriptive approach is applied to the samples investigated in this current study, the median RCC to normal kidney ratio for TRPC1 and TRPC4 is 1.668 and 2.431 respectively, which are comparable. These median values are of limited interpretability, instead identifying the number of samples with upregulation of the TRPC proteins would be more helpful. It does however indicate that overall the upregulation of TRPC1 and TRPC4, and the downregulation of TRPC5 in RCC predominates.

This contrasts with a study by Veliceasa *et al*. investigating the role of the angiogenesis inhibitor thrombospondin-1 (TSP1), in RCC. In this work TSP1 was found to be retained in the cytoplasm of the CRL1933 RCC cell line whereas it was secreted from the cell in the normal kidney cell line (HNK). It was hypothesised that this non-secretion was linked to impaired calcium uptake by the RCC cell. TRPC4 was found to be downregulated in the CRL1933 cell line using RT-PCR compared with the HNK kidney cell line (representing normal kidney). It was hypothesised that TRPC4 downregulation led to impaired calcium intake and thus the non-secretion of the angiogenesis inhibitor TSP-1(Veliceasa et al., 2007). Whilst this may be the case in the CRL1933 cell line, it highlights the problems in extrapolating results from small studies involving a single RCC cell line and the problems of using established RCC cell lines as representative models for RCC.

It is recognised that a weakness in this current study is the small number of samples investigated, and theoretically there may be differences in the cellular composition and variety within RCC samples compared to normal kidney samples, which may contribute to a dilution or concentrating effect on the protein of interest. It is necessary to identify a positive control for TRPC5 to complete its investigation.

Whilst protein translation is tightly regulated, mRNA and protein levels do not always correlate due to the multi-step processes of translation, post-translational modification and protein degradation (Vogel and Marcotte, 2012, de Sousa Abreu et al., 2009). For this reason the investigation of TRPC protein expression was attempted in parallel to the mRNA expression analysis. Western blot results for TRPC 1, 4 and 5 were disappointing. The identity of the striking band between 31 and 36.5 kDa that was upregulated in tumour samples when using the TRPC1 antibody was not resolved. Its presence in the RCC cell lines eliminates the likelihood that it represents a blood component. Although the datasheet for this antibody states it does not cross-react with TRPC4 based on knockout validation results, it also stated that its immunogen shared >50% homology with TRPC4 which was confirmed on analysis using the Uniprot Blast program (Figure 3.24). It is possible that the band observed represents the TRPC4 eta isoform, with a predicted molecular weight of 37 kDa, although long sequence homology was absent. Another possibility is that this represents a TRPC1 protein degradation product. The identity was not clarified by immunoprecipitating the protein using the TRPC1 antibody followed by analysis of the lysate using mass spectrometry. There has been debate in the literature

regarding the specificity of commercially available TRPC antibodies (Flockerzi et al., 2005) (Tajeddine et al., 2010). In addition much of the previously published work has investigated RNA expression, which likely reflects the lack of well-characterised antibodies.

Figure 3.24 – Screenshot of the Uniprot Blast analysis of the TRPC1 antibody immunogen.

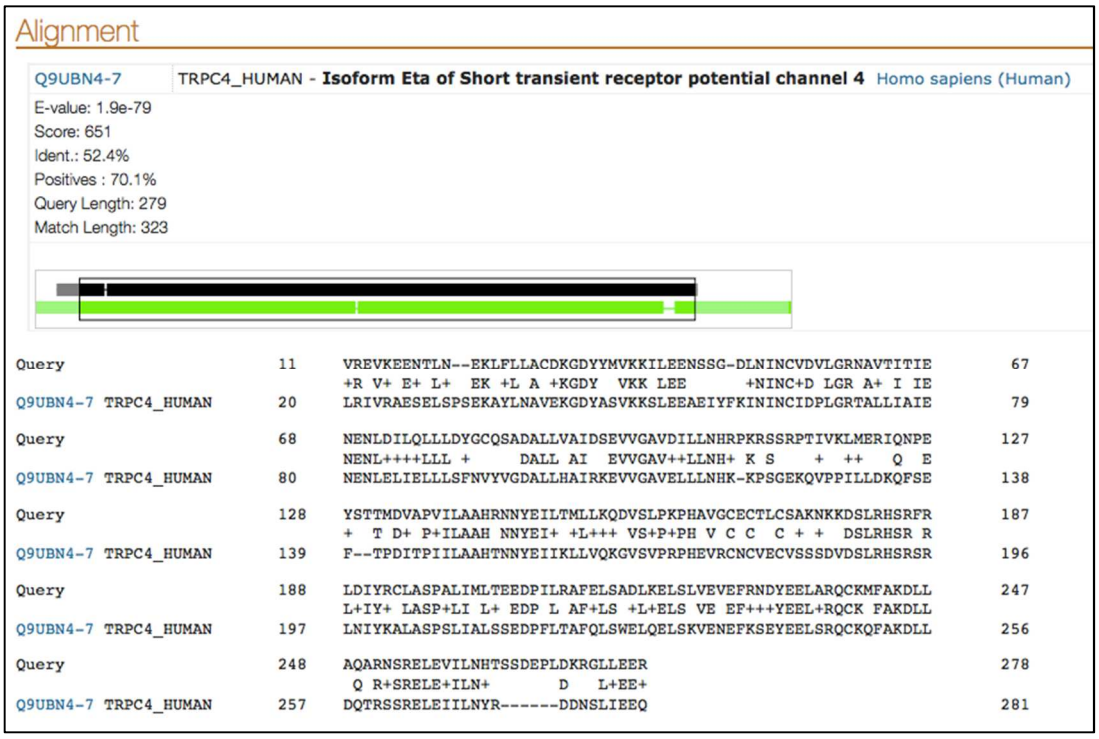

Another possibility is that the altered expression of the TRPC proteins observed in RCC represents their presence in endothelial cells. TRPC1 functions to maintain the barrier function of blood vessels (Abramowitz and Birnbaumer, 2009) and TRPC4 is involved in the regulation of endothelial cell function (Freichel et al., 2001). TRPC4 is upregulated in pulmonary artery endothelial cells in hypoxic conditions and may function mediate the downstream effects of cell proliferation and hypoxia induced changes (Fantozzi et al., 2003). RCC is characterised by its highly vascular nature, therefore this may be very relevant.

Overall in this study whilst expression of TRPC1 and TRPC4 has been confirmed at an mRNA level, the expression of TRPC 1, 4 and 5 could not be confirmed at a protein level. It is likely that the TRPC channels are present at a protein level given the mRNA findings and the rapid cell death seen using the highly specific compound

englerin A which is blocked with knockdown and enhanced with overexpression of the TRPC proteins in cell lines (Carson et al., 2015) (Akbulut et al., 2015). On the basis of this it was felt to be appropriate to continue the investigation of these channels in RCC.

3.6.1.1 Englerin A

The potency of EA on the A498 RCC cell line was reconfirmed in this study, with an EC_{50} determined to be 60 nM, which is comparable to the results preceding this work. Investigation of two other non-cancerous cell lines, namely HEK293 and HUVEC, supported this selectivity and sparing of normal, non-cancerous tissue. This was again supported in a recent extended screen published just after completion of this work (Carson et al., 2015). At the time of this work, other members of the group had hypothesised that cytotoxicity may be a result of the sodium influx upon opening of the TRPC channels. This was supported by the additional cell death observed upon concurrent exposure of the cell lines to EA and the sodium/potassium ATPase inhibitor, ouabain. Ouabain inhibited the corrective transfer of sodium back out of the cell (Ludlow et al., 2017). The additive effect on cell death was reconfirmed here. Ouabain is not licenced for use in the UK. It has a highly toxic profile but has been used to treat cardiac disorders in the past (Furstenwerth, 2010). This may warrant investigation in future work should EA or an effective, less toxic derivative be synthesised.

3.6.1.2 Rosiglitazone and Riluzole

The concept of repurposing of drugs has potential economic and time saving benefits (Ashburn and Thor, 2004). Rosiglitazone and riluzole were investigated as novel drugs for the treatment of RCC. The peak serum concentration of rosiglitazone if taken at a dose of 8 mg per day is 600ng/ml. This equates to a concentration of 1.68 μM (Day and Bailey, 2016).The mean peak serum concentration of riluzole has been determined to be 0.432 mg/l (Groeneveld et al., 2001). The concentrations of both rosiglitazone and riluzole used in this study ranged from 1 to 100 μM, thus should satisfactorily cover the therapeutic range *in-vivo.*

Approximately 10% cell death was observed when rosiglitazone was used at 100 μM. This concentration likely exceeds the maximum tolerated dose in humans. Riluzole did not cause cell death. The low or lack of expression of TRPC5 in ccRCC may

explain these results, as rosiglitazone and riluzole have been observed to activate the TRPC5 channels, (Majeed et al., 2011) (Richter et al., 2014). In this current study conclusions could not be made regarding TRPC5 expression in RCC, but it was suspected that the expression of TRPC5 was low in RCC. This was supported by the study conducted by Park *et al,* which indicated that TRPC5 is predominantly downregulated in RCC (Park et al., 2016). which may contribute to explaining the finding of the lack of effect with rosiglitazone and riluzole. These findings do not support further investigation of rosiglitazone or riluzole as novel therapeutic options in RCC.

3.6.1.3 TRPC channel inhibition

Whilst TRPC channels have been investigated in established RCC cell lines, all the studies to date have looked at activation of the TRPC 1, 4 and 5 channels. Given the availability of a potent TRPC channel inhibitor it was felt to be of interest to investigate the inhibition of these channels to identify if they may also have a growth inhibitory or cell death effect in RCC. This study has demonstrated that the highly potent and selective TRPC 1, 4 and 5 inhibitor, Pico 145, does not alter the growth rate of the A498 cell line at concentrations beyond the IC_{50} values described for inhibiting EA evoked calcium entry into the HEK293 cell line overexpressing TRPC4 and TRPC5 (Rubaiy et al., 2017b) (Rubaiy et al., 2017a). EA was used at a concentration of 10 nM, whereas for this experiement 1 μM EA was used. This IC_{50} may also not represent the IC_{50} for cell death. Whilst it appeared to inhibit the effect of EA on the growth of the A498 cell line, this did not reach statistical significance at 72 hours. This lack of significance may be a result of the small numbers of experiments. In support of this inhibitory action on EA, Pico 145 blocked the adverse reaction to EA in mice (Cheung et al., 2018). The lack of rescue from the effects of EA may indicate that Pico145 is required at higher concentrations of that EA is working through a different mechanism that inhibition of the TRPC channels cannot abrogate. There have been several studies suggesting EA acts through an increase in reactive oxygen species (Sulzmaier et al., 2012), inhibition of the PI3K/AKT (Sourbier et al., 2013) and ERK pathways (Williams et al., 2013), induction of a metabolic stress (Williams et al., 2013), through profound alteration of lipid metabolism and release of acute inflammatory mediators including interleukins, interferons and TNF (Batova et al., 2017), as a component of the response to hypoxia such as the activation of EGFR, and through hypoxia inducible factor-1α (HIF1α) dependent and independent mechanisms (Azimi et al., 2017). The findings in this current study are also based on

one established RCC cell line and may not be representative of primary RCC's. Further investigation is required to explore and fully understand these findings.

Overall, at this present time and with EA in its present form, inhibition of the TRPC 1, 4 and 5 channels does not appear to be a valid therapeutic target due to the on-target side effects affecting other tissues seen in mouse models, where EA caused reduced locomotor activity (Cheung et al., 2018) and death (Carson et al., 2015). Specific and essential to normal renal function, TRPC1 channels play a role in the regulation of glomerular filtration (Abramowitz and Birnbaumer, 2009) and are involved in the important contractile function of glomerular mesangial cells (Du et al., 2007). Beyond the kidney TRPC1 may be involved in lymphocyte activation and development, thus its modulation may seriously compromise the immune system (Mori et al., 2002). Given these, it may be difficult to target the TRPC channels without significant unwanted side effect, although it is recognised that the acceptable risk to benefit ratio of anti-cancer therapies does change depending on the predicted outcome from the cancer treatment.

3.6.2 Spleen Tyrosine Kinase (SYK)

This section of work has identified a differential expression of the SYK isoforms at a protein level in RCC. In primary RCC tissue the expression of SYK(S) was reduced to below the level of detection by Western blot analysis. In matched normal kidney samples there was expression of both isoforms. The differential isoform expression patterns seen in primary RCC and matched normal kidney tissue at a protein emphasised the findings at an mRNA level (Karimzadeh et al., 2018).

Care must be taken in the interpretation of SYK expression levels in tissue samples given that global SYK protein levels have been reported to be as much as six times as abundant in immune cells compared with epithelial cells (Blancato et al., 2014). Flanking sections of each tissue block were cut and examined following H&E staining at the same time as cutting tissue for experimental work to exclude samples with excessive infiltrating inflammatory cells, but it is still possible that these cells were present, which may generate a significant change in the SYK protein expression in these tissue samples. Primary tissue samples also consist of a mixture of other cell types, which may have varying SYK expression.

Whilst acknowledging the potential problems with using established RCC cell lines as accurate models for RCC, but balancing this with their availability, homogeneity and relative ease of growth, Western blot analysis of established RCC cell lines was performed across a panel of established RCC cell lines to find a representative model for further work with SYK inhibitors. In the 12 cell line models investigated, there were two bands observed, consistent with the two SYK isoforms, in only four of these cell lines (786-0, A498, HTB49 and TK10 cell lines). There were no bands detected in the other cell lines investigated (CRL1933, HTB46, HTB47, A704, ACHN, UO31, SN12-K1 and SN12-C). Thus, no cell lines were representative of primary ccRCC tissue samples, thus limiting further work using these cell lines. A possible approach for future work would be transfection of the isoforms into cell lines.

It is not known why the isoform expression is different in the established RCC cell lines examined. A possibility is that the small number of primary RCC and matched normal tissue samples examined in this study are not representative of RCC. It is also possible that alterations in SYK expression are generated with the in-vitro culture of established RCC cells. This theory is supported with the finding that epidermal growth factor (EGF) promotes SYK(L) expression in the SKOC3.ip1 ovarian cancer cell line Prinos et al. (2011). This highlights the limitations of working with established cell lines. This supports the attempts at generating primary RCC cultures in this study with the caveat that the media required to generate primary cultures will likely require supplementation. This may be minimised by performing experiments at an early passage.

The alternative splicing of gene products is a common occurrence within the human body (Wang et al., 2008), where it is estimated to occur in the transcription of up to 95% of multi-exon genes (Pan et al., 2008), and may contribute to cancer development and progression (Venables et al., 2009). The alternate splicing of SYK has been shown to be biologically relevant in a number of different malignancies. SYK(L) contains a 23 amino acid insert that is not present in SYK(S). This insert has been shown to have several functions. Firstly, it contains tyrosine 290, which has been shown to be a site of SYK autophosphorylation in vitro (Furlong et al., 1997). Autophosphorylation is important in allowing the recruitment of other cellular effectors, therefore it may lead to the activation of SYK(L). Evidence against this theory is that this area was not deemed critical to the function of SYK in RBL-2H3 (basophilic leukaemia cell line) or BI-141 (murine T-cell hybridoma cells) cell lines (Latour et al., 1998). Secondly, lack of the linker domain has been linked to the

inability to bind to ITAM's and thus unable to participate in immunoreceptor signalling (Latour et al., 1998). Finally the linker domain contains a nuclear translocation sequence in breast cancer (Wang et al., 2003) and hepatocellular carcinoma (HCC) (Hong et al., 2014), thus explaining the subcellular locations of SYK(L) and SYK(S). This may be very relevant in RCC as the SYK(L) isoform may have a dominant effect on nuclear effectors causing cell proliferation.

3.6.2.1 Other possible downstream effectors linked with SYK

SYK has been shown to interact with varying downstream effectors in different cell lines. The downstream effectors that are particularly relevant to RCC include the mitogen-activated protein kinase (MAPK) pathway (Wan et al., 1996), which is known to be upregulated in RCC and if suppressed may inhibit RCC growth (Huang et al., 2008). SYK has been identified as being important in activating the MAPK pathway in the chicken DT40 bursal lymphoma cell line. SYK is involved in activation of the PI3K-AKT signaling pathway as an oxidative stress response in B cells (Ding et al., 2000) (Pogue et al., 2000). This is also an important pathway in RCC (Guo et al., 2015a). SYK plays a central role in mTOR activation in follicular lymphoma cells where it has been shown to function through Pi3K-independent pathways. Pharmacological SYK inhibition resulted in downregulation of mTOR activity in follicular lymphoma, mantle cell lymphoma, Burkitt lymphoma, and diffuse large B cell lymphoma using cell lines (Leseux et al., 2006). Other downstream signaling pathways include the RAS-ERK pathway in HCC (Mocsai et al., 2010) (Hong et al., 2014). SYK was shown to act as a transcription repressor through down regulation of FRA1 and cyclin D1 ocogenes in MDA-MB-231 breast cancer cell line (Wang et al., 2005). Its role in vascular development as demonstrated in knock-out mouse models may indicate it has a role in angiogenesis which is important in RCC.

3.6.2.2 SYK inhibitors

Small molecule inhibitors of SYK are available. These are currently the focus of several phase I/II trials in various haematological malignancies with some clinical benefit demonstrated. These inhibitors are not isoform specific and their benefit in cancers with differentially expressed SYK isoforms is not known. The development of such inhibitors may be possible but would require preliminary work to determine the individual isoform-specific roles. R406 was chosen to investigate the effect of SYK inhibition on the 786-0 cell line. The peak serum concentration of R406 in

humans when given in doses of 80 – 600 mg as a single daily dose ranged from 501 – 3920 ng/ml, equating to 1.06 μM – 8.33 μM (Baluom et al., 2013). Cell death was seen at concentrations above 1 μM up to 10 μM in this experiment. One of the issues with the SYK inhibitors, like most tyrosine kinase inhibitors, is that R406 also inhibits other kinases such as Lck, Jak, Flt3 and adenosine A3, albeit at much lower potency, but still complicating the understanding of any findings (Braselmann et al., 2006).

In conclusion this work suggests SYK and the differential isoform expression may have a role in renal cell carcinoma. Work is somewhat limited by the lack of commercially available isoform specific SYK antibodies or inhibitors. There may be advances in this area in the future. SYK(L) may act as a tumour promoter where it interacts with downstream effectors in the cell nucleus. It clearly has an important function as it is the predominant isoform in human B cell lymphoid cells (Yagi et al., 1994) where its inhibition can be clinically beneficial. SYK(S) may have an inhibitory role, and its loss may allow the unopposed action of SYK(L).

The expression of SYK in RCC is similar to that in ovarian cancer, where SYK(L) knockdown reduced colony formation of the SLOV3 ovarian cancer cell line (Prinos et al., 2011). Silencing of SYK(L) has been shown to reduce colony formation and viability of the 786-0 and A498 RCC cell lines (Karimzadeh et al., 2018) thus proving a compelling indication to pursue further investigation of this protein as a novel therapeutic target in ccRCC. For the purposes of this section of work, a representative cell line model was required to pursue further investigation therefore work was ceased, awaiting attempts at primary RCC cell growth.

3.6.3 Generation of primary RCC and normal kidney cultures

The drug discovery pathway in oncology begins with the identification of dysregulated genes and/or proteins that may be involved in the uncontrolled growth of the cancer cell. Subsequent *in-vitro* validation of the findings are typically achieved through the use of established cancer cell lines. Their robustness, ease of growth, availability and avoidance of the ethical concerns with the use of human and animal tissue make them a popular alternative to using primary cells, although they may not always replicate their primary cell of origin due to the genetic manipulation required to induce immortality. In addition extended culture and passage can contribute to genetic drift and variation in cell phenotype (Kaur and Dufour, 2012). Primary RCC cultures at an

early passage on the other hand retain many of the phenotypic characteristics of the original tissue and therefore represent a more relevant model (Valente et al., 2011).

To complement the further investigation of the proteins discussed in this chapter and later in the thesis, attempts were made to developing a robust method for the generation of primary RCC cultures. Whilst disappointingly, this section of work did not prove to be successful, it provided insight into the difficulties and challenges encountered, and may be of benefit to others working in this area.

There are a number of papers detailing the establishment and growth of primary RCC and normal kidney cultures. The success rates of these papers varies from 13% (63/498 samples) (Ebert et al., 1990) to 100% (6/6 samples) (Valente et al., 2011). Whilst all the studies have similar sample preparation techniques, from tissue digestion followed by culture, higher success rates are noted to be observed in samples obtained from more advanced tumours or metastatic sites (Anglard et al., 1992). This study included one metastatic site but this was a papillary type tumour and was not successfully cultured. Cellular heterogeneity within the tissue samples is an important consideration. Whilst it would be unlikely to generate completely homogenous cultures by the third passage, characterisation of the cells grown was deemed to be a necessary step. In keeping with many of the published protocols a robust characterisation step involving a combination of genome wide copy number profiling, comparing both cultured cells and the corresponding tissue, and immunocytochemical characterisation to help determine cell origin was planned. Cytokeratin markers were mostly utilised along with carbonic anhydrase IX and vimentin (Cifola et al., 2011) (Kim et al., 2008).

The success rates in this study were low and continued culture *in-vitro* unsuccessful. The same techniques described in some of these papers were followed, but did not yield the same results described. Despite this, it was decided to investigate this area again due to the potential benefits of generating primary cultures and the lack of a representative cell line model for the investigation of SYK.

The pathological characteristics of the tumours were not known at the time of tumour resection and preparation for culture, as renal tumours are commonly diagnosed based on their appearances on imaging and not on a biopsy specimen.

Disappointingly, despite the time-consuming nature of this section of work, the difficulties in culturing primary cells were not overcome. This hindered further planned work on the modulation of TRPC channels and SYK.

3.6.4 Conclusion and future plans

In conclusion, the TRPC channels present an interesting target that inhibits the growth of RCC cell lines both *in-vitro* and *in-vivo*. The lack of antibodies to accurately detect the TRPC channels using Western blot somewhat hinders advancements in this area. The potent and specific action of englerin A within the NCI60 cell panel is remarkable. Despite this there are serious concerns raised regarding the TRPC 1, 4 and 5 channels representing novel therapeutic targets in RCC given the on-target toxicity profile related to their inhibition with Englerin A (Cheung et al., 2018). The TRPC channels also play important roles in normal kidney function, which may be unacceptable when suffering from renal cell carcinoma (Abramowitz and Birnbaumer, 2009) (Du et al., 2007). The future work into these channels would be helped through the development of specific TRPC channel antibodies and exploring ways of delivering this compound or derivatives to the renal cancer cell itself.

The alternative splicing of SYK in RCC compared to matched normal kidney was striking. This along with its position in the intracellular signalling system and its proven function in a number of other cancer types places it in an ideal position as a novel therapeutic target. This work was hindered by the lack of representative RCC cell line models, but despite this, R406, a SYK inhibitor, appeared to cause reduced cell viability between 1 and 10 μM, which was within the tolerated dose range in humans. The question whether this could be replicated in other RCC cell lines and primary RCC tumours was not investigated here. If establishment of cell line models including transfection of SYK isoforms is promising, later development of an isoform specific inhibitor for SYK(L) may be beneficial.

Disappointingly growth of primary ccRCC cell lines was difficult and did not provide primary cell lines for further exploration of the proposed novel therapeutic targets discussed in this chapter. Much of the intended experimental work was hindered as this was planned to be the main concluding section to this work, indeed some of the initial exploration was aimed at optimising the techniques and compounds for use on

the primary cell lines. Despite this, the efforts here will hopefully provide some insight into the difficulties, which may be of benefit to others working in this area.

Chapter 4 Novel therapeutic target discovery in ccRCC through an integrated proteomic and genomic strategy

4.1 Introduction and rationale behind this study

The molecular pathogenesis of sporadic clear cell renal cell carcinoma (ccRCC) is poorly understood despite being extensively characterised at the genetic, epigenetic and transcriptomic level in several studies (Cancer Genome Atlas Research, 2013) (Sato et al., 2013) (Guo et al., 2012) (Dalgliesh et al., 2010) (Pena-Llopis et al., 2012) (Scelo et al., 2014) (Brannon et al., 2010) (Varela et al., 2011). Along with the major finding of *VHL* tumour suppressor gene inactivation in as many as 75% of cases (Young et al., 2009), recurrent mutations in the three genes *PBRM1* (≈40%), *SETD2* (≈19%) and *BAP1* (≈15%) were also observed. To this date, these findings have largely been descriptive and have not generated any further changes in the clinical management and outcome of these patients. The presence of *PBRM1*, *SETD2* and *BAP1* mutations are associated with higher grade tumours and poorer patient survival (Kapur et al., 2013) (Pena-Llopis et al., 2012), therefore appear to have important clinical consequences, however, the drivers of this poor outcome at the protein level remain poorly defined, thus it is not clear how exactly they contribute to tumour biology (Vogelstein et al., 2013) (Pawlowski et al., 2013) (Liu et al., 2017) (Brugarolas, 2013) (Gossage et al., 2014). As discussed in the introduction chapter, a number of studies in other cancer types have recently attempted to address this deficiency in knowledge through the integration of both proteomic and genomic data from the same samples in large bioinformatic analyses (Zhang et al., 2014) (Mertins et al., 2016) (Zhang et al., 2016). Based on these studies, this section of work will adopt an integrative approach, which may have the potential to provide further knowledge into the functional effect of the recurrent mutations in *VHL*, *PBRM1*, *SETD2* and *BAP1*, leading to the identification of novel therapeutic targets in ccRCC.

4.2.1 Aims and hypotheses

The aim of this section of work was to undertake a detailed proteomic analysis of ccRCC tissue compared with normal kidney, selected on the basis of the underlying genomic changes. This data will be used to attempt to identify how these genomic changes contribute to ccRCC biology. A number of proteins will be taken forward for

further studies into their potential as novel therapeutic targets based on their expression patterns in ccRCC compared to normal kidney tissue.

4.3 Study design

The following details the study design adopted in the detailed planning and undertaking of this study, which is summarised in Figure 4.1.

4.3.1 Strategy overview

The main strategy was to identify a number of genetically annotated frozen ccRCC and normal kidney tissue blocks from the RTB with a plan to undertake a detailed proteomic study using mass spectrometry to identify differentially expressed proteins within the genetic groupings. The ccRCC and normal kidney samples would be matched whenever possible. This study was made possible through the group's involvement in the EU-funded Cancer Genomics of the Kidney (CAGEKID) project (Scelo et al., 2014), through which selected frozen ccRCC tissue had undergone whole genome sequencing. To be deemed suitable for inclusion into the study and taking into account potential heterogeneity between tissue blocks, it was planned that each tissue block underwent a histopathological review (as described in section 4.4.1.2) and the presence of the chosen genetic mutations confirmed (as described in section 4.4.1.1). The main proteomic analysis was planned to be undertaken using tandem mass spectrometry (MS/MS) in our laboratory. Alongside this, international collaboration with two other expert groups was planned, through which the same samples would be subject to SWATH-MS (Zurich, Switzerland), and antibody array analysis (DKFZ, Germany) to allow complementary analysis and independent confirmation of the findings. Following the analysis, interpretation of the proteomic data in the context of the mutational profile present would be undertaken in an integrated analysis with assistance from Dr Lara Feulner (visiting academic clinician). The latter two analyses will not be discussed in detail in this chapter, instead they will form an integral part of a larger bioinformatics analysis following the completion of this thesis.

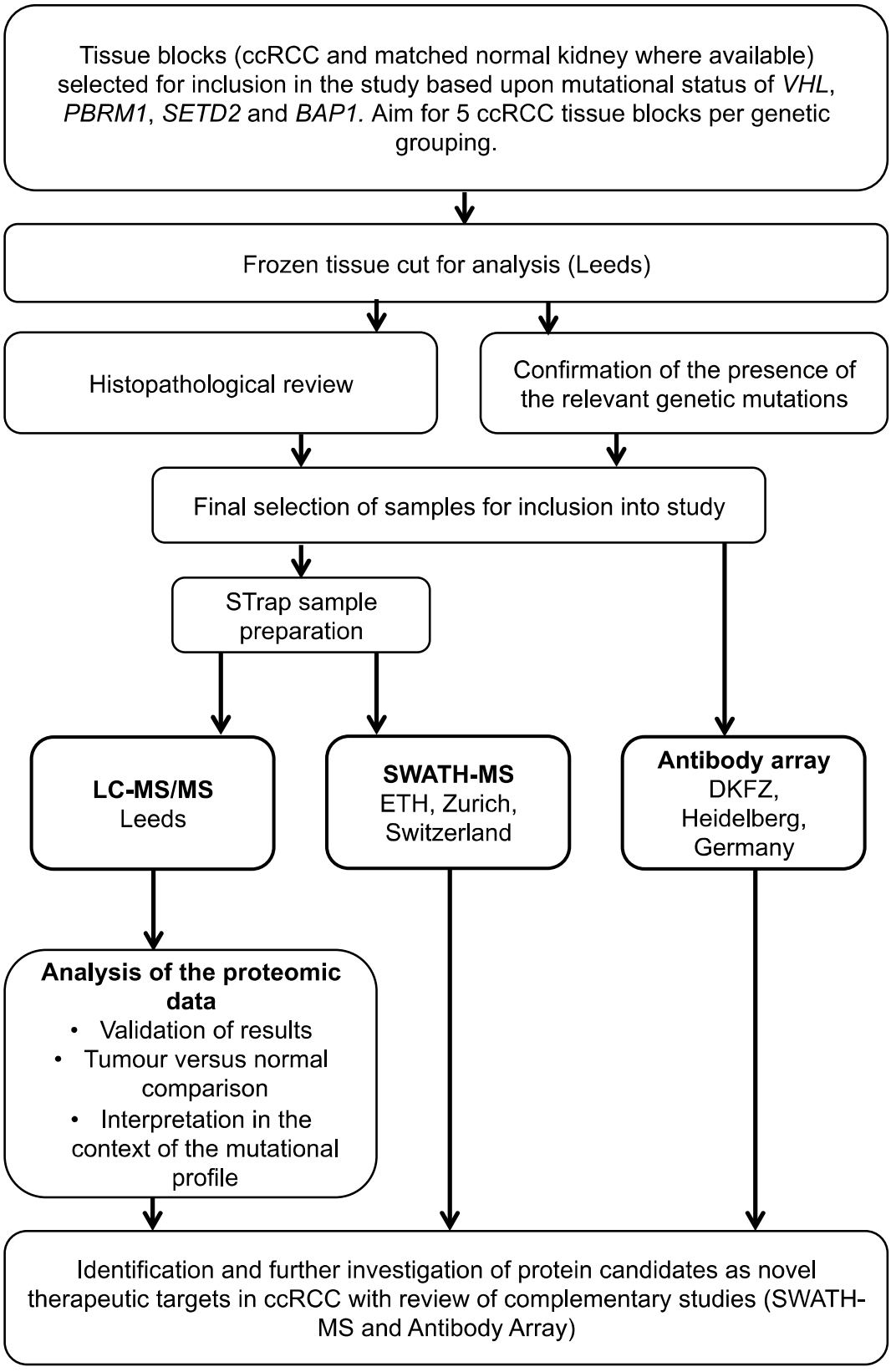

Figure 4.1 – Project Summary

4.3.2 Choice of genetic mutations

Genetically defined fresh-frozen tissue samples from surgically resected primary ccRCC and matched normal renal tissue were selected for inclusion based on the mutational profile present. Careful consideration was given to the choice of genetic mutations to be represented within this study, particularly given the relatively small numbers of samples. This included taking into account the published evidence behind the consequence of a mutation of that particular gene, the type of mutation, the expected frequency of the genetic mutation and the availability of tissue blocks. Missense mutations were excluded on the basis that they are more likely to result in a normally functioning or partly functional protein, unlike the other mutation types. Samples with *VHL* inactivation due to hypermethylation of one or both alleles were also excluded. Based on this, samples with the four most common genetic mutations in ccRCC were selected (Table 4.1).

Table 4.1 – Genetically annotated groups chosen for further analysis.

The following genetically annotated groups were chosen for proteomic analysis within this study.

Genetic grouping (based on four 'driver' mutations	*VHL*	*PBRM1*	*SETD2*	*BAP1*
***VHL* mutation only**	**Present**	**Absent**	**Absent**	**Absent**
***VHL* + *PBRM1* mutation**	**Present**	**Present**	**Absent**	**Absent**
***VHL* + *SETD2* mutation**	**Present**	**Absent**	**Present**	**Absent**
***VHL* + *BAP1* mutation**	**Present**	**Absent**	**Absent**	**Present**
***VHL, PBRM1, SETD2* and *BAP1* wild-type (no mutation)**	**Absent**	**Absent**	**Absent**	**Absent**
***PBRM1* mutation only**	**Absent**	**Present**	**Absent**	**Absent**

4.3.3 Numbers of samples

A target of 5 representative ccRCC tissue samples were planned per genetic group. Initially a larger number of patients would be selected for inclusion in the study, as it was anticipated that a number of tissue samples would be excluded due to inadequate quality upon histopathological review or may not have the chosen genetic

mutation in the available blocks. These tissue blocks were from the Leeds Multidisciplinary RTB and the International Agency for Research on Cancer (IARC), Lyon, France. All samples included in the CAGEKID study were subject to uniform standard operating procedures (SOPs) for handling and storage. A number of matched normal kidney samples were planned for inclusion (target of 50% of ccRCC samples) to allow a normal to tumour comparison to be made in the later analysis.

4.3.4 Sample preparation and processing

4.3.4.1 Sample cutting sequence

Careful consideration was given to the cutting sequence for each tissue block to ensure that each Eppendorf contained a representative quantity of tissue from the whole tissue sample, thus limiting the impact of intratumoural heterogeneity (Figure 4.2). A plan was made for two 5μm thick flanking and middle sections for histopathological review (as described in section 4.4.1.2). Sections were cut for DNA extraction for genetic mutation confirmation and for protein extraction for analysis using LC-MS/MS, SWATH-MS, and antibody array analysis. A sample of each tissue block was also collected for a parallel independent study that enriched for surface membrane proteins through a modified tissue lysis protocol followed by analysis using LC-MS/MS. Whilst this study is not discussed any further here, it was aimed that the results would be later reviewed to complement the results from this analysis. Provisional experiments determined the protein yield for samples cut with a surface area of $3cm^2$ x 10μm thick equivalent to be on average, 1000μg (range 250-2500μg). This helped determine the quantity of tissue needed to be cut for this experiment.

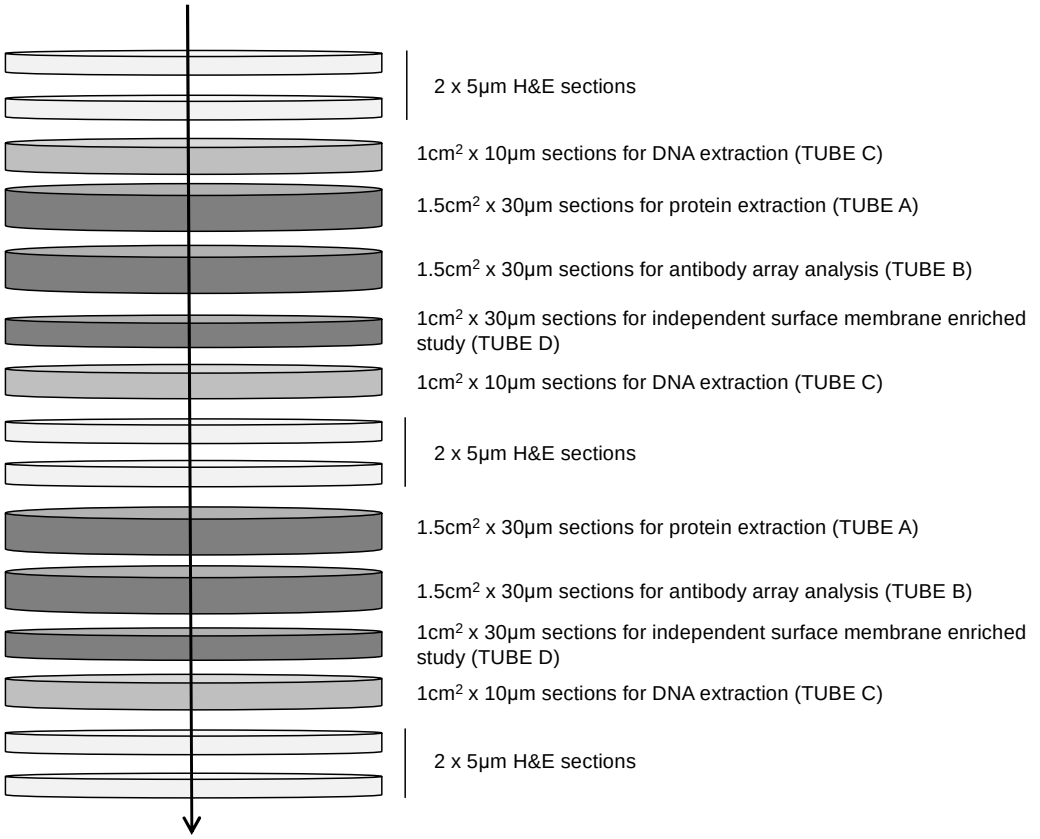

Figure 4.2 –Cutting sequence for each frozen tissue block.

Two 5µm flanking and middle sections were cut for histopathology review. Frozen issue was cut using a Leica Cryostat and placed in four eppendorf tubes. The sample in tube A was processed for LC-MS/MS and SWATH-MS and Tube B couriered to Germany for antibody array analysis. DNA extraction was performed on the sample in tube C for later genetic mutation confirmation. The content of tube D was used for an independent study that enriched for surface membrane proteins through a modified tissue lysis protocol and was analysed by LC-MS/MS (not discussed here)

4.3.4.2 Protein extraction

The suspension trapping (STrap) sample preparation method was chosen for peptide preparation. Developed in this laboratory, a single pipette tip per sample, loaded with both quartz fiber filters and reverse phase membrane (c_{18}) disk plugs stacked on top of one another enabled rapid SDS based protein extraction, followed by protein digestion and peptide clean up (Zougman et al., 2014). Preliminary experiments identified frequent blockage of the quartz filters and C18 disk plugs following centrifugation, particularly in ccRCC samples. Additional centrifugation compounded the problem due to further compression of the filters into the narrowing pipette tip. It was concluded that the digested blood proteins present in the highly vascular ccRCC (Aziz et al., 2013) was the cause, and the method was adapted by separating the

filter and C18 disc plugs into two separate pipette tips which improved sample flow-through.

4.3.5 Quality control

Data obtained from mass spectrometry can fluctuate over time, particularly with studies involving large numbers of samples that require prolonged analysis time (Watrous et al., 2017). There are many potential reasons for these signal drifts, including slight variations in mobile phase preparations, fluctuations in the high performance liquid chromatography (HPLC) retention times, varying complexity of the biological sample and changes in the sensitivity of the mass spectrometer. For this reason, a quality control sample (471 N) was planned to be run at the start, middle and end of the MS analysis to ensure correlation between the three mass spectra obtained.

4.4 Results (Sample selection and processing)

4.4.1 Sample preparation

38 tumour blocks and 26 normal kidney blocks were initially selected for cutting based on the availability of the tissue blocks, genetic grouping and type of mutation present. Small numbers of patients within the *VHL + SETD2* mutation and *VHL + BAP1* mutation groups necessitated access of samples from the International Agency for Research on Cancer (IARC), Lyon, France. Additional tumour blocks from the same patient were then also accessed either due to small sample size or inadequate predefined quality. Overall there were sections cut from 125 tumour tissue blocks, representing 38 patients. Sections were also cut from 53 matched normal kidney tissue blocks, representing 26 patients. Dr Karen Dunn (postgraduate researcher) assisted in the cutting of tissue samples and in the preparation of tissue lysates.

4.4.1.1 Confirmation of genetic mutations

Given the extensive intratumoural heterogeneity previously described in RCC (Gerlinger et al., 2014), reconfirmation of the chosen genetic mutations was undertaken through targeted sequencing (Table 4.1). This work was undertaken by Dr Claire Taylor, Senior Researcher, Genomics Facility, University of Leeds. When included, the matched normal kidney samples were analysed in parallel for germline

mutations in the chosen genes. Two ccRCC tumour blocks originally identified as having both *VHL* and *PBRM1* mutations were identified as having a *VHL* mutation only (340 T and 357 T). Two patients previously identified as having none of the genetic mutations were found to have a *VHL* mutation only (031 T and 400 T) and two patients originally identified to have a *PBRM1* mutation only were found to have a VHL mutation in addition to the *PBRM1* mutation (377 T and 404 T). One patient with a *VHL* and a *PBRM1* mutation was also found to have that *PBRM1* mutation in the normal kidney sample (370 N), which was confirmed as not containing any ccRCC tissue on histopathological review of flanking sections, thus confirming its presence in the germline. This sample was removed from the analysis. This impacted on the numbers of patients in each of the genetic groupings, especially the *VHL* + *BAP1* mutation group and the *PBRM1* mutation only group which were left with 2 and 1 samples respectively.

As known, a small number of mutations in other genes were identified within these samples, for the purposes of this study it was not feasible to account for lower frequency genes.

4.4.1.2 Histopathological review of tissue sections

An expert pathologist with a specialist interest in RCC (Dr. Pat Harnden) reviewed each slide for confirmation of the diagnosis and assessment of the grade, presence or absence of necrosis and fibrosis, percentage of viable tumour cells, presence or absence of medulla in the sample and degree of inflammation.

13 tumour samples were excluded as they did not meet pre-determined criteria. The histopathological review assisted in the selection of the predetermined number of normal kidney samples (13) for inclusion in the study. Summary details of the ccRCC tumour samples and normal kidney samples are shown in Table 4.2 and Table 4.3 respectively. A more detailed review is included in Appendix 4.

Table 4.2 – Summary of histopathological review of ccRCC tissue sections

Extent of necrosis and degree of inflammation was graded from 0-2, the higher the figure, the more extensive the finding.

Sample Number	Section number	Genetic group (based on four 'driver' mutations)	ISUP grade review	Extent of necrosis (0-2)	% viable tumour cells	Degree of inflammation (0-2)	% fibrosis or exudate
031 T	1	*VHL* mutation only	2-3	0-2	60-70	0-1	30-40
340 T	1	*VHL* mutation only	2	0	70-75	0	25-30
344 T	1	*VHL* mutation only	2	0	75-80	0	20-25
357 T	1	*VHL* mutation only	2	1	40-50	2	50-60
364 T	1	*VHL* mutation only	2	0	75	0	25
400 T	1	*VHL* mutation only	2	0	75	0	25
417 T	1	*VHL* mutation only	2	0	70	1	30
422 T	1	*VHL* mutation only	2	0	70-80	0-1	2-30
426 T	1	*VHL* mutation only	1	0	70	1	30
370 T	1	*VHL* + *PBRM1* mutation	3	0	70	0	30
377 T	1	*VHL* + *PBRM1* mutation	3	0	80	0	20
382 T	1	*VHL* + *PBRM1* mutation	2	0	90	0	10
404 T	1	*VHL* + *PBRM1* mutation	1	0	90	0	10
413 T	1	*VHL* + *PBRM1* mutation	3	0	60-70	1	30-40
231 T	1	*VHL* + *SETD2* mutation	2	0	70	0	30
371 T	1	*VHL* + *SETD2* mutation	2	0	80	0	20

Sample Number	Section number	Genetic group (based on four 'driver' mutations)	ISUP grade review	Extent of necrosis (0-2)	% viable tumour cells	Degree of inflammation (0-2)	% fibrosis or exudate
RS114563 T	1	*VHL* + *SETD2* mutation	2	0	70	0	30
RS114585 T	1	*VHL* + *SETD2* mutation	2	0	70	0	30
255 T	1	*VHL* + *BAP1* mutation	2	0	60	2	60
RS114494 T	1	*VHL* + *BAP1* mutation	2	0	70	0	30
128 T	1	No mutation group	4 and rhabdoid	0	70	0	30
233 T	1	No mutation group	2	0	70	1	30
409 T	1	No mutation group	3	0	60-70	1	30-40
471 T	1	No mutation group	2	0	70	0	30
396 T	1	*PBRM1* mutation only	1	0	75	0	25

Table 4.3 – Summary of histopathological review of normal kidney tissue sections

Extent of necrosis and degree of inflammation was graded from 0-2, the higher the figure, the more extensive the finding.

Sample Number	Section number	Genetic group (based on four 'driver' mutations)	Cortex (%)	Medulla (%)	Degree of inflammation	% fibrosis or exudate
344 N	1	*VHL* mutation only	100	0	1	0
357 N	1	*VHL* mutation only	100	0	1	0
364 N	1	*VHL* mutation only	100	0	1	0
400 N	1	*VHL* mutation only	100	0	1	0
417 N	1	*VHL* mutation only	100	0	1	0-1
370 N	1	*VHL* + *PBRM1* mutation	100	0	1	0
377 N	1	*VHL* + *PBRM1* mutation	100	0	0-1	0
382 N	1	*VHL* + *PBRM1* mutation	100	0	1	0
404 N	1	*VHL* + *PBRM1* mutation	100	0	1	0
231 N	1	*VHL* + *SETD2* mutation	90-100	0-10	1	5
371 N	1	*VHL* + *SETD2* mutation	100	0	1	0
409 N	1	No mutation group	100	0	2	5
471 N	1	No mutation group	100	0	1	0
396 N	1	*PBRM1* mutation only	100	0	1	0-10

4.4.2 Overview and patient demographics

Following a rigorous histopathological and genomic review, 25 tumour samples and 13 matched normal kidney samples were subject to proteomic analysis (Figure 4.3). The median age of patients at sample collection was 62 years (range 40-82 years). The male to female ratio was 14:11. A range of stages and grades were represented in the study. Detailed summaries of the ccRCC tumour samples entered into the study are shown in Table 4.4 and Table 4.5.

In total, quantitative measurements for 3332 proteins were obtained from the samples analysed. Proteins identified on the basis of one peptide (n=134) were excluded from further analysis due to the lower confidence that these represented a true discovery.

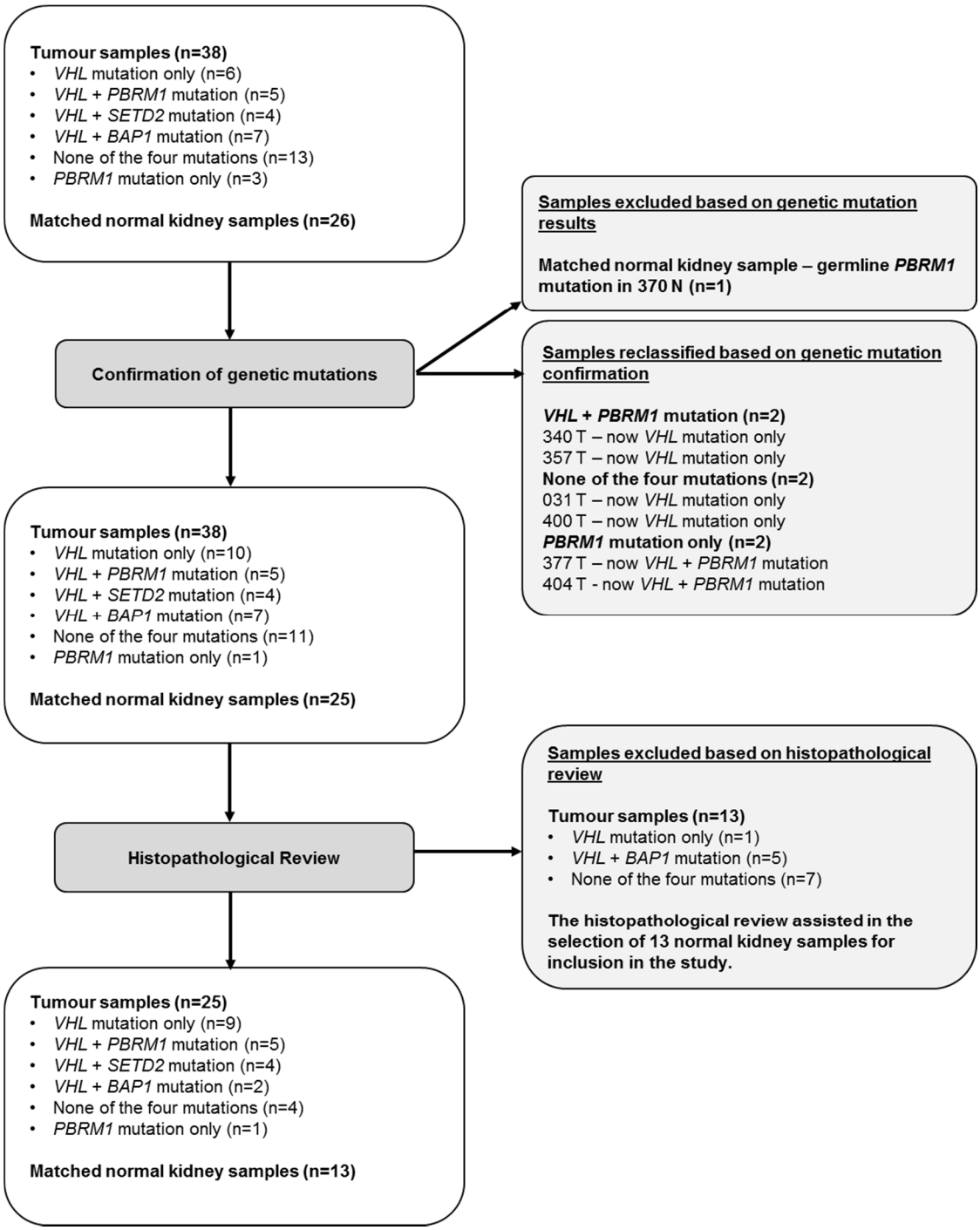

Figure 4.3 - Consort diagram detailing samples entered into the study.

Table 4.4 – Patient demographics and characteristics of tumour samples entered into the study

Gender	Male	14 (56%)
	Female	11 (44%)
Age (years)	Median	62
	Range	40-82
Stage	I	7 (28%)
	II	3 (12%)
	III	8 (32%)
	IV	7 (28%)
Grade	1	3 (12%)
	2	12 (48%)
	3	5 (20%)
	4	4 (16%)
	No consensus	1 (4%)
Genetic grouping based on four 'driver' mutations	*VHL* mutation only	9 (36%)
	VHL + *PBRM1* mutation	5 (20%)
	VHL + *SETD2* mutation	4 (16%)
	VHL + *BAP1* mutation	2 (8%)
	None of the four mutations	4 (16%)
	PBRM1 mutation *only*	1 (4%)
Country of residence	UK	22 (88%)
	Russia	3 (12%)

Table 4.5 – Detailed demographics and characteristics of patients' tumour samples entered into the study

Sample number	Genetic group (based on four 'driver' mutations)	Age	Gender	Stage	Grade	Geographical origin of tissue block	Number of other genetic mutations detected	Other mutations detected	Matched normal included in study?
031 T	*VHL* mutation only	71	F	IV	4	Leeds	0		N
340 T	*VHL* mutation only	40	M	III	2	Leeds	2	ANPEP, ZFHX4	N
344 T	*VHL* mutation only	65	F	I	2	Leeds	3	ARID1A, MDN1, ZFHX4	Y
357 T	*VHL* mutation only	45	M	IV	2	Leeds	1	DMD	Y
364 T	*VHL* mutation only	77	F	I	2	Leeds	2	SST, KDM5C	Y
400 T	*VHL* mutation only	54	F	I	2	Leeds	0		Y
417 T	*VHL* mutation only	49	F	I	2	Leeds	2	KMT2C, MTOR	Y
422 T	*VHL* mutation only	67	M	IV	2	Leeds	2	ATM, CSMD3	N
426 T	*VHL* mutation only	46	M	I	1	Leeds	3	ARID1A, KMT2C, TENM1	N
370 T	*VHL* + *PBRM1* mutation	54	M	IV	3	Leeds	0		N

Sample number	**Genetic group (based on four 'driver' mutations)**	**Age**	**Gender**	**Stage**	**Grade**	**Geographical origin of tissue block**	**Number of other genetic mutations detected**	**Other mutations detected**	**Matched normal included in study?**
377 T	*VHL* + *PBRM1* mutation	60	M	III	3	Leeds	2	COL11A1, FAT1	Y
382 T	*VHL* + *PBRM1* mutation	73	M	I	2	Leeds	3	NRXN1, TENM1, TRRAP	Y
404 T	*VHL* + *PBRM1* mutation	65	F	III	1	Leeds	5	ANPEP, AR1d1A, COL11A1, DST, TRRAP	Y
413 T	*VHL* + *PBRM1* mutation	61	M	III	4	Leeds	8	ABCA13, ANPEP, ATM, DMD, MUC17, PTK7, ZAN, ZNF469	N
231 T	*VHL* + *SETD2* mutation	53	F	IV	2	Leeds	2	ATM, 2FHX4	Y
371 T	*VHL* + *SETD2* mutation	67	M	I	2	Leeds	2	CACNA1, NRXN1	Y

Sample number	**Genetic group (based on four 'driver' mutations)**	**Age**	**Gender**	**Stage**	**Grade**	**Geographical origin of tissue block**	**Number of other genetic mutations detected**	**Other mutations detected**	**Matched normal included in study?**
RS114563 T	*VHL* + *SETD2* mutation	54	M	III	No consensus	Russia	0		N
RS114585 T	*VHL* + *SETD2* mutation	62	F	IV	2	Russia	2	KDM5C, TP53	N
255 T	*VHL* + *BAP1* mutation	82	M	II	3	Leeds	1	ANPEP	N
RS114494 T	*VHL* + *BAP1* mutation	56	F	II	2	Russia	3	ABCA13, DHAH7, DOCK8	N
128 T	No mutation group	57	F	III	4	Leeds	0		N
233 T	No mutation group	64	M	IV	4	Leeds	0		N
409 T	No mutation group	62	F	II	3	Leeds	1	MTOR	Y
471 T	No mutation group	66	M	III	3	Leeds	4	ANK2, KDM5C, MTOR, USP24	Y
396 T	*PBRM1* mutation only	69	M	III	1	Leeds	3	COL11A1, PRKDC, ZAN	Y

4.4.3 Quality control

From the single sample (471 N) analysed across the study, 3332 proteins were included in this correlation analysis. The spectra obtained were analysed for differences using one-way ANOVA for repeated measures. This demonstrated no evidence of a statistical difference in the pairwise comparisons between the three sample runs [F(2,6662)=1.185 p=0.306]. The Pearson's correlation coefficients for each pairwise combination were 0.99 and the corresponding *p*-values were <0.001 (Figure 4.4), indicating a strong association between the LFQ intensities of each run. This gives confidence that sample drift will have had a negligible effect on results obtained.

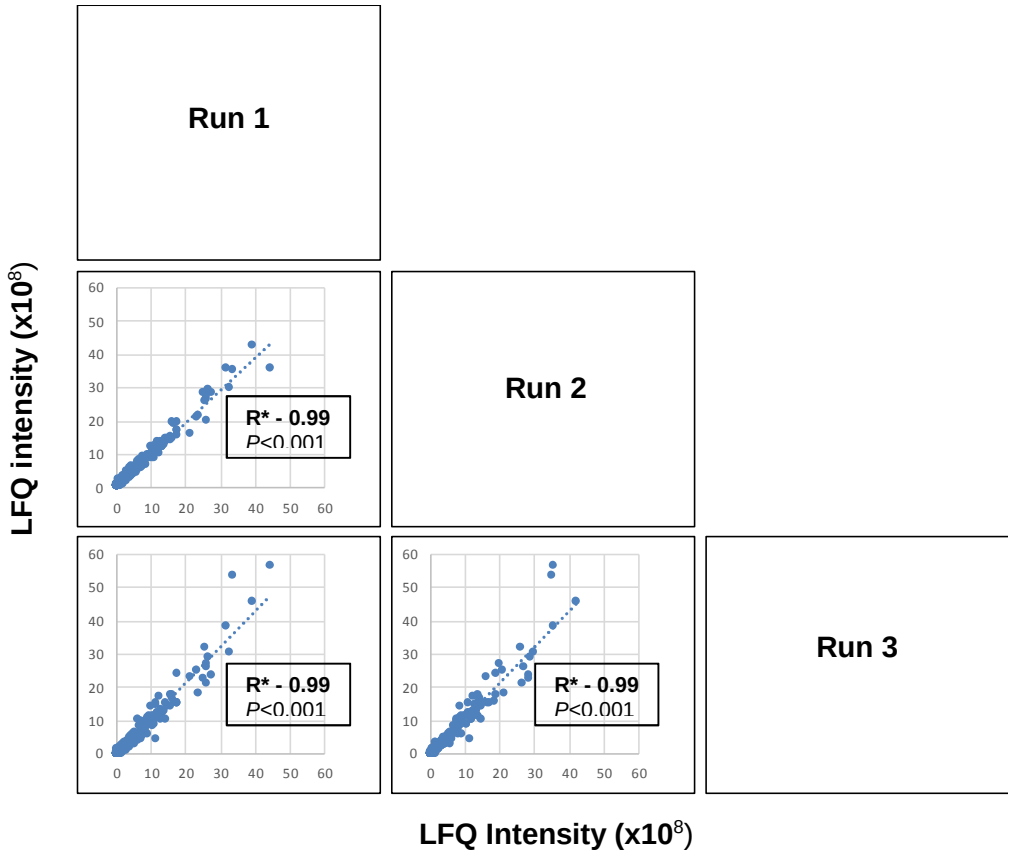

Figure 4.4 –Correlation between the LFQ intensities of the proteins identified in 3 runs of R471 normal tissue used as a quality control sample.

Sample number R471N was run at the start, middle and end of the MS analysis. This figure shows the correlation of the LFQ intensities for the 3332 proteins identified between each of the three runs. (r* = Pearson's correlation coefficient and the dashed line represents the line of best fit) The *p* value is a test of the null hypothesis that the correlation is equal to 0. The LFQ intensities for albumin and cytoplasmic actin 1 are not shown in the figure for clarity, as their LFQ intensity scores were much larger than the other identified proteins, although these two proteins were included in the statistical analysis.

4.5 Analysis of data from LC-MS/MS analysis (Leeds data)

4.5.1 Principal component analysis

From this point forward, statistical analyses were undertaken using the R statistical package. Principal component analysis (PCA) of the LFQ intensity data for all identified proteins within the LC-MS/MS analysis was performed (Figure 4.5). A clear separation between normal kidney (N) and ccRCC tumour (T) samples was observed.

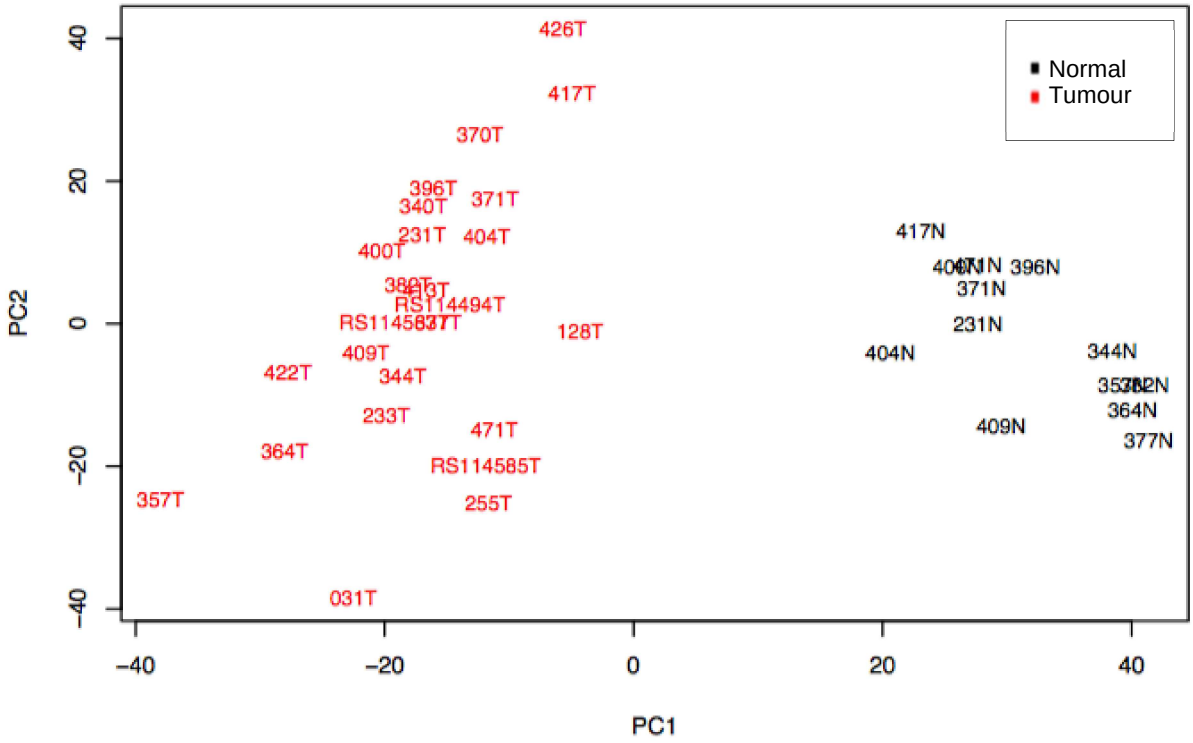

Figure 4.5 – First principal component analysis (PCA) of ccRCC tumour (T) and normal kidney (N) samples within the proteomic study based on LFQ intensity.

There was no separation within this PCA between the genetic groups included in the study (Figure 4.6). This was the same pattern for the second and third PCA.

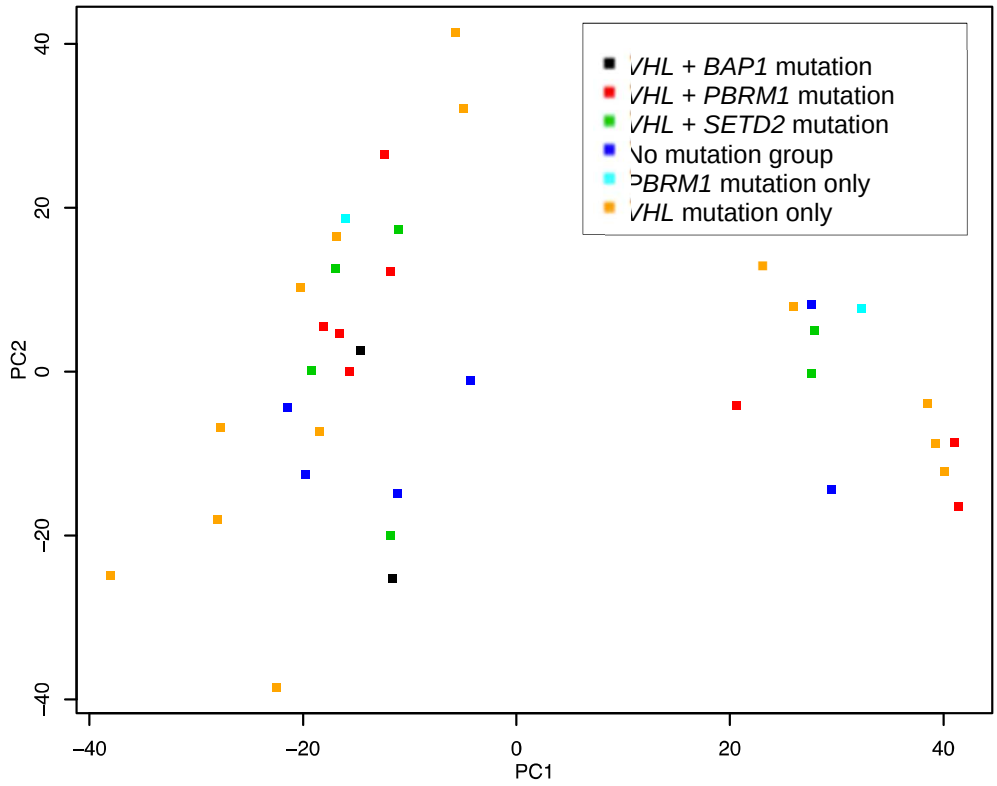

Figure 4.6 - First principal component analysis of ccRCC tumour (T) and normal kidney (N) samples marked according to their different genetic groupings.

4.5.2 Hierarchical clustering

Hierarchical clustering also demonstrated this separation of normal kidney and ccRCC tumour samples at the first major branch of the dendrogram (Figure 4.7). A second major branch separated the ccRCC tumour samples into two groups. This was the same for the normal kidney samples. The samples contained in the groups after the second branch mostly demonstrated concordance in the tumour and normal kidney samples, except for 344, 471 and 382. The reasons for the second branch within the ccRCC tumour samples are unclear. No correlation between the genetic groupings and branches were observed. Other factors such as gender, age and tumour characteristics were assessed but provided no explanation. A heatmap demonstrating the differential clustering between normal kidney and ccRCC samples is shown in Figure 4.8. When the tumour samples were analysed without normal kidney there was no clustering observed that related to the genetic groupings (Figure 4.9).

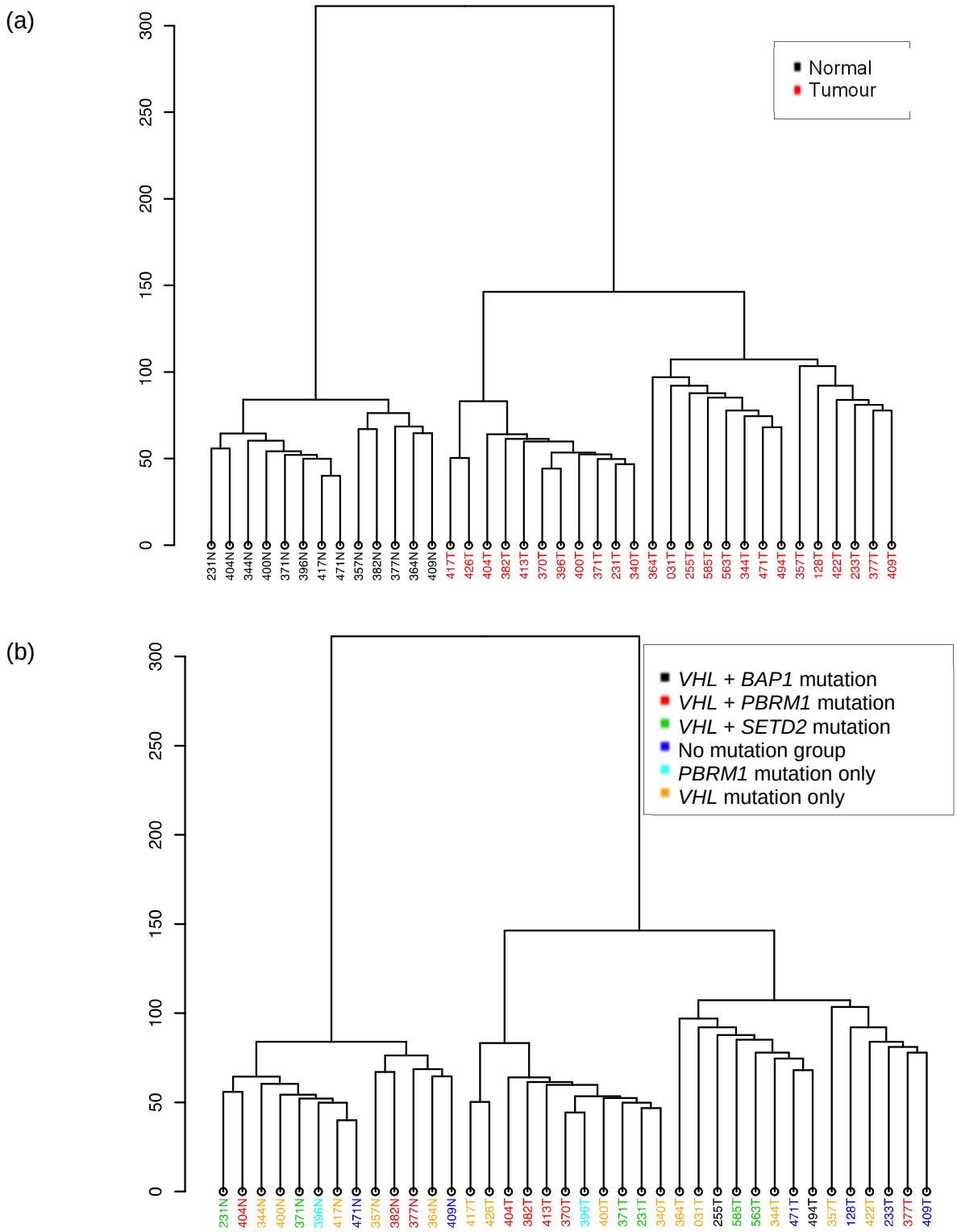

Figure 4.7 – Dendrogram showing hierarchical clustering of ccRCC tumour and normal kidney samples

Hierarchical clustering of (a) all normal and tumour samples from the study (b) the tumour and normal kidney samples coloured based on genetic grouping, is shown.

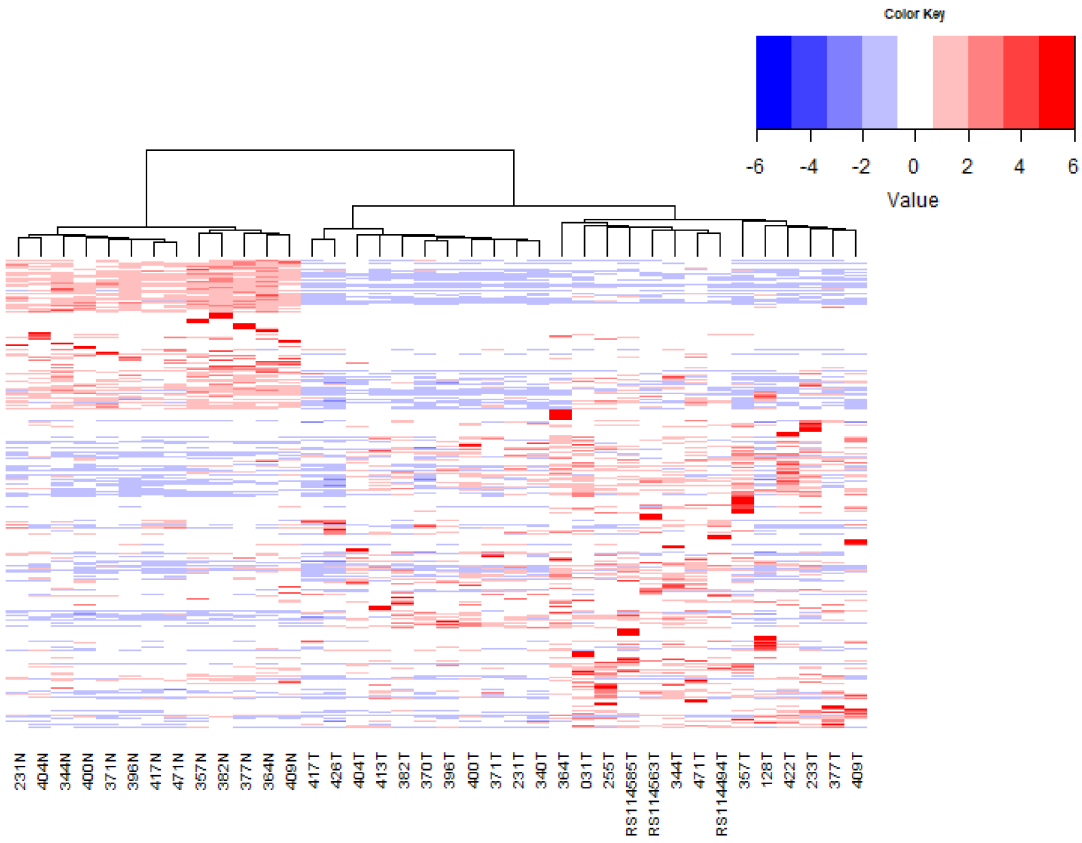

Figure 4.8 – Heatmap showing differential protein abundance between normal kidney and ccRCC tumour samples using LFQ intensity.

Courtesy of Dr Lara Fuelner

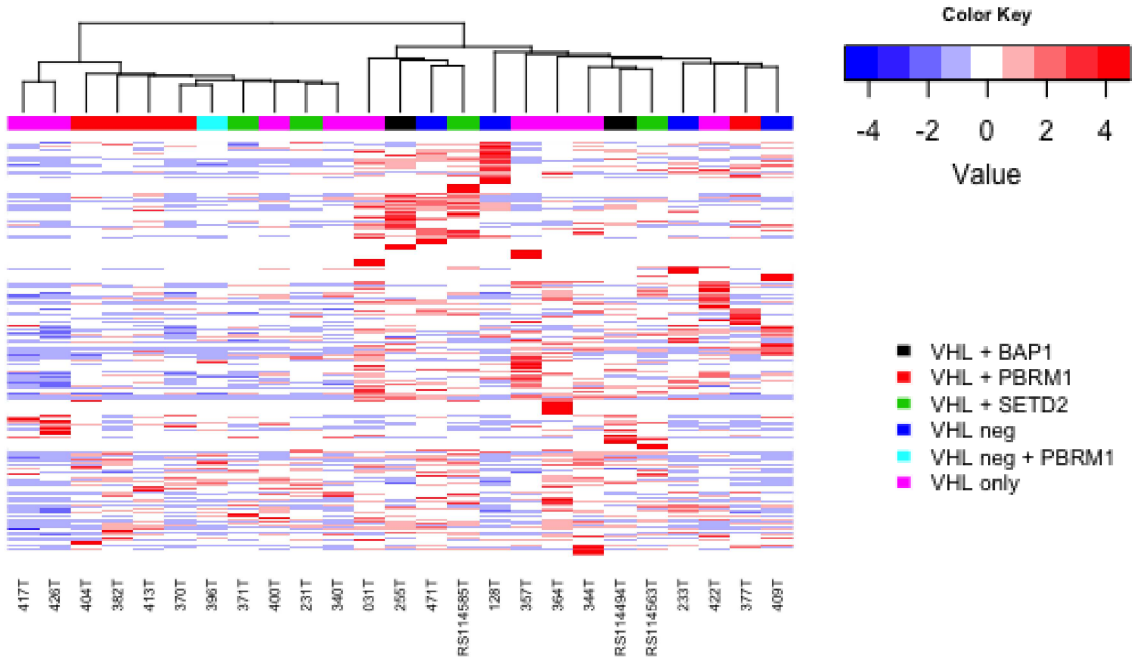

Figure 4.9 – Heatmap of ccRCC tumour samples demonstrating the genetic groupings using LFQ intensity

Courtesy of Dr Lara Fuelner

4.5.3 Analysis of tumour versus normal tissue across all proteins

Overall 3136 proteins were identified by LC-MS/MS in the Leeds analysis. Using the definition of upregulation an downregulation as over, or less than 2 times the LFQ intensity respectively, compared to the average LFQ intensity for the normal samples, 1323 of the proteins were upregulated in tumours (>2x) and 1314 were downregulated in tumours (>2x) The Wilcoxon test was applied to each protein to identify global differences in protein expression between the average LFQ intensity results of all ccRCC tumour and normal kidney samples. Overall 1337 (42.6%) proteins were identified to have a statistically significant difference (p<0.05) between tumour and normal kidney. The q value is a statistical measure of the number of statistically significant proteins that are wrongly identified as such. In this analysis the q value indicated that there was an 11.5% potential for false discoveries amongst these identified proteins. 32 proteins were below the level of detection in the normal kidney samples but were identified in over half of the ccRCC samples (see appendix). Conversely, there were 79 proteins detected in over half the normal samples but absent in the tumours.

On the same analysis of tumour versus normal kidney samples but on the basis of the peptide count, there were 1485 (47.4%) proteins with a statistically significant difference based on the Wilcoxon test. The q value indicated that there was a 10.5% potential of false discoveries amongst these proteins.

4.5.3.1 Proof of principle

Prior to proceeding with further analysis, seven of the differentially expressed proteins which were upregulated in ccRCC were selected and their expression reviewed in relation to published experience as a proof of principle. This provided confidence in the results obtained (Table 4.6, Figure 4.10 and Figure 4.11).

Table 4.6 – Proteins identified as being upregulated in ccRCC samples in the LC-MS/MS study.

Ten proteins from the 1337 identified as being upregulated in ccRCC samples in the LC-MS/MS analysis were reviewed and compared to published expression findings. The average LFQ intensity ratio of tumour to normal kidney for each protein is included, along with the *p*-value from a statistical comparison using the average LFQ intensity for tumour versus normal kidney using Wilcoxon matched pairs test. 1337 proteins were identified as being significantly upregulated in ccRCC tumour compared with normal kidney (Wilcoxon test).

Protein name	Gene name	Number of samples with protein detected		Average LFQ intensity fold difference (T/N)	*p*-value	Supportive references
		Normal	Tumour			
Carbonic anhydrase 9	CA9	0	19	14762445	<0.001	(Soyupak et al., 2005), (Liao et al., 1997)
Gamma-enolase	ENO2	0	24	108357601	<0.001	(Sanders and Diehl, 2015) (Sun et al., 2010)
Fatty acid-binding protein, brain	FABP7	0	15	415913481	<0.001	(Zhou et al., 2015) (Domoto et al., 2007)
NADH dehydrogenase [ubiquinone] 1 alpha subcomplex subunit 4-like 2	NDUFA4L2	0	21	43232961	<0.001	(Liu et al., 2016) (Minton et al., 2016)
Protein AHNAK2	AHNAK2	0	14	19467657	<0.001	(Wang et al., 2017)
Cell surface glycoprotein MUC18	MCAM	0	22	9573301	<0.001	(Wragg et al., 2016)
Chondroitin sulfate proteoglycan 4	CSPG4	0	17	9141129	<0.001	(Geldres et al., 2014)

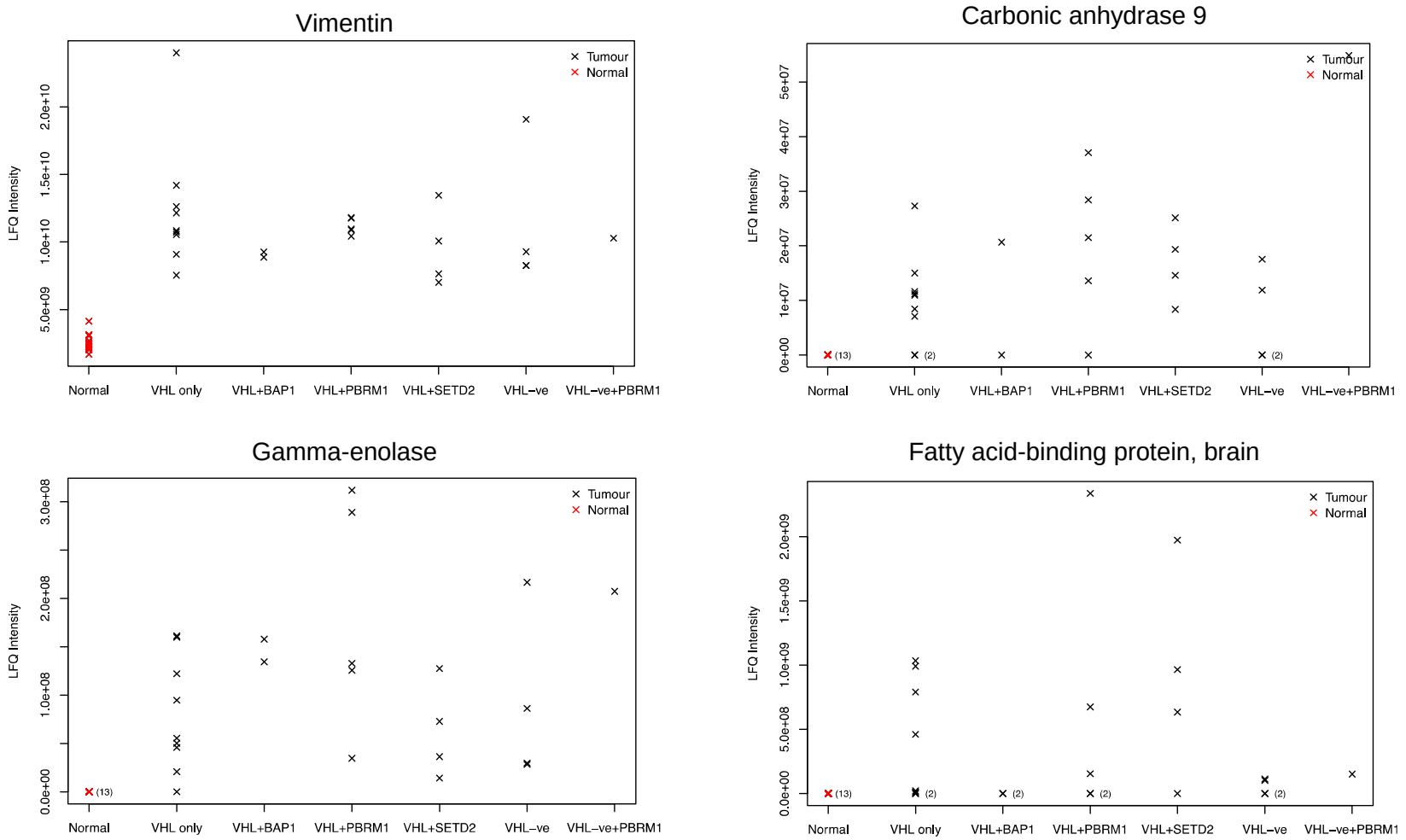

Figure 4.10 – Dot plots of LFQ intensities of proteins identified as being upregulated in ccRCC samples in the LC-MS/MS study

Each sample is arranged by its genetic group. The normal samples are included in red on the left side of the figure.

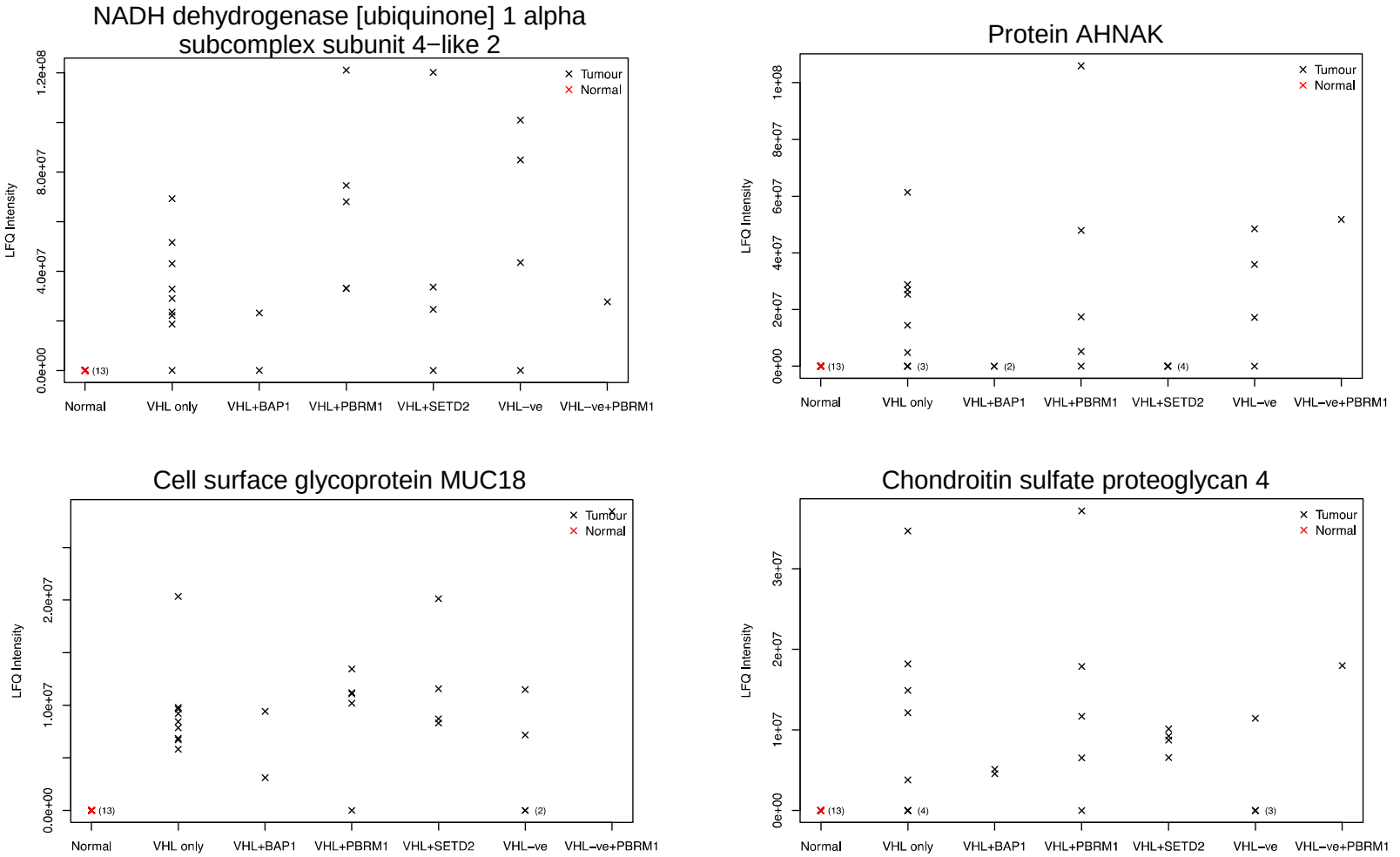

Figure 4.11 - Dot plots of LFQ intensities of proteins identified as being upregulated in ccRCC samples in the LC-MS/MS study

Each sample is arranged by its genetic group. The normal samples are included in red on the left side of the figure.

4.5.3.2 Canonical pathway analysis

The averaged LFQ intensity data for all the ccRCC tumour samples and normal kidney samples were next inputted into Ingenuity ® Pathway Analysis (IPA) (Qiagen, Redwood City). IPA contains a comprehensive knowledge-base from which uploaded protein expression profiles can be compared so as to predict expression changes in upstream molecules and to identify enriched canonical pathways.

Pre-analysis settings specified inclusion of proteins with a two-fold cut off in LFQ intensity difference between tumour and normal kidney, human as the species, experimentally derived confidence and included all tissues and cell lines within IPA knowledge base. Canonical pathway enrichment within IPA was performed using Fisher's exact test with a significance cut off $p<0.05$. IPA uses a z-score algorithm, such that an activation z-score ≥ 2 is considered activated and ≤ 2 is considered inhibited. z-score is a statistical measure of the match between expected relationship direction and observed gene expression It is weighted by the underlying findings, the relationship bias, and dataset bias. A review of the subsequent analysis identified upregulation and downregulation a dominant theme in a number of signalling pathways (Table 4.7).

Table 4.7 Enriched canonical pathways in ccRCC tumour compared with normal kidney

Upregulated	**Downregulated**
Carbohydrate biosynthesis	Alcohol degradation
Nucleoside / nucleotide biosynthesis	Amino acid degradation
Apoptosis signalling pathways	Fatty acid and lipid degradation
Integrin signalling	
Cellular growth, proliferation and development	
Cellular immune response	
Cellular injury and stress	
Growth factor signalling (VEGF, PDGF)	

The subsequent analysis identified enrichment of several pathways, of which the most significant top 20 are shown in Figure 4.12.. In particular there were a group of

pathways related to metabolism and energy production. In terms of energy metabolism, these were decreased expression of proteins involved in oxidative phosphorylation, evidence of mitochondrial dysfunction, an increase in the expression of proteins involved in carbohydrate biosynthesis (glycolysis, glycogen degradation and gluconeogenesis), and evidence of reduced ketolysis and ketogenesis. There were decreased expression of proteins involved in the TCA cycle, along with fatty acid β-oxidation, valine, tryptophan, and ethanol degradation. There was predominance of decreased expression of proteins involved in serotonin degradation. Within the cellular immune response pathways, the antigen presentation pathway, caveolar-mediated endocytosis signalling, IL-8 signalling, interferon signalling and, leucocyte extravasation signalling pathways were enriched. The VEGF and PDGF pathways were predominantly enriched with upregulated proteins, although this did not reach statistical significance with a *z*-score of 1.147 for each (Figure 4.13)

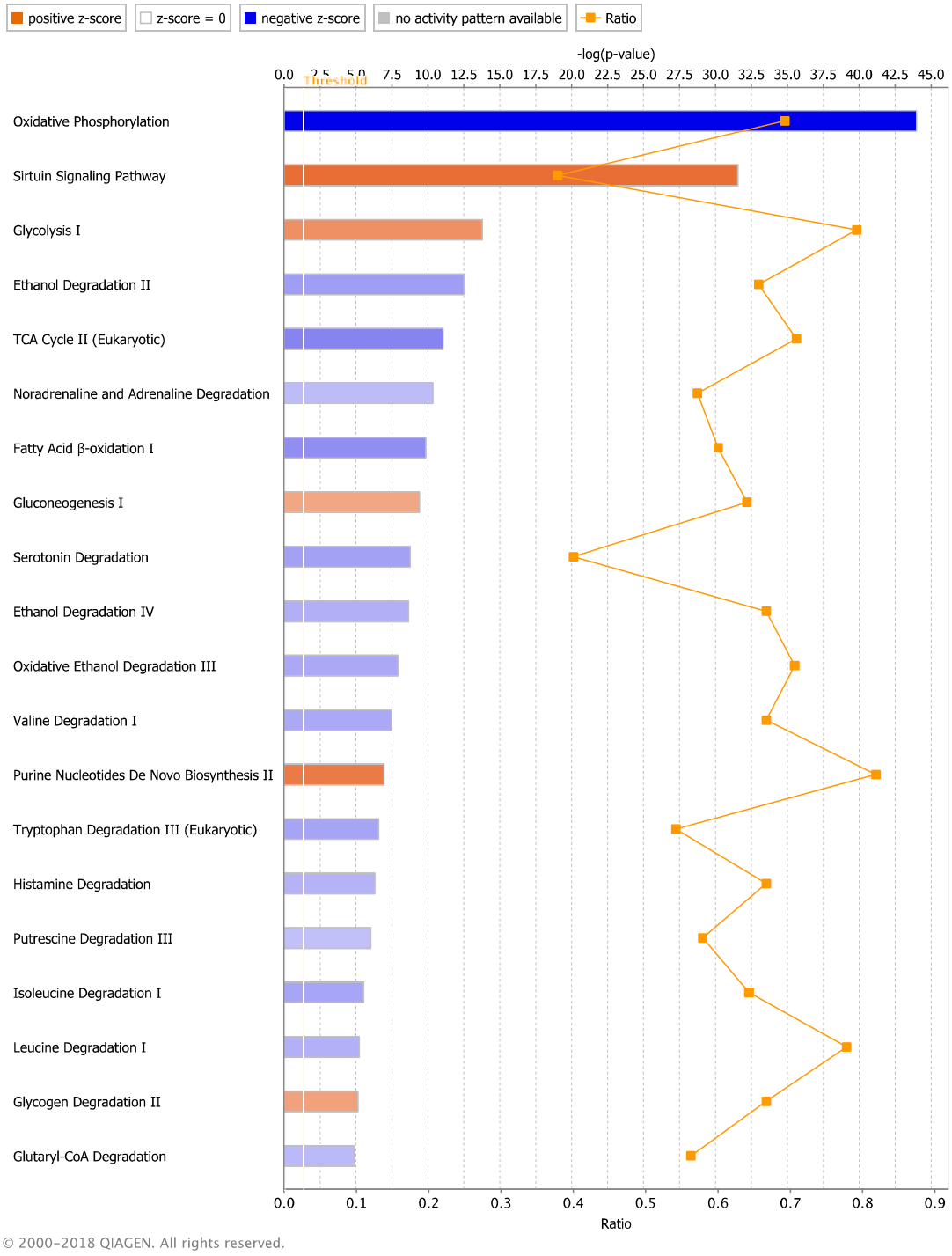

Figure 4.12 - The 20 most significantly altered canonical pathways in ccRCC when comparing average LFQ intensities of tumour versus normal tissue.

The orange bars represent canonical pathways with a *z*-score of greater than 2, thus indicating upregulation of the pathway. The blue bars represent canonical pathways with a *z*-score of less than -2, indicating downregulation of the pathway. The horizontal axis for the bars indicate the –log *p*-value. The orange line represents the ratio of proteins detected to the total number of proteins expected in that pathway.

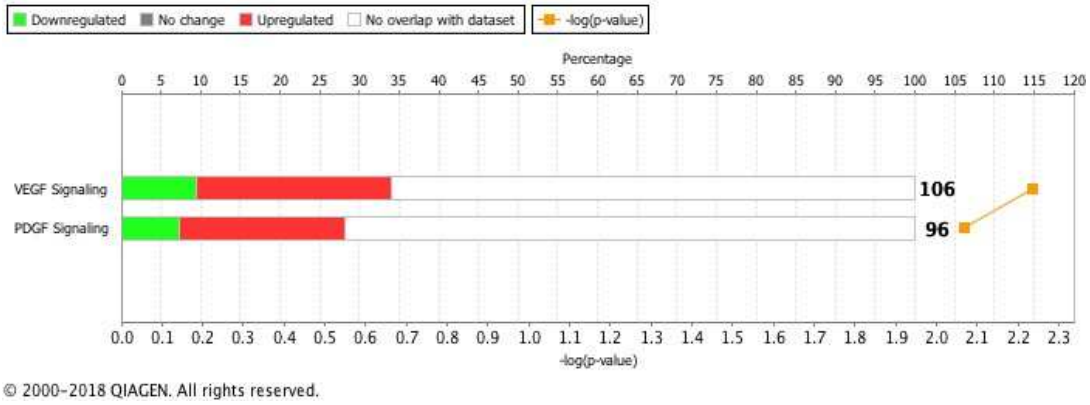

Figure 4.13 - Vascular endothelial growth factor (VEGF) and platelet derived growth factor (PDGF) signalling pathway enrichment.

The red bars indicate the proportion of unregulated proteins in relation to total proteins expected in the pathway. The green bars indicate the proportion of downregulated proteins in relation to the total proteins expected. These pathways were enriched with upregulated proteins with a positive *z*-score, suggesting upregulation of these pathways, although the *z*-score was <2 (1.147 for each), therefore it is not possible to say these pathways were activated.

4.5.3.3 Upstream regulator analysis

A further analysis to identify the predicted upstream regulators was undertaken. From this analysis, two statistical measures are computed for each protein, an activation *z*-score and p□value of overlap. The activation *z*-score is used to describe the activation state and the p□value of overlap describes the significance of the overlap between the dataset and the knowledge base using Fisher's Exact Test, with significance generally attributed to p□values <0.01. Upstream transcriptional regulators were identified based on a *z*-score of ≤2 or ≥2, and a *p*-value of overlap of ≤0.01. 24 upstream targets were predicted to be activated (Table 4.8). 8 of these regulators had already been identified within the MS analysis, although the expression pattern of TRAP1 was not in agreement with the predicted expression state. 14 molecules were predicted to be downregulated (Table 4.9). 6 of these regulators had been identified in the MS analysis and there was agreement in the state of activation in all except MAPK1 and OGA. They were 4-fold and 150000-fold upregulated in the MS analysis, respectively, yet were predicted to be inhibited based on the other protein expression levels.

Table 4.8 – Upstream regulators that are predicted to be activated in ccRCC compared with normal kidney tissue.

Upstream Analysis within IPA uses a z-score algorithm, such that an activation z-score ≥ 2 is considered activated and ≤ 2 is considered inhibited (p<0.01). The expression fold change refers to the findings from the MS analysis

Upstream regulator	Expression fold change	Activation z-score	p-value of overlap
RAC-alpha serine/threonine-protein kinase (*Akt*)		2.832	0.00851
Epidermal growth factor receptor (*EGFR*)	1268797	2.565	0.0000874
Interferon-induced, double-stranded RNA-activated protein kinase (*EIF2AK2*)	192545	3.206	0.00345
Endothelial PAS domain-containing protein 1 (*EPAS1*)		2.395	0.000235
Oestrogen-related receptor gamma (*ESRRG*)		2.224	0.0000667
Guanine nucleotide-binding protein subunit alpha-12 (*GNA12*)		2.557	0.00128
Hypoxia-inducible factor 1-alpha (*HIF1A*)		3.552	2.99E-08
Interferon alpha/beta receptor 2 (*IFNAR2*)		2.449	0.0053
Interferon regulatory factor 9 (*IRF9*)		2	0.00365
Transcription factor jun-B (*JUNB*)		2.219	0.00409
JmjC domain-containing protein 5 (*KDM8*)		2.449	0.0000112
Myc proto-oncogene protein (*MYC*)		3.521	2.62E-09
Enhancer of filamentation 1 (*NEDD9*)		2.534	0.0000927
Protein NLRC5 (*NLRC5*)		2.407	0.000902
p38 mitogen-activated protein kinase family (P38 MAPK)		4.373	0.0024
Phosphoinositide 3-kinase family (PI3K)		3.035	0.0000613
Pyruvate kinase PKM (*PKM*)	96377	2.432	0.0000262
Transcription factor p65 *(*RELA*)	245441	3.494	0.000616
Transcription activator BRG1 (*SMARCA4*)		3.244	0.00619
Signal transducer and activator of transcription 1-alpha/beta (*STAT1*)	1358.883	2.531	0.00113
E3 ubiquitin-protein ligase synoviolin (*SYVN1*)		3.212	6.33E-07
Transforming growth factor beta-1 proprotein (*TGFB1*)	131973	3.577	0.000671
Protein-glutamine gamma-glutamyltransferase 2 (*TGM2*)	9.43	3.273	0.00438
Heat shock protein 75 kDa, mitochondrial (*TRAP1*)	-1.788	2.864	2.01E-09

Table 4.9 – Upstream regulators that are predicted to be downregulated in ccRCC compared with normal kidney tissue.

Upstream Analysis within IPA uses a z-score algorithm, such that an activation z-score ≥ 2 is considered activated and ≤ 2 is considered inhibited (p<0.01). The expression fold change refers to the findings from the MS analysis

Upstream regulator	**Expression fold change**	**Activation z-score**	**p-value of overlap**
Apoptosis-inducing factor 1, mitochondrial (*AIFM1*)	-4.519	-2.2	0.0000874
Transcription regulator protein BACH1 (*BACH1*)		-2.177	0.00744
Collagen alpha-1(XVIII) chain (*COL18A1*)	-2.638	-2.35	0.00465
Cystatin-D (*CST5*)		-2.452	3.59E-11
28S ribosomal protein S29, mitochondrial (*DAP3*)	-127554.85	-2.236	0.00966
Egl nine homolog 1 (*EGLN*)		-3.448	0.0000242
Mitogen-activated protein kinase 1 (*MAPK1*)	4.259	-2.785	6.52E-07
Protein Mdm4 (*MDM4*)		-2.8	0.0000345
Protein O-GlcNAcase (*OGA*)	151097	-2.508	0.0000122
Secretory phospholipase A2 receptor (*PLA2R1*)		-2.737	5.28E-13
Scaffold attachment factor B1 (*SAFB*)	-172701	-2.309	0.00286
Suppressor of cytokine signaling 1 (*SOCS1*)		-2.54	0.00439
Transcription factor EB (*TFEB*)		-2.121	0.000787
WNT1-inducible-signaling pathway protein 2 (*WISP2*)		-3.148	0.00808

Amongst the 24 upstream regulators that were predicted to be upregulated in ccRCC, many of them are already known and have previously been documented in the literature. HIF1A (Krieg et al., 2000) and EPAS1 (HIF2A) (Frew and Moch, 2015) are identified to be upregulated as expected. Other known activated regulators include Akt (Hara et al., 2005) in which the inhibition is being investigated in a number of clinical trials (Jonasch et al., 2017). EGFR has been identified to be upregulated in 83.8% (n=771) of ccRCC samples examined using a tissue microarray and was associated with a high tumour grade (Minner et al., 2012). A number of the regulators have not yet been investigated in RCC including GNA12, KDM8, SMARCA4 and SYVN1.

4.5.4 Analysis of proteomic changes across the genetic groups

Identified proteins were analysed for differential expression across each genetically defined group according to the LFQ intensity using a Kruskal-Wallis test. 48 proteins

were found to have a statistically significant difference ($p<0.05$) across one or more group, although the *q*-value indicated that 99.9% of these proteins would be predicted to be false discoveries. A further post-hoc pairwise comparison using Wilcoxon test was performed to identify the group associated with the significant difference. When the same analysis was repeated using the average peptide count, there were 43 proteins identified with a *p*-value <0.05. The *q*-value again indicated that 99.9% of these proteins would be predicted to be false discoveries. Dot plots for each protein were constructed using the R statistical package, as in Figure 4.10, and each were reviewed. No protein was observed to have a clear difference between groups. Due to the small sample sizes and exploratory nature of this study it is not possible to define proteins that are differentially expressed across the genetic groups, and possibly there may not be any.

4.5.4.1 Canonical pathway analysis

Through the IPA software, the next approach of inputting the LFQ expression fold change relative to normal kidney for each of the six genetic groups was undertaken. Firstly an analysis of canonical pathway enrichment was reviewed. On review there were no changes in canonical pathway activation across the groups, particularly the top 20 ranked according to their *p*-value (Figure 4.14). Given the very small numbers of samples in the PBRM1 mutation only group and the VHL + BAP1 mutation group caution was used in the interpretation of the proteomic profile results.

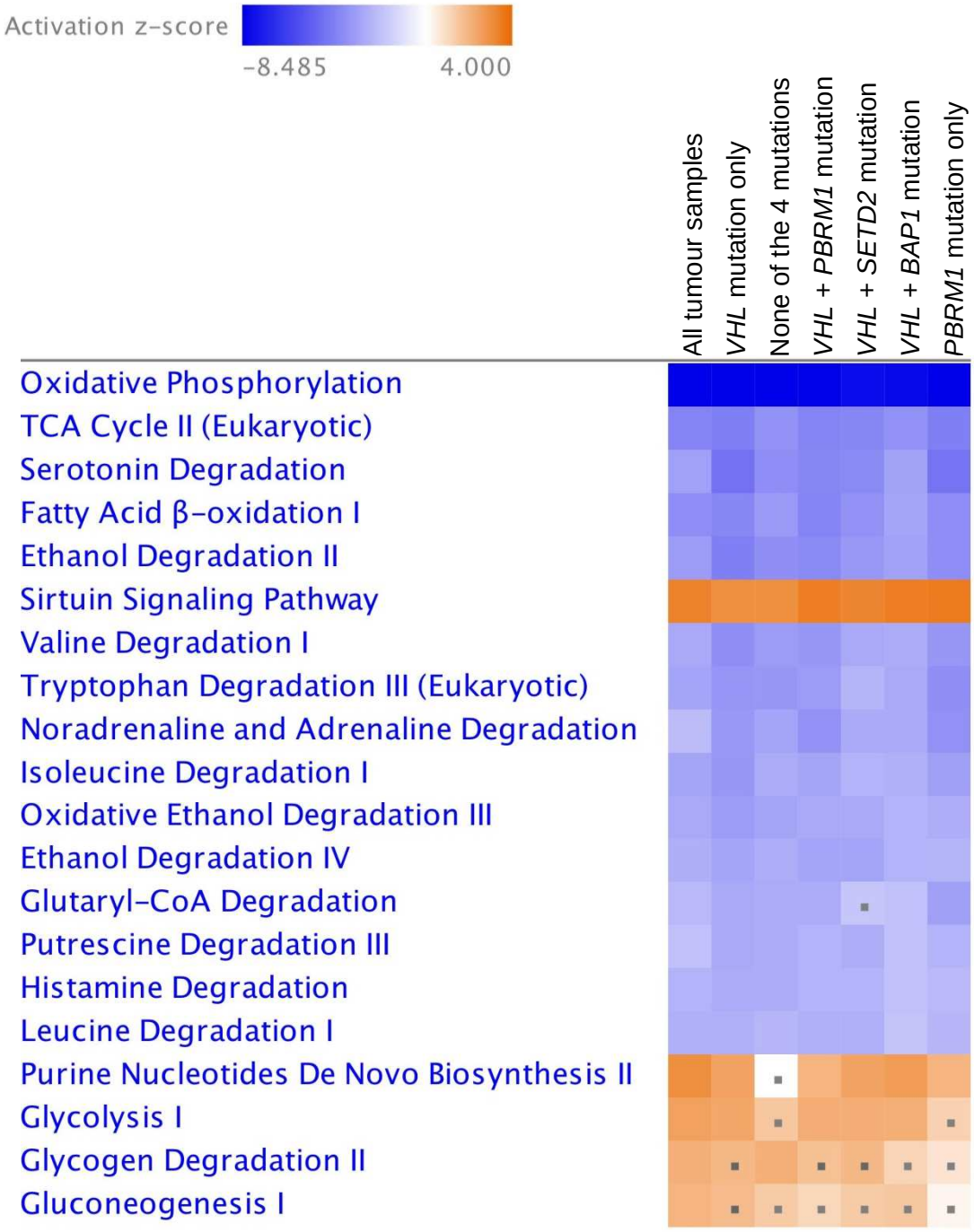

Figure 4.14 –Enriched canonical pathways on comparison of all genetic groups.

The LFQ intensity data was inputted into IPA and an analysis of the canonical pathways that are enriched with proteins, was performed. The results are based on an activation z-score, such that a score ≥2 is considered to be upregulated and a score ≤2 is considered to be downregulated. The colour key is indicated at the top of the figure. Squares may be coloured with a z-score between -2 and 2. They are highlighted with a small square inside, therefore not classified as upregulated or downregulated.

4.5.4.2 Upstream regulator analysis

On analysis of predicted upstream regulators based on the proteomic profile for each genetic group, a number of regulators were identified (Table 4.10, Table 4.11, Table 4.12, Table 4.13, Table 4.14 and Table 4.15). These were grouped together for review in Table 4.16 and Table 4.17. A number of observations were made. Firstly JmjC domain-containing protein 5 (*KDM8*) was predicted to be upregulated across all genetic groups, as was Heat shock protein 75 kDa, mitochondrial (*TRAP1)*. PKM is also predicted to be upregulated across the groups except the *PMRM1* mutation only group. In the analysis of the effect of *VHL* mutation, Hypoxia-inducible factor 1-alpha (*HIF1A*) was predicted to be upregulated in the *VHL* mutation groups as was Transforming growth factor beta-1 proprotein (*TGFB1*). Guanine nucleotide-binding protein subunit alpha-12 (*GNA12*) was upregulated in the no mutation group but not in the VHL mutation only group.

A number of upstream regulators were identified to be downregulated across all samples, namely Apoptosis-inducing factor 1, mitochondrial (*AIFM1*), 28S ribosomal protein S29, mitochondrial (*DAP3*) and Secretory phospholipase A2 receptor (*PLA2R1*). Krueppel-like factor 11 (*KLF11*) is downregulated in samples containing a VHL mutation and Scaffold attachment factor B1 (*SAFB*) is downregulated in the no mutation group. Sterol regulatory element-binding protein 1 (*SREBF1*) was downregulated in the *VHL+PBRM1* mutation group and the *PBRM1* mutation only group.

Table 4.10 – *VHL* mutation only group - Upstream molecules that are predicted to be (a) activated and (b) inhibited in ccRCC compared with normal kidney tissue

Upstream Analysis within IPA uses a z-score algorithm, such that an activation z-score ≥ 2 is considered activated and ≤ 2 is considered inhibited (p<0.05). The expression fold change is the fold difference between ccRCC and normal kidney for that genetic group from the MS analysis.

(a) Upstream regulator	Expression fold change	Activation z-score	p-value of overlap
Epidermal growth factor receptor (*EGFR*)	1058923	2.417	0.000112
Interferon-induced, double-stranded RNA-activated protein kinase (*EIF2AK2*)	534845.4	3.426	0.00999
Oestrogen-related receptor gamma (*ESRRG*)		2.224	0.0000301
Hypoxia-inducible factor 1-alpha (*HIF1A*)		3.671	1.31E-07
Interferon alpha/beta receptor 2 (*IFNAR2*)		2.449	0.00306
JmjC domain-containing protein 5 (*KDM8*)		2.449	0.00000586
Myc proto-oncogene protein (*MYC*)		3.562	6.78E-09
Enhancer of filamentation 1 (*NEDD9*)		2.331	0.000145
Protein NLRC5 (*NLRC5*)		2.407	0.000499
Phosphoinositide 3-kinase family (PI3K)		2.585	0.000247
Pyruvate kinase PKM (*PKM*)	6.838	2.23	0.0000537
Transcription factor p65 (*RELA*)	194223.2	2.977	0.0000793
Transcription activator BRG1 (*SMARCA4*)		2	0.00447
E3 ubiquitin-protein ligase synoviolin (*SYVN1*)		2.556	0.0000122
Transforming growth factor beta-1 proprotein (*TGFB1*)	366589.9	3.563	0.000437
Heat shock protein 75 kDa, mitochondrial (*TRAP1)*	-2.956	3.014	3.07E-11

(b) Upstream regulator	**Expression fold change**	**Activation z-score**	**p-value of overlap**
Apoptosis-inducing factor 1, mitochondrial (*AIFM1*)	-8.669	-2.2	0.0000512
Collagen alpha-1(XVIII) chain (*COL18A1*)	-3.232	-2.688	0.00447
Cystatin-D (*CST5*)		-2.205	4.39E-10
28S ribosomal protein S29, mitochondrial (*DAP3*)	-127555	-2.236	0.00607
Egl nine homolog 1 (*EGLN*)		-3.448	0.00000361
Oestrogen receptor		-4.035	0.00488
Krueppel-like factor 11 (*KLF11*)		-2.58	0.0000184
Mitogen-activated protein kinase 1 (*MAPK1*)	3.323	-2.669	0.0000122
Protein Mdm4 (*MDM4*)		-2.621	0.000165
Secretory phospholipase A2 receptor (*PLA2R1*)		-3.128	7.25E-14
Peroxisome proliferator-activated receptor alpha (*PPARA*)		-2.557	0.0000681
SAM pointed domain-containing Ets transcription factor (*SPDEF*)		-2.53	0.00000153

Table 4.11 – No mutation group - Upstream molecules that are predicted to be (a) activated and (b) inhibited in ccRCC compared with normal kidney tissue

Upstream Analysis within IPA uses a z-score algorithm, such that an activation z-score ≥ 2 is considered activated and ≤ 2 is considered inhibited (p<0.05). The expression fold change is the fold difference between ccRCC and normal kidney for that genetic group from the MS analysis.

(a) Upstream regulator	Expression fold change	Activation z-score	p-value of overlap
Bromodomain-containing protein 7 (*BRD7*)		2.219	0.00952
Epidermal growth factor receptor (*EGFR*)	2047451	2.837	0.00000133
Oestrogen-related receptor gamma (*ESRRG*)		2.224	0.0000118
Guanine nucleotide-binding protein subunit alpha-12 (*GNA12*)		2.198	0.00191
JmjC domain-containing protein 5 (*KDM8*)		2.449	0.00000276
Protein NLRC5 (*NLRC5*)		2.191	0.00232
Phosphoinositide 3-kinase family (PI3K)		2.568	0.000896
Pyruvate kinase PKM (*PKM*)	6.657	2.432	0.00000227
E3 ubiquitin-protein ligase synoviolin (*SYVN1*)		2.335	2.87E-07
Heat shock protein 75 kDa, mitochondrial (*TRAP1)*	-1.479	2.546	4.77E-09

(b) Upstream regulator	Expression fold change	Activation z-score	p-value of overlap
Apoptosis-inducing factor 1, mitochondrial (*AIFM1*)	-2.567	-2.2	0.0000274
Collagen alpha-1(XVIII) chain (*COL18A1*)	-2.414	-2.496	0.004
28S ribosomal protein S29, mitochondrial (*DAP3*)	-127554.85	-2.236	0.0035
Egl nine homolog 1 (*EGLN*)		-3.157	0.000161
Mitogen-activated protein kinase 1 (*MAPK1*)	4.094	-2.401	0.007
Protein Mdm4 (*MDM4*)		-2.425	0.000694
Protein O-GlcNAcase (*OGA*)	587926	-2.034	0.000277
Secretory phospholipase A2 receptor (*PLA2R1*)		-3.128	7.08E-15
Peroxisome proliferator-activated receptor alpha (*PPARA*)		-2.897	1.16E-07
Scaffold attachment factor B1 (*SAFB*)	-172701	-2.111	0.00115

Table 4.12 – *VHL* + *PBRM1* mutation group - Upstream molecules that are predicted to be (a) activated and (b) inhibited in ccRCC compared with normal kidney tissue

Upstream Analysis within IPA uses a z-score algorithm, such that an activation z-score ≥ 2 is considered activated and ≤ 2 is considered inhibited (p<0.05). The expression fold change is the fold difference between ccRCC and normal kidney for that genetic group from the MS analysis.

(a) Upstream regulator	Expression fold change	Activation z-score	p-value of overlap
Hypoxia-inducible factor 1-alpha (*HIF1A*)		2.532	0.00000212
JmjC domain-containing protein 5 (*KDM8*)		2.236	0.0000818
Pyruvate kinase PKM (*PKM*)	481881	2.012	0.0000884
Transforming growth factor beta-1 proprotein (*TGFB1*)	1	3.021	0.00167
Heat shock protein 75 kDa, mitochondrial (*TRAP1)*	-1.709	3.637	3.6E-10

(b) Upstream regulator	Expression fold change	Activation z-score	p-value of overlap
Apoptosis-inducing factor 1, mitochondrial (*AIFM1*)	-4.352	-2.2	0.0000252
28S ribosomal protein S29, mitochondrial (*DAP3*)	-127555	-2.236	0.00324
Egl nine homolog 1 (*EGLN*)		-3.033	0.0000125
Krueppel-like factor 11 (*KLF11*)		-2	0.0029
Mitogen-activated protein kinase 1 (*MAPK1*)	4.755	-2.692	0.000129
Protein Mdm4 (*MDM4*)		-2.425	0.000632
Protein O-GlcNAcase (*OGA*)	285141	-2.302	0.0000411
Secretory phospholipase A2 receptor (*PLA2R1*)		-2.591	1.19E-13
Peroxisome proliferator-activated receptor alpha (*PPARA*)		-2.182	4.83E-07
Sterol regulatory element-binding protein 1 (*SREBF1*)		-2.03	9.72E-12
Transcription factor EB (*TFEB*)		-2.646	0.000935

Table 4.13 – *VHL + SETD2* mutation group - Upstream molecules that are predicted to be (a) activated and (b) inhibited in ccRCC compared with normal kidney tissue

Upstream Analysis within IPA uses a z-score algorithm, such that an activation z-score ≥ 2 is considered activated and ≤ 2 is considered inhibited ($p<0.05$). The expression fold change is the fold difference between ccRCC and normal kidney for that genetic group from the MS analysis.

(a) Upstream regulator	Expression fold change	Activation z-score	p-value of overlap
RAC-alpha serine/threonine-protein kinase (*Akt*)		2.018	0.00427
Oestrogen-related receptor gamma (*ESRRG*)		2.224	0.0000115
Hypoxia-inducible factor 1-alpha (*HIF1A*)		2.533	4.45E-07
JmjC domain-containing protein 5 (*KDM8*)		2.449	0.00000271
Phosphoinositide 3-kinase family (*PI3K*)		2.13	0.00086
Pyruvate kinase PKM (*PKM*)	7.658	2.87	0.0000993
Transcription factor p65 (*RELA*)	1	2.902	0.00827
Syntenin-2 (*SDCBP*)	-52382.538	2.207	0.00344
Structural maintenance of chromosomes protein 3 (*SMC3*)	1	2	0.00498
Transforming growth factor beta-1 proprotein (*TGFB1*)	1	2.428	0.0037
Heat shock protein 75 kDa, mitochondrial (*TRAP1)*	-2.449	3.173	4.47E-10

(b) Upstream regulator	Expression fold change	Activation z-score	p-value of overlap
Apoptosis-inducing factor 1, mitochondrial (*AIFM1*)	-5.065	-2.2	0.0000269
28S ribosomal protein S29, mitochondrial (*DAP3*)	-127554.85	-2.236	0.00344
28S ribosomal protein S29, mitochondrial (*DAP3*)		-2.492	0.0000503
Egl nine homolog 1 (*EGLN*)		-2	0.00311
Krueppel-like factor 11 (*KLF11*)	5.317	-2.774	0.000816
Mitogen-activated protein kinase 1 (*MAPK1*)		-2.216	0.00498
Protein Mdm4 (*MDM4*)	1	-2.682	0.00000435
Protein O-GlcNAcase (*OGA*)		-2.878	2.48E-16
Transcription factor EB (*TFEB*)		-2.333	0.0000186

Table 4.14 – *VHL* + *BAP1* mutation group - Upstream molecules that are predicted to be (a) activated and (b) inhibited in ccRCC compared with normal kidney tissue

Upstream Analysis within IPA uses a z-score algorithm, such that an activation z-score ≥ 2 is considered activated and ≤ 2 is considered inhibited (p<0.05). The expression fold change is the fold difference between ccRCC and normal kidney for that genetic group from the MS analysis.

(a) Upstream regulator	Expression fold change	Activation z-score	p-value of overlap
Fibroblast growth factor 7 (*FGF7*)		2.387	0.000153
JmjC domain-containing protein 5 (*KDM8*)		2.236	0.0000701
Pyruvate kinase PKM (*PKM*)	6.79	2.23	0.0000102
Protein tyrosine phosphatase type IVA 3 (*PTP4A3*)		2.194	0.00408
Heat shock protein 75 kDa, mitochondrial (*TRAP1)*	1.735	2.523	2.34E-09

(b) Upstream regulator	Expression fold change	Activation z-score	p-value of overlap
Apoptosis-inducing factor 1, mitochondrial (*AIFM1*)	-2.193	-2.2	0.0000215
28S ribosomal protein S29, mitochondrial (*DAP3*)	-127555	-2.236	0.00281
Egl nine homolog 1 (*EGLN*)		-3.017	0.000249
Mitogen-activated protein kinase 1 (*MAPK1*)	4.281	-3.025	0.000861
Protein Mdm4 (*MDM4*)		-2.619	0.0000533
Secretory phospholipase A2 receptor (*PLA2R1*)		-2.261	3E-18
Peroxisome proliferator-activated receptor alpha (*PPARA*)		-2.354	0.0000342
Scaffold attachment factor B1 (*SAFB*)	-172701	-2.53	0.00259

Table 4.15 – *PBRM1* mutation only group - Upstream molecules that are predicted to be (a) activated and (b) inhibited in ccRCC compared with normal kidney tissue

Upstream Analysis within IPA uses a z-score algorithm, such that an activation z-score ≥ 2 is considered activated and ≤ 2 is considered inhibited (p<0.05). The expression fold change is the fold difference between ccRCC and normal kidney for that genetic group from the MS analysis.

(a) Upstream regulator	Expression fold change	Activation z-score	p-value of overlap
JmjC domain-containing protein 5 (*KDM8*)		2	0.00181
Protein tyrosine phosphatase type IVA 3 (*PTP4A3*)		2.411	0.000826
Heat shock protein 75 kDa, mitochondrial (*TRAP1)*	-4.928	4.021	4.22E-13
Tribbles homolog 3 (*TRIB3*)		2.236	0.00808

(b) Upstream regulator	Expression fold change	Activation z-score	p-value of overlap
Apoptosis-inducing factor 1, mitochondrial (*AIFM1*)	-11.771	-2.2	0.0000322
28S ribosomal protein S29, mitochondrial (*DAP3*)	-127555	-2.236	0.00403
Krueppel-like factor 11 (*KLF11*)		-2.449	0.000607
Nuclear factor erythroid 2-related factor 2 (*NFE2L2*)		-2.588	0.000227
Secretory phospholipase A2 receptor (*PLA2R1*)		-3.262	5E-16
Peroxisome proliferator-activated receptor alpha (*PPARA*)		-2.534	0.0000048 3
SHC-transforming protein 1 (*SHC1*)		-2.178	0.00374
Osteopontin (*SPP1*)		-3.158	5.65E-09
Sterol regulatory element-binding protein 1 (*SREBF1*)		-2.514	8.29E-12
Transcription factor EB (*TFEB*)		-2.828	0.000195
Tumor protein p73 (*TP73*)		-3.119	0.00123

Table 4.16 – Upstream regulators that are predicted to be upregulated in each genetic group compared with normal kidney tissue.

Grey shading indicates upregulation in that particular genetic group

Upstream regulator	VHL mutation only	No mutation group	VHL + PBRM1 mutation	VHL + SETD2 mutation	VHL + BAP1 mutation	PBRM1 mutation only
RAC-alpha serine/threonine-protein kinase (*Akt*)				⇑		
Bromodomain-containing protein 7 (*BRD7*)		⇑				
Epidermal growth factor receptor (*EGFR*)	⇑	⇑				
Interferon-induced, double-stranded RNA-activated protein kinase (*EIF2AK2*)	⇑					
Oestrogen-related receptor gamma (*ESRRG*)	⇑	⇑		⇑		
Fibroblast growth factor 7 (*FGF7*)					⇑	
Guanine nucleotide-binding protein subunit alpha-12 (*GNA12*)		⇑				
Hypoxia-inducible factor 1-alpha (*HIF1A*)	⇑		⇑	⇑		
Interferon alpha/beta receptor 2 (*IFNAR2*)	⇑					
JmjC domain-containing protein 5 (*KDM8*)	⇑	⇑	⇑	⇑	⇑	⇑
Myc proto-oncogene protein (*MYC*)	⇑					
Enhancer of filamentation 1 (*NEDD9*)	⇑					
Protein NLRC5 (*NLRC5*)	⇑	⇑				
Phosphoinositide 3-kinase family (PI3K)	⇑	⇑		⇑		
Pyruvate kinase PKM (*PKM*)	⇑	⇑	⇑	⇑	⇑	
Protein tyrosine phosphatase type IVA 3 (*PTP4A3*)					⇑	⇑
Transcription factor p65 (*RELA*)	⇑			⇑		
Syntenin-2 (*SDCBP*)				⇑		
Transcription activator BRG1 (*SMARCA4*)	⇑					
Structural maintenance of chromosomes protein 3 (*SMC3*)				⇑		
E3 ubiquitin-protein ligase synoviolin (*SYVN1*)	⇑	⇑				
Transforming growth factor beta-1 proprotein (*TGFB1*)	⇑		⇑	⇑		
Heat shock protein 75 kDa, mitochondrial (*TRAP1)*	⇑	⇑	⇑	⇑	⇑	⇑
Tribbles homolog 3 (*TRIB3*)						⇑

Table 4.17 – Upstream regulators that are predicted to be downregulated in each genetic group compared with normal kidney tissue.

Grey shading indicates downregulation in that particular genetic group

Upstream regulator	VHL mutation only	No mutation group	VHL + PBRM1 mutation	VHL + SETD2 mutation	VHL + BAP1	PBRM1 mutation only
Apoptosis-inducing factor 1, mitochondrial (*AIFM1*)	⇓	⇓	⇓	⇓	⇓	⇓
Collagen alpha-1(XVIII) chain (*COL18A1*)	⇓	⇓				
Cystatin-D (*CST5*)	⇓					
28S ribosomal protein S29, mitochondrial (*DAP3*)	⇓	⇓	⇓	⇓	⇓	⇓
Egl nine homolog 1 (*EGLN*)	⇓	⇓	⇓	⇓	⇓	
Krueppel-like factor 11 (*KLF11*)	⇓		⇓	⇓		⇓
Mitogen-activated protein kinase 1 (*MAPK1*)	⇓	⇓	⇓	⇓	⇓	
Protein Mdm4 (*MDM4*)	⇓	⇓	⇓	⇓	⇓	
Nuclear factor erythroid 2-related factor 2 (*NFE2L2*)						⇓
Protein O-GlcNAcase (*OGA*)		⇓	⇓	⇓		
Secretory phospholipase A2 receptor (*PLA2R1*)	⇓	⇓	⇓	⇓	⇓	⇓
Peroxisome proliferator-activated receptor alpha (*PPARA*)	⇓	⇓	⇓		⇓	⇓
Scaffold attachment factor B1 (*SAFB*)		⇓			⇓	
SHC-transforming protein 1 (*SHC1*)						⇓
Osteopontin (*SPP1*)						⇓
SAM pointed domain-containing Ets transcription factor (*SPDEF*)	⇓					
Sterol regulatory element-binding protein 1 (*SREBF1*)			⇓			⇓
Transcription factor EB (*TFEB*)			⇓	⇓		⇓
Tumor protein p73 (*TP73*)						⇓

4.5.5 Selection of novel proteins as therapeutic targets

Following on from this work, several proteins were selected for further investigation as novel therapeutic targets in ccRCC. A list of desired criteria was considered. These included upregulation in the majority of tumour samples whilst having a low

expression in normal kidney samples, not ubiquitous expression in other tissues, relevant biological function of the selected protein and finally the availability of antibodies and small molecule inhibitors. An initial shortlist of proteins was created and each one was considered, with two being then discussed in Chapter 5.

Table 4.18 – Proteins chosen for consideration of further investigation as novel therapeutic targets in ccRCC

Protein	Gene	Function (www.uniprot.org)	Investigations in		Inhibitor availability
			RCC	Other cancers	
Protein diaphanous homolog 1	*DIAPH1*	Assembly of actin structures. Required for cytokinesis. Promotes cell migration - essential for cell adhesion to collagen.	None	In the HCT-116 colorectal cancer cell line controls cellular adhesion by stabilising microtubules. Its loss resulted in reduced metastatic potential (Lin et al., 2015)	None available
Protein NDRG1	*NDRG1*	Ubiquitously expressed in normal tissue. Stress/hypoxia responsive protein. Involved in cell growth and differentiation	Association between primary tissue expression and favourable prognosis. In-vitro studies demonstrated enhanced RCC cell line invasiveness and cell proliferation with silencing (Hosoya et al., 2013)	Decreased expression in colorectal carcinoma tissue compared with normal colon and loss is associated with poorer OS and recurrence (Mao et al., 2013). Cell proliferation and invasiveness enhanced with knock-down in a gastric cancer cell line (Chang et al., 2016)	None available
Peptidyl-prolyl cis-trans isomerase FKBP1A	*FKBP1A*	Role in immunoregulation and cellular processes involving protein folding, trafficking and cell cycle regulation. Ubiquitous expression in cells. Binding to rapamycin mediates the immunosuppressive effects (Fong et al., 2003)	None	None	Inhibited by FK506 (tacrolimus) and rapamycin

Protein	Gene	Function (www.uniprot.org)	Investigations in		Inhibitor availability
			RCC	Other cancers	
Tumour protein D54	*TPD52L2*	Regulation of cell proliferation	None	Knock-down in the U251 glioma cell line reduced cell invasiveness, colony formation and induced G0/G1 cell cycle arrest (Wang et al., 2014)	None
Proliferation-associated protein 2G4	*PA2G4*	May play a role in ERBB3 signal transduction (Yoo et al., 2000). May be involved in growth regulation	None	Expression upregulated in the transition from normal to hormone sensitive to hormone resistant prostate cancer (Gannon et al., 2008).	WS6 available. It is an inducer of β cell proliferation (Sigma Aldrich)
ATP-dependent 6-phosphofructokinase, platelet type	*PFKP*	A key enzyme in the glycolytic pathway	Known to be upregulated in ccRCC at an mRNA and protein level. Knockdown work induced cell cycle arrest and reduced proliferation in the 786-0 and Caki-1 cell lines (Wang et al., 2016a)	none	Not available
Prostaglandin G/H synthase 1	*PTSG1*	More commonly known as cyclooxygenase-1 (COX-1). PTGS1 catalyses the conversion of arachidonate to prostaglandin H2 (PGH2), a committed step in prostanoid synthesis. The prostanoids are the principal proteins responsible for production of inflammatory	By IHC, the cytoplasmic and cytomembranous staining intensity in RCC correlates with tumour grade, renal vein invasion, tumour size and perirenal fat	Abnormal prostaglandin generation is felt to play a pivotal role in the evolution of most epithelial cancers from precursor lesions, this includes breast, colorectal and prostate	Available - The selective PTGS1 inhibitor SC-560 was shown to inhibit ovarian cancer cell growth in vivo and increase apoptosis in vitro (Daikoku et al., 2005).

Protein	Gene	Function (www.uniprot.org)	Investigations in		Inhibitor availability
			RCC	Other cancers	
		prostaglandins (Ricciotti and FitzGerald, 2011).	invasion (Osman and Youssef, 2015). In both ovarian cancer and RCC PTGS1 and VEGF expression were found to correlate, suggesting their interaction. The non-steroidal anti-inflammatory drugs (NSAIDs) bind to the cyclooxygenase active site and inhibit PTGS1 with varying selectivity (Patrono et al., 2004).	cancer (Singh Ranger, 2016) (Mauro et al., 2010). PTGS1 has been shown to be overexpressed in a number of different cancers compared with adjacent normal tissue, including endometrial, oral, ovarian	
EH domain-containing protein 2	*EHD2*	May play a role in membrane trafficking between plasma membrane and endosomes	Previously noted to be upregulated in ccRCC (Zaravinos et al., 2014)	Reduced expression in breast cancer tissue compared with adjacent normal breast tissue. Overexpression repressed and knock down of EHD2 promoted migration and invasion of the breast cancer cell lines, MCF-7 and MDA-MB-435 (Yang et al., 2015).	None available

Protein	Gene	Function (www.uniprot.org)	Investigations in		Inhibitor availability
			RCC	Other cancers	
Protein ANHNAK2	*AHNAK2*	Regulation of RNA splicing	Identified as being upregulated in ccRCC primary tissue. Knockdown inhibited cell proliferation, colony formation and proliferation in Caki-1 cell line (Wang et al., 2017)	Upregulated in pancreatic adenocarcinoma relative to normal pancreas using IHC (Lu et al., 2017)	None available
Gamma-interferon-inducible protein 16	*IFI16*	Involved in transcriptional regulation. Possibly involved in p53-related tumour suppression	None	Downregulated in prostate cancer compared to prostate cancer cell lines (Alimirah et al., 2007). Expression decreased in hepatocellular carcinoma primary tissue and cell lines relative to normal liver tissue. Overexpression decreased cell migrational ability and colony formation whilst increasing apoptosis (Lin et al., 2017)	None available
Neutral cholesterol ester hydrolase 1	*NCEH1*	Tumour cell migration, lipid metabolism, ether lipid metabolism	None	Upregulated in breast, ovarian, pancreatic cancers and melanoma. Inhibition in PC3 prostate cancer cell lines reduced invasiveness, migration	Available - JW480 (Sigma Aldrich)

Protein	Gene	Function (www.uniprot.org)	Investigations in		Inhibitor availability
			RCC	Other cancers	
				and cell viability (Chang et al., 2011)	
ERO1-like protein	*ERO1A*	Involved in oxidative protein folding in the endoplasmic reticulum. Regulates the MHC class molecule	None	Expressed in oesophageal and gastric cancer cell lines (Battle et al., 2013). Related to the expression of PD-L1 in triple negative breast cancer (Tanaka et al., 2017)	Available
Proteasome subunit beta type 9	*PSMB9*	This protein forms a subunit of the immunoproteasome, a complex macromolecular structure involved in protein degradation and antigen presentation (Ferrington and Gregerson, 2012). The immunoproteasome is an alternative form of the constitutive proteasome that is not normally active in normal cells of the body but is expressed at high levels in cancer tissues. Its synthesis is induced by cytokines such as TNF-α and INF-γ (Ho et al., 2007).	None	PSMB9 has been shown to be upregulated in a number of other cancers including AML, prostate cancer and malignant melanoma (Rouette et al., 2016) (Kageshita et al., 1999).	Inhibitors are available that are non-discriminatory in their action against all constitutive and immune-proteasome complexes and may have other actions (Kondagunta et al., 2004). These have been introduced into clinical practice for the treatment of multiple myeloma and are the subject of multiple ongoing clinical trials (Hideshima et al., 2001).

Protein	Gene	Function (www.uniprot.org)	Investigations in		Inhibitor availability
			RCC	Other cancers	
Prolyl 4-hydroxylase subunit alpha 1	*P4HA1*	Involved in biogenesis of collagen. Directly upregulated by HIF1 =under hypoxic conditions, where it may have a role in extracellular remodelling.	Identified as an upregulated gene in ccRCC (Hirota et al., 2006)	Increased levels predice poor outcome in patients with breast cancer (Gilkes et al., 2013)	Available
Prolyl 4-hydroxylase subunit alpha 2	*P4HA2*	Involved in biogenesis of collagen	None	Upregulated at an mRNA level in breast cancer tissue compared with normal breast tissue. Silencing reduced cell growth and metastases in xenograft models (Xiong et al., 2014)	Available
Fatty acid binding protein, brain	*FABP7*	Thought to be involved in fatty acid uptake, transport and metabolism	Identified to be upregulated in ccRCC and correlated with advanced stage and poorer survival. Overexpression enhanced cell growth in RCC cell lines (Zhou et al., 2015)	Associated with the basal breast cancer phenotype where higher expression was associated with a better outcome (Zhang et al., 2010)	None available
Protein FAM49B	*FAM49B*	Regulator of mitochondrial function	None	Silencinig in pancreatic adenocarcinoma cell lines enhanced cell proliferation and invasiveness (Chattaragada et al., 2018)	None available
Synaptogyrin-2	*SYNGR2*	May play a role in regulated exocytosis	None	None	None available

Protein	Gene	Function (www.uniprot.org)	Investigations in		Inhibitor availability
			RCC	Other cancers	
Testin	*TES*	It is found at areas of cell-to-cell contact and focal adhesions. Its location suggests it may have a role in cell adherence, communication and cell mobility.		This protein has been described as being overexpressed in a gastric cancer cell line (GTL-16) where it co-amplifies with MET (Han et al., 2003). Although conflictingly it has also been demonstrated to be lost in multiple other cancers, including head and neck squamous cell carcinoma (Gunduz et al., 2009), breast, pancreatic, haematological (Tatarelli et al., 2000) (Sarti et al., 2005), glioblastoma (Mueller et al., 2007), prostate cancer (Chene et al., 2004) and colorectal cancer (Huili et al., 2016).	None available

4.6 Discussion

This chapter has described a comprehensive proteomic study in the context of using genomically defined tissues. Three profiling platforms, LC-MS/MS, SWATH-MS and antibody arrays, were used to analyse 25 ccRCC tissue samples and 13 matched normal kidney samples. Whilst the SWATH-MS and antibody array data is not discussed here, they will contribute to future work beyond this thesis. Overall, the expression of 3136 unique proteins was examined, of which 1337 (42.6%) were identified to have a statistically significant difference between the tumour and normal kidney samples. Two proteins were taken forward for further investigation, discussed in the next chapter of this thesis.

Each sample underwent a comprehensive histopathological review and confirmation of the genetic mutation of interest to identify high quality tissue samples and avoid potential intratumoural heterogeneity affecting the results. The importance of this was highlighted in the 6 samples that were found to have a different mutational profile than when originally sequenced. Interestingly four of the tumour samples that were initially characterised as not having a *VHL* mutation were later found to have a somatic *VHL* mutation. If we consider the findings of the two phylogenetic studies of intratumoural genetic heterogeneity in ccRCC, this would not be expected as these studies consistently demonstrated that VHL mutations when present, were always positioned in the trunks of the phylogenetic trees, and were never subclonal. They were therefore ubiquitous throughout the multiregional biopsies (Gerlinger et al., 2014) (Sankin et al., 2014). Further investigation established that the *VHL* mutations were in fact present in exon 1 of the *VHL* gene but were not initially detected due to read quality. It is known that approximately 28% of VHL mutations are reported to occur in the large, GC-rich exon 1. The failure to detect these mutations were attributed to difficulties amplifying GC-rich regions, which is well documented in the literature (Hube et al., 2005). Normal kidney sample number 370 N was found to harbour a germline mutation in PBRM1, which has been reported in a small number of studies, one in a family with a predisposition to RCC (Benusiglio et al., 2015). This normal kidney sample was excluded from the subsequent analysis to prevent interference with the final results.

Proof of principle of our approach was obtained at the beginning and throughout the study in the identification of proteins already known and expected to be dysregulated in ccRCC.

4.6.1 Analysis of tumour versus normal tissue across all proteins

This study clearly distinguished between normal kidney and ccRCC tissue at a proteomic level as observed following principal component analysis and hierarchical clustering. Interestingly the tumours separated into two distinct clusters based on the protein profile. This clustering pattern did not relate to patient demographics, tumour characteristics and importantly the presence of one of the top four frequently occurring genetic mutations (*VHL, PBRM1, SETD2* and *BAP1*). Further work to explore the difference between the two groups was undertaken by Dr Lara Feulner, who identified 117 proteins differentially expressed between the two groups. These proteins enriched the EIF2 signalling and mTOR signalling pathways in the first cluster, which is particularly interesting given the use of mTOR inhibitors in the clinic. In the everolimus versus placebo phase III trial in the second line setting in RCC, the response rate was approximately 5% in patients receiving everolimus (Motzer et al., 2008). It would be interesting to apply this analysis to patients receiving everolimus to identify if it can predict response. The EIF2 signalling pathway is involved in protein synthesis, in particular translation initiation. Phosphorylation causes general repression of mRNA translation. Perhaps it is not surprising that these two pathways are enriched together as they appear to be interlinked. (Burwick and Aktas, 2017). Rapamycin, an mTOR inhibitor, indirectly increases phosphorylation of EIF2α in rapamycin sensitive and oestrogen-dependent MCF-7 breast cancer cell lines highlighting the modulating effect mTOR has on the EIF2 pathway (Tuval-Kochen et al., 2013). A study investigating other targets of sorafenib has demonstrated increased EIF2α phosphorylation in U937 leukaemia cell lines (Rahmani et al., 2007). Given these findings and the role of this signalling pathway, it warrants further investigation in the future.

In the comparison between the average LFQ intensity values for each protein identified in ccRCC and normal kidney tissue, not taking into account the genetic mutations present, several enriched canonical pathways were identified particularly related to metabolism. The Warburg effect, first proposed by Otto Heinrich Warburg, describes the dependence of cancer cells on aerobic glycolysis for ATP production (Warburg, 1956), whereas normal kidney cells rely on mitochondrial oxidative

phosphorylation as the primary source of energy. In keeping with this finding and as proof of principle of our approach, there was increased abundance of proteins involved in carbohydrate biosynthesis and the generation of precursor molecules for the production of fatty acids, non-essential amino acids and nucleotides (Vander Heiden et al., 2009). It was expected that the VEGF and PDGF signalling pathways would be significantly enriched given the predominance of samples with VHL mutation (80%), although this was not the case. Whilst VEGF and PDGF pathways were observed to be enriched with upregulated proteins, this was not statistically significant (*z*-score 1.147). It is not known why this is the case, it may possibly be related to small sample size or the dilutional effect of the VHL wild-type samples.

Twenty-four upstream molecules were identified to be upregulated and fourteen were identified to be downregulated in this analysis. HIF1A and EPAS1 (HIF2A) were upregulated, which adds to the proof of principle of the approach. A number of novel proteins were identified, not having previously been investigated. These included JmjC domain-containing protein 5, encoded by the *KDM8* gene. This protein has H3K36me2 histone demethylase and hydroxylase activities, and is required for cell cycle progression by directly regulating transcription. It has been investigated in a number of different cancer types including breast cancer tissue where it was observed to be upregulated by IHC relative to normal breast tissue. Silencing in MCF7 breast cancer cells resulted in reduced cell growth (Hsia et al., 2010). It has been hypothesised to play a role in microtubule stabilisation. Its use with vinblastine and colchicine enhanced cell death in the HeLa cell line (Wu et al., 2016). There may be a link between upregulation of JmjC domain-containing protein 5 and the increased carbohydrate metabolism observed. It directly binds M2-PK, the M2 splice variant of pyruvate kinase which channels energy production through lactate synthesis. It then shuttles M2-PK to the cell nucleus where it activates HIF-1A transcription and thus the downstream glycolytic cascade (Lichner et al., 2017). Histone demethylase inhibitors are currently in development but none specific to JmjC domain-containing protein 5 have yet been identified. This warrants further investigation in the future (Larkin et al., 2012).

4.6.2 Analysis of proteomic changes across the genetic groups

This is the first study to begin to integrate the proteomic and genomic data from the same sample in ccRCC. *PBRM1* encodes polybromo-1 (also known as BAF180), a subunit of the SWI/SNF complex that mediates ATP-dependent chromatin

remodelling processes that are implicated in replication, transcription, DNA repair and control of cell differentiation and proliferation (Reisman et al., 2009). There are a small number of studies investigating the biological consequences of a *PBRM1* inactivating mutation. These have highlighted the role of *PBRM1* in the regulation of p53 transcriptional activity and the regulation of p53 mediated replicative senescence through p21 induction (Burrows et al., 2010). It is known that p53 regulates P21 expression, which induces cell cycle arrest (Xia et al., 2008). Knockdown of *PBRM1* in ccRCC cell lines has been shown to increase their proliferation, colony formation and cell migration (Varela et al., 2011). Similarly restoration of *PBRM1* expression in breast cancer cell lines was shown to reduce colony number and size (Xia et al., 2008). Gene expression profiling has indicated that it regulates pathways associated with chromosomal instability, cellular proliferation, extracellular matrix organisation, cell adhesion and ion transport. The gene signature group was enriched with hypoxic markers (Varela et al., 2011) (Wang et al., 2016b). *PBRM1* may also function to limit the over amplification of HIF in *VHL* deficient tumours through limiting the interplay between HIF and STAT3 (Nargund et al., 2017), possibly explaining why VHL inactivation alone is not sufficient to promote the development of ccRCC (Mack et al., 2003). *SETD2* encodes a histone H3K36 methyltransferase that is involved in histone remodelling processes (Sun et al., 2005). Tumours with a *SETD2* mutation have been described to have a distinct gene expression profile compared with other non-*SETD2* mutated tumours. Large-scale transcriptional deregulation was noted with 298 genes showing significant differences in expression, all twofold or less (Dalgliesh et al., 2010). Similar to tumours with a *PBRM1* mutation, those with a *SETD2* mutation also fell into a hypoxic gene expression signature group (Dalgliesh et al., 2010). *BAP1* encodes ubiquitin carboxyl-terminal hydrolase *BAP1*. This protein has been found to have a number of roles. Firstly it interacts with host cell factor-1 (HCF-1) where it regulates cell cycle progression (Misaghi et al., 2009). It also interacts with BRCA1 where it regulates the DNA damage response (Pena-Llopis et al., 2012) and may have a broad role in nuclear ubiquitin-dependent regulatory processes. It was suggested that *BAP1* has an indirect role in mTORC1 activation (Hsieh et al., 2017).

Initial analysis for differential protein expression within each genetic group versus normal using a Kruskal-Wallis test did not confidently identify any proteins with a clear difference between the groups. This was supported by an individual review of the dot plot for LFQ intensity for each protein produced through the R statistical package. This was an interesting finding given the postulated functional differences described in the paragraph above. In keeping with the lack of differential protein expression

across the genetic groups, an analysis of the most significantly enriched canonical pathways seen in the global tumour versus normal kidney comparison did not highlight any change in the upregulated or downregulated status across all genetic groups.

A number of upstream molecules were identified to be upregulated across the different genetic groups. As discussed before, JmjC domain-containing protein 5 (encoded by *KDM8*) was upregulated in all genetic groups investigated, as was heat shock protein 75 kDa, mitochondrial (encoded by *TRAP1*). Heat shock protein 75 kDa has been shown to bind to and inhibit succinate dehydrogenase resulting in the stabilisation of HIF1A (Sciacovelli et al., 2013). There was disagreement in the MS analysis and the prediction of the upstream activation state. Despite being found to have a decreased fold change in 4/5 groups (range x 1.5-5) except VHL+BAP1 in the MS analysis, the IPA software predicted it to be upregulated based on the profile of other proteins. It is known to be expressed in RCC tissue and to a lower degree in normal kidney tissue at an mRNA and protein level which is consistent with the upstream regulator analysis (Si et al., 2015). These findings may reflect the small sample numbers and inadvertent choice of normal kidney samples with high expression of heat shock protein 75 kDa, mitochondrial, or may demonstrate the limitations of predicting upstream pathways in this software. The predicted state was based upon the differential expression of 19-20 downstream proteins, of which three were not as predicted in the MS analysis, namely pyruvate kinase M1/2, seryl-tRNA synthetase and glycyl-tRNA synthetase.

HIF1α was predicted to be upregulated in the three of the four groups with *VHL* mutation, (not in the *VHL+BAP1* mutation group). This is as would be expected with the knowledge of *VHL*. The small sample numbers in the *VHL+BAP1* mutation group (2) may mean it is not representative. The VEGF and PDGF signalling pathways were not identified as being differentially expressed based on a significant *z*-score cut-off as 2. Transforming growth factor beta-1 proprotein (encoded by *TGFB1*) was similarly observed to be upregulated in the same three groups with VHL mutation. This link between VHL loss and transforming growth factor beta-1 proprotein upregulation has been commented on before in ccRCC in which its activity was attenuated upon reintroduction of functioning VHL in ccRCC cell lines (Bostrom et al., 2013). Small molecule inhibitors are being developed and some have been used in clinical trials, one of which included one patient with RCC in a phase I setting having failed sorafenib

or sunitinib (Morris et al., 2014). This patient did not have a response. The development of these inhibitors continues and may hold promise for the future (de Gramont et al., 2017). It may be that a patient may be predicted to respond if they have a VHL mutation according to the expression patterns in this study.

VHL wild-type tumours are a particular subtype of RCC that were explored further in this study. Despite similar morphological features to tumours with a *VHL* mutation, they have a worse prognosis (Dagher et al., 2016). The no mutation group was analysed in relation to the other groups with a VHL mutation. Two upstream proteins were observed to be upregulated in the no mutation/VHL wild-type group, namely guanine nucleotide-binding protein subunit alpha-12, encoded by GNA12, and bromodomain-containing protein 7, encoded by BRD7. Guanine nucleotide-binding protein subunit alpha-12, which was previously identified as being upregulated in our comparison between the average LFQ intensity of all tumour samples compared to all normal kidney samples, was upregulated in the no mutation group and not in the other groups. Encoded by the *GNA12* gene, it forms the α-subunit of a heterotrimeric G protein, which function to transmit many signals to effector molecules within the cell (Udayappan and Casey, 2017). Guanine nucleotide-binding protein subunit alpha-12 has been previously identified to be upregulated at a RNA level in oral squamous cell carcinoma (Cheong et al., 2009), breast cancer (Kelly et al., 2006a) and prostate cancer (Kelly et al., 2006b). Silencing of guanine nucleotide-binding protein subunit alpha-12reduced cell growth, invasiveness and metastatic potential in each of these cancer types, but it has not yet been investigated in RCC. A link with VHL was not found in the literature, thus no explanation was found for its upregulation in VHL wild-type tumours. Inhibition of the guanine nucleotide-binding protein subunit alpha-12 and 13 subtypes has been shown to enhance the effect of bortezomib, a non-selective proteasomal inhibitor, through repression of PSMB5 (Yang et al., 2010).

There were 19 proteins identified to be downregulated in one or more of the genetic groups in this study. They are not discussed further at this point due to their downregulated nature. Overall they provide further information into the biology of renal cell carcinoma with regards to the genetic mutations present.

4.6.3 Selection of proteins for further investigation

To conclude the study, the proteins were reviewed, with an aim to select two to further investigate their potential as novel therapeutic targets in ccRCC. From the list of interesting proteins in terms of their selective expression in ccRCC, relevant biological function and the availability of antibodies to perform proteomic investigations, two were selected to investigate in the next chapter of this thesis. Prostaglandin G/H synthase 1, which is also known as cyclooxygenase-1 (COX-1) was selected based on the dot plot of its expression according to its LFQ intensities in all samples (Figure 4.15).

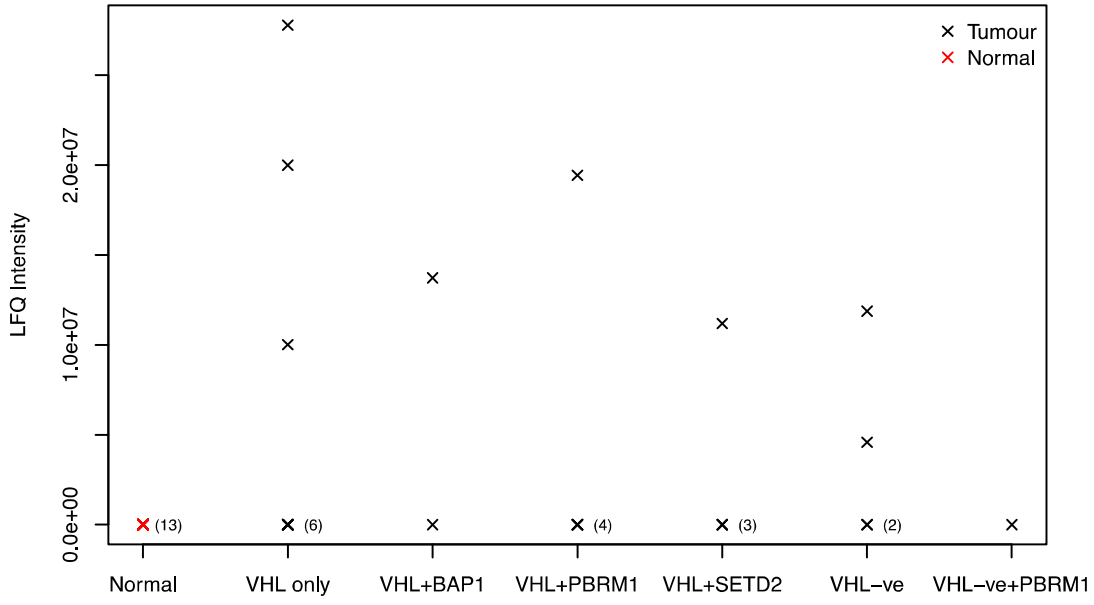

Figure 4.15 – Dot plot for cyclooxygenase-1 (COX-1) expression according to the LFQ intensity readings from the proteomic study

COX-1 inhibitors are a commonly utilised drug in the clinic today, having anti-inflammatory and analgesic effects. Further investigation would focus on whether this finding is confirmed in the complementary studies and whether there is a cell line model on which COX-1 inhibitors can be investigated.

The second chosen protein was proteasome subunit beta type-9 (PSMB9) which is a proteasomal subunit that functions to cleave redundant proteins within a cell. It was markedly upregulated in all ccRCC tumour samples whilst having low or no expression in the normal kidney samples.

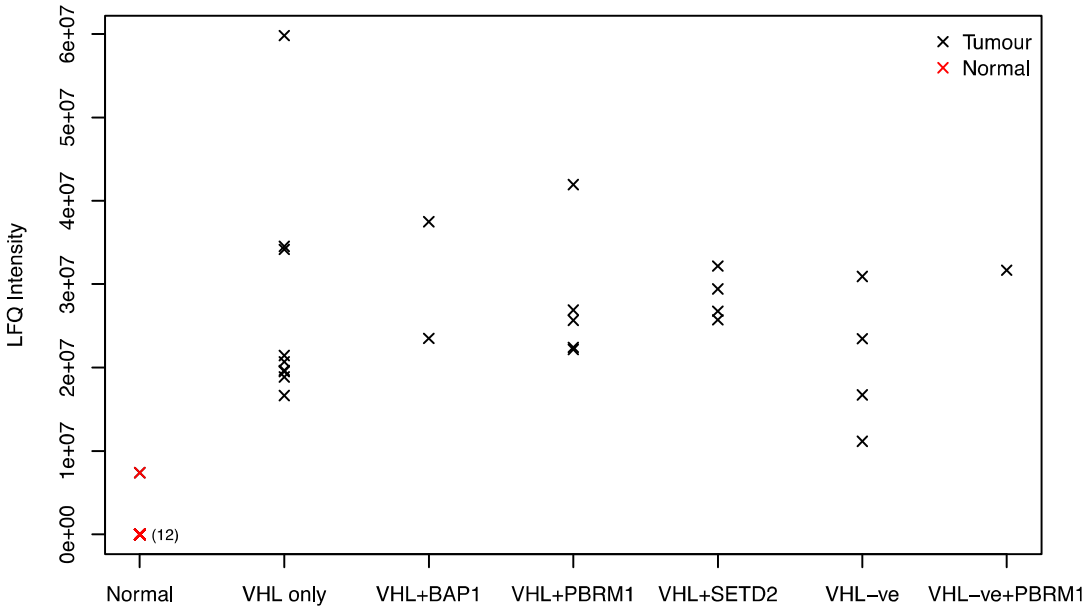

Figure 4.16 – Dot plot for proteasome subunit beta type-9 (PSMB9) expression according to LFQ intensity readings from the proteomic study.

4.6.4 Conclusion

In conclusion, to our knowledge this study is one of the most comprehensive proteomic studies in ccRCC that also takes account of the genetic profile of the tissue samples. Several novel and interesting upstream proteins have been identified to be upregulated across the genetic groups through an analysis using the Ingenuity® Pathway Analysis (IPA) software, and two proteins have been selected for further investigation in the next chapter in this thesis.

A number of interesting observations were made. Firstly, there was no significant difference in the expression of any particular protein observed across the genetic groups. Investigation of enriched canonical pathways did not identify significant differences across the genetic groups either. It may be that the tumours displaying different genetic mutations may converge on similar cellular processes and canonical pathways due to exposure to common selective pressures from the microenvironment or constraints inherited from the parental founder cell (Venkatesan and Swanton, 2016). This would explain the convergence upon the pathways involved in glucose metabolism, nucleoside and nucleotide biosynthesis, cellular growth, proliferation and development and growth factor signalling. Secondly the tumours clustered into two

groups on hierarchical clustering and principal component analysis. Whilst the tumours did not cluster based upon the genetic groups, 17 proteins were differentially expressed between these two clusters and these proteins enriched the EIF2 and mTOR signalling pathways. The significance of this is not yet known.

It is recognised that there were some limitations to this study that could not be addressed despite the comprehensive planning stages. The main limitation was the relatively small numbers of samples, as it was designed to be an exploratory pilot study for a larger future study. It was difficult to obtain tissue samples for the VHL+BAP1 and PBRM1 mutation only genetic groups due to the lack of tissue samples. Prior to commencing the study this was anticipated to be an issue. The design of this study did not take into account the presence of other genetic mutations in the selection of tissue samples. The impact of the additional mutations is unknown but are likely to have influenced the observed protein expression profiles. An example of a genetic mutation that may be significant is *TP53*, which is associated with higher-grade tumours and poorer overall survival (Gerlinger et al., 2014) (Manley et al., 2016). There are also limitations in the technology employed for this study. Despite the recent advances in mass spectrophotometric analysis, low protein coverage is still a problem in the absence of extensive fractionation which precludes analysis of numerous samples due to analysis time required.

Overall, to date this study has been the first attempt to our knowledge at integrating the proteomic and selected genomic profile of the same tissue sample in ccRCC. It has given an insight into the biology of ccRCC and demonstrates the feasibility of undertaking such a study at a larger scale. The inclusion of a bioinformatic analysis would be beneficial to the analysis of such a study.

Chapter 5 Initial investigations into COX-1 and PSMB9 as potential therapeutic targets in ccRCC

5.1 Introduction

This chapter describes the results of the initial investigations of the two candidate novel therapeutic targets in ccRCC, namely cyclooxygenase-1 (COX-1) and proteasome subunit beta type-9 (PSMB9). Both were discovered to be upregulated in ccRCC compared with the matched normal kidney counterparts in the previous proteomic analysis of ccRCC tissue compared with normal kidney, selected on the basis of underlying genomic changes (see Chapter 4).

5.2 Cyclooxygenase-1 (COX-1)

5.2.1 COX-1 expression in the LC-MS/MS study

COX-1 was identified to be expressed in 8/25 (32%) of ccRCC samples (R031, R233, R255, R340, R371, R377, R417 and R471) whilst it was detected in 0/13 of the normal kidney samples included in the detailed proteomic analysis of ccRCC tissue compared with normal kidney (Figure 5.1). There was no pattern of increased COX-1 expression across the selected genetic groupings. There was no correlation between COX-1 expression and tumour grade.

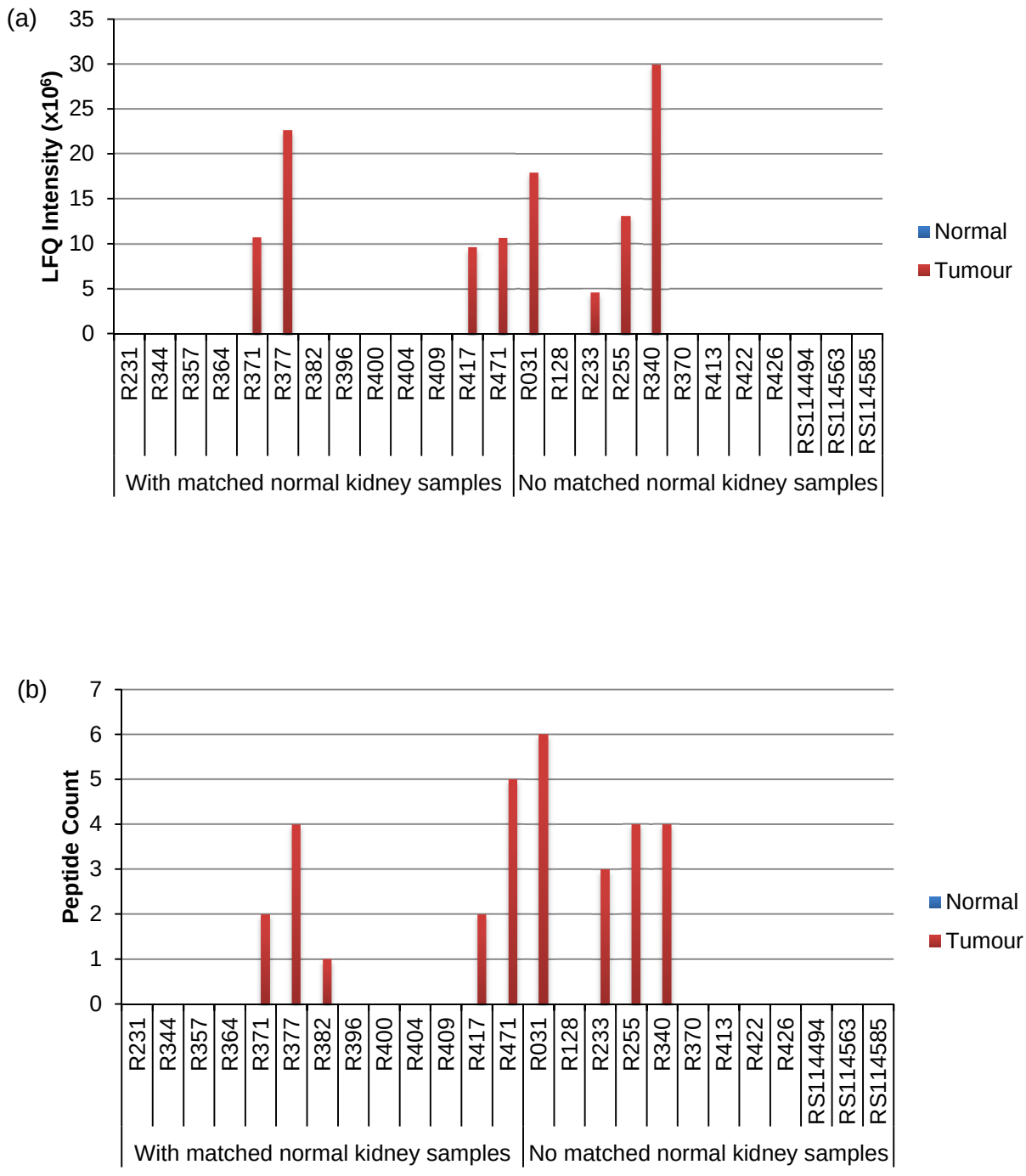

Figure 5.1 – COX-1 expression in the proteomic analysis of ccRCC tissue compared with normal kidney using LC-MS/MS (a) LFQ intensity results (b) peptide count results

5.2.2 COX-1 expression in the SWATH-MS study

To further confirm this finding the data obtained from the SWATH-MS analysis of the same samples was reviewed (Figure 5.2). In this analysis COX-1 was detected in all samples including normal kidney. Defining upregulation as an intensity level of over twice the matched normal kidney sample, COX-1 was upregulated in 6/13 (46%) of the matched samples (R364, R371, R377, R404, R417 and R471). The samples previously identified in the LC-MS/MS analysis were again identified in this study and represented the samples with the highest COX-1 intensity levels.

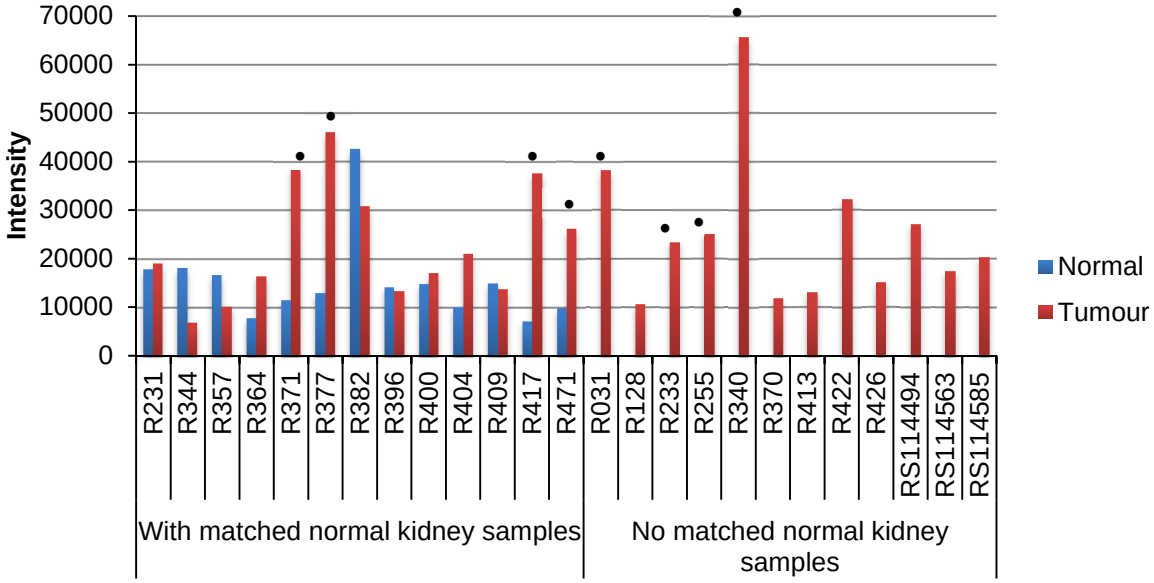

Figure 5.2 - COX-1 expression (intensity) in the proteomic analysis of ccRCC compared with normal kidney using SWATH-MS.
(• indicates samples in which COX-1 was identified to be expressed in the LC-MS/MS study)

An association between the results obtained from the LC-MS/MS and SWATH-MS analyses was next investigated (Figure 5.3). The corresponding Pearson's correlation coefficient (r) was determined to be 0.87 ($p<0.001$) suggesting there was a correlation.

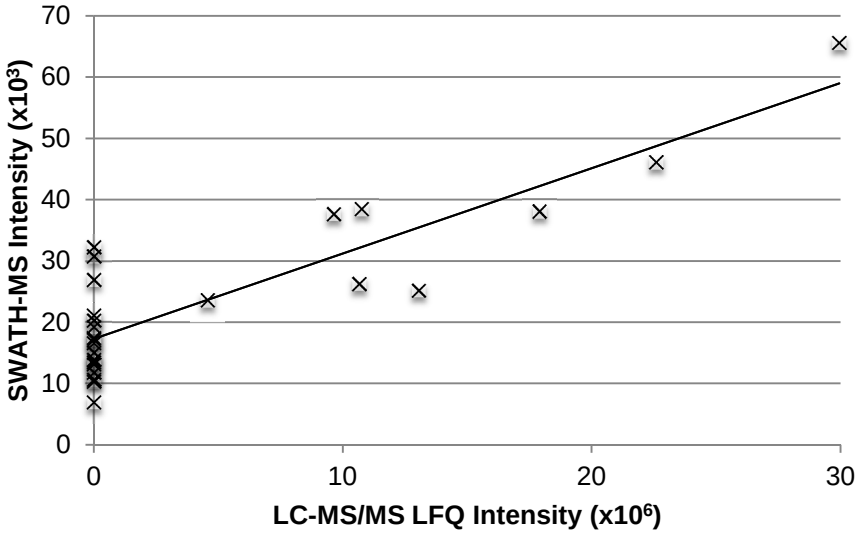

Figure 5.3 – Graph demonstrating the association between the LFQ intensities of COX-1 identified in the samples analysed by LC-MS/MS and the intensity of the same samples analysed by SWATH-MS.
The Pearson's correlation coefficient (R) was 0.87 ($p<0.001$).

5.2.3 COX-1 expression in a membrane enriched LC-MS/MS study

During sample preparation for the section of work described in chapter 4, tissue sections were also cut for a parallel but independent study to be undertaken by another member of the group. Whilst the samples used in this second parallel study overlapped heavily with those in this section of work, some samples were excluded due to lack of tissue availability. This parallel study involved an adapted protein lysis and extraction technique to allow for membrane protein enrichment (the method is not described in this thesis) followed by analysis by LC-MS/MS. The data obtained for COX-1 was also analysed (Figure 5.4). Similar to the initial analysis using the data obtained from the LC-MS/MS study, COX-1 was not identified in any (0/13) of the normal kidney samples. It was however detected in 16/20 (80%) ccRCC samples.

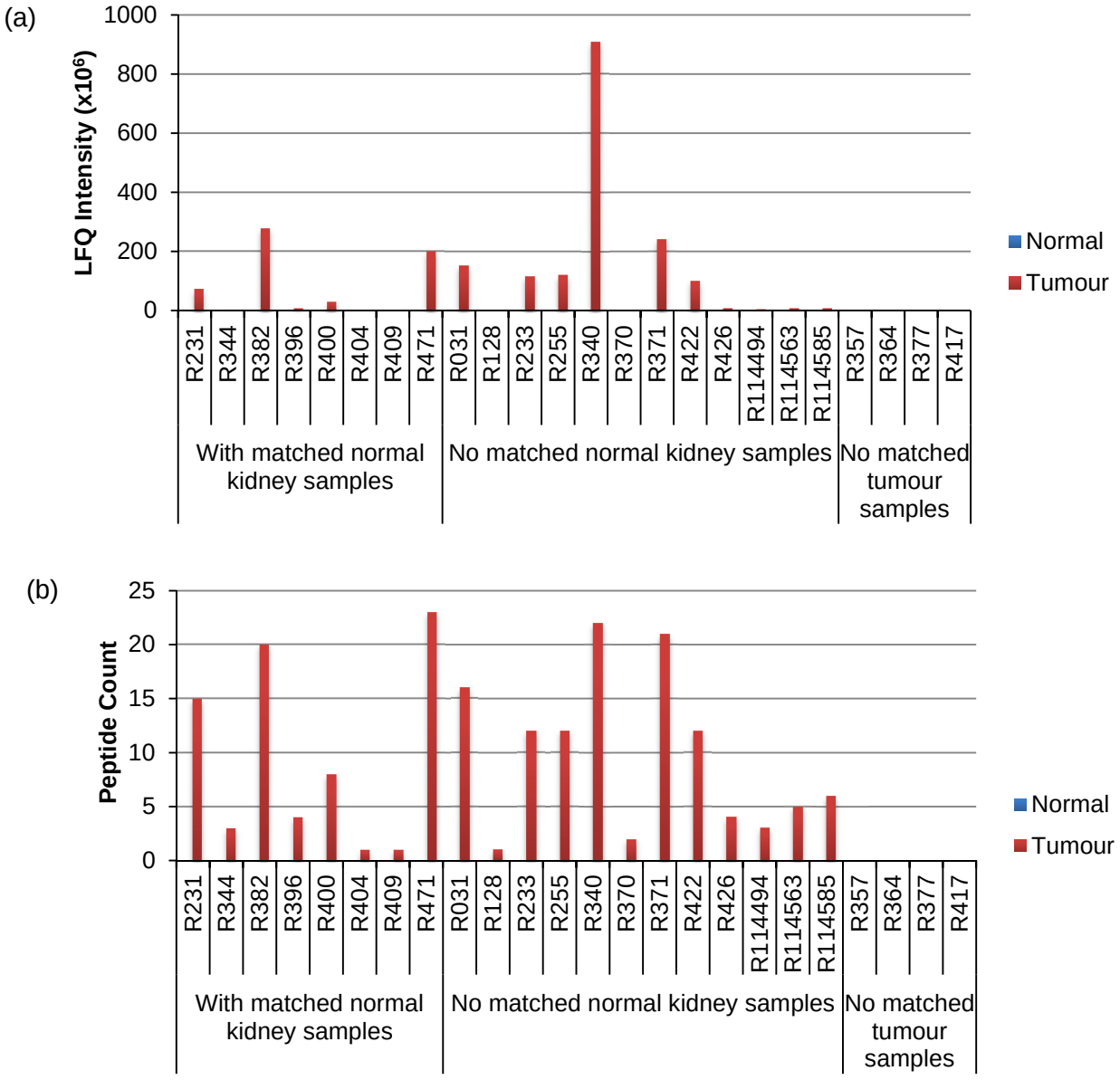

Figure 5.4 - COX-1 expression in a parallel but independent study investigating membrane protein enrichment followed by analysis using LC-MS/MS.
(a) LFQ intensity results (b) peptide count results

Overall these three complementary mass spectrometry analyses are supportive of the discovery that COX-1 is upregulated in a number of ccRCC samples compared with matched normal kidney. There was significant overlap in the peptides identified between the three approaches. These results support its further investigation as a novel therapeutic target in ccRCC.

5.2.4 Western blot analysis of COX-1 expression in ccRCC

COX-1 protein expression was next investigated in ccRCC tumour and normal kidney samples through Western blot analysis. It is known that COX-2, a second protein encoded by a different gene, PTGS2 (chromosome 1q31.1), shares 65% homology with COX-1 at the protein level (www.uniprot.org). As well as sharing similar structural properties, it also catalyses the synthesis of prostanoids (Daikoku et al., 2005). Unlike COX-1, which is reported to be present in a broad range of cells, with constant expression under most physiological and pathological conditions (Wang and Dubois, 2006), COX-2 is an immediate early response gene which is not normally expressed in most cells. Following discussions with Dr. Louise Coletta (Pre-Clinical Translation and Imaging Research Group, University of Leeds) who has a special research focus on COX-2, the colorectal cancer cell line HT-29 was identified as expressing COX-1 and minimal COX-2, and conversely, the HCA7 colorectal cancer cell line was identified as expressing high levels of COX-2, but only minimal expression of COX-1.

Due to the cross-reactivity of most of the available COX-1 and COX-2 antibodies and the similarities in molecular weight, care was taken in their selection for this study. Prior to analysing the lysates prepared in the proteomic study, antibodies were optimised using paired ccRCC tumour and normal kidney lysates selected from frozen stocks. Preliminary experiments confirmed the expected COX isoform expression patterns in the positive control cell lines (Figure 5.5).These Western blots demonstrate a dominant band and some lesser bands in each lysate at the expected molecular weight (range 56-72 kDa) for the majority of the COX-1 isoforms (69, 65, 62, 56, and 72 kDa). These lesser bands may represent the multiple forms or alternatively may reflect some degradation, although unlikely given the care taken with the sample handling and processing. There was a further band at approximately 37 kDa in the tumour sample of R051.

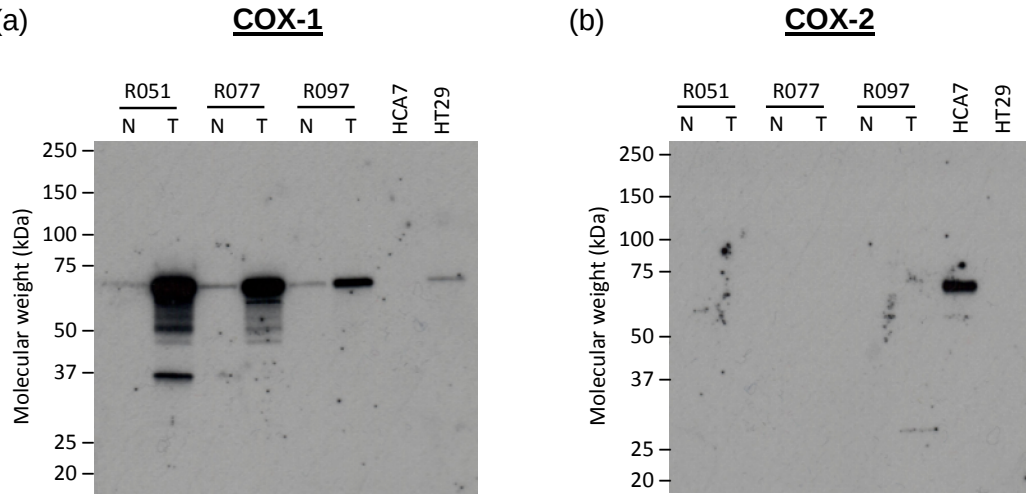

Figure 5.5 - Western blot analysis of three ccRCC tumour (T) and paired normal (N) tissue lysates and the positive control cell lines HCA7 and HT29 for (a) COX-1 and (b) COX-2.
5 μg of protein was loaded per well. A parallel gel was checked for equal loading using Coomassie blue staining. No bands were seen with a no primary antibody control. The expected molecular weight for the COX-1 isoforms are 69, 65, 62, 56, and 72 kDa. The expected molecular weight for COX-2 is 69 kDa.

Overall there was an increased expression of COX-1 in each paired tumour sample compared with the normal kidney counterpart. COX-2 expression was below the threshold of detection in these ccRCC and normal kidney lysates, whilst being detectable in the positive control HCA7 cell line. It was not detected an any of the mass spectrometry analyses. Selected samples from the proteomic study were next subject to Western blot analysis together with the positive control cell lines (Figure 5.6).

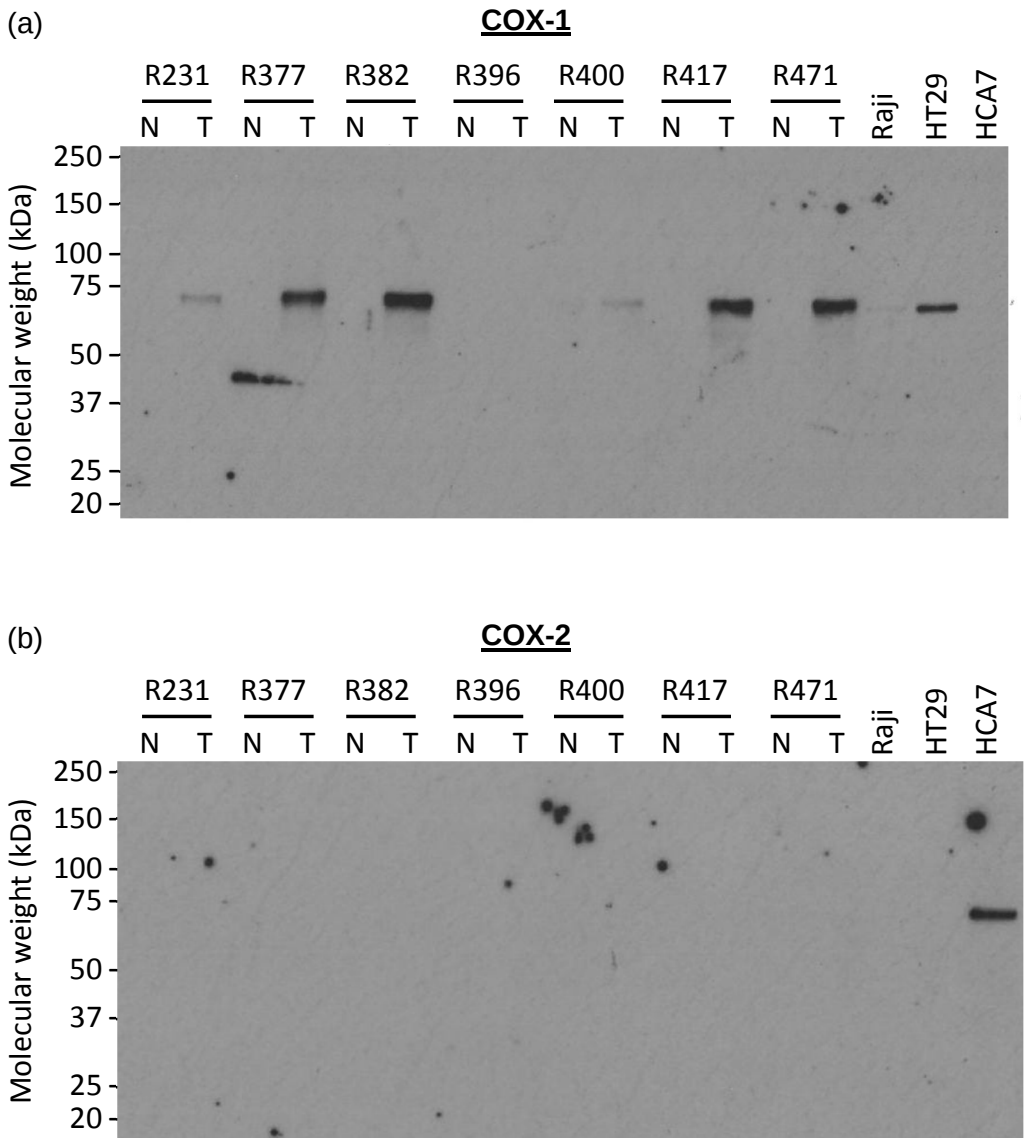

Figure 5.6 – Western blot analysis of seven ccRCC tumour (T) and paired normal (N) tissue lysates chosen from the proteomic study for (a) COX-1 and (b) COX-2.

5 μg of protein was loaded per well and equal loading checked on a parallel Coomassie stained gel. Three positive control cell lines were included in this gel. HT29 and Raji as a positive control for COX-1 and HCA7 as a positive control for COX-2. No bands were seen with a no primary antibody control.

A dominant band (~69 kDa) was seen in each tumour sample (although only faint in R396) and in the positive control cell line lysate consistent with COX-1. This band was upregulated in all ccRCC samples compared with the matched normal kidney samples thus further confirming the upregulation of COX-1 in ccRCC.

5.2.5 Immunohistochemical analysis of COX-1 in ccRCC

Initial workup experiments were carried out to determine the correct antibody concentration using cytospins of the positive control cell lines previously studied using Western blot. HT29 cells stained for COX-1, with minimal staining for COX-2. The HCA7 cells stained strongly for COX-2 and had minimal staining for COX-1.

Tissue samples R377, R417 and R231 were selected for immunohistochemistry (IHC) based on the previous Western blot and mass spectrometry results (although R231 was negative by MS). There was increased staining for COX-1 in all tumour samples in comparison with their normal counterparts (Figure 5.7), which had no or minimal COX-1 detected. There was no staining for COX-2 in all samples and all irrelevant primary and no primary antibody controls were negative. The staining location was cytoplasmic/membranous. These results supported the previous analyses using mass spectrometry and Western blotting.

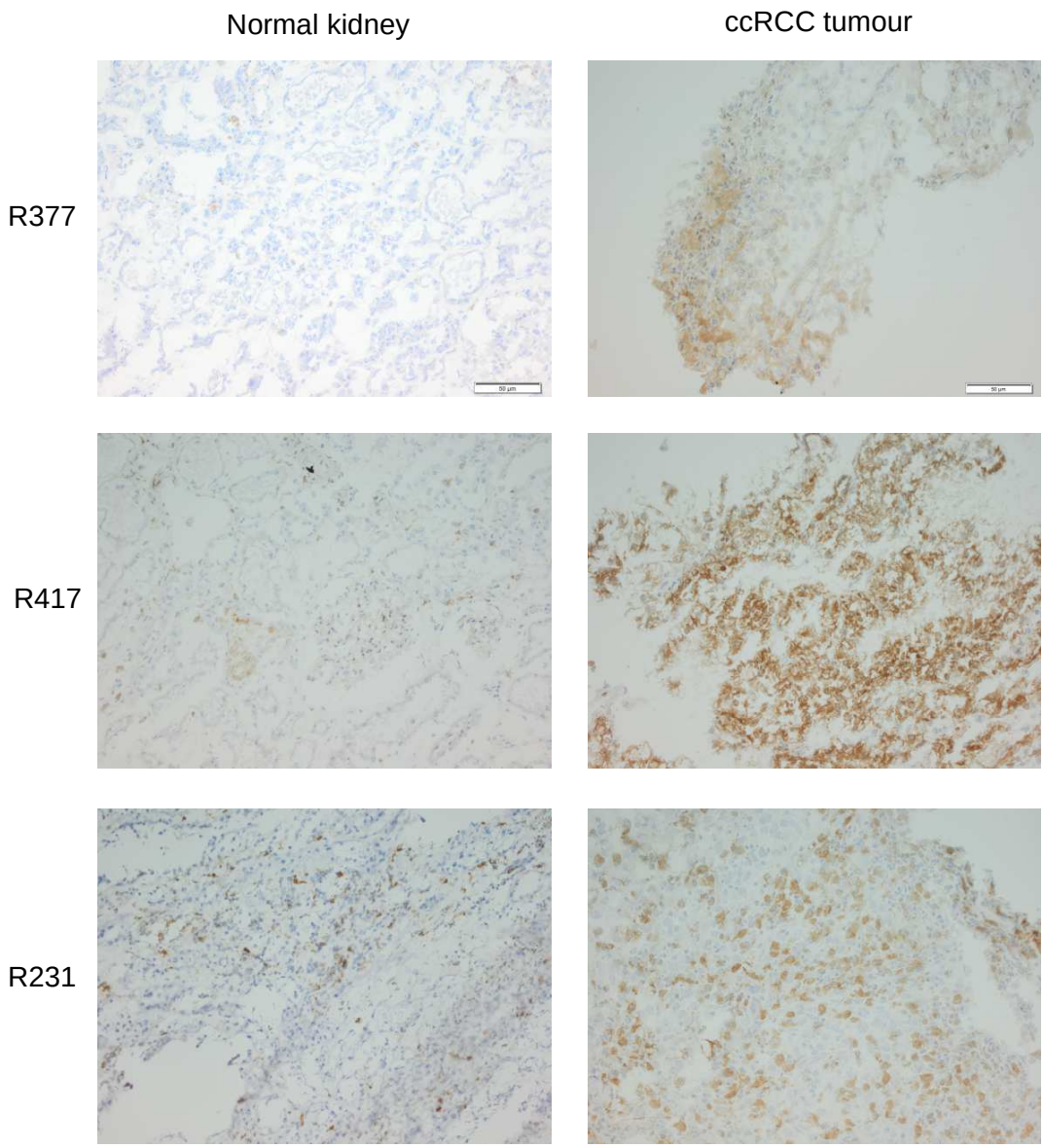

Figure 5.7 – Immunohistochemistry of ccRCC and the matched normal kidney sections for COX-1
Three patient samples were selected based on previous Western blot and mass spectrometry results. No staining was observed in the irrelevant primary and no primary antibody controls (magnification x 160)

5.2.6 Western blot analysis of COX-1 in RCC cell lines

To identify cell lines with a similar COX-1 and COX-2 expression pattern as observed in ccRCC, twelve established RCC cell lines (786-0, A498, CRL1933, HTB46, HTB47, HTB49, A704, ACHN, UO31, SN12-K1 and TK10), the normal kidney cell line (HK2) and the positive control cell lines (HT29 and HCA7) were examined by Western blotting. Four bands were observed across the lysates with varying intensities when blotted for COX-1 (Figure 5.8). The molecular weights for the COX-1 isoforms are 69, 65, 62, 56, 72 and 72 kDa, thereby providing an explanation for the lower three bands, but not the band at approximately 100 kDa. The positive control cell lines had one band consistent with COX-1. There are multiple bands present in most cell lines suggestive of COX-1 expression but the main isoform is slightly smaller than the dominant one seen in RCC tissue and HT29 positive control. This dominant band was not present in the normal kidney cell line (HK2). COX-2 was not observed in any of the ccRCC cell line lysates, although was present in the HCA7 positive control lysate, again this is as seen in RCC tissue.

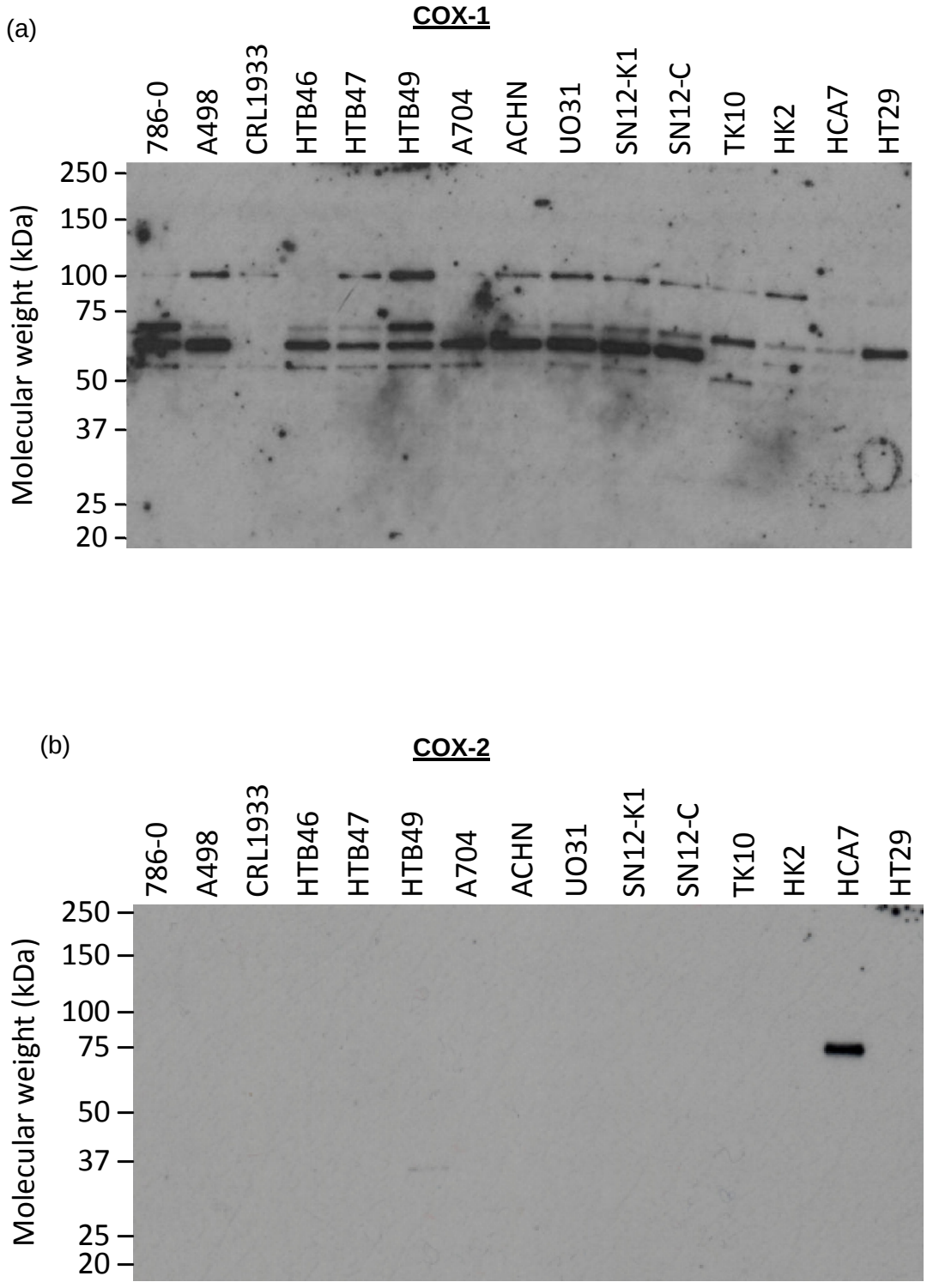

Figure 5.8 - Western blot analysis of RCC cell line lysates and positive control cell lines for (a) COX-1 and (b) COX-2.

A single band is observed in the HT29 and HCA7 positive control cell lines consistent with COX-1 and COX-2 respectively. 5 μg of protein was loaded per well and equal loading was confirmed with a parallel gel stained with Coomassie blue. No bands were seen with a no primary antibody control.

5.2.7 Investigation of COX-1 inhibition in RCC cell lines

Despite the lack of an established RCC cell line with an identical COX-1 expression pattern to primary RCC tissues, several cell lines were selected for investigation of COX-1 and COX-2 inhibition using commercially available inhibitors. The cell lines 786-0, A498, CRL1933 and TK10 were selected to cover a range of expression patterns of the three COX-1 bands of 50 - 75 kDa, visible on Western blot analysis (Figure 5.9). Four COX inhibitors were selected for investigation based on their differing inhibitory values for COX-1 and COX-2 (Table 5.1).

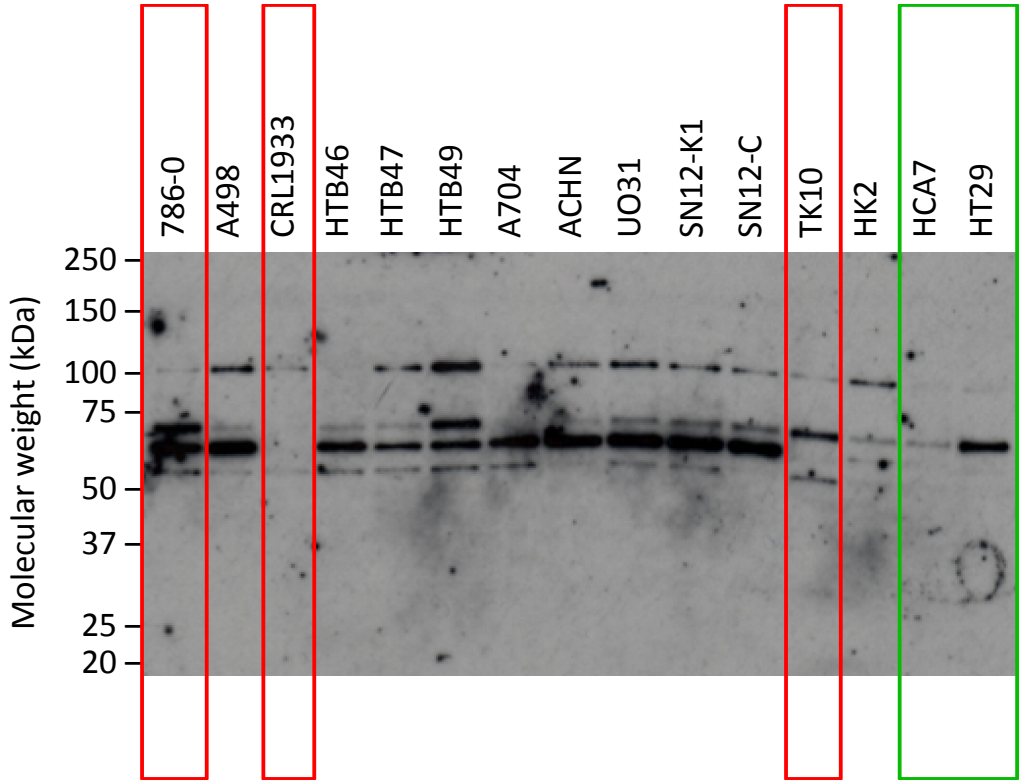

Figure 5.9 – Selection of cell lines for investigation of COX inhibition based on the pattern of band expression for COX-1 using Western blot.
The cell lines selected for further investigation of COX-1 and COX-2 inhibition are highlighted in red. The positive control cell lines are highlighted in green. No bands were seen with a no primary antibody control.

Table 5.1 – COX-1 and COX-2 inhibitors selected for investigation in this study.
Four COX inhibitors were selected based upon their IC_{50} values for inhibiting COX-1 and COX-2. DMSO was used as the organic solvent for all inhibitors

COX Inhibitor	Max. solubility in organic solvent (mg/ml) / (mM)	Stock Conc. (mM)	IC_{50} COX-1 (μM)		IC_{50} COX-2 (μM)		References
			Recombinant protein	Human monocytes	Recombinant protein	Human monocytes	
SC-560	35.0 / 100	100	0.009	0.005	6.30	1.4	(Smith et al., 1998)
FR122047	1.00 / 2	2	0.028	N/A	65.0	N/A	(Ochi et al., 2000),
Indomethacin	17.5 / 50	50	1.670	0.009	24.6	0.31	(Barnett et al., 1994)
Celecoxib	10.0 / 26	25	15.00	82	0.04	6.8	(Penning et al., 1997)

5.2.7.1 SC-560

SC-560 is a highly selective COX-1 inhibitor with an approximately 700 fold higher selectivity for COX-1 than COX-2. Cytotoxicity was observed at concentrations above 1 μM (Figure 5.10). The three RCC cell lines exhibited a range of sensitivities to SC-560. The CRL 1933 cell line was the most sensitive.

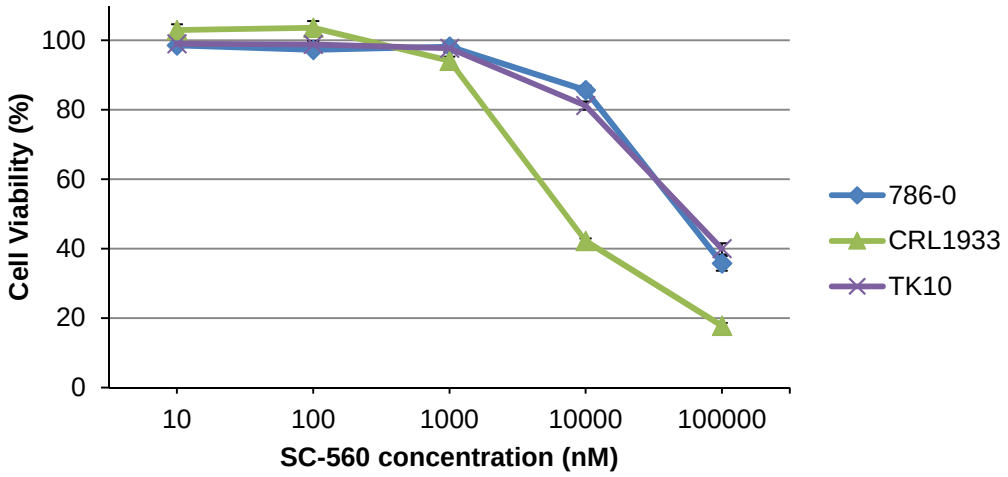

Figure 5.10 – Investigation of COX inhibition in RCC cell lines using the selective COX-1 inhibitor, SC-560.
Cell viability was expressed relative to the vehicle control. 786-0, CRL1933 and TK10 cells were seeded at 1000, 2000, 1500 cells/well respectively. (There were 3 independent repeats per experiment, each with 3 replicates per condition). The error bars represent the standard error of the mean for each concentration of SC-560.

The A498 RCC cell line was next chosen to investigate the effect of COX-1 inhibition on cell growth. Cell confluence was measured each hour for 72 hours using the Incucyte® equipment and software. SC-560 inhibited cell growth at concentrations above 1 μM (Figure 5.11).

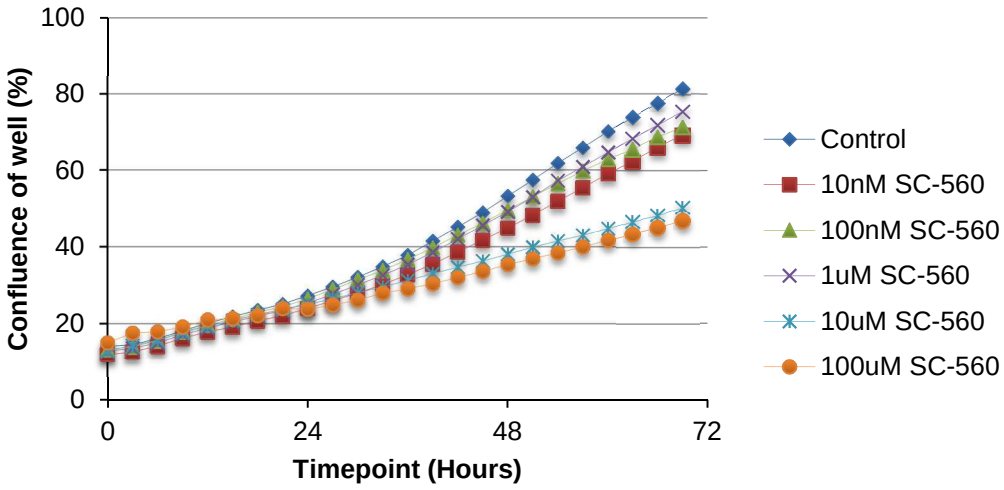

Figure 5.11 – Incucyte analysis of A498 RCC cell line growth over 72 hours of exposure to the selective COX-1 inhibitor, SC560.
This graph represents one experiment with three replicates and is representative of the three independent repeats.

5.2.7.2 FR122047

FR122047 is another selective inhibitor of COX-1. The IC_{50} for COX-1 is 28nM and for COX-2 is 65 μM. There was no cell death seen with concentrations up to 2μM (Figure 5.12). The poor solubility of this compound in the selected organic solvent did not allow its investigation at higher concentrations.

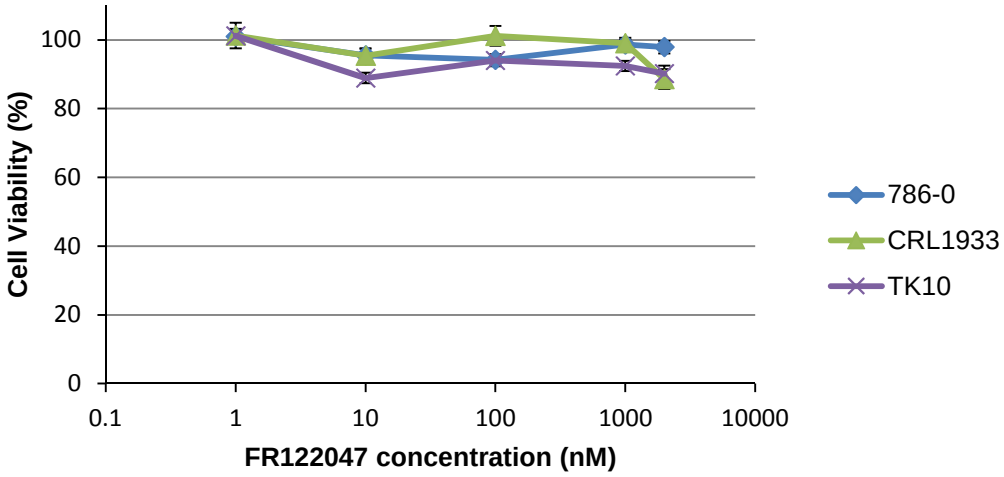

Figure 5.12 - Investigation of COX inhibition in RCC cell lines using the selective COX-1 inhibitor, FR122047.

Cell viability was expressed relative to the vehicle control. 786-0, CRL1933 and TK10 cells were seeded at 1000, 2000, 1500 cells/well respectively. (There were 3 independent repeats per experiment, each with 3 replicates per condition). The error bars represent the standard error of the mean for each concentration of FR122047.

5.2.7.3 Indomethacin

Indomethacin is a less selective COX-1 inhibitor, with a 14 fold higher selectivity for inhibition of COX-1 than COX-2. Its IC_{50} values are 1.67 and 24.6 μM for COX-1 and COX-2 respectively. Approximately 20% cell death was seen at 50 μM (Figure 5.13).

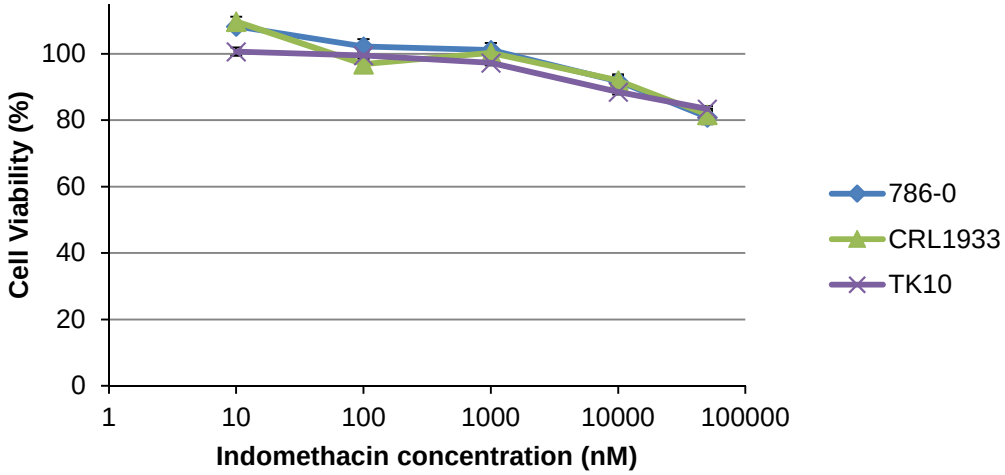

Figure 5.13 - Investigation of COX inhibition in RCC cell lines using the COX inhibitor Indomethacin.

Cell viability was expressed relative to the vehicle control. 786-0, CRL1933 and TK10 cells were seeded at 1000, 2000, 1500 cells/well respectively. (There were 3 independent repeats per experiment, each with 3 replicates per condition). The error bars represent the standard error of the mean for each concentration of Indomethacin.

5.2.7.4 Celecoxib

Finally a selective COX-2 inhibitor was chosen to investigate the possibility that COX-2 was being expressed at lower levels than our detection capabilities, but that its inhibition, rather than COX-1 was resulting in cell death. Celecoxib was chosen due to its IC_{50} values of 15 μM and 40 nM for COX-1 and COX-2 respectively. Cytotoxicity was observed in the CRL1933 cell line at concentrations above 1 μM and in the 786-0 and TK10 cell lines at concentrations above 10 μM (Figure 5.14).

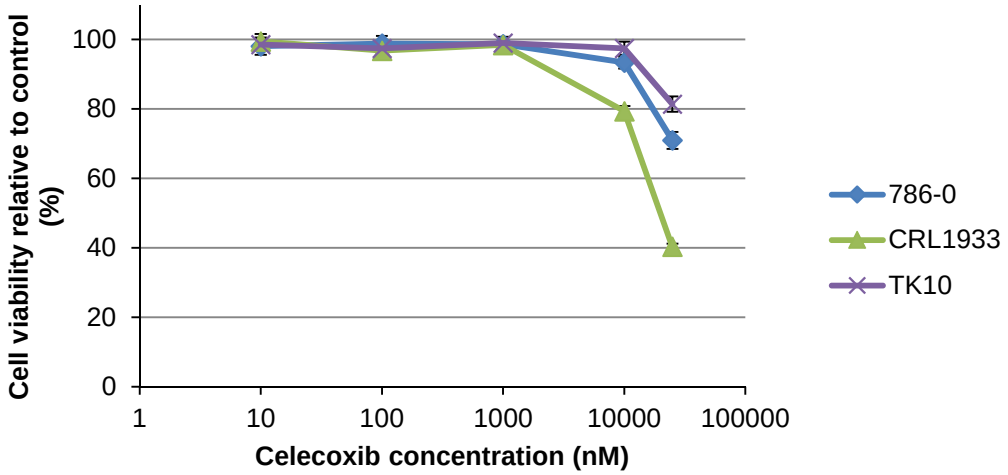

Figure 5.14 - Investigation of COX inhibition in the RCC cell lines using the selective COX-2 inhibitor Celecoxib.

The cell viability was expressed relative to the vehicle control. 786-0, CRL1933 and TK10 cells were seeded at 1000, 2000, 1500 cells/well respectively. (There were 3 independent repeats per experiment, each with replicates per condition). The error bars represent the standard error of the mean for each concentration of Celecoxib

This concluded the investigation of COX-1 in RCC. Whilst it is upregulated in ccRCC at a protein level as evidenced in the MS analyses and Western blot analysis, there were no representative RCC cell line model identified.

5.3 Proteasome subunit beta type-9 (PSMB9)

5.3.1 Proteasomal subunit expression in the proteomic study

On initial review of the data obtained from the LC-MS/MS analysis of primary ccRCC and matched normal kidney tissue, the proteasome subunit beta type-9 (PSMB9) was identified as being expressed in all ccRCC samples included in the study but was expressed in only one matched normal sample, LR404, at a low level (Figure 5.16).

PSMB9 is a subunit of the proteasome complex, which acts to cleave redundant proteins. Proteasomal inhibitors are in clinical use in the treatment of multiple myeloma and are being investigated in other cancer types. Inflammatory cytokines induce a change from the constitutively expressed proteasomal subunits PSMB5, PSMB6 and PSMB7 to the immunoproteasomal subunits PSMB8, PSMB9 and PSMB10 respectively, which is thought to be an adaptive response (Ho et al., 2007) (Kloetzel, 2001). To further investigate this, this analysis was expanded to include the six proteasomal subunits mentioned (Figure 5.15 and Figure 5.16)

Of the constitutive proteasomal subunits, proteasome subunit beta type-5 (PSMB5) was expressed in all 13 normal samples included in the study. It was expressed in 5/25 (20%) of the ccRCC samples, but at lower levels than the normal kidney samples overall. These 5 samples did not have matched normal kidney therefore the expression relative to the matched normal sample could not be ascertained. Proteasome subunit beta type-6 (PSMB6) was again expressed in all normal samples and 18/25 of the ccRCC samples, but overall its expression was lower than in the normal kidney samples. Proteasome subunit beta type-7 was only detected in one normal sample, LR377, and was not detected in any of the ccRCC samples

The proteasomal subunits belonging to the immunoproteasome were next investigated. Proteasome subunit beta type-8 (PSMB8) was expressed in 21/25 (84%) of ccRCC samples and in only 2/13 (15%) of the normal kidney samples. In these two normal kidney samples, the expression levels were lower than the matched ccRCC samples. PSMB9 was expressed in all 25 ccRCC samples and only 1/13 (8%) of the normal kidney samples, where the expression in the matched ccRCC sample was much higher. Proteasome subunit beta type-10 (PSMB10) was expressed in

5/25 (20%) of the ccRCC samples but was not found to be expressed in any of the normal kidney samples (Figure 5.16).

Overall this data demonstrates a shift between the predominant expression of the constitutive members of the proteasome in normal kidney samples to an predominance in expression of the immunoproteasomal subunits in ccRCC.

This pattern of expression was replicated in the data obtained from the analysis of the samples using SWATH-MS. As with the analysis of COX-1, there was an intensity reading for each protein in every sample. Defining upregulation as an intensity level of over twice the matched normal kidney sample, and down regulation the opposite, PSMB5 was downregulated in 1/13 (8%) (LR344) and upregulated in 1/13 (8%) (LRV231) of the ccRCC samples. PSMB6 was downregulated in 4/13 (31%) of the ccRCC samples and PSMB7 was not differentially expressed between ccRCC and normal kidney. PSMB8 was upregulated in 10/13 (77%) of ccRCC samples and PSMB9 was upregulated in 10/13 (77%) of ccRCC samples compared with matched normal kidney. PSMB10 was not detected in the SWATH-MS analysis. Overall these results demonstrated a striking upregulation of PSMB8 and PSMB9 in ccRCC compared to normal kidney (Figure 5.17 and Figure 5.18).

These results were again supported by the LC-MS/MS study that enriched for surface membrane proteins (Figure 5.19 and Figure 5.20).

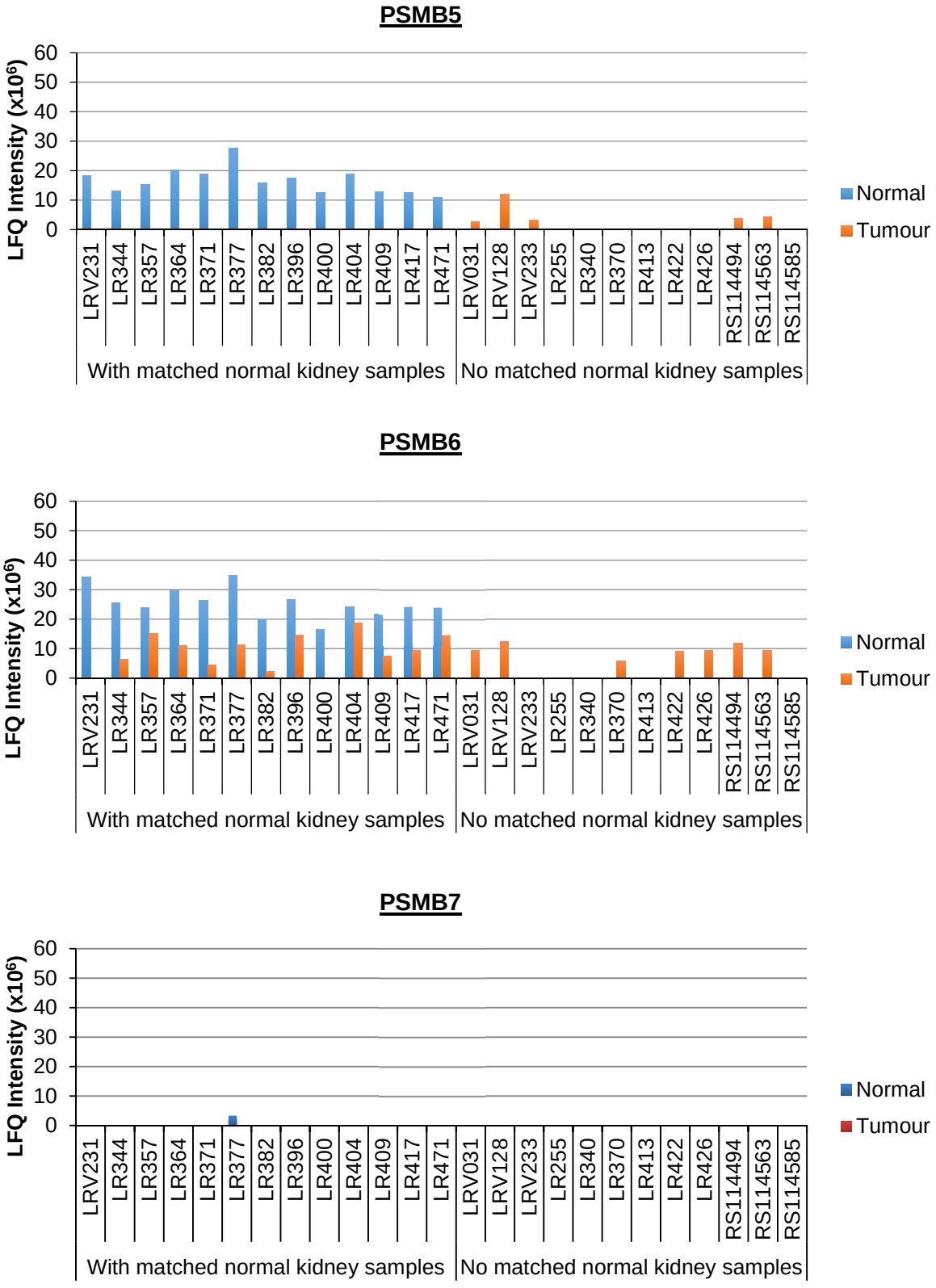

Figure 5.15 – Expression of the consitiutive proteasomal subunits (PSMB5, PSMB6 and PSMB7) in primary RCC and normal kidney from the proteomic study using LC-MS/MS.

(n=13 matched pairs plus 12 additional unmatched ccRCC samples)

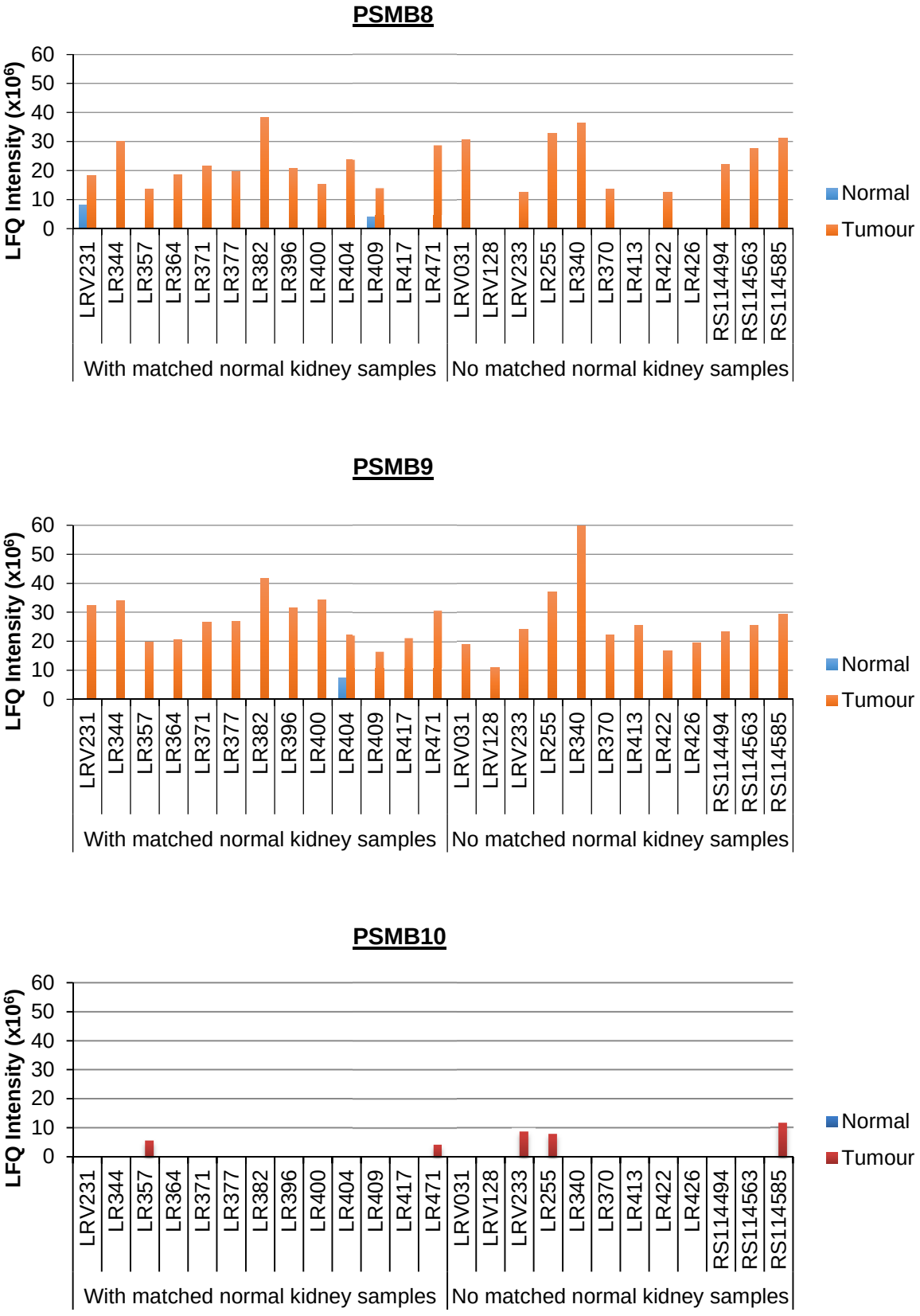

Figure 5.16 - Expression of the immunoproteasomal subunits (PSMB8, PSMB9 and PSMB10) in primary RCC and normal kidney from the proteomic study using LC-MS/MS

(n=13 matched pairs plus 12 additional unmatched ccRCC samples).

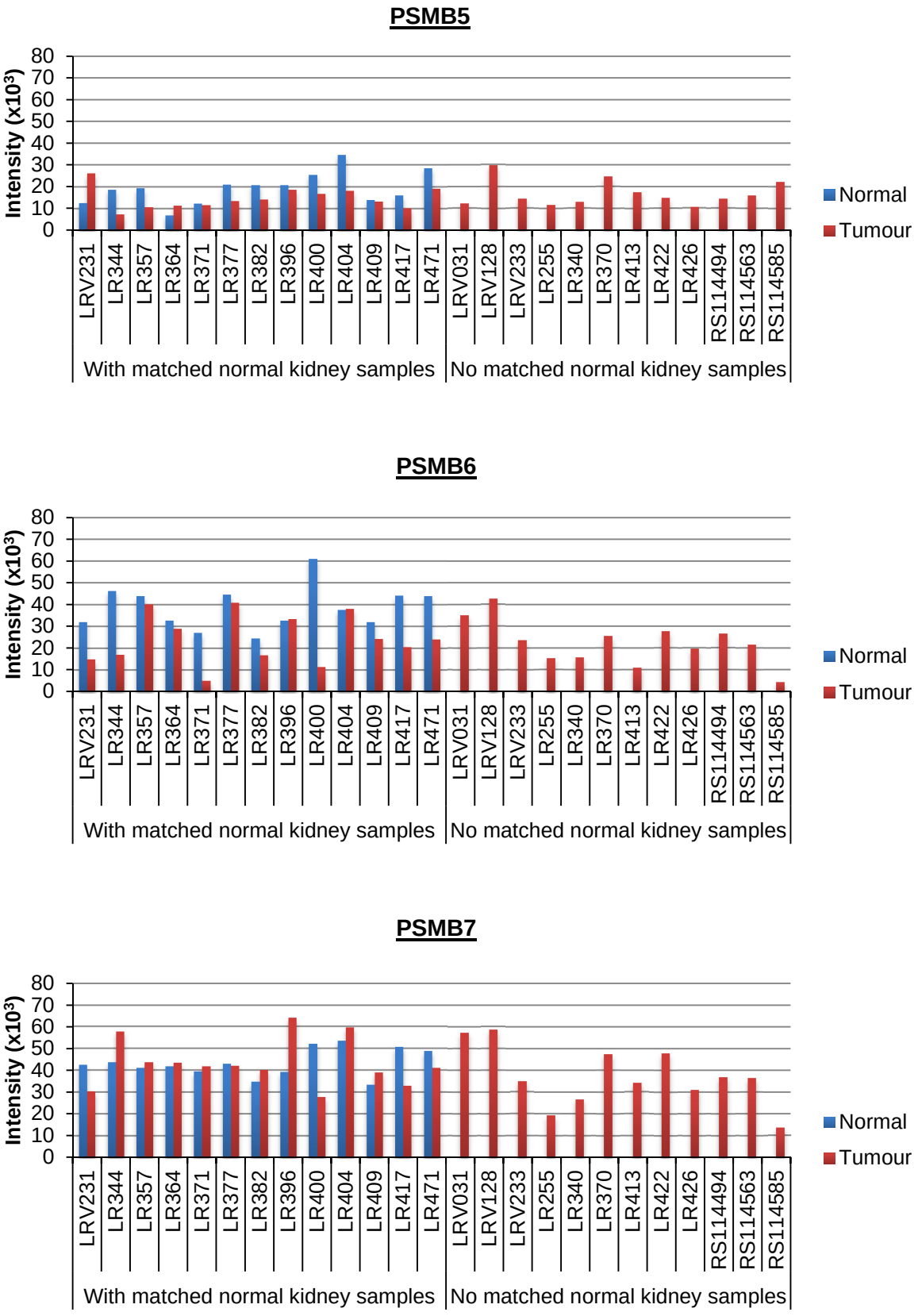

Figure 5.17 - Expression of the consitiutive proteasomal subunits (PSMB5, PSMB6 and PSMB7) in primary RCC and normal kidney from the proteomic study using SWATH-MS

(n=13 matched pairs plus 12 additional unmatched ccRCC samples).

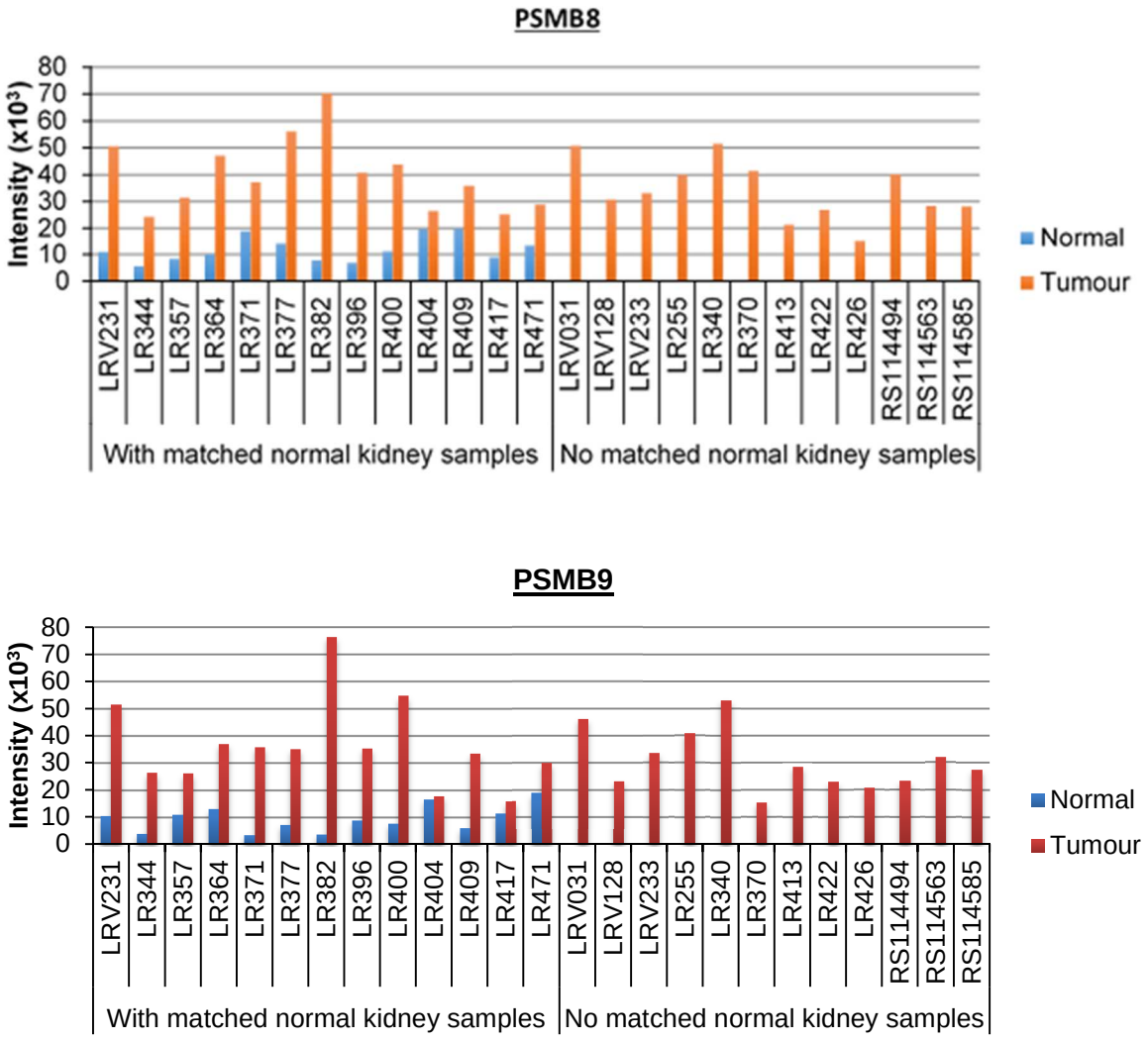

Figure 5.18 - Expression of the consitiutive proteasomal subunits (PSMB8 and PSMB9) in primary RCC and normal kidney from the proteomic study using SWATH-MS.

(n=13 matched pairs plus 12 additional unmatched ccRCC samples PSMB10 was not detected in this analysis)

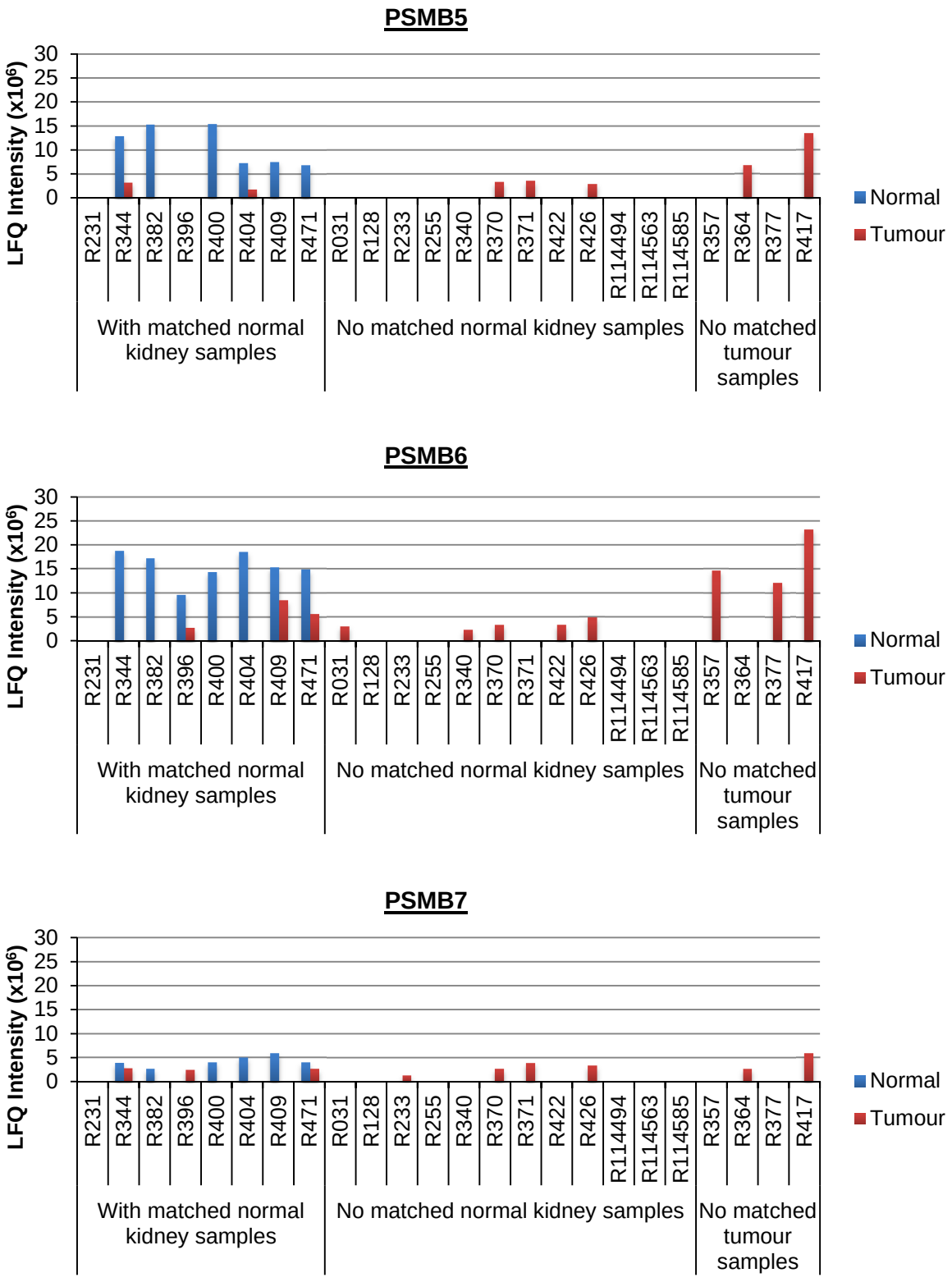

Figure 5.19 - Expression of the consitiutive proteasomal subunits (PSMB5, PSMB6 and PSMB7) in primary RCC and normal kidney from the membrane-enriched proteomic study using LC-MS/MS.

(n=8 matched pairs plus 12 additional unmatched ccRCC samples and 4 unmatched normal kidney samples)

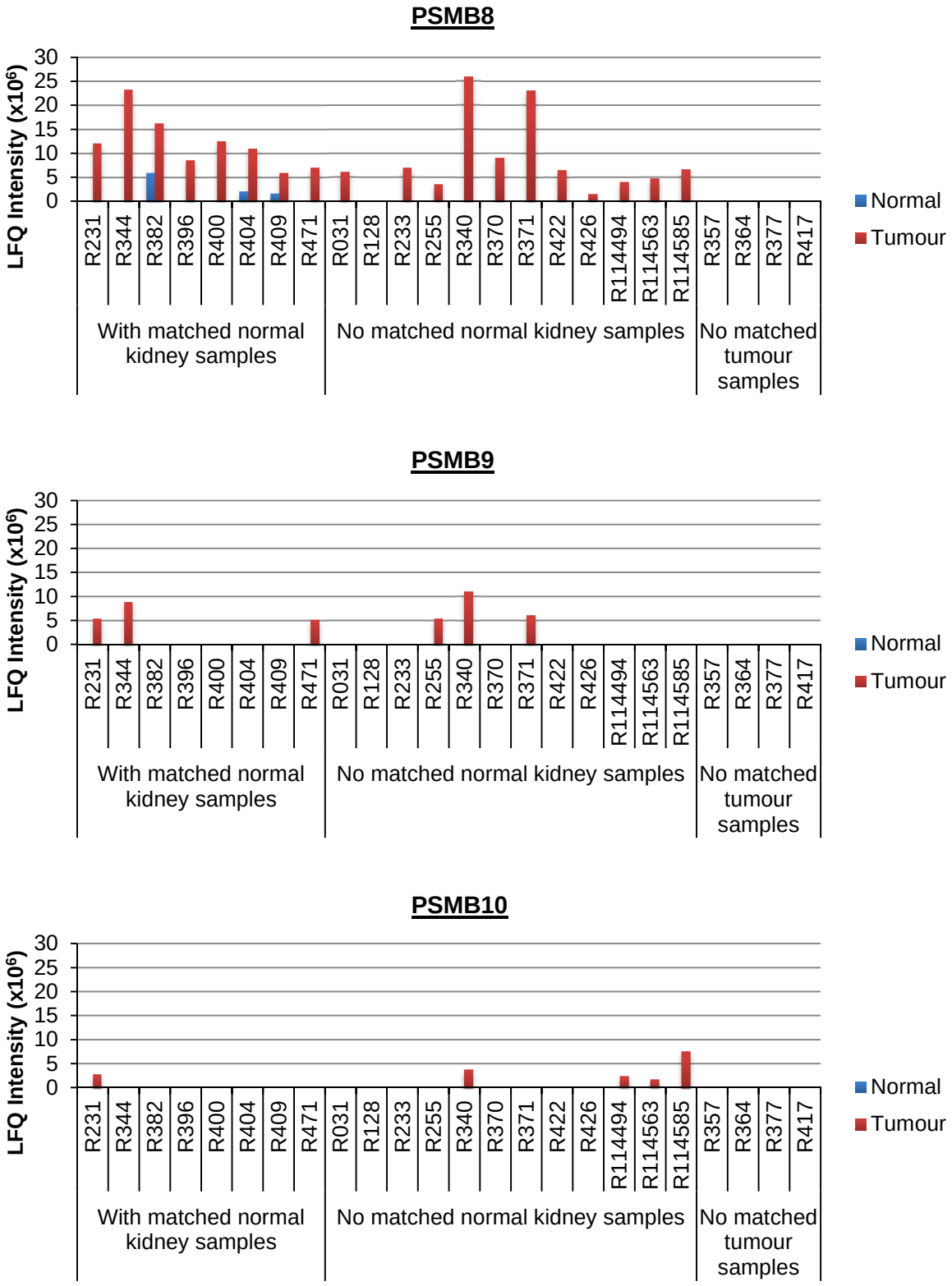

Figure 5.20 - Expression of the consitiutive proteasomal subunits (PSMB8, PSMB9 and PSMB10) in primary RCC and normal kidney from the membrane-enriched proteomic study using LC-MS/MS.

(n=8 matched pairs plus 12 additional unmatched ccRCC samples and 4 unmatched normal kidney samples)

5.3.2 Western blot analysis of PSMB9 expression in ccRCC tissue

PSMB9 protein expression was next investigated by Western blotting of tissue samples (Figure 5.21). Three samples (RR051, R077 and R097) were electrophoresed on a polyacrylamide gel. The Western blot demonstrated upregulation of PSMB9 in the three ccRCC samples compared with their matched normal kidney. The band was seen in the matched normal kidney, but was faint. There were two positive control cell lines, mouse spleen and Raji cells were chosen based upon the antibody datasheet and previous publications. PSMB9 has been noted to exist as two isoforms in humans, weighing 23 kDa and 22 kDa, and in mice as one isoform weighing 23 kDa.

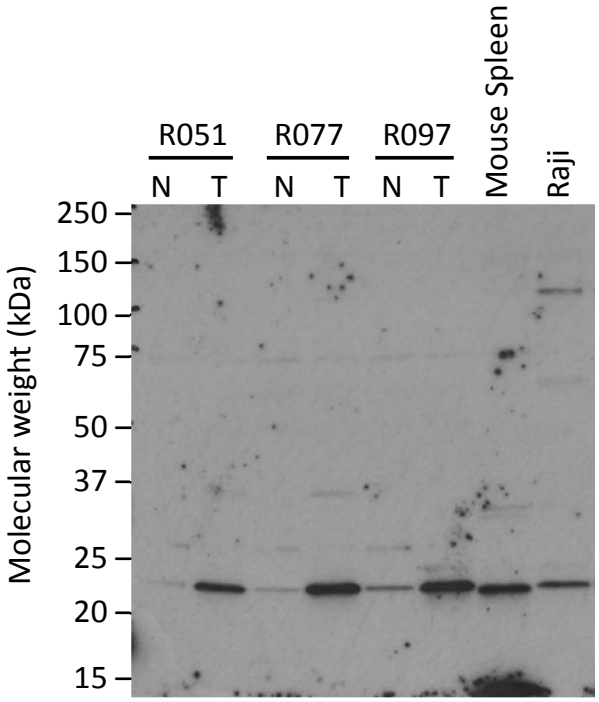

Figure 5.21 - Western blot analysis of three ccRCC tumour and paired normal tissue lysates (not included in the proteomic study) for PSMB9.

Two positive control cell lines are included in this blot. 5 μg of protein was loaded per well. Equal loading was confirmed using Coomassie blue staining of an equally loaded parallel gel. PSMB9 has two known isoforms measuring 23 and 22 kDa.

The band seen with mouse spleen was noted to be at a slightly lower molecular weight than the band seen in the other lysates. The reason for this is not known and is not explained by the expected molecular weights of PSMB9 (www.uniprot.org). This was assumed to be related to interspecies variation. The Raji cell line lysate was chosen to proceed as a positive control.

Seven samples from the proteogenomic study were next selected and blotted for PSMB9. Whilst upregulation of PSMB9 compared with the matched normal kidney samples was observed in all seven ccRCC samples, they were observed to be a higher molecular weight than the positive control cell line. The bands observed in the ccRCC samples were also broader than the bands seen previously, leading to the conclusion that they had gained a post-translational modification in the handling between the lysis and running the gel (Figure 5.22).

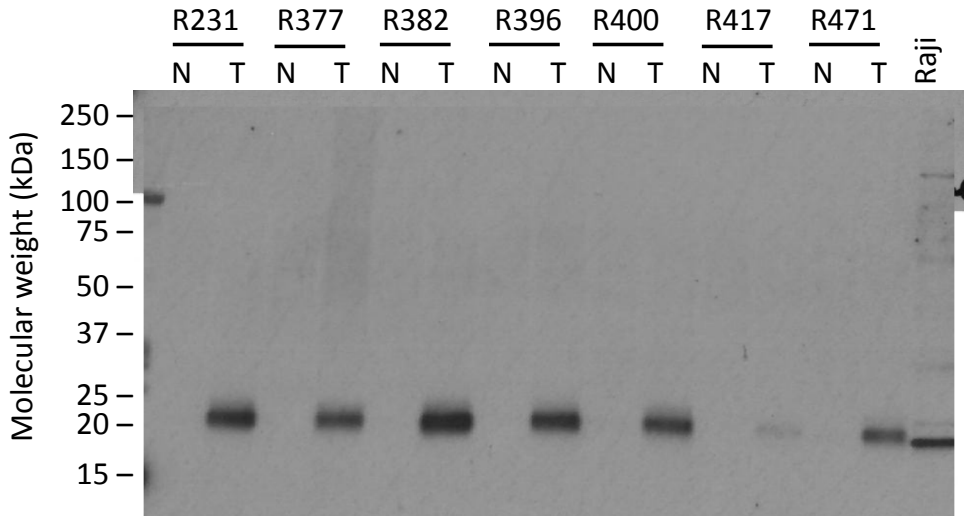

Figure 5.22- Western blot analysis of seven ccRCC tumour and paired normal tissue lysates for PSMB9.

These lysates were used in the proteogenomic study. This blot demonstrates a band between 25 and 20 kDa, consistent with PSMB9. This band is not seen in the paired normal tissue. 5 μg protein load per well.

5.3.3 Western blot analysis of PSMB9 expression in RCC cell lines

PSMB9 expression was investigated in RCC cell lines using Western blot. Twelve RCC cell lines (786-0, A498, CRL1933, HTB46, HTB47, HTB49, A704, ACHN, UO31, SN12-K1 and TK10) and the normal kidney cell line (HK2) were investigated. PSMB9 was expressed in all cell lines except CRL1933 (Figure 5.23). There were faint bands seen at approximately 100 kDa. These were not present in a no primary antibody control. Analysis of the immunogen for this primary antibody suggests it does not react with any other protein.

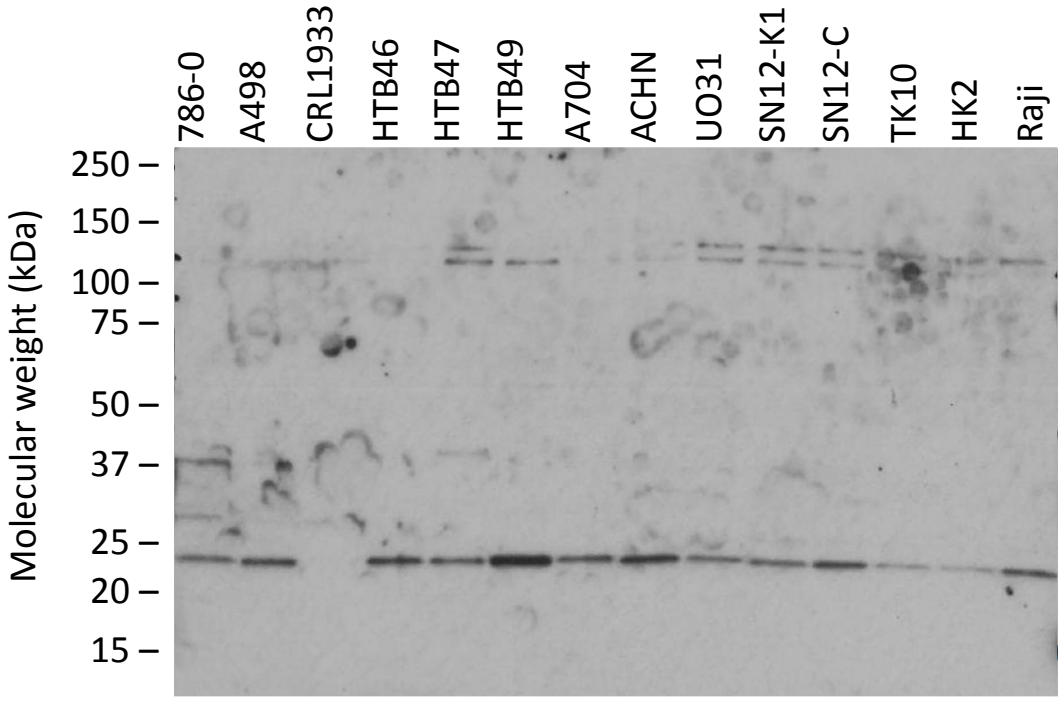

Figure 5.23 – Western blot analysis of RCC cell line lysates for PSMB9. 5 μg of protein was loaded per well. Equal loading was confirmed with an equally loaded gel run In parallel and stained with Coomassie blue.

5.4 Discussion

Following on from the detailed proteomic analysis performed in Chapter 4, this section of work has further contributed to the characterisation of the expression of two proteins, namely COX-1 and PSMB9, which had been identified as being differentially expressed in ccRCC compared to matched normal tissue.

5.4.1 COX-1

5.4.1.1 COX-1 protein expression in ccRCC

COX-1 has been identified as being upregulated in 31–50% of the ccRCC samples included in this proteomic study (LC-MS/MS and SWATH-MS) and in the independent membrane enriched LC-MS/MS study. The findings of these three parallel analyses all correlated with one another. This finding was further confirmed using Western blot (WB) analysis of tissue samples. Two samples were observed to have upregulation of COX-1 using WB that had not been highlighted in the MS studies (R231 and R382).

The SWATH-MS analysis identified COX-1 presence in all samples including normal kidney, although at an overall lower intensity than in the ccRCC samples. This is likely to relate to the higher sensitivity of the SWATH-MS in analysing samples (Guo et al., 2015b). In this case, the analysis of the SWATH-MS data was based around one specific peptide sequence per protein, in this case 'LQPFNEYR', which theoretically if not carefully chosen correctly could mean the identification of other proteins, or the non-detection of appropriate proteins. To confirm this peptide sequence is unique, it was entered into the BLAST application (www.uniprot.org) and was found to be specific to all six known isoforms of COX-1 and reassuringly had no homology for any other proteins. This peptide sequence only appeared in the membrane enriched study and not the other LC-MS/MS study. This may be due to the sensitivity of LC-MS/MS or MaxQuant, the MS spectra database. Immunohistochemistry on three cases of matched ccRCC ad normal kidney samples demonstrated upregulation of COX-1, which correlated with the Western blot results. The location of staining was cytoplasmic/membranous which concurs with the staining patterns seen in RCC according to 'The Human Protein Atlas' (www.proteinatlas.org). Multiple bands were observed in a panel of 12 established RCC cell lines and one normal kidney cell line using Western blotting, thus there was no cell line model fully representative of the primary ccRCC samples in term of this Western blot pattern.

COX-1 belongs to the cyclooxygenase family and exists alongside a second isoenzyme, COX-2. They are encoded by separate genes, PTGS1 on chromosome 9q33.2 and PTGS2 located on chromosome 1q31.1. They share 65% homology in their protein sequences (www.uniprot.org) resulting in similar structural and kinetic properties (Daikoku et al., 2005). COX-1 is a key protein involved in prostanoid synthesis and is ubiquitously expressed in a broad range of cells, with constant expression under most physiological and pathological conditions. It catalyses the conversion of arachidonate to the key upstream prostanoid prostaglandin H2 (PGH2), which in turn is subsequently metabolised to the downstream prostaglandin isoforms D2, E2, F2, I2 and thromboxane A2 (TXA2) (Mauro et al., 2010) (Feng et al., 1993). The prostanoids have various roles including that of cell homeostasis, involvement in vasoconstriction and proliferation of vascular smooth muscle cells, and in the regulation of immune function and kidney development (Patrono et al., 2001) (Williams et al., 1999). COX-1 exists as 6 isoforms weighing 69, 65, 62, 56 and 72 kDa. The specific function of each isoform is unknown. Like COX-1, COX-2 catalyses the synthesis of prostanoids, although it is an immediate early response gene which is not normally expressed in most cells (Wang and Dubois, 2006), It is the principal isozyme responsible for production of inflammatory prostaglandins, thereby positioned to play a potential role in carcinogenesis. This has led to the development of selective COX-2 inhibitors and a large number of studies investigating COX-2 in different cancer types. Given its similar structural and biological properties, its protein expression was also investigated in the proteomic study. COX-2 was not identified in any of the ccRCC and normal kidney samples in any of the MS analyses, suggesting either its absence or presence below the level of detection. Further to this, Western blotting for COX-2 across 10 ccRCC and adjacent normal kidney samples, and a 12 established RCC cell lines, and immunohistochemistry of 3 paired ccRCC and normal kidney samples did not detect any COX-2 expression.

COX-1 expression has been previously investigated in RCC, but focusing in particular on correlation with prognostic features of the tumour. A study of 42 paired RCC samples (86% ccRCC) using qRT-PCR demonstrated a significantly higher level of mRNA for COX-1 in RCC compared with matched normal kidney. This was confirmed at the protein level by immunohistochemistry of 196 RCC (77% ccRCC) and 91 adjacent normal paraffin-embedded tissue samples. High expression of COX-1

correlated with larger tumour size, pathological stage, TNM stage and tumour recurrence. Survival analysis indicated that patients with high expression of COX-1 had a shorter overall survival time (Yu et al., 2013). A similar study using immunohistochemical analysis of 64 RCC (70% ccRCC) paraffin embedded tissue samples identified high COX-1 expression in 62.5% of cases, with a similar correlation with tumor size, grade and stage (Osman and Youssef, 2015).

COX-1 has been shown to be upregulated at a protein and mRNA level in other cancer types compared to the adjacent matched normal tissue including untreated epithelial ovarian cancer (Gupta et al., 2003), and cervical adeno- and squamous cell carcinoma (Sales et al., 2002). Using Immunohistochemical staining and RT-PCR, COX-1 was shown to exhibit increasing expression in the progression from normal oral mucosa, through hyperplasia, dysplasia and carcinoma (Mauro et al., 2010). Similarly COX-1 has been shown to be upregulated in breast cancer (Hwang et al., 1998) and prostate cancer (Kirschenbaum et al., 2000) using Western blot.

5.4.1.2 COX-1 inhibition in ccRCC

The cyclooxygenase inhibitors include the non-steroidal anti-inflammatory drugs (NSAIDs), each having varying selectivity for COX-1 and COX-2, but none are specific for either COX protein. Four inhibitors were selected based upon their varying selectivity for COX-1 and COX-2 but recognizing that the IC_{50} values very much depend upon the method in which they were derived. Table 5.1 details the IC_{50} values for both COX-1 and COX-2 from studies using recombinant protein and also human monocytes. The solubilised recombinant protein or the cells were incubated with arachidonic acid and the IC_{50} was determined from measurement of the converted prostaglandin E2 (PGE2). There will be variability between these models and they are unlikely to reflect the IC_{50} values when studied using *in-vivo* models. In this study, the selective COX-1 inhibitors SC-560 and indomethacin both induced cell death *in-vitro* at concentrations above 1 μM. In addition to the variability in IC_{50} values, this may also suggest that the COX-1 inhibitor is acting through a different pathway or on an alternative target at the higher concentrations, for example COX-2 given its distinct homology with COX-1 and despite it not being detected in this study. For this reason a highly selective COX-2 inhibitor, celecoxib was also used with IC_{50} values for COX-1 and COX-2 of 15 μM and 0.04 μM respectively in recombinant protein models. Cell death was seen at concentrations between 1 and 25 μM, which still does not exclude

cell death as a result of COX-1 or other pathway inhibition. The COX inhibitor FR122047 did not cause cell death up to concentrations of 2 μM. Retrospectively it would have been useful to source a positive control cell line to provide confidence in the results. Overall, the COX-1 inhibitors cause cell death in established RCC cell lines albeit at much higher concentrations and are therefore still of potential interest in this investigation.

At this point it is useful to mention some of the inhibitors that have been investigated using *in-vivo* models and their beneficial effects in the cancer setting. SC-560 was demonstrated to reduce the growth of a mouse model of epithelial ovarian cancer, in which genetic and oncogenic modifications were experimentally engineered into mouse ovarian surface epithelial cells that were subsequently allografted into host mice to produce tumours (Daikoku et al., 2005). Similar to RCC, COX-2 was not expressed in this tumour type, and in turn the selective COX-2 inhibitor had little effect on tumour growth (Daikoku et al., 2005). Whilst this highly engineered cell type may not be representative of primary tumours, it is still a significant finding. Aspirin is an example of a potent COX inhibitor with a 50-100 fold selectivity for COX-1 (Patrono et al., 2004). Population-based studies have established that the long-term intake of COX inhibitors such as aspirin are associated with a significant reduction in the incidence and mortality from colorectal cancer (Gupta and Dubois, 2001) (Rothwell et al., 2010). Unlike RCC, COX-2 but not COX-1 is overexpressed in most colonic cancers and in polyps of patients suffering from familial adenomatous polyposis (FAP) (Nugent et al., 1993) (Janne and Mayer, 2000). Whilst the beneficial effect of aspirin is attributed to COX-2 inhibition in intestinal epithelial cells, stromal cells or endothelial cells of newly formed blood vessels, it is interesting that the dosages required to terminate COX-2 function in nucleated cells is much higher than that obtained from taking the low dose (75 to 100 mg) aspirin used here (Patrono et al., 2004), but that COX-1 activity in activated platelets is permanently inactivated with low dose aspirin. It is hypothesised that activated platelets may serve as an induction signal for COX-2 expression in adjacent cells (Patrono et al., 2001). Upon activation, platelets release large amounts of arachidonic acid, which in turn is rapidly metabolised by multiple enzymatic pathways, the best characterized within platelets is the conversion to TXA2. The protein 15(S)-hydroxyeicosatetraenoic acid (HETE) is a pro-angiogenic downstream platelet product. HETE promotes angiogenic responses in both human dermal microvascular endothelial cells and HUVEC cells by up-regulating VEGF through the PIK3-Akt and p38 MAPK signaling pathways

(Rauzi et al., 2016). The other possibility is that the protective effect is from a COX-independent pathway (Patrono et al., 2001).

Several studies have attempted to explore how COX-1 may contribute to carcinogenesis given the preventative effect of aspirin. A correlation between vascular endothelial growth factor (VEGF) and COX-1 expression was observed in a number of cancer types including ovarian carcinoma (Gupta et al., 2003), RCC (Osman and Youssef, 2015), cervical cancer (Kim et al., 2003) and oesophageal cancer (von Rahden et al., 2005). In both ovarian cancer and RCC, immunohistochemistry was used to demonstrate that areas of tissue sections with high expression of VEGF were also positive for COX-1 (Osman and Youssef, 2015) (Kim et al., 2003). This finding was reproduced using *in-situ* hybridisation and RT-PCR in human epithelial ovarian cancer and oesophageal cancer respectively (Gupta et al., 2003) (von Rahden et al., 2005). Other work has shown that COX-1 regulates angiogenesis in endothelial cells through observations following its inhibition in established endothelial cell lines *in-vitro* (Tsujii et al., 1998). Either way it is not yet known if the upregulation of COX-1 is an innocent bystander or if it has a functional role.

To date there have not been any other studies investigating the inhibition of COX-1 in RCC cell lines nor RCC. This study has highlighted the upregulation of COX-1, but not COX-2 in RCC and confirms cell death in RCC cell lines upon inhibition of COX-1 but only at high concentrations. It is not known whether this is due to specific COX-1 inhibition or not. COX-1 inhibitors are in routine use in the clinical setting and are fairly well tolerated, but their use is somewhat limited by the toxicity profile, particularly with long-term use. Examples of the side effects include gastric ulceration, renal injury, and prolongation of bleeding time. With this in mind and the high concentrations of COX-1 inhibitors required for cell death *in-vitro*, it is unlikely that COX-1 represents a viable option for treatment of RCC.

5.4.2 Proteasome subunit beta type-9 (PSMB9)

The regulation of protein production and destruction is critical to cell survival. More than 80% of cellular proteins are degraded by the ubiquitin-proteasome system (Ho et al., 2007). Redundant proteins are recognised and marked for degradation via the attachment of multiple ubiquitin molecules, which are subsequently recognised by

the proteasomal complexes, of which three major variations exist in humans, the constitutive proteasome, the immunoproteasome and the thymo-proteasome (present exclusively in cortical thymic epithelial cells) (Murata et al., 2009). My work has identified a switch between predominance of the constitutive proteasome in normal kidney and the immunoproteasome in ccRCC samples.

5.4.2.1 Proteasomal subunit expression in ccRCC

PSMB9 is an immunoproteasomal subunit, which along with the other two immunoproteasomal subunits (PSMB8 and PSMB10) were found to be upregulated in ccRCC compared to normal kidney. Conversely the three members of the constitutive proteasome (PSMB5, PSMB6 and PSMB7) have been found to be downregulated in ccRCC. This finding was also confirmed in the SWATH-MS and the membrane enriched LC-MS/MS analyses.

The 26S proteasome complex is almost exclusively found in humans. It consists of a 20S core particle with two 19S regulatory cap subunits. The 20S core particle is composed of four stacked rings of seven subunits each, forming a central pore. The outer two rings contain the constitutively expressed α-subunits and the inner two rings contain the β-subunits (Figure 5.24). The α-subunits control the entry of tagged proteins into the proteasomal complex (Smith et al., 2007) and predominantly act to provide structure, whilst the β-subunits contain the protease active sites. In humans the inner rings of the 20S core particle consists mainly of the β-catalytic subunits, PSMB5, PSMB6 and PSMB7 each with different specificities considered caspase-like, chymotrypsin-like and trypsin-like (Table 5.2) (Heinemeyer et al., 1997) (Groll et al., 2001). In response to inflammatory cytokines such as interferon-γ and TNF-α, the β-subunits PSMB6, PSMB7 and PSMB5 are replaced by PSMB9, PSMB10 and PSMB8, respectively, to form the immunoproteasome (Ferrington and Gregerson, 2012) (Ho et al., 2007) (Kloetzel, 2001). The immunoproteasome is associated with adaptive immune responses, for example generation of antigenic peptide fragments for major histocompatibility complex 1 (MHC1) through its increased chymotrypsin-like and trypsin-like activities, and in the positive selection of CD8+T cells. Through its regulation of protein homeostasis, it is hypothesised to be protective against oxidative stress. The immunoproteasome may also have a role in cytokine production as evident in the reduction in cytokine response to influenza in LMP2-/- mice (Angeles

et al., 2012) (de Verteuil et al., 2010) (Seliger et al., 1997) (Murata et al., 2009) (Kaur and Batra, 2016).

The thymo-proteasome is present exclusively in cortical thymic epithelial cells and has a role in the selection of CDS8+ T cells (Murata et al., 2009). The study of the proteasome is difficult, contributed to by the lack of selective inhibitors and the existence of hybrid variants containing immunoproteasome and proteasome subunits (Kaur and Batra, 2016).

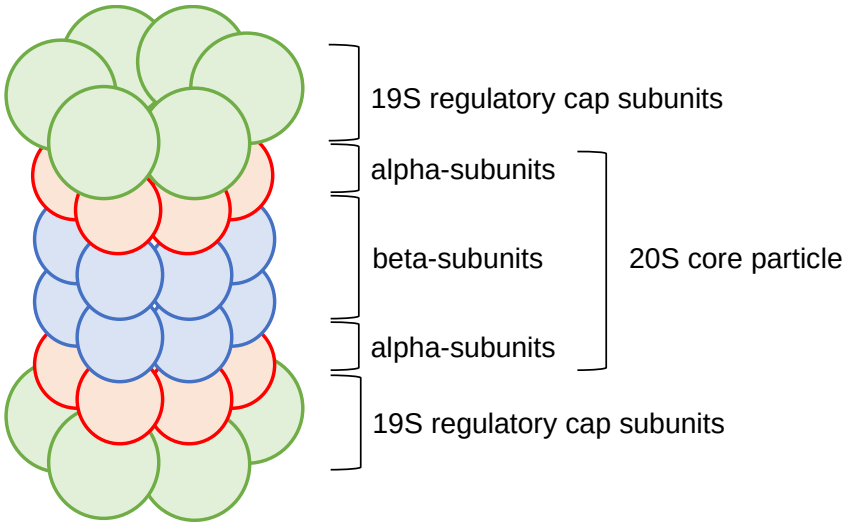

Figure 5.24 – Schematic diagram showing structure of the 26S proteasome

Table 5.2 – Nomenclature and activity of the proteasome catalytic subunits
(Heinemeyer et al., 1997)

β-subunit	Uniprot nomenclature	Alternative names	Activity
β5	PSMB5		Chymotrypsin-like
β1	PSMB6		Caspase-like
β2	PSMB7		Trypsin-like
β5i	PSMB8	LMP7	Chymotrypsin-like
β1i	PSMB9	LMP2	Caspase-like
β2i	PSMB10	MECL-1	Trypsin-like

PSMB9 and PSMB10 have previously been identified as being upregulated in RCC amongst a panel of other genes, in a study using oligonucleotide microarrays to molecularly subtype 31 adult renal tumours, of which 13/31 were ccRCC (Schuetz et al., 2005). A second study investigating all 6 β-subunits in 54 RCC samples using RT-PCR focused mainly on correlation with prognosis. Expression of PSMB8 and PSMB9 was low in high grade tumours and low levels of expression of the immunoproteasomal subunits was associated with a poor overall survival, leading the authors to conclude that RCC with low levels of immunoproteasome subunit expression may not be presenting antigen appropriately, thereby evading immune surveillance. There was no comparison with normal kidney tissue in this study. (Murakami et al., 2001). This is a significant conclusion, particularly if consideration of PSMB9 inhibition is being considered. In support of the lack of expression in normal kidney, a study using IHC staining for PSMB9 observed scattered and weak cytoplasmic staining in a small number of normal kidney samples, although the main aim of this study was to compare expression in renal oncocytoma and the chromophobe variant of RCC in the search for a molecular marker to differentiate between the two (Zheng et al., 2013). Finally in a study of exploring the data from The Cancer Genome Atlas (TCGA) transcriptomic analyses identified PSMB5 and PSMB6 as being downregulated in RCC and PSMB7, PSMB8, PSMB9 and PSMB10 as being upregulated compared to normal tissue (Rouette et al., 2016).

PSMB9 and the other immunoproteasome subunits have been characterised in other cancer types and have been found to vary in expression compared to normal tissue. Examples of downregulation include uterine leiomyosarcoma, where PSMB9 was observed to be downregulated compared with normal uterine tissue in 46/54 (85%) patients using IHC of tissue samples (Hayashi et al., 2011). Another study has observed that 36% of PSMB9 deficient mouse models spontaneously developed uterine leiomyosarcoma by 12 months old (Hayashi and Faustman, 2002). Similarly, in oesophageal squamous cell carcinoma downregulation of PSMB9 and PSMB8 were significantly associated with more advanced tumour stage and positive lymph node status (Liu et al., 2009)

An example of the upregulation of the immunoproteasomal subunits is breast cancer. An analysis of The Cancer Genome Atlas (TCGA) transcriptomic analyses identified that high expression of the immunoproteasome genes, in particular PSMB8 and PSMB9, is associated with improved breast cancer survival. This was hypothesised to be a surrogate marker of the paracrine secretion of interferon (INF) by infiltrating lymphocytes thus resulting in the improved survival (Adams, 2004). In AML, oxidative stress preferentially induces immunoproteasome expression over the constitutive proteasome. A number of prostate cancer cell lines overexpress PSMB9, leading to the finding of high levels of staining in primary tumour tissue compared with normal prostate tissue using IHC (FFPE tissue). In the PC3 cell line DAPI and PSMB9 were found to co-localise when investigated using immunofluorescence, suggesting PSMB9 presence in the cell nucleus where it may participate in transcriptional regulation. Transient knock-down of PSMB9 in PC3 cells caused a growth inhibitory effect (Wehenkel et al., 2012)

In melanoma the expression pattern of the proteasomal subunits are more complicated. Melanocytes grown *in*-vitro do not express PSMB9, but in a study involving the immunohistochemical staining of 98 melanoma and 10 nevi lesions, PSMB9 was identified as being upregulated in nevi and melanoma lesions, but less frequently expressed in the melanoma lesions than the naevi leading the authors to hypothesise that the loss was a mechanism for escape from immune recognition (Kageshita et al., 1999).

5.4.3 Proteasome Inhibitors

These ubiquitin-orientated proteasomal pathways were first considered as novel targets in cancer in the 1990's (Tew, 2016), which led to the subsequent development of Bortezomib (PS-341), an unselective proteasomal inhibitor, which is licensed for use in the treatment of multiple myeloma and mantle cell lymphoma in the UK (Adams et al., 1999). The disruption of protein homeostasis through the use of Bortezomib and the other proteasomal inhibitors has validated the proteasome as an anticancer target, but the clinical application of these inhibitors have been limited due to lack of efficacy and toxicity in their current form. Bortezomib has other indirect effects including preventing activation of the NF-κB pathway (through stabilisation of IκB) and stabilisation of proapoptotic proteins, including cyclin dependent kinase inhibitors (p21 and p27) and tumour suppressors (p53). Its anti-cancer effect has been investigated using the NCI 60 cell panel where it was active against a wide range of cancer cell lines including RCC cell lines at nanomolar concentrations (Adams et al., 1999). This had led to the investigation of bortezomib in RCC where it has been shown to induce apoptosis in the R11 and 444 RCC cell lines at concentrations of less than 1 μM (An et al., 2004). This has progressed to several phase II clinical trials in RCC. In a phase II study which included 21 patients with advanced RCC there was one partial response within the group in a patient with clear cell pathology (Davis et al., 2004). A second trial of bortezomib in advanced RCC (67% ccRCC) demonstrated that out of 37 patients, 4 had a partial response and 14 had stable disease (Kondagunta et al., 2004). A combination of sorafenib and bortezomib was investigated in the first line in a phase II trial involving 17 patients with advanced ccRCC demonstrated 1 partial response and 12 with stable disease. The combination was not superior to single agent sorafenib (Rao and Lauer, 2015). The combination of bortezomib and the histone deacetylase inhibitor belinostat was observed to increase apoptosis and inhibit renal cancer growth in RCC cell lines (Asano et al., 2015). Bortezomib has been used *in-vitro* with other cancer cell lines including ovarian (Frankel et al., 2000), mantle cell lymphoma (Pham et al., 2003), pancreatic cancer (Shah et al., 2001) (Bold et al., 2001), NSCLC (Ling et al., 2003), prostate cancer (Adams et al., 1999) and squamous cell carcinoma head and neck (Sunwoo et al., 2001). In multiple myeloma, bortezomib has been shown to directly inhibit proliferation and induce apoptosis of human multiple myeloma cell lines and freshly isolated patient MM cells. It inhibits MAPK growth signaling along with other mechanisms including abrogating paracrine growth in the bone marrow by altering cellular interactions and cytokine secretion in the bone marrow millieu. This paper

laid the basis for clinical trials in patients with multiple myeloma (Hideshima et al., 2001).

The finding of the upregulation of the immunoproteasome, and not the constitutive proteasome in a number of cancers has led to the development of specific inhibitors of the immunoproteasome. An example is UK-101, which is a selective small molecule inhibitor of PSMB9. When used the molecular weight of PSMB9 shifts upwards suggesting the attachment of the inhibitor. This compound induced apoptosis in the PC-3 prostate cancer cell line, independent of the NF-κB pathway, both *in-vitro* and when implanted into a mouse model (Wehenkel et al., 2012).

Overall, whilst upregulation of the immunoproteasome subunits have been reported at an mRNA and DNA level, this is the first reported analysis to identify upregulation of the immunoproteasome subunits in ccRCC at a protein level. If we consider what makes a good therapeutic target, the immunoproteasome subunits fulfill some of the criteria, namely the striking differential expression between normal and tumour tissue, the availability of antibodies and inhibitors for investigation and the high unmet clinical need for further treatments for patients suffering from advanced ccRCC. This study complements those already done investigating the immunoproteasome in RCC, and warrants further follow-up through the investigation of knockdown models and the use of specific immunoproteasome inhibitors. Bortezomib has been extensively investigated in RCC but was limited by its non-selective mechanism of action. Selective immunoproteasome inhibitors were not available at the time of this work. Two unanswered findings were firstly that of the Western blot demonstrating a band at a lower molecular weight than tissue samples in mouse spleen (Figure 5.21). It is assumed that this represents an alternative isoform of PSMB9, that is described in humans but not in mice. The Western blot of tumour samples included in the proteomic study appear to weigh heavier than the Raji cell line positive control (Figure 5.22). Unlike the bands seen in the previous blot, these bands appeared larger suggesting a gained modification between the mass spectrometry and the Western blot analysis. Despite this the differences in band intensity is striking with upregulation in the tumour samples.

The findings here highlight upregulation of the immunoproteasome in ccRCC. It is not known if this change from the constitutive proteasome subunits is an adaptive result

of cell stress or cytokine release from infiltrating inflammatory cells and is simply a bystander change, or it is a driver of malignant change itself. This area remains interesting and warrants further work.

5.4.4 Conclusion

Overall, expression of the immunoproteasome in ccRCC warrants further investigation using RNA interference models and small molecule inhibitors. COX-1 on the other hand is unlikely to represent a therapeutic target in ccRCC. The data generated through this work is will be of benefit to others in this group and is available for future analysis.

Chapter 6 Overall Discussion

The overarching aim of this study was to identify novel potential therapeutic targets in clear cell RCC. Two approaches were taken to try and achieve this. Firstly, potential targets recently identified by our collaborators, but still at a very early stage of validation, were explored further. Secondly, a de novo discovery approach was undertaken, using parallel multi-platform proteomic profiling, using genetically characterised tumours.

Despite early promise, particularly with respect to EA, neither of the existing candidate targets examined in this work demonstrated sufficient potential to warrant further investigation. However, the reasons for this are different for EA and SYK. In the case of EA, demonstrated to be a highly potent and specific activator of TRPC channels in vitro, the cytotoxicity of this compound at nanomolar concentrations was confirmed, with relative inactivity against a normal kidney cell line (HEK293) and non-cancer cell controls, (HUVEC). Furthermore, expression of the target, TRPC4/5 was confirmed in primary RCC tissues, albeit at the level of mRNA rather than protein. However, the relative expression of TRPC4/5 in tumour relative to normal was not uniformly significantly elevated. Indeed, the ubiquitous expression of TRPC channels in normal tissues is widely acknowledged (Bon and Beech, 2013), thus raising the concern that exposure to EA in humans may be associated with significant toxicity. Notably, it has been reported that locals native to a region of Zimbabwe where the plant Phyllanthus Engleri is known to grow is known as the ‘suicide plant’ when the smoke of the root is inhaled (Watt and Breyer-Brandwijk, 1927). In parallel to the work undertaken in this study, toxicity studies in mice and rats have been undertaken by our group and others, confirming the highly toxic nature of EA (Carson et al., 2015) (Cheung et al., 2018). Critically, these studies, using TRPC knock-out mouse models, have demonstrated irrefutably that the observed toxicity represents an ‘on-target’ effect. Whilst VEGFR TKIs also have a number of well recognised on-target toxicities, these are manageable and the risk-benefit ratio favours their use. In the case of EA, the toxicity appears to be severe and, as yet, poorly defined. Thus, disappointingly, it is apparent that whilst EA is capable of efficiently killing renal cancer cells in vitro, it is also associated with a level of toxicity that renders the TRPC channels an unlikely future therapeutic target in RCC.

SYK as a therapeutic target was principally proposed based on the observation of differential expression of SYK isoforms at an mRNA level in RCC versus normal kidney. This finding was confirmed at a protein level although no representative RCC cell line model was identified. SYK inhibitors are in clinical trials and one is currently undergoing a licensing review in the UK. SYK inhibition using a small molecule inhibitor was shown to cause cell death in the 786-0 RCC cell line at concentrations above 1 μM. In summary it is difficult to say that SYK inhibition holds promise as a therapeutic target given the lack of isoform specific inhibitors and the need for further investigations into the biological function of each isoform in RCC. It may be that the observed change is simply a passenger rather than a driver. Its expression in other cancer types has mostly been reported relative to normal tissue as opposed to differential isoform expression. Despite this, it is worth exploring further given the striking change at a protein level and the effect in other cancer types.

We also undertook one of the most comprehensive proteomic studies to date in ccRCC, particularly in the context of using genomically defined tissues. Across the three profiling platforms employed, in total, the relative expression of 3136 unique proteins were examined both within tumours and when compared to matched controls. 1337 proteins were identified to have a statistical significant difference between ccRCC and normal kidney, in particular 32 proteins were identified to be upregulated in ccRCC whilst not being detected in the normal kidney samples included in this study. Using a global tumour versus normal comparison of protein expression, two differentially expressed proteins, cyclooxygenase-1 (COX-1) and proteasome subunit beta type-9 (PSMB9), were taken forward for further investigation. COX-1 is unlikely to represent a therapeutic target in ccRCC based on the lack of potency of COX-1 inhibition *in vitro*. It remains unclear whether PSMB9 really holds any promise as a therapeutic target, and further work is needed to establish the role, if any, of this protein in ccRCC growth and development. Disappointingly, protein expression was not significantly different between genetic groups. Given, for example, the higher grade and stage of cancers associated with a BAP1 mutation, it was hoped that the drivers of such a phenotype at a protein level would be identified. Such changes must be apparent, but the small sample size and the heterogeneity of mutational status beyond the key genes that we focused on, are likely to have hindered their detection. Thus, whilst descriptively ccRCC is well characterised at the genetic level, exploiting this information for patient benefit remains elusive. Interestingly, one hope for the future may come from the concept of

synthetic lethality and the sensitivity of SETD2 deficient cancers to WEE1 inhibition (Pfister et al., 2015). SETD2 encodes a H3K36 methyltransferase, which when lost results in loss of H3K36me3. This in turn results in reduced expression of a ribonucleotide reductase subunit (RRM2). WEE1 also regulates RRM2 expression and inhibition of WEE1 results in RRM2 degradation. RRM2 is essential for the maintenance of dNTP levels and thus DNA replication. A phase II clinical trial currently in recruitment is investigating the use of adavosertib (a WEE1 inhibitor) in the second line setting in patients with a SETD2 mutation (NCT03284385).

Given the tremendous changes that have taken place in terms of the treatment landscape in RCC in recent years, it is reasonable to ask whether novel therapeutic targets are even needed in this disease. Combination immunotherapy using ipilimumab plus nivolumab has recently been licensed in the front-line setting by the European Medicines Agency and now awaits NICE appraisal before uptake in the UK. Furthermore, promising data is emerging for the combination of immunotherapy with anti-VEGF agents, in particular TKIs (Motzer et al., 2018a) (Motzer et al., 2018b) (Choueiri et al., 2018b). Deep and durable responses have been noted with both of these approaches and it is possible, although not yet established, that some patients may even be cured using such combinations. Nevertheless, several gaps remain. Firstly, not all patients will benefit from these approaches. In the landmark CheckMate 214 trial, 20% of patients had PD as their best response (Motzer et al., 2018b). Secondly, these combinations are toxic. Combination immunotherapy was associated with 40% grade 3-4 toxicity, 35% of patients required high dose steroids to manage immune related adverse events (irAE) and there were seven treatment related deaths reported in the ipilimumab plus nivolumab arm (Motzer et al., 2018b). Thirdly not all patients are suitable for these treatments, due to poor performance status or co-morbidities. Fourthly, they come with a significant financial burden that is now a significant issue for increasingly overstretched and financially constrained health systems. For example, one year of ipilimumab plus nivolumab would be estimated to cost in excess of £120,000 per patient, which accounts for drug costs alone. An emerging priority, therefore, is to at least identify those patients most likely to benefit from these drugs. In this regard, transcriptomic signatures, gene mutation status such as PBRM1 and the gut microbiome have all shown early promise, but rigorous validation of these findings is required before their routine application in the clinic (Motzer et al., 2018a) (Miao et al., 2018) (Routy et al., 2018).

Non-clear cell carcinomas make up a small but significant minority of RCCs and it is arguable that in fact it is in this setting that the greatest priority for identifying novel therapeutic targets lies. The cell of origin, genetics, biology and clinical behaviour of these tumours is distinct to clear cell RCCs and, even within the non-clear cell types, there is great variation. Type I papillary tumours, for example, are characterised by MET alterations, whereas type 2 tumors are characterized by CDKN2A silencing, SETD2 mutations and TFE3 fusions (Linehan et al., 2016). Despite this, approaches to the management of patients with these types of RCC are based on the biology of clear cell RCC, and response rates to VEGFR TKI are recognized to be lower (Armstrong et al., 2016). Even in MET driven papillary RCCs, the activity of the MET inhibitor savolitinib was only 18% amongst 43 patients (Choueiri et al., 2017b). Whether a drug such as cabozantinib, that combines VEGF and MET activity, is more efficacious remains to be established. Overall, it is evident that rational novel therapeutic strategies are urgently needed for this group of patients, particularly as access to novel agents is being increasingly restricted to those with ccRCC.

Bibliography

Cancer Research UK, http://www.cancerresearchuk.org/health-professional/cancer-statistics/statistics-by-cancer-type/bladder-cancer#heading-Six*, [Accessed October 2015].* [Online].

ABRAMOWITZ, J. & BIRNBAUMER, L. 2009. Physiology and pathophysiology of canonical transient receptor potential channels. *FASEB J,* 23**,** 297-328.

ADAMS, J. 2004. The development of proteasome inhibitors as anticancer drugs. *Cancer Cell,* 5**,** 417-21.

ADAMS, J., PALOMBELLA, V. J., SAUSVILLE, E. A., JOHNSON, J., DESTREE, A., LAZARUS, D. D., MAAS, J., PIEN, C. S., PRAKASH, S. & ELLIOTT, P. J. 1999. Proteasome inhibitors: a novel class of potent and effective antitumor agents. *Cancer Res,* 59**,** 2615-22.

AKBULUT, Y., GAUNT, H. J., MURAKI, K., LUDLOW, M. J., AMER, M. S., BRUNS, A., VASUDEV, N. S., RADTKE, L., WILLOT, M., HAHN, S., SEITZ, T., ZIEGLER, S., CHRISTMANN, M., BEECH, D. J. & WALDMANN, H. 2015. (-)-Englerin A is a Potent and Selective Activator of TRPC4 and TRPC5 Calcium Channels. *Angew Chem Int Ed Engl,* 54**,** 3787-91.

ALIMIRAH, F., CHEN, J., DAVIS, F. J. & CHOUBEY, D. 2007. IFI16 in human prostate cancer. *Mol Cancer Res,* 5**,** 251-9.

AMIN, M. B., EDGE, S., GREENE, F. L., BYRD, D. R., BROOKLAND, R. K., WASHINGTON, M. K., GERSHENWALD, J. E., COMPTON, C. C., HESS, K. R., SULLIVAN, D. C., JESSUP, J. M., BRIERLEY, J. D., GASPAR, L. E., SCHILSKY, R. L., BALCH, C. M., WINCHESTER, D. P., ASARE, E. A., MADERA, M., GRESS, D. M. & MEYER, L. R. 2017. *AJCC Cancer Staging Manual*, New York: Springer; 2017.

AN, J., SUN, Y., FISHER, M. & RETTIG, M. B. 2004. Maximal apoptosis of renal cell carcinoma by the proteasome inhibitor bortezomib is nuclear factor-kappaB dependent. *Mol Cancer Ther,* 3**,** 727-36.

ANGELES, A., FUNG, G. & LUO, H. 2012. Immune and non-immune functions of the immunoproteasome. *Front Biosci (Landmark Ed),* 17**,** 1904-16.

ANGLARD, P., TRAHAN, E., LIU, S., LATIF, F., MERINO, M. J., LERMAN, M. I., ZBAR, B. & LINEHAN, W. M. 1992. Molecular and cellular

characterization of human renal cell carcinoma cell lines. *Cancer Res,* 52**,** 348-56.

ARMSTRONG, A. J., HALABI, S., EISEN, T., BRODERICK, S., STADLER, W. M., JONES, R. J., GARCIA, J. A., VAISHAMPAYAN, U. N., PICUS, J., HAWKINS, R. E., HAINSWORTH, J. D., KOLLMANNSBERGER, C. K., LOGAN, T. F., PUZANOV, I., PICKERING, L. M., RYAN, C. W., PROTHEROE, A., LUSK, C. M., OBERG, S. & GEORGE, D. J. 2016. Everolimus versus sunitinib for patients with metastatic non-clear cell renal cell carcinoma (ASPEN): a multicentre, open-label, randomised phase 2 trial. *Lancet Oncol,* 17**,** 378-88.

ARROWSMITH, J. & MILLER, P. 2013. Trial watch: phase II and phase III attrition rates 2011-2012. *Nat Rev Drug Discov,* 12**,** 569.

ASANO, T., SATO, A., ISONO, M., OKUBO, K., ITO, K. & ASANO, T. 2015. Bortezomib and belinostat inhibit renal cancer growth synergistically by causing ubiquitinated protein accumulation and endoplasmic reticulum stress. *Biomed Rep,* 3**,** 797-801.

ASHBURN, T. T. & THOR, K. B. 2004. Drug repositioning: identifying and developing new uses for existing drugs. *Nat Rev Drug Discov,* 3**,** 673-83.

AZIMI, I., MILEVSKIY, M. J. G., KAEMMERER, E., TURNER, D., YAPA, K., BROWN, M. A., THOMPSON, E. W., ROBERTS-THOMSON, S. J. & MONTEITH, G. R. 2017. TRPC1 is a differential regulator of hypoxia-mediated events and Akt signalling in PTEN-deficient breast cancer cells. *J Cell Sci,* 130**,** 2292-2305.

AZIZ, S. A., SZNOL, J., ADENIRAN, A., COLBERG, J. W., CAMP, R. L. & KLUGER, H. M. 2013. Vascularity of primary and metastatic renal cell carcinoma specimens. *J Transl Med,* 11**,** 15.

BAKHEET, T. M. & DOIG, A. J. 2009. Properties and identification of human protein drug targets. *Bioinformatics,* 25**,** 451-457.

BALUOM, M., GROSSBARD, E. B., MANT, T. & LAU, D. T. 2013. Pharmacokinetics of fostamatinib, a spleen tyrosine kinase (SYK) inhibitor, in healthy human subjects following single and multiple oral dosing in three phase I studies. *Br J Clin Pharmacol,* 76**,** 78-88.

BARNETT, J., CHOW, J., IVES, D., CHIOU, M., MACKENZIE, R., OSEN, E., NGUYEN, B., TSING, S., BACH, C., FREIRE, J. & ET AL. 1994. Purification, characterization and selective inhibition of human prostaglandin G/H synthase 1 and 2 expressed in the baculovirus system. *Biochim Biophys Acta,* 1209**,** 130-9.

BATOVA, A., ALTOMARE, D., CREEK, K. E., NAVIAUX, R. K., WANG, L., LI, K., GREEN, E., WILLIAMS, R., NAVIAUX, J. C., DICCIANNI, M. & YU, A. L. 2017. Englerin A induces an acute inflammatory response and reveals lipid metabolism and ER stress as targetable vulnerabilities in renal cell carcinoma. *PLoS One,* 12**,** e0172632.

BATTLE, D. M., GUNASEKARA, S. D., WATSON, G. R., AHMED, E. M., SAYSELL, C. G., ALTAF, N., SANUSI, A. L., MUNIPALLE, P. C., SCOONES, D., WALKER, J., VISWANATH, Y. & BENHAM, A. M. 2013. Expression of the endoplasmic reticulum oxidoreductase Ero1alpha in gastro-intestinal cancer reveals a link between homocysteine and oxidative protein folding. *Antioxid Redox Signal,* 19**,** 24-35.

BEAR, A., CLAYMAN, R. V., ELBERS, J., LIMAS, C., WANG, N., STONE, K., GEBHARD, R., PRIGGE, W. & PALMER, J. 1987. Characterization of two human cell lines (TK-10, TK-164) of renal cell cancer. *Cancer Res,* 47**,** 3856-62.

BENEMEI, S., PATACCHINI, R., TREVISANI, M. & GEPPETTI, P. 2015. TRP channels. *Curr Opin Pharmacol,* 22**,** 18-23.

BENHAMOU, M., RYBA, N. J., KIHARA, H., NISHIKATA, H. & SIRAGANIAN, R. P. 1993. Protein-tyrosine kinase p72syk in high affinity IgE receptor signaling. Identification as a component of pp72 and association with the receptor gamma chain after receptor aggregation. *J Biol Chem,* 268**,** 23318-24.

BENUSIGLIO, P. R., COUVE, S., GILBERT-DUSSARDIER, B., DEVEAUX, S., LE JEUNE, H., DA COSTA, M., FROMONT, G., MEMETEAU, F., YACOUB, M., COUPIER, I., LEROUX, D., MEJEAN, A., ESCUDIER, B., GIRAUD, S., GIMENEZ-ROQUEPLO, A. P., BLONDEL, C., FROUIN, E., TEH, B. T., FERLICOT, S., BRESSAC-DE PAILLERETS, B., RICHARD, S. & GAD, S. 2015. A germline mutation in PBRM1 predisposes to renal cell carcinoma. *J Med Genet,* 52**,** 426-30.

BERGSMA, D. J., EDER, C., GROSS, M., KERSTEN, H., SYLVESTER, D., APPELBAUM, E., CUSIMANO, D., LIVI, G. P., MCLAUGHLIN, M. M., KASYAN, K. & ET AL. 1991. The cyclophilin multigene family of peptidyl-prolyl isomerases. Characterization of three separate human isoforms. *J Biol Chem,* 266**,** 23204-14.

BEROUKHIM, R., BRUNET, J. P., DI NAPOLI, A., MERTZ, K. D., SEELEY, A., PIRES, M. M., LINHART, D., WORRELL, R. A., MOCH, H., RUBIN, M. A., SELLERS, W. R., MEYERSON, M., LINEHAN, W. M., KAELIN, W. G., JR. & SIGNORETTI, S. 2009. Patterns of gene expression and copy-number alterations in von-hippel lindau disease-associated and sporadic clear cell carcinoma of the kidney. *Cancer Res,* 69**,** 4674-81.

BLANCATO, J., GRAVES, A., RASHIDI, B., MORONI, M., TCHOBE, L., OZDEMIRLI, M., KALLAKURY, B., MAKAMBI, K. H., MARIAN, C. & MUELLER, S. C. 2014. SYK allelic loss and the role of Syk-regulated genes in breast cancer survival. *PLoS One,* 9**,** e87610.

BOLD, R. J., VIRUDACHALAM, S. & MCCONKEY, D. J. 2001. Chemosensitization of pancreatic cancer by inhibition of the 26S proteasome. *J Surg Res,* 100**,** 11-7.

BON, R. S. & BEECH, D. J. 2013. In pursuit of small molecule chemistry for calcium-permeable non-selective TRPC channels -- mirage or pot of gold? *Br J Pharmacol,* 170**,** 459-74.

BOSTROM, A. K., LINDGREN, D., JOHANSSON, M. E. & AXELSON, H. 2013. Effects of TGF-beta signaling in clear cell renal cell carcinoma cells. *Biochem Biophys Res Commun,* 435**,** 126-33.

BRANNON, A. R., REDDY, A., SEILER, M., ARREOLA, A., MOORE, D. T., PRUTHI, R. S., WALLEN, E. M., NIELSEN, M. E., LIU, H., NATHANSON, K. L., LJUNGBERG, B., ZHAO, H., BROOKS, J. D., GANESAN, S., BHANOT, G. & RATHMELL, W. K. 2010. Molecular Stratification of Clear Cell Renal Cell Carcinoma by Consensus Clustering Reveals Distinct Subtypes and Survival Patterns. *Genes Cancer,* 1**,** 152-163.

BRASELMANN, S., TAYLOR, V., ZHAO, H., WANG, S., SYLVAIN, C., BALUOM, M., QU, K., HERLAAR, E., LAU, A., YOUNG, C., WONG, B. R., LOVELL, S., SUN, T., PARK, G., ARGADE, A., JURCEVIC, S., PINE, P., SINGH, R., GROSSBARD, E. B., PAYAN, D. G. & MASUDA, E. S. 2006. R406, an orally available spleen tyrosine kinase inhibitor blocks fc receptor signaling and reduces immune complex-mediated inflammation. *J Pharmacol Exp Ther,* 319**,** 998-1008.

BROOKS, S. A., BRANNON, A. R., PARKER, J. S., FISHER, J. C., SEN, O., KATTAN, M. W., HAKIMI, A. A., HSIEH, J. J., CHOUEIRI, T. K., TAMBOLI, P., MARANCHIE, J. K., HINDS, P., MILLER, C. R., NIELSEN, M. E. & RATHMELL, W. K. 2014. ClearCode34: A prognostic risk predictor for localized clear cell renal cell carcinoma. *Eur Urol,* 66**,** 77-84.

BRUGAROLAS, J. 2013. PBRM1 and BAP1 as novel targets for renal cell carcinoma. *Cancer J,* 19**,** 324-32.

BUCHNER, M., FUCHS, S., PRINZ, G., PFEIFER, D., BARTHOLOME, K., BURGER, M., CHEVALIER, N., VALLAT, L., TIMMER, J., GRIBBEN, J. G., JUMAA, H., VEELKEN, H., DIERKS, C. & ZIRLIK, K. 2009. Spleen tyrosine kinase is overexpressed and represents a potential therapeutic target in chronic lymphocytic leukemia. *Cancer Res,* 69**,** 5424-32.

BURROWS, A. E., SMOGORZEWSKA, A. & ELLEDGE, S. J. 2010. Polybromo-associated BRG1-associated factor components BRD7 and BAF180 are critical regulators of p53 required for induction of replicative senescence. *Proc Natl Acad Sci U S A,* 107**,** 14280-5.

BURWICK, N. & AKTAS, B. H. 2017. The eIF2-alpha kinase HRI: a potential target beyond the red blood cell. *Expert Opin Ther Targets,* 21**,** 1171-1177.

CAIRNS, P. 2010. Renal cell carcinoma. *Cancer Biomark,* 9**,** 461-73.

CANCER GENOME ATLAS RESEARCH, N. 2013. Comprehensive molecular characterization of clear cell renal cell carcinoma. *Nature,* 499**,** 43-9.

CANCER RESEARCH UK. *Kidney cancer statistics* [Online]. Available: https://www.cancerresearchuk.org/health-professional/cancer-statistics/statistics-by-cancer-type/kidney-cancer [Accessed November 2018.

CARSON, C., RAMAN, P., TULLAI, J., XU, L., HENAULT, M., THOMAS, E., YEOLA, S., LAO, J., MCPATE, M., VERKUYL, J. M., MARSH, G., SARBER, J., AMARAL, A., BAILEY, S., LUBICKA, D., PHAM, H., MIRANDA, N., DING, J., TANG, H. M., JU, H., TRANTER, P., JI, N., KRASTEL, P., JAIN, R. K., SCHUMACHER, A. M., LOUREIRO, J. J., GEORGE, E., BERELLINI, G., ROSS, N. T., BUSHELL, S. M., ERDEMLI, G. & SOLOMON, J. M. 2015. Englerin A Agonizes the TRPC4/C5 Cation Channels to Inhibit Tumor Cell Line Proliferation. *PLoS One,* 10**,** e0127498.

CHAN, A. C., VAN OERS, N. S., TRAN, A., TURKA, L., LAW, C. L., RYAN, J. C., CLARK, E. A. & WEISS, A. 1994. Differential expression of ZAP-70 and Syk protein tyrosine kinases, and the role of this family of protein tyrosine kinases in TCR signaling. *J Immunol,* 152**,** 4758-66.

CHANG, J. W., NOMURA, D. K. & CRAVATT, B. F. 2011. A potent and selective inhibitor of KIAA1363/AADACL1 that impairs prostate cancer pathogenesis. *Chem Biol,* 18**,** 476-84.

CHANG, X., XU, X., XUE, X., MA, J., LI, Z., DENG, P., CHEN, J., ZHANG, S., ZHI, Y. & DAI, D. 2016. NDRG1 Controls Gastric Cancer Migration and Invasion through Regulating MMP-9. *Pathol Oncol Res,* 22**,** 789-96.

CHATTARAGADA, M. S., RIGANTI, C., SASSOE, M., PRINCIPE, M., SANTAMORENA, M. M., ROUX, C., CURCIO, C., EVANGELISTA, A., ALLAVENA, P., SALVIA, R., RUSEV, B., SCARPA, A., CAPPELLO, P. & NOVELLI, F. 2018. FAM49B, a novel regulator of mitochondrial function and integrity that suppresses tumor metastasis. *Oncogene,* 37**,** 697-709.

CHEN, J., LUAN, Y., YU, R., ZHANG, Z., ZHANG, J. & WANG, W. 2014. Transient receptor potential (TRP) channels, promising potential diagnostic and therapeutic tools for cancer. *Biosci Trends,* 8**,** 1-10.

CHEN, X., YANG, L. & ZHAI, S. D. 2012. Risk of cardiovascular disease and all-cause mortality among diabetic patients prescribed rosiglitazone or pioglitazone: a meta-analysis of retrospective cohort studies. *Chin Med J (Engl),* 125**,** 4301-6.

CHENE, L., GIROUD, C., DESGRANDCHAMPS, F., BOCCON-GIBOD, L., CUSSENOT, O., BERTHON, P. & LATIL, A. 2004. Extensive analysis of the 7q31 region in human prostate tumors supports TES as the best candidate tumor suppressor gene. *Int J Cancer,* 111**,** 798-804.

CHEONG, S. C., CHANDRAMOULI, G. V., SALEH, A., ZAIN, R. B., LAU, S. H., SIVAKUMAREN, S., PATHMANATHAN, R., PRIME, S. S., TEO, S. H., PATEL, V. & GUTKIND, J. S. 2009. Gene expression in human oral squamous cell carcinoma is influenced by risk factor exposure. *Oral Oncol,* 45**,** 712-9.

CHEUNG, S. Y., HENROT, M., AL-SAAD, M., BAUMANN, M., MULLER, H., UNGER, A., RUBAIY, H. N., MATHAR, I., DINKEL, K., NUSSBAUMER, P., KLEBL, B., FREICHEL, M., RODE, B., TRAINOR, S., CLAPCOTE, S. J., CHRISTMANN, M., WALDMANN, H., ABBAS, S. K., BEECH, D. J. & VASUDEV, N. S. 2018. TRPC4/TRPC5 channels mediate adverse reaction to the cancer cell cytotoxic agent (-)-Englerin A. *Oncotarget,* 9**,** 29634-29643.

CHOUEIRI, T. K., ESCUDIER, B., POWLES, T., TANNIR, N. M., MAINWARING, P. N., RINI, B. I., HAMMERS, H. J., DONSKOV, F., ROTH, B. J., PELTOLA, K., LEE, J. L., HENG, D. Y. C., SCHMIDINGER, M., AGARWAL, N., STERNBERG, C. N., MCDERMOTT, D. F., AFTAB, D. T., HESSEL, C., SCHEFFOLD, C., SCHWAB, G., HUTSON, T. E., PAL, S., MOTZER, R. J. & INVESTIGATORS, M. 2016. Cabozantinib versus everolimus in advanced renal cell carcinoma (METEOR): final results from a randomised, open-label, phase 3 trial. *Lancet Oncol,* 17**,** 917-927.

CHOUEIRI, T. K., HALABI, S., SANFORD, B. L., HAHN, O., MICHAELSON, M. D., WALSH, M. K., FELDMAN, D. R., OLENCKI, T., PICUS, J., SMALL, E. J., DAKHIL, S., GEORGE, D. J. & MORRIS, M. J. 2017a. Cabozantinib Versus Sunitinib As Initial Targeted Therapy for Patients With Metastatic Renal Cell Carcinoma of Poor or Intermediate Risk: The Alliance A031203 CABOSUN Trial. *J Clin Oncol,* 35**,** 591-597.

CHOUEIRI, T. K., HESSEL, C., HALABI, S., SANFORD, B., MICHAELSON, M. D., HAHN, O., WALSH, M., OLENCKI, T., PICUS, J., SMALL, E. J., DAKHIL, S., FELDMAN, D. R., MANGESHKAR, M., SCHEFFOLD, C., GEORGE, D. & MORRIS, M. J. 2018a. Cabozantinib versus sunitinib as initial therapy for metastatic renal cell carcinoma of intermediate or poor risk

(Alliance A031203 CABOSUN randomised trial): Progression-free survival by independent review and overall survival update. *Eur J Cancer,* 94**,** 115-125.

CHOUEIRI, T. K., LARKIN, J., OYA, M., THISTLETHWAITE, F., MARTIGNONI, M., NATHAN, P., POWLES, T., MCDERMOTT, D., ROBBINS, P. B., CHISM, D. D., CHO, D., ATKINS, M. B., GORDON, M. S., GUPTA, S., UEMURA, H., TOMITA, Y., COMPAGNONI, A., FOWST, C., DI PIETRO, A. & RINI, B. I. 2018b. Preliminary results for avelumab plus axitinib as first-line therapy in patients with advanced clear-cell renal-cell carcinoma (JAVELIN Renal 100): an open-label, dose-finding and dose-expansion, phase 1b trial. *Lancet Oncol,* 19**,** 451-460.

CHOUEIRI, T. K., PLIMACK, E., ARKENAU, H. T., JONASCH, E., HENG, D. Y. C., POWLES, T., FRIGAULT, M. M., CLARK, E. A., HANDZEL, A. A., GARDNER, H., MORGAN, S., ALBIGES, L. & PAL, S. K. 2017b. Biomarker-Based Phase II Trial of Savolitinib in Patients With Advanced Papillary Renal Cell Cancer. *J Clin Oncol,* 35**,** 2993-3001.

CHOW, S., GALVIS, V., PILLAI, M., LEACH, R., KEENE, E., SPENCER-SHAW, A., SHABLAK, A., SHANKS, J., LIPTROT, T., THISTLETHWAITE, F. & HAWKINS, R. E. 2016. High-dose interleukin2 - a 10-year single-site experience in the treatment of metastatic renal cell carcinoma: careful selection of patients gives an excellent outcome. *J Immunother Cancer,* 4**,** 67.

CHOW, S., LEACH, R., SPENCER-SHAW, A., SHAHEEN, F., THISTLETHWAITE, F. C. & HAWKINS, R. E. 2018. High dose Interleukin2 (HD IL2) in metastatic renal cell carcinoma (mRCC) after prior therapy: A single centre experience. *Journal of Clinical Oncology,* 36**,** e16558-e16558.

CHOW, W. H., DONG, L. M. & DEVESA, S. S. 2010. Epidemiology and risk factors for kidney cancer. *Nat Rev Urol,* 7**,** 245-57.

CIFOLA, I., BIANCHI, C., MANGANO, E., BOMBELLI, S., FRASCATI, F., FASOLI, E., FERRERO, S., DI STEFANO, V., ZIPETO, M. A., MAGNI, F., SIGNORINI, S., BATTAGLIA, C. & PEREGO, R. A. 2011. Renal cell carcinoma primary cultures maintain genomic and phenotypic profile of parental tumor tissues. *BMC Cancer,* 11**,** 244.

COOPMAN, P. J., DO, M. T., BARTH, M., BOWDEN, E. T., HAYES, A. J., BASYUK, E., BLANCATO, J. K., VEZZA, P. R., MCLESKEY, S. W., MANGEAT, P. H. & MUELLER, S. C. 2000. The Syk tyrosine kinase suppresses malignant growth of human breast cancer cells. *Nature,* 406**,** 742-7.

COOPMAN, P. J. & MUELLER, S. C. 2006. The Syk tyrosine kinase: a new negative regulator in tumor growth and progression. *Cancer Lett,* 241**,** 159-73.

COX, J., HEIN, M. Y., LUBER, C. A., PARON, I., NAGARAJ, N. & MANN, M. 2014. Accurate proteome-wide label-free quantification by delayed normalization and maximal peptide ratio extraction, termed MaxLFQ. *Mol Cell Proteomics,* 13**,** 2513-26.

COX, J. & MANN, M. 2008. MaxQuant enables high peptide identification rates, individualized p.p.b.-range mass accuracies and proteome-wide protein quantification. *Nat Biotechnol,* 26**,** 1367-72.

COX, J., MATIC, I., HILGER, M., NAGARAJ, N., SELBACH, M., OLSEN, J. V. & MANN, M. 2009. A practical guide to the MaxQuant computational platform for SILAC-based quantitative proteomics. *Nat Protoc,* 4**,** 698-705.

COX, J., NEUHAUSER, N., MICHALSKI, A., SCHELTEMA, R. A., OLSEN, J. V. & MANN, M. 2011. Andromeda: a peptide search engine integrated into the MaxQuant environment. *J Proteome Res,* 10**,** 1794-805.

DAGHER, J., DELAHUNT, B., RIOUX-LECLERCQ, N., EGEVAD, L., SRIGLEY, J. R., COUGHLIN, G., DUNGLINSON, N., GIANDUZZO, T., KUA, B., MALONE, G., MARTIN, B., PRESTON, J., POKORNY, M., WOOD, S., YAXLEY, J. & SAMARATUNGA, H. 2017. Clear cell renal cell carcinoma: validation of World Health Organization/International Society of Urological Pathology grading. *Histopathology,* 71**,** 918-925.

DAGHER, J., KAMMERER-JACQUET, S. F., BRUNOT, A., PLADYS, A., PATARD, J. J., BENSALAH, K., PERRIN, C., VERHOEST, G., MOSSER, J., LESPAGNOL, A., VIGNEAU, C., DUGAY, F., BELAUD-ROTUREAU, M. A. & RIOUX-LECLERCQ, N. 2016. Wild-type VHL Clear Cell Renal Cell Carcinomas Are a Distinct Clinical and Histologic Entity: A 10-Year Follow-up. *Eur Urol Focus,* 1**,** 284-290.

DAIKOKU, T., WANG, D. Z., TRANGUCH, S., MORROW, J. D., ORSULIC, S., DUBOIS, R. N. & DEY, S. K. 2005. Cyclooxygenase-1 is a potential target for prevention and treatment of ovarian epithelial cancer. *Cancer Research,* 65**,** 3735-3744.

DALGLIESH, G. L., FURGE, K., GREENMAN, C., CHEN, L., BIGNELL, G., BUTLER, A., DAVIES, H., EDKINS, S., HARDY, C., LATIMER, C., TEAGUE, J., ANDREWS, J., BARTHORPE, S., BEARE, D., BUCK, G., CAMPBELL, P. J., FORBES, S., JIA, M., JONES, D., KNOTT, H., KOK, C. Y., LAU, K. W., LEROY, C., LIN, M. L., MCBRIDE, D. J., MADDISON, M., MAGUIRE, S., MCLAY, K., MENZIES, A., MIRONENKO, T., MULDERRIG, L., MUDIE, L., O'MEARA, S., PLEASANCE, E., RAJASINGHAM, A., SHEPHERD, R., SMITH, R., STEBBINGS, L., STEPHENS, P., TANG, G., TARPEY, P. S., TURRELL, K., DYKEMA, K. J., KHOO, S. K., PETILLO, D., WONDERGEM, B., ANEMA, J., KAHNOSKI, R. J., TEH, B. T., STRATTON, M. R. & FUTREAL,

P. A. 2010. Systematic sequencing of renal carcinoma reveals inactivation of histone modifying genes. *Nature,* 463**,** 360-3.

DAMANN, N., VOETS, T. & NILIUS, B. 2008. TRPs in our senses. *Curr Biol,* 18**,** R880-9.

DAVIS, N. B., TABER, D. A., ANSARI, R. H., RYAN, C. W., GEORGE, C., VOKES, E. E., VOGELZANG, N. J. & STADLER, W. M. 2004. Phase II trial of PS-341 in patients with renal cell cancer: a University of Chicago phase II consortium study. *J Clin Oncol,* 22**,** 115-9.

DAY, C. & BAILEY, C. J. 2016. Rosiglitazone. *Reference Module in Biomedical Sciences.* Elsevier.

DE GRAMONT, A., FAIVRE, S. & RAYMOND, E. 2017. Novel TGF-beta inhibitors ready for prime time in onco-immunology. *Oncoimmunology,* 6**,** e1257453.

DE SOUSA ABREU, R., PENALVA, L. O., MARCOTTE, E. M. & VOGEL, C. 2009. Global signatures of protein and mRNA expression levels. *Mol Biosyst,* 5**,** 1512-26.

DE VELASCO, G., CULHANE, A. C., FAY, A. P., HAKIMI, A. A., VOSS, M. H., TANNIR, N. M., TAMBOLI, P., APPLEMAN, L. J., BELLMUNT, J., KIMRYN RATHMELL, W., ALBIGES, L., HSIEH, J. J., HENG, D. Y., SIGNORETTI, S. & CHOUEIRI, T. K. 2017. Molecular Subtypes Improve Prognostic Value of International Metastatic Renal Cell Carcinoma Database Consortium Prognostic Model. *Oncologist,* 22**,** 286-292.

DE VERTEUIL, D., MURATORE-SCHROEDER, T. L., GRANADOS, D. P., FORTIER, M. H., HARDY, M. P., BRAMOULLE, A., CARON, E., VINCENT, K., MADER, S., LEMIEUX, S., THIBAULT, P. & PERREAULT, C. 2010. Deletion of immunoproteasome subunits imprints on the transcriptome and has a broad impact on peptides presented by major histocompatibility complex I molecules. *Mol Cell Proteomics,* 9**,** 2034-47.

DELAHUNT, B., CHEVILLE, J. C., MARTIGNONI, G., HUMPHREY, P. A., MAGI-GALLUZZI, C., MCKENNEY, J., EGEVAD, L., ALGABA, F., MOCH, H., GRIGNON, D. J., MONTIRONI, R., SRIGLEY, J. R. & MEMBERS OF THE, I. R. T. P. 2013. The International Society of Urological Pathology (ISUP) grading system for renal cell carcinoma and other prognostic parameters. *Am J Surg Pathol,* 37**,** 1490-504.

DHENNIN-DUTHILLE, I., GAUTIER, M., FAOUZI, M., GUILBERT, A., BREVET, M., VAUDRY, D., AHIDOUCH, A., SEVESTRE, H. & OUADID-AHIDOUCH, H. 2011. High expression of transient receptor potential channels

in human breast cancer epithelial cells and tissues: correlation with pathological parameters. *Cell Physiol Biochem,* 28**,** 813-22.

DIMASI, J. A., GRABOWSKI, H. G. & HANSEN, R. W. 2016. Innovation in the pharmaceutical industry: New estimates of R&D costs. *J Health Econ,* 47**,** 20-33.

DING, J., TAKANO, T., GAO, S., HAN, W., NODA, C., YANAGI, S. & YAMAMURA, H. 2000. Syk is required for the activation of Akt survival pathway in B cells exposed to oxidative stress. *J Biol Chem,* 275**,** 30873-7.

DIZON, D. S., DAMSTRUP, L., FINKLER, N. J., LASSEN, U., CELANO, P., GLASSPOOL, R., CROWLEY, E., LICHENSTEIN, H. S., KNOBLACH, P. & PENSON, R. T. 2012. Phase II activity of belinostat (PXD-101), carboplatin, and paclitaxel in women with previously treated ovarian cancer. *Int J Gynecol Cancer,* 22**,** 979-86.

DOMOTO, T., MIYAMA, Y., SUZUKI, H., TERATANI, T., ARAI, K., SUGIYAMA, T., TAKAYAMA, T., MUGIYA, S., OZONO, S. & NOZAWA, R. 2007. Evaluation of S100A10, annexin II and B-FABP expression as markers for renal cell carcinoma. *Cancer Sci,* 98**,** 77-82.

DU, J., SOURS-BROTHERS, S., COLEMAN, R., DING, M., GRAHAM, S., KONG, D. H. & MA, R. 2007. Canonical transient receptor potential 1 channel is involved in contractile function of glomerular mesangial cells. *J Am Soc Nephrol,* 18**,** 1437-45.

DUPASQUIER, S., DELMARCELLE, A. S., MARBAIX, E., COSYNS, J. P., COURTOY, P. J. & PIERREUX, C. E. 2014. Validation of housekeeping gene and impact on normalized gene expression in clear cell renal cell carcinoma: critical reassessment of YBX3/ZONAB/CSDA expression. *BMC Mol Biol,* 15**,** 9.

EBERT, T., BANDER, N. H., FINSTAD, C. L., RAMSAWAK, R. D. & OLD, L. J. 1990. Establishment and characterization of human renal cancer and normal kidney cell lines. *Cancer Res,* 50**,** 5531-6.

EINSTEIN, D. J. & MCDERMOTT, D. F. 2017. Combined blockade of vascular endothelial growth factor and programmed death 1 pathways in advanced kidney cancer. *Clin Adv Hematol Oncol,* 15**,** 478-488.

ESCUDIER, B., EISEN, T., STADLER, W. M., SZCZYLIK, C., OUDARD, S., SIEBELS, M., NEGRIER, S., CHEVREAU, C., SOLSKA, E., DESAI, A. A., ROLLAND, F., DEMKOW, T., HUTSON, T. E., GORE, M., FREEMAN, S., SCHWARTZ, B., SHAN, M., SIMANTOV, R., BUKOWSKI, R. M. & GROUP, T. S. 2007. Sorafenib in advanced clear-cell renal-cell carcinoma. *N Engl J Med,* 356**,** 125-34.

ESCUDIER, B., EISEN, T., STADLER, W. M., SZCZYLIK, C., OUDARD, S., STAEHLER, M., NEGRIER, S., CHEVREAU, C., DESAI, A. A., ROLLAND, F., DEMKOW, T., HUTSON, T. E., GORE, M., ANDERSON, S., HOFILENA, G., SHAN, M., PENA, C., LATHIA, C. & BUKOWSKI, R. M. 2009. Sorafenib for treatment of renal cell carcinoma: Final efficacy and safety results of the phase III treatment approaches in renal cancer global evaluation trial. *J Clin Oncol,* 27**,** 3312-8.

ESCUDIER, B., PORTA, C., SCHMIDINGER, M., RIOUX-LECLERCQ, N., BEX, A., KHOO, V., GRUENVALD, V., HORWICH, A. & ON BEHALF OF THE, E. G. C. 2016. Renal cell carcinoma: ESMO Clinical Practice Guidelines for diagnosis, treatment and follow-up†. *Annals of Oncology,* 27**,** v58-v68.

EUROPEAN ASSOCIATION OF UROLOGY. 2018. *EAU – ESTRO – ESUR – SIOG Guidelines on Renal Cell Carcinoma* [Online]. Available: http://uroweb.org/guideline/renal-cell-carcinoma/#1 [Accessed November 2018.

FAJARDO, A. M., BROWNE, T., GRAFF, H., KLEIER, K., NELTNER, K., MCCALL, C., MEYER, B., DOUGLASS, L. & CARTER, J. 2015. Targeting PAK1 activity in breast cancer: Inhibition of cell growth, survival, motility, and signaling. *Cancer Research,* 75.

FANTOZZI, I., ZHANG, S., PLATOSHYN, O., REMILLARD, C. V., COWLING, R. T. & YUAN, J. X. 2003. Hypoxia increases AP-1 binding activity by enhancing capacitative Ca2+ entry in human pulmonary artery endothelial cells. *Am J Physiol Lung Cell Mol Physiol,* 285**,** L1233-45.

FENG, L., SUN, W., XIA, Y., TANG, W. W., CHANMUGAM, P., SOYOOLA, E., WILSON, C. B. & HWANG, D. 1993. Cloning two isoforms of rat cyclooxygenase: differential regulation of their expression. *Arch Biochem Biophys,* 307**,** 361-8.

FERGUSON, R. E., CARROLL, H. P., HARRIS, A., MAHER, E. R., SELBY, P. J. & BANKS, R. E. 2005. Housekeeping proteins: a preliminary study illustrating some limitations as useful references in protein expression studies. *Proteomics,* 5**,** 566-71.

FERRINGTON, D. A. & GREGERSON, D. S. 2012. Immunoproteasomes: structure, function, and antigen presentation. *Prog Mol Biol Transl Sci,* 109**,** 75-112.

FLANIGAN, R. C., MICKISCH, G., SYLVESTER, R., TANGEN, C., VAN POPPEL, H. & CRAWFORD, E. D. 2004. Cytoreductive nephrectomy in patients with metastatic renal cancer: a combined analysis. *J Urol,* 171**,** 1071-6.

FLOCKERZI, V., JUNG, C., ABERLE, T., MEISSNER, M., FREICHEL, M., PHILIPP, S. E., NASTAINCZYK, W., MAURER, P. & ZIMMERMANN, R. 2005. Specific detection and semi-quantitative analysis of TRPC4 protein expression by antibodies. *Pflugers Arch,* 451**,** 81-6.

FOGH, J., FOGH, J. M. & ORFEO, T. 1977. One hundred and twenty-seven cultured human tumor cell lines producing tumors in nude mice. *J Natl Cancer Inst,* 59**,** 221-6.

FONG, S., MOUNKES, L., LIU, Y., MAIBAUM, M., ALONZO, E., DESPREZ, P. Y., THOR, A. D., KASHANI-SABET, M. & DEBS, R. J. 2003. Functional identification of distinct sets of antitumor activities mediated by the FKBP gene family. *Proc Natl Acad Sci U S A,* 100**,** 14253-8.

FRANK, I., BLUTE, M. L., CHEVILLE, J. C., LOHSE, C. M., WEAVER, A. L. & ZINCKE, H. 2002. An outcome prediction model for patients with clear cell renal cell carcinoma treated with radical nephrectomy based on tumor stage, size, grade and necrosis: the SSIGN score. *J Urol,* 168**,** 2395-400.

FRANKEL, A., MAN, S., ELLIOTT, P., ADAMS, J. & KERBEL, R. S. 2000. Lack of multicellular drug resistance observed in human ovarian and prostate carcinoma treated with the proteasome inhibitor PS-341. *Clin Cancer Res,* 6**,** 3719-28.

FREICHEL, M., SUH, S. H., PFEIFER, A., SCHWEIG, U., TROST, C., WEISSGERBER, P., BIEL, M., PHILIPP, S., FREISE, D., DROOGMANS, G., HOFMANN, F., FLOCKERZI, V. & NILIUS, B. 2001. Lack of an endothelial store-operated Ca2+ current impairs agonist-dependent vasorelaxation in TRP4-/- mice. *Nat Cell Biol,* 3**,** 121-7.

FREW, I. J. & MOCH, H. 2015. A clearer view of the molecular complexity of clear cell renal cell carcinoma. *Annu Rev Pathol,* 10**,** 263-89.

FRIEDBERG, J. W., SHARMAN, J., SWEETENHAM, J., JOHNSTON, P. B., VOSE, J. M., LACASCE, A., SCHAEFER-CUTILLO, J., DE VOS, S., SINHA, R., LEONARD, J. P., CRIPE, L. D., GREGORY, S. A., STERBA, M. P., LOWE, A. M., LEVY, R. & SHIPP, M. A. 2010. Inhibition of Syk with fostamatinib disodium has significant clinical activity in non-Hodgkin lymphoma and chronic lymphocytic leukemia. *Blood,* 115**,** 2578-85.

FUHRMAN, S. A., LASKY, L. C. & LIMAS, C. 1982. Prognostic significance of morphologic parameters in renal cell carcinoma. *Am J Surg Pathol,* 6**,** 655-63.

FURLONG, M. T., MAHRENHOLZ, A. M., KIM, K. H., ASHENDEL, C. L., HARRISON, M. L. & GEAHLEN, R. L. 1997. Identification of the major sites

of autophosphorylation of the murine protein-tyrosine kinase Syk. *Biochim Biophys Acta,* 1355**,** 177-90.

FURSTENWERTH, H. 2010. Ouabain - the insulin of the heart. *Int J Clin Pract,* 64**,** 1591-4.

FUTTERER, K., WONG, J., GRUCZA, R. A., CHAN, A. C. & WAKSMAN, G. 1998. Structural basis for Syk tyrosine kinase ubiquity in signal transduction pathways revealed by the crystal structure of its regulatory SH2 domains bound to a dually phosphorylated ITAM peptide. *J Mol Biol,* 281**,** 523-37.

FYFE, G., FISHER, R. I., ROSENBERG, S. A., SZNOL, M., PARKINSON, D. R. & LOUIE, A. C. 1995. Results of treatment of 255 patients with metastatic renal cell carcinoma who received high-dose recombinant interleukin-2 therapy. *J Clin Oncol,* 13**,** 688-96.

GANNON, P. O., KOUMAKPAYI, I. H., LE PAGE, C., KARAKIEWICZ, P. I., MES-MASSON, A. M. & SAAD, F. 2008. Ebp1 expression in benign and malignant prostate. *Cancer Cell Int,* 8**,** 18.

GANTI, S., TAYLOR, S. L., ABU ABOUD, O., YANG, J., EVANS, C., OSIER, M. V., ALEXANDER, D. C., KIM, K. & WEISS, R. H. 2012. Kidney tumor biomarkers revealed by simultaneous multiple matrix metabolomics analysis. *Cancer Res,* 72**,** 3471-9.

GASHAW, I., ELLINGHAUS, P., SOMMER, A. & ASADULLAH, K. 2011. What makes a good drug target? *Drug Discovery Today,* 16**,** 1037-1043.

GEAHLEN, R. L. 2014. Getting Syk: spleen tyrosine kinase as a therapeutic target. *Trends Pharmacol Sci,* 35**,** 414-22.

GELDRES, C., SAVOLDO, B., HOYOS, V., CARUANA, I., ZHANG, M., YVON, E., DEL VECCHIO, M., CREIGHTON, C. J., ITTMANN, M., FERRONE, S. & DOTTI, G. 2014. T lymphocytes redirected against the chondroitin sulfate proteoglycan-4 control the growth of multiple solid tumors both in vitro and in vivo. *Clin Cancer Res,* 20**,** 962-71.

GERLINGER, M., HORSWELL, S., LARKIN, J., ROWAN, A. J., SALM, M. P., VARELA, I., FISHER, R., MCGRANAHAN, N., MATTHEWS, N., SANTOS, C. R., MARTINEZ, P., PHILLIMORE, B., BEGUM, S., RABINOWITZ, A., SPENCER-DENE, B., GULATI, S., BATES, P. A., STAMP, G., PICKERING, L., GORE, M., NICOL, D. L., HAZELL, S., FUTREAL, P. A., STEWART, A. & SWANTON, C. 2014. Genomic architecture and evolution of clear cell renal cell carcinomas defined by multiregion sequencing. *Nat Genet,* 46**,** 225-33.

GIARD, D. J., AARONSON, S. A., TODARO, G. J., ARNSTEIN, P., KERSEY, J. H., DOSIK, H. & PARKS, W. P. 1973. In vitro cultivation of human tumors: establishment of cell lines derived from a series of solid tumors. *J Natl Cancer Inst,* 51**,** 1417-23.

GILKES, D. M., CHATURVEDI, P., BAJPAI, S., WONG, C. C., WEI, H., PITCAIRN, S., HUBBI, M. E., WIRTZ, D. & SEMENZA, G. L. 2013. Collagen prolyl hydroxylases are essential for breast cancer metastasis. *Cancer Res,* 73**,** 3285-96.

GONZALEZ, N., CARDAMA, G. A., COMIN, M. J., SEGATORI, V. I., PIFANO, M., ALONSO, D. F., GOMEZ, D. E. & MENNA, P. L. 2017. Pharmacological inhibition of Rac1-PAK1 axis restores tamoxifen sensitivity in human resistant breast cancer cells. *Cell Signal,* 30**,** 154-161.

GOODMAN, P. A., WOOD, C. M., VASSILEV, A., MAO, C. & UCKUN, F. M. 2001. Spleen tyrosine kinase (Syk) deficiency in childhood pro-B cell acute lymphoblastic leukemia. *Oncogene,* 20**,** 3969-78.

GOSSAGE, L., EISEN, T. & MAHER, E. R. 2015. VHL, the story of a tumour suppressor gene. *Nat Rev Cancer,* 15**,** 55-64.

GOSSAGE, L., MURTAZA, M., SLATTER, A. F., LICHTENSTEIN, C. P., WARREN, A., HAYNES, B., MARASS, F., ROBERTS, I., SHANAHAN, S. J., CLAAS, A., DUNHAM, A., MAY, A. P., ROSENFELD, N., FORSHEW, T. & EISEN, T. 2014. Clinical and pathological impact of VHL, PBRM1, BAP1, SETD2, KDM6A, and JARID1c in clear cell renal cell carcinoma. *Genes Chromosomes Cancer,* 53**,** 38-51.

GRAHAM, F. L., SMILEY, J., RUSSELL, W. C. & NAIRN, R. 1977. Characteristics of a human cell line transformed by DNA from human adenovirus type 5. *J Gen Virol,* 36**,** 59-74.

GROENEVELD, G. J., VAN KAN, H. J., TORANO, J. S., VELDINK, J. H., GUCHELAAR, H. J., WOKKE, J. H. & VAN DEN BERG, L. H. 2001. Inter- and intraindividual variability of riluzole serum concentrations in patients with ALS. *J Neurol Sci,* 191**,** 121-5.

GROLL, M., KOGUCHI, Y., HUBER, R. & KOHNO, J. 2001. Crystal structure of the 20 S proteasome:TMC-95A complex: a non-covalent proteasome inhibitor. *J Mol Biol,* 311**,** 543-8.

GROSSMAN, H. B., WEDEMEYER, G. & REN, L. Q. 1985. Human renal carcinoma: characterization of five new cell lines. *J Surg Oncol,* 28**,** 237-44.

GUNDUZ, E., GUNDUZ, M., BEDER, L., NAGATSUKA, H., FUKUSHIMA, K., SUTCU, R., DELIBAS, N., YAMANAKA, N., SHIMIZU, K. & NAGAI, N. 2009. Downregulation of TESTIN and its association with cancer history and a tendency toward poor survival in head and neck squamous cell carcinoma. *Arch Otolaryngol Head Neck Surg,* 135**,** 254-60.

GUO, G., GUI, Y., GAO, S., TANG, A., HU, X., HUANG, Y., JIA, W., LI, Z., HE, M., SUN, L., SONG, P., SUN, X., ZHAO, X., YANG, S., LIANG, C., WAN, S., ZHOU, F., CHEN, C., ZHU, J., LI, X., JIAN, M., ZHOU, L., YE, R., HUANG, P., CHEN, J., JIANG, T., LIU, X., WANG, Y., ZOU, J., JIANG, Z., WU, R., WU, S., FAN, F., ZHANG, Z., LIU, L., YANG, R., LIU, X., WU, H., YIN, W., ZHAO, X., LIU, Y., PENG, H., JIANG, B., FENG, Q., LI, C., XIE, J., LU, J., KRISTIANSEN, K., LI, Y., ZHANG, X., LI, S., WANG, J., YANG, H., CAI, Z. & WANG, J. 2012. Frequent mutations of genes encoding ubiquitin-mediated proteolysis pathway components in clear cell renal cell carcinoma. *Nat Genet,* 44**,** 17-9.

GUO, H., GERMAN, P., BAI, S., BARNES, S., GUO, W., QI, X., LOU, H., LIANG, J., JONASCH, E., MILLS, G. B. & DING, Z. 2015a. The PI3K/AKT Pathway and Renal Cell Carcinoma. *J Genet Genomics,* 42**,** 343-53.

GUO, T., KOUVONEN, P., KOH, C. C., GILLET, L. C., WOLSKI, W. E., RÖST, H. L., ROSENBERGER, G., COLLINS, B. C., BLUM, L. C., GILLESSEN, S., JOERGER, M., JOCHUM, W. & AEBERSOLD, R. 2015b. Rapid mass spectrometric conversion of tissue biopsy samples into permanent quantitative digital proteome maps. *Nature Medicine,* 21**,** 407-413.

GUPTA, K., MILLER, J. D., LI, J. Z., RUSSELL, M. W. & CHARBONNEAU, C. 2008. Epidemiologic and socioeconomic burden of metastatic renal cell carcinoma (mRCC): a literature review. *Cancer Treat Rev,* 34**,** 193-205.

GUPTA, R. A. & DUBOIS, R. N. 2001. Colorectal cancer prevention and treatment by inhibition of cyclooxygenase-2. *Nat Rev Cancer,* 1**,** 11-21.

GUPTA, R. A., TEJADA, L. V., TONG, B. J., DAS, S. K., MORROW, J. D., DEY, S. K. & DUBOIS, R. N. 2003. Cyclooxygenase-1 is overexpressed and promotes angiogenic growth factor production in ovarian cancer. *Cancer Research,* 63**,** 906-911.

HAAB, B. B. 2005. Antibody arrays in cancer research. *Mol Cell Proteomics,* 4**,** 377-83.

HAAS N, M. J., UZZO RG, ET AL 2015. Initial results from ASSURE (E2805): Adjuvant sorafenib or sunitinib for unfavorable renal carcinoma, an ECOG-ACRIN-led, NCTN phase III trial. 2015 Genitourinary Cancers Symposium. Abstract 403. .

HAKIMI, A. A., REZNIK, E., LEE, C. H., CREIGHTON, C. J., BRANNON, A. R., LUNA, A., AKSOY, B. A., LIU, E. M., SHEN, R., LEE, W., CHEN, Y., STIRDIVANT, S. M., RUSSO, P., CHEN, Y. B., TICKOO, S. K., REUTER, V. E., CHENG, E. H., SANDER, C. & HSIEH, J. J. 2016. An Integrated Metabolic Atlas of Clear Cell Renal Cell Carcinoma. *Cancer Cell,* 29**,** 104-116.

HAN, S. Y., DRUCK, T. & HUEBNER, K. 2003. Candidate tumor suppressor genes at FRA7G are coamplified with MET and do not suppress malignancy in a gastric cancer. *Genomics,* 81**,** 105-107.

HARA, S., OYA, M., MIZUNO, R., HORIGUCHI, A., MARUMO, K. & MURAI, M. 2005. Akt activation in renal cell carcinoma: contribution of a decreased PTEN expression and the induction of apoptosis by an Akt inhibitor. *Ann Oncol,* 16**,** 928-33.

HARRISON, M. L., ISAACSON, C. C., BURG, D. L., GEAHLEN, R. L. & LOW, P. S. 1994. Phosphorylation of human erythrocyte band 3 by endogenous p72syk. *J Biol Chem,* 269**,** 955-9.

HARSHMAN, L. C., DRAKE, C. G. & CHOUEIRI, T. K. 2014. PD-1 blockade in renal cell carcinoma: to equilibrium and beyond. *Cancer Immunol Res,* 2**,** 1132-41.

HAYASHI, T. & FAUSTMAN, D. L. 2002. Development of spontaneous uterine tumors in low molecular mass polypeptide-2 knockout mice. *Cancer Res,* 62**,** 24-7.

HAYASHI, T., HORIUCHI, A., SANO, K., HIRAOKA, N., KASAI, M., ICHIMURA, T., SUDO, T., TAGAWA, Y., NISHIMURA, R., ISHIKO, O., KANAI, Y., YAEGASHI, N., ABURATANI, H., SHIOZAWA, T. & KONISHI, I. 2011. Potential role of LMP2 as tumor-suppressor defines new targets for uterine leiomyosarcoma therapy. *Sci Rep,* 1**,** 180.

HE, B., LIU, F., RUAN, J., LI, A., CHEN, J., LI, R., SHEN, J., ZHENG, D. & LUO, R. 2012. Silencing TRPC1 expression inhibits invasion of CNE2 nasopharyngeal tumor cells. *Oncol Rep,* 27**,** 1548-54.

HEINEMEYER, W., FISCHER, M., KRIMMER, T., STACHON, U. & WOLF, D. H. 1997. The active sites of the eukaryotic 20 S proteasome and their involvement in subunit precursor processing. *J Biol Chem,* 272**,** 25200-9.

HENG, D. Y., MACKENZIE, M. J., VAISHAMPAYAN, U. N., BJARNASON, G. A., KNOX, J. J., TAN, M. H., WOOD, L., WANG, Y., KOLLMANNSBERGER, C., NORTH, S., DONSKOV, F., RINI, B. I. & CHOUEIRI, T. K. 2012. Primary anti-vascular endothelial growth factor (VEGF)-refractory metastatic renal cell carcinoma: clinical characteristics, risk factors, and subsequent therapy. *Ann Oncol,* 23**,** 1549-55.

HENG, D. Y., XIE, W., REGAN, M. M., WARREN, M. A., GOLSHAYAN, A. R., SAHI, C., EIGL, B. J., RUETHER, J. D., CHENG, T., NORTH, S., VENNER, P., KNOX, J. J., CHI, K. N., KOLLMANNSBERGER, C., MCDERMOTT, D. F., OH, W. K., ATKINS, M. B., BUKOWSKI, R. M., RINI, B. I. & CHOUEIRI, T. K. 2009. Prognostic factors for overall survival in patients with metastatic renal cell carcinoma treated with vascular endothelial growth factor-targeted agents: results from a large, multicenter study. *J Clin Oncol,* 27**,** 5794-9.

HIDESHIMA, T., RICHARDSON, P., CHAUHAN, D., PALOMBELLA, V. J., ELLIOTT, P. J., ADAMS, J. & ANDERSON, K. C. 2001. The proteasome inhibitor PS-341 inhibits growth, induces apoptosis, and overcomes drug resistance in human multiple myeloma cells. *Cancer Res,* 61**,** 3071-6.

HIROTA, E., YAN, L., TSUNODA, T., ASHIDA, S., FUJIME, M., SHUIN, T., MIKI, T., NAKAMURA, Y. & KATAGIRI, T. 2006. Genome-wide gene expression profiles of clear cell renal cell carcinoma: identification of molecular targets for treatment of renal cell carcinoma. *Int J Oncol,* 29**,** 799-827.

HO, Y. K., BARGAGNA-MOHAN, P., WEHENKEL, M., MOHAN, R. & KIM, K. B. 2007. LMP2-specific inhibitors: chemical genetic tools for proteasome biology. *Chem Biol,* 14**,** 419-30.

HOELLER, C., THALLINGER, C., PRATSCHER, B., BISTER, M. D., SCHICHER, N., LOEWE, R., HEERE-RESS, E., ROKA, F., SEXL, V. & PEHAMBERGER, H. 2005. The non-receptor-associated tyrosine kinase Syk is a regulator of metastatic behavior in human melanoma cells. *J Invest Dermatol,* 124**,** 1293-9.

HONG, J., YUAN, Y., WANG, J., LIAO, Y., ZOU, R., ZHU, C., LI, B., LIANG, Y., HUANG, P., WANG, Z., LIN, W., ZENG, Y., DAI, J. L. & CHUNG, R. T. 2014. Expression of variant isoforms of the tyrosine kinase SYK determines the prognosis of hepatocellular carcinoma. *Cancer Res,* 74**,** 1845-56.

HOSOYA, N., SAKUMOTO, M., NAKAMURA, Y., NARISAWA, T., BILIM, V., MOTOYAMA, T., TOMITA, Y. & KONDO, T. 2013. Proteomics identified nuclear N-myc downstream-regulated gene 1 as a prognostic tissue biomarker candidate in renal cell carcinoma. *Biochim Biophys Acta,* 1834**,** 2630-9.

HSIA, D. A., TEPPER, C. G., POCHAMPALLI, M. R., HSIA, E. Y., IZUMIYA, C., HUERTA, S. B., WRIGHT, M. E., CHEN, H. W., KUNG, H. J. & IZUMIYA, Y. 2010. KDM8, a H3K36me2 histone demethylase that acts in the cyclin A1 coding region to regulate cancer cell proliferation. *Proc Natl Acad Sci U S A,* 107**,** 9671-6.

HSIEH, J. J., CHEN, D., WANG, P. I., MARKER, M., REDZEMATOVIC, A., CHEN, Y. B., SELCUKLU, S. D., WEINHOLD, N., BOUVIER, N., HUBERMAN, K. H., BHANOT, U., CHEVINSKY, M. S., PATEL, P., PINCIROLI, P., WON, H. H., YOU, D., VIALE, A., LEE, W., HAKIMI, A. A., BERGER, M. F., SOCCI, N. D., CHENG, E. H., KNOX, J., VOSS, M. H., VOI, M. & MOTZER, R. J. 2017. Genomic Biomarkers of a Randomized Trial Comparing First-line Everolimus and Sunitinib in Patients with Metastatic Renal Cell Carcinoma. *Eur Urol,* 71**,** 405-414.

HU, A., NOBLE, W. S. & WOLF-YADLIN, A. 2016. Technical advances in proteomics: new developments in data-independent acquisition. *F1000Res,* 5.

HUANG, D., DING, Y., LUO, W. M., BENDER, S., QIAN, C. N., KORT, E., ZHANG, Z. F., VANDENBELDT, K., DUESBERY, N. S., RESAU, J. H. & TEH, B. T. 2008. Inhibition of MAPK kinase signaling pathways suppressed renal cell carcinoma growth and angiogenesis in vivo. *Cancer Res,* 68**,** 81-8.

HUBE, F., REVERDIAU, P., IOCHMANN, S. & GRUEL, Y. 2005. Improved PCR method for amplification of GC-rich DNA sequences. *Mol Biotechnol,* 31**,** 81-4.

HUILI, L., HUANG, K., GAO, L., WANG, L., NIU, Y., LIU, H., WANG, Z., WANG, L., WANG, G. & WANG, J. 2016. TES inhibits colorectal cancer progression through activation of p38. *Oncotarget*.

HWANG, D., SCOLLARD, D., BYRNE, J. & LEVINE, E. 1998. Expression of cyclooxygenase-1 and cyclooxygenase-2 in human breast cancer. *Journal of the National Cancer Institute,* 90**,** 455-460.

JAFFE, E. A., NACHMAN, R. L., BECKER, C. G. & MINICK, C. R. 1973. Culture of human endothelial cells derived from umbilical veins. Identification by morphologic and immunologic criteria. *J Clin Invest,* 52**,** 2745-56.

JANNE, P. A. & MAYER, R. J. 2000. Chemoprevention of colorectal cancer. *N Engl J Med,* 342**,** 1960-8.

JIANG, H. N., ZENG, B., ZHANG, Y., DASKOULIDOU, N., FAN, H., QU, J. M. & XU, S. Z. 2013. Involvement of TRPC channels in lung cancer cell differentiation and the correlation analysis in human non-small cell lung cancer. *PLoS One,* 8**,** e67637.

JIMENEZ, N., KROUWER, V. J. & POST, J. A. 2013. A new, rapid and reproducible method to obtain high quality endothelium in vitro. *Cytotechnology,* 65**,** 1-14.

JONASCH, E., GAO, J. & RATHMELL, W. K. 2014. Renal cell carcinoma. *BMJ,* 349**,** g4797.

JONASCH, E., HASANOV, E., CORN, P. G., MOSS, T., SHAW, K. R., STOVALL, S., MARCOTT, V., GAN, B., BIRD, S., WANG, X., DO, K. A., ALTAMIRANO, P. F., ZURITA, A. J., DOYLE, L. A., LARA, P. N., JR. & TANNIR, N. M. 2017. A randomized phase 2 study of MK-2206 versus everolimus in refractory renal cell carcinoma. *Ann Oncol,* 28**,** 804-808.

JUNG, M., RAMANKULOV, A., ROIGAS, J., JOHANNSEN, M., RINGSDORF, M., KRISTIANSEN, G. & JUNG, K. 2007. In search of suitable reference genes for gene expression studies of human renal cell carcinoma by real-time PCR. *BMC Mol Biol,* 8**,** 47.

JUNG, S., MUHLE, A., SCHAEFER, M., STROTMANN, R., SCHULTZ, G. & PLANT, T. D. 2003. Lanthanides potentiate TRPC5 currents by an action at extracellular sites close to the pore mouth. *J Biol Chem,* 278**,** 3562-71.

KAGESHITA, T., HIRAI, S., ONO, T., HICKLIN, D. J. & FERRONE, S. 1999. Down-regulation of HLA class I antigen-processing molecules in malignant melanoma: association with disease progression. *Am J Pathol,* 154**,** 745-54.

KAPUR, P., PENA-LLOPIS, S., CHRISTIE, A., ZHREBKER, L., PAVIA-JIMENEZ, A., RATHMELL, W. K., XIE, X. J. & BRUGAROLAS, J. 2013. Effects on survival of BAP1 and PBRM1 mutations in sporadic clear-cell renal-cell carcinoma: a retrospective analysis with independent validation. *Lancet Oncol,* 14**,** 159-67.

KARIMZADEH, M., JANDAGHI, P., PAPADAKIS, A. I., TRAINOR, S., RUNG, J., GONZALEZ-PORTA, M., SCELO, G., VASUDEV, N. S., BRAZMA, A., HUANG, S., BANKS, R. E., LATHROP, M., NAJAFABADI, H. S. & RIAZALHOSSEINI, Y. 2018. Aberration hubs in protein interaction networks highlight actionable targets in cancer. *Oncotarget,* 9**,** 25166-25180.

KARPOVA, M. B., SCHOUMANS, J., ERNBERG, I., HENTER, J. I., NORDENSKJOLD, M. & FADEEL, B. 2005. Raji revisited: cytogenetics of the original Burkitt's lymphoma cell line. *Leukemia,* 19**,** 159-61.

KAUR, G. & BATRA, S. 2016. Emerging role of immunoproteasomes in pathophysiology. *Immunol Cell Biol,* 94**,** 812-820.

KAUR, G. & DUFOUR, J. M. 2012. Cell lines: Valuable tools or useless artifacts. *Spermatogenesis,* 2**,** 1-5.

KAWATA, N., NAGANE, Y., YAMAGUCHI, K., ICHINOSE, T., HIRAKATA, H. & TAKAHASHI, S. 2008. How do symptoms have an impact on the prognosis of renal cell carcinoma? *Int J Urol,* 15**,** 299-303.

KELLNER, R., LICHTENFELS, R., ATKINS, D., BUKUR, J., ACKERMANN, A., BECK, J., BRENNER, W., MELCHIOR, S. & SELIGER, B. 2002. Targeting of tumor associated antigens in renal cell carcinoma using proteome-based analysis and their clinical significance. *Proteomics,* 2**,** 1743-51.

KELLY, P., MOELLER, B. J., JUNEJA, J., BOODEN, M. A., DER, C. J., DAAKA, Y., DEWHIRST, M. W., FIELDS, T. A. & CASEY, P. J. 2006a. The G12 family of heterotrimeric G proteins promotes breast cancer invasion and metastasis. *Proc Natl Acad Sci U S A,* 103**,** 8173-8.

KELLY, P., STEMMLE, L. N., MADDEN, J. F., FIELDS, T. A., DAAKA, Y. & CASEY, P. J. 2006b. A role for the G12 family of heterotrimeric G proteins in prostate cancer invasion. *J Biol Chem,* 281**,** 26483-90.

KIM, F. J., CAMPAGNA, A., KHANDRIKA, L., KOUL, S., BYUN, S. S., VANBOKHOVEN, A., MOORE, E. E. & KOUL, H. 2008. Individualized medicine for renal cell carcinoma: establishment of primary cell line culture from surgical specimens. *J Endourol,* 22**,** 2361-6.

KIM, M. H., SEO, S. S., SONG, Y. S., KANG, D. H., PARK, I. A., KANG, S. B. & LEE, H. P. 2003. Expression of cyclooxygenase-1 and-2 associated with expression of VEGF in primary cervical cancer and at metastatic lymph nodes. *Gynecologic Oncology,* 90**,** 83-90.

KIM, S. P., CRISPEN, P. L., THOMPSON, R. H., WEIGHT, C. J., BOORJIAN, S. A., COSTELLO, B. A., LOHSE, C. M. & LEIBOVICH, B. C. 2012. Assessment of the pathologic inclusion criteria from contemporary adjuvant clinical trials for predicting disease progression after nephrectomy for renal cell carcinoma. *Cancer,* 118**,** 4412-20.

KIRSCHENBAUM, A., KLAUSNER, A. P., LEE, R., UNGER, P., YAO, S., LIU, X. H. & LEVINE, A. C. 2000. Expression of cyclooxygenase-1 and cyclooxygenase-2 in the human prostate. *Urology,* 56**,** 671-6.

KLOETZEL, P. M. 2001. Antigen processing by the proteasome. *Nat Rev Mol Cell Biol,* 2**,** 179-87.

KOBAYASHI, T., NAKAMURA, S., TANIGUCHI, T. & YAMAMURA, H. 1990. Purification and characterization of a cytosolic protein-tyrosine kinase from porcine spleen. *Eur J Biochem,* 188**,** 535-40.

KOLETSKY, A. J., HARDING, M. W. & HANDSCHUMACHER, R. E. 1986. Cyclophilin: distribution and variant properties in normal and neoplastic tissues. *J Immunol,* 137**,** 1054-9.

KONDAGUNTA, G. V., DRUCKER, B., SCHWARTZ, L., BACIK, J., MARION, S., RUSSO, P., MAZUMDAR, M. & MOTZER, R. J. 2004. Phase II trial of bortezomib for patients with advanced renal cell carcinoma. *J Clin Oncol,* 22**,** 3720-5.

KRIEG, M., HAAS, R., BRAUCH, H., ACKER, T., FLAMME, I. & PLATE, K. H. 2000. Up-regulation of hypoxia-inducible factors HIF-1alpha and HIF-2alpha under normoxic conditions in renal carcinoma cells by von Hippel-Lindau tumor suppressor gene loss of function. *Oncogene,* 19**,** 5435-43.

KRISENKO, M. O. & GEAHLEN, R. L. 2015. Calling in SYK: SYK's dual role as a tumor promoter and tumor suppressor in cancer. *Biochim Biophys Acta,* 1853**,** 254-63.

LARKIN, J., GOH, X. Y., VETTER, M., PICKERING, L. & SWANTON, C. 2012. Epigenetic regulation in RCC: opportunities for therapeutic intervention? *Nat Rev Urol,* 9**,** 147-55.

LATIF, F., TORY, K., GNARRA, J., YAO, M., DUH, F. M., ORCUTT, M. L., STACKHOUSE, T., KUZMIN, I., MODI, W., GEIL, L. & ET AL. 1993. Identification of the von Hippel-Lindau disease tumor suppressor gene. *Science,* 260**,** 1317-20.

LATOUR, S., ZHANG, J., SIRAGANIAN, R. P. & VEILLETTE, A. 1998. A unique insert in the linker domain of Syk is necessary for its function in immunoreceptor signalling. *EMBO J,* 17**,** 2584-95.

LAYTON, T., STALENS, C., GUNDERSON, F., GOODISON, S. & SILLETTI, S. 2009. Syk tyrosine kinase acts as a pancreatic adenocarcinoma tumor suppressor by regulating cellular growth and invasion. *Am J Pathol,* 175**,** 2625-36.

LEE, G. K., PARK, H. J., MACLEOD, M., CHANDLER, P., MUNN, D. H. & MELLOR, A. L. 2002. Tryptophan deprivation sensitizes activated T cells to apoptosis prior to cell division. *Immunology,* 107**,** 452-60.

LEIBOVICH, B. C., BLUTE, M. L., CHEVILLE, J. C., LOHSE, C. M., FRANK, I., KWON, E. D., WEAVER, A. L., PARKER, A. S. & ZINCKE, H. 2003. Prediction of progression after radical nephrectomy for patients with clear cell renal cell carcinoma: a stratification tool for prospective clinical trials. *Cancer,* 97**,** 1663-71.

LESEUX, L., HAMDI, S. M., AL SAATI, T., CAPILLA, F., RECHER, C., LAURENT, G. & BEZOMBES, C. 2006. Syk-dependent mTOR activation in follicular lymphoma cells. *Blood,* 108**,** 4156-62.

LIAO, S. Y., AURELIO, O. N., JAN, K., ZAVADA, J. & STANBRIDGE, E. J. 1997. Identification of the MN/CA9 protein as a reliable diagnostic biomarker of clear cell carcinoma of the kidney. *Cancer Res,* 57**,** 2827-31.

LICHNER, Z., MAC-WAY, F. & YOUSEF, G. M. 2017. Obstacles in Renal Regenerative Medicine: Metabolic and Epigenetic Parallels Between Cellular Reprogramming and Kidney Cancer Oncogenesis. *Eur Urol Focus*.

LIN, W., ZHAO, Z., NI, Z., ZHAO, Y., DU, W. & CHEN, S. 2017. IFI16 restoration in hepatocellular carcinoma induces tumour inhibition via activation of p53 signals and inflammasome. *Cell Prolif,* 50.

LIN, Y. N., BHUWANIA, R., GROMOVA, K., FAILLA, A. V., LANGE, T., RIECKEN, K., LINDER, S., KNEUSSEL, M., IZBICKI, J. R. & WINDHORST, S. 2015. Drosophila homologue of Diaphanous 1 (DIAPH1) controls the metastatic potential of colon cancer cells by regulating microtubule-dependent adhesion. *Oncotarget,* 6**,** 18577-89.

LINEHAN, W. M., SPELLMAN, P. T., RICKETTS, C. J., CREIGHTON, C. J., FEI, S. S., DAVIS, C., WHEELER, D. A., MURRAY, B. A., SCHMIDT, L., VOCKE, C. D., PETO, M., AL MAMUN, A. A., SHINBROT, E., SETHI, A., BROOKS, S., RATHMELL, W. K., BROOKS, A. N., HOADLEY, K. A., ROBERTSON, A. G., BROOKS, D., BOWLBY, R., SADEGHI, S., SHEN, H., WEISENBERGER, D. J., BOOTWALLA, M., BAYLIN, S. B., LAIRD, P. W., CHERNIACK, A. D., SAKSENA, G., HAAKE, S., LI, J., LIANG, H., LU, Y., MILLS, G. B., AKBANI, R., LEISERSON, M. D., RAPHAEL, B. J., ANUR, P., BOTTARO, D., ALBIGES, L., BARNABAS, N., CHOUEIRI, T. K., CZERNIAK, B., GODWIN, A. K., HAKIMI, A. A., HO, T. H., HSIEH, J., ITTMANN, M., KIM, W. Y., KRISHNAN, B., MERINO, M. J., MILLS SHAW, K. R., REUTER, V. E., REZNIK, E., SHELLEY, C. S., SHUCH, B., SIGNORETTI, S., SRINIVASAN, R., TAMBOLI, P., THOMAS, G., TICKOO, S., BURNETT, K., CRAIN, D., GARDNER, J., LAU, K., MALLERY, D., MORRIS, S., PAULAUSKIS, J. D., PENNY, R. J., SHELTON, C., SHELTON, W. T., SHERMAN, M., THOMPSON, E., YENA, P., AVEDON, M. T., BOWEN, J., GASTIER-FOSTER, J. M., GERKEN, M., LERAAS, K. M., LICHTENBERG, T. M., RAMIREZ, N. C., SANTOS, T., WISE, L., ZMUDA, E., DEMCHOK, J. A., FELAU, I., HUTTER, C. M., SHETH, M., SOFIA, H. J., TARNUZZER, R., WANG, Z., YANG, L., ZENKLUSEN, J. C., ZHANG, J., AYALA, B., BABOUD, J., CHUDAMANI, S., LIU, J., LOLLA, L., NARESH, R., et al. 2016. Comprehensive Molecular Characterization of Papillary Renal-Cell Carcinoma. *N Engl J Med,* 374**,** 135-45.

LINEHAN, W. M., WALTHER, M. M. & ZBAR, B. 2003. The genetic basis of cancer of the kidney. *J Urol,* 170**,** 2163-72.

LING, Y. H., LIEBES, L., JIANG, J. D., HOLLAND, J. F., ELLIOTT, P. J., ADAMS, J., MUGGIA, F. M. & PEREZ-SOLER, R. 2003. Mechanisms of proteasome inhibitor PS-341-induced G(2)-M-phase arrest and apoptosis in human non-small cell lung cancer cell lines. *Clin Cancer Res,* 9**,** 1145-54.

LIU, L., GUO, R., ZHANG, X., LIANG, Y., KONG, F., WANG, J. & XU, Z. 2017. Loss of SETD2, but not H3K36me3, correlates with aggressive clinicopathological features of clear cell renal cell carcinoma patients. *Biosci Trends,* 11**,** 214-220.

LIU, L., LAN, G., PENG, L., XIE, X., PENG, F., YU, S., WANG, Y. & TANG, X. 2016. NDUFA4L2 expression predicts poor prognosis in clear cell renal cell carcinoma patients. *Ren Fail,* 38**,** 1199-205.

LIU, Q., HAO, C., SU, P. & SHI, J. 2009. Down-regulation of HLA class I antigen-processing machinery components in esophageal squamous cell carcinomas: association with disease progression. *Scand J Gastroenterol,* 44**,** 960-9.

LONSER, R. R., GLENN, G. M., WALTHER, M., CHEW, E. Y., LIBUTTI, S. K., LINEHAN, W. M. & OLDFIELD, E. H. 2003. von Hippel-Lindau disease. *Lancet,* 361**,** 2059-67.

LU, D., WANG, J., SHI, X., YUE, B. & HAO, J. 2017. AHNAK2 is a potential prognostic biomarker in patients with PDAC. *Oncotarget,* 8**,** 31775-31784.

LUDLOW, M. J., GAUNT, H. J., RUBAIY, H. N., MUSIALOWSKI, K. E., BLYTHE, N. M., VASUDEV, N. S., MURAKI, K. & BEECH, D. J. 2017. (-)-Englerin A-evoked Cytotoxicity Is Mediated by Na+ Influx and Counteracted by Na+/K+-ATPase. *J Biol Chem,* 292**,** 723-731.

MA, Y., DAI, H., KONG, X. & WANG, L. 2012. Impact of thawing on reference gene expression stability in renal cell carcinoma samples. *Diagn Mol Pathol,* 21**,** 157-63.

MACK, F. A., RATHMELL, W. K., ARSHAM, A. M., GNARRA, J., KEITH, B. & SIMON, M. C. 2003. Loss of pVHL is sufficient to cause HIF dysregulation in primary cells but does not promote tumor growth. *Cancer Cell,* 3**,** 75-88.

MAJEED, Y., BAHNASI, Y., SEYMOUR, V. A., WILSON, L. A., MILLIGAN, C. J., AGARWAL, A. K., SUKUMAR, P., NAYLOR, J. & BEECH, D. J. 2011. Rapid and contrasting effects of rosiglitazone on transient receptor potential TRPM3 and TRPC5 channels. *Mol Pharmacol,* 79**,** 1023-30.

MANLEY, B. J., ZABOR, E. C., CASUSCELLI, J., TENNENBAUM, D. M., REDZEMATOVIC, A., BECERRA, M. F., BENFANTE, N., SATO, Y., MORIKAWA, T., KUME, H., FUKAYAMA, M., HOMMA, Y., OGAWA, S., ARCILA, M. E., VOSS, M. H., FELDMAN, D. R., COLEMAN, J. A., REUTER, V. E., MOTZER, R. J., RUSSO, P., HSIEH, J. J. & HAKIMI, A. A. 2016. Integration of Recurrent Somatic Mutations with Clinical Outcomes: A Pooled Analysis of 1049 Patients with Clear Cell Renal Cell Carcinoma. *Eur Urol Focus*.

MAO, Z., SUN, J., FENG, B., MA, J., ZANG, L., DONG, F., ZHANG, D. & ZHENG, M. 2013. The metastasis suppressor, N-myc downregulated gene 1 (NDRG1), is a prognostic biomarker for human colorectal cancer. *PLoS One,* 8**,** e68206.

MARAFIOTI, T., POZZOBON, M., HANSMANN, M. L., DELSOL, G., PILERI, S. A. & MASON, D. Y. 2004. Expression of intracellular signaling molecules in classical and lymphocyte predominance Hodgkin disease. *Blood,* 103**,** 188-93.

MAURO, A., LIPARI, L., LEONE, A., TORTORICI, S., BURRUANO, F., PROVENZANO, S., GERBINO, A. & BUSCEMI, M. 2010. Expression of cyclooxygenase-1 and cyclooxygenase-2 in normal and pathological human oral mucosa. *Folia Histochem Cytobiol,* 48**,** 555-63.

MEDICINES AND HEALTHCARE PRODUCTS REGULATORY AGENCY. *Rosiglitazone: recommended withdrawal from clinical use* [Online]. Available: https://www.gov.uk/drug-safety-update/rosiglitazone-recommended-withdrawal-from-clinical-use [Accessed November 2018.

MEJEAN, A., RAVAUD, A., THEZENAS, S., COLAS, S., BEAUVAL, J. B., BENSALAH, K., GEOFFROIS, L., THIERY-VUILLEMIN, A., CORMIER, L., LANG, H., GUY, L., GRAVIS, G., ROLLAND, F., LINASSIER, C., LECHEVALLIER, E., BEISLAND, C., AITCHISON, M., OUDARD, S., PATARD, J. J., THEODORE, C., CHEVREAU, C., LAGUERRE, B., HUBERT, J., GROSS-GOUPIL, M., BERNHARD, J. C., ALBIGES, L., TIMSIT, M. O., LEBRET, T. & ESCUDIER, B. 2018. Sunitinib Alone or after Nephrectomy in Metastatic Renal-Cell Carcinoma. *N Engl J Med,* 379**,** 417-427.

MERTINS, P., MANI, D. R., RUGGLES, K. V., GILLETTE, M. A., CLAUSER, K. R., WANG, P., WANG, X., QIAO, J. W., CAO, S., PETRALIA, F., KAWALER, E., MUNDT, F., KRUG, K., TU, Z., LEI, J. T., GATZA, M. L., WILKERSON, M., PEROU, C. M., YELLAPANTULA, V., HUANG, K. L., LIN, C., MCLELLAN, M. D., YAN, P., DAVIES, S. R., TOWNSEND, R. R., SKATES, S. J., WANG, J., ZHANG, B., KINSINGER, C. R., MESRI, M., RODRIGUEZ, H., DING, L., PAULOVICH, A. G., FENYO, D., ELLIS, M. J., CARR, S. A. & NCI, C. 2016. Proteogenomics connects somatic mutations to signalling in breast cancer. *Nature,* 534**,** 55-62.

MIAO, D., MARGOLIS, C. A., GAO, W., VOSS, M. H., LI, W., MARTINI, D. J., NORTON, C., BOSSE, D., WANKOWICZ, S. M., CULLEN, D., HORAK, C., WIND-ROTOLO, M., TRACY, A., GIANNAKIS, M., HODI, F. S., DRAKE, C. G., BALL, M. W., ALLAF, M. E., SNYDER, A., HELLMANN, M. D., HO, T., MOTZER, R. J., SIGNORETTI, S., KAELIN, W. G., JR., CHOUEIRI, T. K. & VAN ALLEN, E. M. 2018. Genomic correlates of response to immune checkpoint therapies in clear cell renal cell carcinoma. *Science,* 359**,** 801-806.

MINNER, S., RUMP, D., TENNSTEDT, P., SIMON, R., BURANDT, E., TERRACCIANO, L., MOCH, H., WILCZAK, W., BOKEMEYER, C., FISCH, M., SAUTER, G. & EICHELBERG, C. 2012. Epidermal growth factor receptor protein expression and genomic alterations in renal cell carcinoma. *Cancer,* 118**,** 1268-75.

MINOBE, K., ONDA, M., IIDA, A., KASUMI, F., SAKAMOTO, G., NAKAMURA, Y. & EMI, M. 1998. Allelic loss on chromosome 9q is associated with lymph node metastasis of primary breast cancer. *Jpn J Cancer Res,* 89**,** 916-22.

MINTON, D. R., FU, L., MONGAN, N. P., SHEVCHUK, M. M., NANUS, D. M. & GUDAS, L. J. 2016. Role of NADH Dehydrogenase (Ubiquinone) 1 Alpha Subcomplex 4-Like 2 in Clear Cell Renal Cell Carcinoma. *Clin Cancer Res,* 22**,** 2791-801.

MISAGHI, S., OTTOSEN, S., IZRAEL-TOMASEVIC, A., ARNOTT, D., LAMKANFI, M., LEE, J., LIU, J., O'ROURKE, K., DIXIT, V. M. & WILSON, A. C. 2009. Association of C-terminal ubiquitin hydrolase BRCA1-associated protein 1 with cell cycle regulator host cell factor 1. *Mol Cell Biol,* 29**,** 2181-92.

MOCSAI, A., HUMPHREY, M. B., VAN ZIFFLE, J. A., HU, Y., BURGHARDT, A., SPUSTA, S. C., MAJUMDAR, S., LANIER, L. L., LOWELL, C. A. & NAKAMURA, M. C. 2004. The immunomodulatory adapter proteins DAP12 and Fc receptor gamma-chain (FcRgamma) regulate development of functional osteoclasts through the Syk tyrosine kinase. *Proc Natl Acad Sci U S A,* 101**,** 6158-63.

MOCSAI, A., RULAND, J. & TYBULEWICZ, V. L. 2010. The SYK tyrosine kinase: a crucial player in diverse biological functions. *Nat Rev Immunol,* 10**,** 387-402.

MOHAMMADI, B., LANG, N., DENGLER, R. & BUFLER, J. 2002. Interaction of high concentrations of riluzole with recombinant skeletal muscle sodium channels and adult-type nicotinic receptor channels. *Muscle Nerve,* 26**,** 539-45.

MORI, Y., WAKAMORI, M., MIYAKAWA, T., HERMOSURA, M., HARA, Y., NISHIDA, M., HIROSE, K., MIZUSHIMA, A., KUROSAKI, M., MORI, E.,

GOTOH, K., OKADA, T., FLEIG, A., PENNER, R., IINO, M. & KUROSAKI, T. 2002. Transient receptor potential 1 regulates capacitative Ca(2+) entry and Ca(2+) release from endoplasmic reticulum in B lymphocytes. *J Exp Med,* 195**,** 673-81.

MORONI, M., SOLDATENKOV, V., ZHANG, L., ZHANG, Y., STOICA, G., GEHAN, E., RASHIDI, B., SINGH, B., OZDEMIRLI, M. & MUELLER, S. C. 2004. Progressive loss of Syk and abnormal proliferation in breast cancer cells. *Cancer Res,* 64**,** 7346-54.

MORRIS, J. C., TAN, A. R., OLENCKI, T. E., SHAPIRO, G. I., DEZUBE, B. J., REISS, M., HSU, F. J., BERZOFSKY, J. A. & LAWRENCE, D. P. 2014. Phase I study of GC1008 (fresolimumab): a human anti-transforming growth factor-beta (TGFbeta) monoclonal antibody in patients with advanced malignant melanoma or renal cell carcinoma. *PLoS One,* 9**,** e90353.

MOTZER, R. J., BACIK, J., MURPHY, B. A., RUSSO, P. & MAZUMDAR, M. 2002. Interferon-alfa as a comparative treatment for clinical trials of new therapies against advanced renal cell carcinoma. *J Clin Oncol,* 20**,** 289-96.

MOTZER, R. J., BANDER, N. H. & NANUS, D. M. 1996. Renal-cell carcinoma. *N Engl J Med,* 335**,** 865-75.

MOTZER, R. J., ESCUDIER, B., MCDERMOTT, D. F., GEORGE, S., HAMMERS, H. J., SRINIVAS, S., TYKODI, S. S., SOSMAN, J. A., PROCOPIO, G., PLIMACK, E. R., CASTELLANO, D., CHOUEIRI, T. K., GURNEY, H., DONSKOV, F., BONO, P., WAGSTAFF, J., GAULER, T. C., UEDA, T., TOMITA, Y., SCHUTZ, F. A., KOLLMANNSBERGER, C., LARKIN, J., RAVAUD, A., SIMON, J. S., XU, L. A., WAXMAN, I. M., SHARMA, P. & CHECKMATE, I. 2015a. Nivolumab versus Everolimus in Advanced Renal-Cell Carcinoma. *N Engl J Med,* 373**,** 1803-13.

MOTZER, R. J., ESCUDIER, B., OUDARD, S., HUTSON, T. E., PORTA, C., BRACARDA, S., GRUNWALD, V., THOMPSON, J. A., FIGLIN, R. A., HOLLAENDER, N., KAY, A., RAVAUD, A. & GROUP, R.-S. 2010. Phase 3 trial of everolimus for metastatic renal cell carcinoma : final results and analysis of prognostic factors. *Cancer,* 116**,** 4256-65.

MOTZER, R. J., ESCUDIER, B., OUDARD, S., HUTSON, T. E., PORTA, C., BRACARDA, S., GRUNWALD, V., THOMPSON, J. A., FIGLIN, R. A., HOLLAENDER, N., URBANOWITZ, G., BERG, W. J., KAY, A., LEBWOHL, D., RAVAUD, A. & GROUP, R.-S. 2008. Efficacy of everolimus in advanced renal cell carcinoma: a double-blind, randomised, placebo-controlled phase III trial. *Lancet,* 372**,** 449-56.

MOTZER, R. J., HUTSON, T. E., GLEN, H., MICHAELSON, M. D., MOLINA, A., EISEN, T., JASSEM, J., ZOLNIEREK, J., MAROTO, J. P., MELLADO, B.,

MELICHAR, B., TOMASEK, J., KREMER, A., KIM, H. J., WOOD, K., DUTCUS, C. & LARKIN, J. 2015b. Lenvatinib, everolimus, and the combination in patients with metastatic renal cell carcinoma: a randomised, phase 2, open-label, multicentre trial. *Lancet Oncol,* 16**,** 1473-1482.

MOTZER, R. J., HUTSON, T. E., TOMCZAK, P., MICHAELSON, M. D., BUKOWSKI, R. M., OUDARD, S., NEGRIER, S., SZCZYLIK, C., PILI, R., BJARNASON, G. A., GARCIA-DEL-MURO, X., SOSMAN, J. A., SOLSKA, E., WILDING, G., THOMPSON, J. A., KIM, S. T., CHEN, I., HUANG, X. & FIGLIN, R. A. 2009. Overall survival and updated results for sunitinib compared with interferon alfa in patients with metastatic renal cell carcinoma. *J Clin Oncol,* 27**,** 3584-90.

MOTZER, R. J., HUTSON, T. E., TOMCZAK, P., MICHAELSON, M. D., BUKOWSKI, R. M., RIXE, O., OUDARD, S., NEGRIER, S., SZCZYLIK, C., KIM, S. T., CHEN, I., BYCOTT, P. W., BAUM, C. M. & FIGLIN, R. A. 2007. Sunitinib versus interferon alfa in metastatic renal-cell carcinoma. *N Engl J Med,* 356**,** 115-24.

MOTZER, R. J., NOSOV, D., EISEN, T., BONDARENKO, I., LESOVOY, V., LIPATOV, O., TOMCZAK, P., LYULKO, O., ALYASOVA, A., HARZA, M., KOGAN, M., ALEKSEEV, B. Y., STERNBERG, C. N., SZCZYLIK, C., CELLA, D., IVANESCU, C., KRIVOSHIK, A., STRAHS, A., ESTEVES, B., BERKENBLIT, A. & HUTSON, T. E. 2013. Tivozanib versus sorafenib as initial targeted therapy for patients with metastatic renal cell carcinoma: results from a phase III trial. *J Clin Oncol,* 31**,** 3791-9.

MOTZER, R. J., POWLES, T., ATKINS, M. B., ESCUDIER, B., MCDERMOTT, D. F., SUAREZ, C., BRACARDA, S., STADLER, W. M., DONSKOV, F., LEE, J.-L., HAWKINS, R. E., RAVAUD, A., ALEKSEEV, B. Y., STAEHLER, M. D., UEMURA, M., DONALDSON, F., LI, S., HUSENI, M. A., SCHIFF, C. & RINI, B. I. 2018a. IMmotion151: A Randomized Phase III Study of Atezolizumab Plus Bevacizumab vs Sunitinib in Untreated Metastatic Renal Cell Carcinoma (mRCC). *Journal of Clinical Oncology,* 36**,** 578-578.

MOTZER, R. J., TANNIR, N. M., MCDERMOTT, D. F., AREN FRONTERA, O., MELICHAR, B., CHOUEIRI, T. K., PLIMACK, E. R., BARTHELEMY, P., PORTA, C., GEORGE, S., POWLES, T., DONSKOV, F., NEIMAN, V., KOLLMANNSBERGER, C. K., SALMAN, P., GURNEY, H., HAWKINS, R., RAVAUD, A., GRIMM, M. O., BRACARDA, S., BARRIOS, C. H., TOMITA, Y., CASTELLANO, D., RINI, B. I., CHEN, A. C., MEKAN, S., MCHENRY, M. B., WIND-ROTOLO, M., DOAN, J., SHARMA, P., HAMMERS, H. J., ESCUDIER, B. & CHECKMATE, I. 2018b. Nivolumab plus Ipilimumab versus Sunitinib in Advanced Renal-Cell Carcinoma. *N Engl J Med,* 378**,** 1277-1290.

MUELLER, W., NUTT, C. L., EHRICH, M., RIEMENSCHNEIDER, M. J., VON DEIMLING, A., VAN DEN BOOM, D. & LOUIS, D. N. 2007. Downregulation of

RUNX3 and TES by hypermethylation in glioblastoma. *Oncogene,* 26**,** 583-93.

MURAKAMI, Y., KANDA, K., YOKOTA, K., KANAYAMA, H. & KAGAWA, S. 2001. Prognostic significance of immuno-proteosome subunit expression in patients with renal-cell carcinoma: a preliminary study. *Mol Urol,* 5**,** 113-9.

MURATA, S., YASHIRODA, H. & TANAKA, K. 2009. Molecular mechanisms of proteasome assembly. *Nat Rev Mol Cell Biol,* 10**,** 104-15.

NAITO, S., VON ESCHENBACH, A. C., GIAVAZZI, R. & FIDLER, I. J. 1986. Growth and metastasis of tumor cells isolated from a human renal cell carcinoma implanted into different organs of nude mice. *Cancer Res,* 46**,** 4109-15.

NAKAIGAWA, N., YAO, M., BABA, M., KATO, S., KISHIDA, T., HATTORI, K., NAGASHIMA, Y. & KUBOTA, Y. 2006. Inactivation of von Hippel-Lindau gene induces constitutive phosphorylation of MET protein in clear cell renal carcinoma. *Cancer Res,* 66**,** 3699-705.

NAKASHIMA, H., NATSUGOE, S., ISHIGAMI, S., OKUMURA, H., MATSUMOTO, M., HOKITA, S. & AIKOU, T. 2006. Clinical significance of nuclear expression of spleen tyrosine kinase (Syk) in gastric cancer. *Cancer Lett,* 236**,** 89-94.

NARGUND, A. M., PHAM, C. G., DONG, Y., WANG, P. I., OSMANGEYOGLU, H. U., XIE, Y., ARAS, O., HAN, S., OYAMA, T., TAKEDA, S., RAY, C. E., DONG, Z., BERGE, M., HAKIMI, A. A., MONETTE, S., LEKAYE, C. L., KOUTCHER, J. A., LESLIE, C. S., CREIGHTON, C. J., WEINHOLD, N., LEE, W., TICKOO, S. K., WANG, Z., CHENG, E. H. & HSIEH, J. J. 2017. The SWI/SNF Protein PBRM1 Restrains VHL-Loss-Driven Clear Cell Renal Cell Carcinoma. *Cell Rep,* 18**,** 2893-2906.

NATIONAL INSTITUTE FOR HEALTH AND CARE EXCELLENCE (NICE) 2001. NICE technology appraisal guidance [TA20]. Guidance on the use of riluzole for the treatment of motor neurone disease.

NISSEN, S. E. & WOLSKI, K. 2007. Effect of rosiglitazone on the risk of myocardial infarction and death from cardiovascular causes. *N Engl J Med,* 356**,** 2457-71.

NUGENT, K. P., FARMER, K. C., SPIGELMAN, A. D., WILLIAMS, C. B. & PHILLIPS, R. K. 1993. Randomized controlled trial of the effect of sulindac on duodenal and rectal polyposis and cell proliferation in patients with familial adenomatous polyposis. *Br J Surg,* 80**,** 1618-9.

OCHI, T., MOTOYAMA, Y. & GOTO, T. 2000. The analgesic effect profile of FR122047, a selective cyclooxygenase-1 inhibitor, in chemical nociceptive models. *Eur J Pharmacol,* 391**,** 49-54.

OSMAN, W. M. & YOUSSEF, N. S. 2015. Combined use of COX-1 and VEGF immunohistochemistry refines the histopathologic prognosis of renal cell carcinoma. *International Journal of Clinical and Experimental Pathology,* 8**,** 8165-8177.

PALAPATTU, G. S., KRISTO, B. & RAJFER, J. 2002. Paraneoplastic syndromes in urologic malignancy: the many faces of renal cell carcinoma. *Rev Urol,* 4**,** 163-70.

PALSDOTTIR, H. B., HARDARSON, S., PETURSDOTTIR, V., JONSSON, A., JONSSON, E., SIGURDSSON, M. I., EINARSSON, G. V. & GUDBJARTSSON, T. 2012. Incidental detection of renal cell carcinoma is an independent prognostic marker: results of a long-term, whole population study. *J Urol,* 187**,** 48-53.

PAN, Q., SHAI, O., LEE, L. J., FREY, B. J. & BLENCOWE, B. J. 2008. Deep surveying of alternative splicing complexity in the human transcriptome by high-throughput sequencing. *Nat Genet,* 40**,** 1413-5.

PANER, G. P., STADLER, W. M., HANSEL, D. E., MONTIRONI, R., LIN, D. W. & AMIN, M. B. 2018. Updates in the Eighth Edition of the Tumor-Node-Metastasis Staging Classification for Urologic Cancers. *Eur Urol,* 73**,** 560-569.

PARDOLL, D. M. 2012. The blockade of immune checkpoints in cancer immunotherapy. *Nat Rev Cancer,* 12**,** 252-64.

PARK, Y. R., CHUN, J. N., SO, I., KIM, H. J., BAEK, S., JEON, J. H. & SHIN, S. Y. 2016. Data-driven Analysis of TRP Channels in Cancer: Linking Variation in Gene Expression to Clinical Significance. *Cancer Genomics Proteomics,* 13**,** 83-90.

PATRONO, C., COLLER, B., FITZGERALD, G. A., HIRSH, J. & ROTH, G. 2004. Platelet-active drugs: the relationships among dose, effectiveness, and side effects: the Seventh ACCP Conference on Antithrombotic and Thrombolytic Therapy. *Chest,* 126**,** 234S-264S.

PATRONO, C., PATRIGNANI, P. & GARCIA RODRIGUEZ, L. A. 2001. Cyclooxygenase-selective inhibition of prostanoid formation: transducing biochemical selectivity into clinical read-outs. *J Clin Invest,* 108**,** 7-13.

PAUL, S. M., MYTELKA, D. S., DUNWIDDIE, C. T., PERSINGER, C. C., MUNOS, B. H., LINDBORG, S. R. & SCHACHT, A. L. 2010. How to improve

R&D productivity: the pharmaceutical industry's grand challenge. *Nat Rev Drug Discov,* 9**,** 203-14.

PAWLOWSKI, R., MUHL, S. M., SULSER, T., KREK, W., MOCH, H. & SCHRAML, P. 2013. Loss of PBRM1 expression is associated with renal cell carcinoma progression. *Int J Cancer,* 132**,** E11-7.

PENA-LLOPIS, S., VEGA-RUBIN-DE-CELIS, S., LIAO, A., LENG, N., PAVIA-JIMENEZ, A., WANG, S., YAMASAKI, T., ZHREBKER, L., SIVANAND, S., SPENCE, P., KINCH, L., HAMBUCH, T., JAIN, S., LOTAN, Y., MARGULIS, V., SAGALOWSKY, A. I., SUMMEROUR, P. B., KABBANI, W., WONG, S. W., GRISHIN, N., LAURENT, M., XIE, X. J., HAUDENSCHILD, C. D., ROSS, M. T., BENTLEY, D. R., KAPUR, P. & BRUGAROLAS, J. 2012. BAP1 loss defines a new class of renal cell carcinoma. *Nat Genet,* 44**,** 751-9.

PENNACCHIETTI, S., MICHIELI, P., GALLUZZO, M., MAZZONE, M., GIORDANO, S. & COMOGLIO, P. M. 2003. Hypoxia promotes invasive growth by transcriptional activation of the met protooncogene. *Cancer Cell,* 3**,** 347-61.

PENNING, T. D., TALLEY, J. J., BERTENSHAW, S. R., CARTER, J. S., COLLINS, P. W., DOCTER, S., GRANETO, M. J., LEE, L. F., MALECHA, J. W., MIYASHIRO, J. M., ROGERS, R. S., ROGIER, D. J., YU, S. S., ANDERSON, G. D., BURTON, E. G., COGBURN, J. N., GREGORY, S. A., KOBOLDT, C. M., PERKINS, W. E., SEIBERT, K., VEENHUIZEN, A. W., ZHANG, Y. Y. & ISAKSON, P. C. 1997. Synthesis and Biological Evaluation of the 1,5-Diarylpyrazole Class of Cyclooxygenase-2 Inhibitors: Identification of 4-[5-(4-Methylphenyl)-3- (trifluoromethyl)-1H-pyrazol-1-yl]benzenesulfonamide (SC-58635, Celecoxib). *Journal of Medicinal Chemistry,* 40**,** 1347-1365.

PEREGO, R. A., BIANCHI, C., CORIZZATO, M., EROINI, B., TORSELLO, B., VALSECCHI, C., DI FONZO, A., CORDANI, N., FAVINI, P., FERRERO, S., PITTO, M., SARTO, C., MAGNI, F., ROCCO, F. & MOCARELLI, P. 2005. Primary cell cultures arising from normal kidney and renal cell carcinoma retain the proteomic profile of corresponding tissues. *J Proteome Res,* 4**,** 1503-10.

PERROUD, B., ISHIMARU, T., BOROWSKY, A. D. & WEISS, R. H. 2009. Grade-dependent proteomics characterization of kidney cancer. *Mol Cell Proteomics,* 8**,** 971-85.

PFALLER, W. & GSTRAUNTHALER, G. 1998. Nephrotoxicity testing in vitro--what we know and what we need to know. *Environ Health Perspect,* 106 Suppl 2**,** 559-69.

PFISTER, S. X., MARKKANEN, E., JIANG, Y., SARKAR, S., WOODCOCK, M., ORLANDO, G., MAVROMMATI, I., PAI, C. C., ZALMAS, L. P., DROBNITZKY, N., DIANOV, G. L., VERRILL, C., MACAULAY, V. M., YING, S., LA THANGUE, N. B., D'ANGIOLELLA, V., RYAN, A. J. & HUMPHREY, T. C. 2015. Inhibiting WEE1 Selectively Kills Histone H3K36me3-Deficient Cancers by dNTP Starvation. *Cancer Cell,* 28**,** 557-568.

PHAM, L. V., TAMAYO, A. T., YOSHIMURA, L. C., LO, P. & FORD, R. J. 2003. Inhibition of constitutive NF-kappa B activation in mantle cell lymphoma B cells leads to induction of cell cycle arrest and apoptosis. *J Immunol,* 171**,** 88-95.

PHELAN, K. D., SHWE, U. T., ABRAMOWITZ, J., WU, H., RHEE, S. W., HOWELL, M. D., GOTTSCHALL, P. E., FREICHEL, M., FLOCKERZI, V., BIRNBAUMER, L. & ZHENG, F. 2013. Canonical transient receptor channel 5 (TRPC5) and TRPC1/4 contribute to seizure and excitotoxicity by distinct cellular mechanisms. *Mol Pharmacol,* 83**,** 429-38.

PODOLANCZUK, A., LAZARUS, A. H., CROW, A. R., GROSSBARD, E. & BUSSEL, J. B. 2009. Of mice and men: an open-label pilot study for treatment of immune thrombocytopenic purpura by an inhibitor of Syk. *Blood,* 113**,** 3154-60.

POGUE, S. L., KUROSAKI, T., BOLEN, J. & HERBST, R. 2000. B cell antigen receptor-induced activation of Akt promotes B cell survival and is dependent on Syk kinase. *J Immunol,* 165**,** 1300-6.

PREVARSKAYA, N., FLOURAKIS, M., BIDAUX, G., THEBAULT, S. & SKRYMA, R. 2007a. Differential role of TRP channels in prostate cancer. *Biochem Soc Trans,* 35**,** 133-5.

PREVARSKAYA, N., ZHANG, L. & BARRITT, G. 2007b. TRP channels in cancer. *Biochim Biophys Acta,* 1772**,** 937-46.

PRINOS, P., GARNEAU, D., LUCIER, J. F., GENDRON, D., COUTURE, S., BOIVIN, M., BROSSEAU, J. P., LAPOINTE, E., THIBAULT, P., DURAND, M., TREMBLAY, K., GERVAIS-BIRD, J., NWILATI, H., KLINCK, R., CHABOT, B., PERREAULT, J. P., WELLINGER, R. J. & ELELA, S. A. 2011. Alternative splicing of SYK regulates mitosis and cell survival. *Nat Struct Mol Biol,* 18**,** 673-9.

R CORE DEVELOPMENT TEAM 2010. R: A language and environment for statistical computing. Vienna, Austria: R Foundation for Statistical Computing.

RABJERG, M., MIKKELSEN, M. N., WALTER, S. & MARCUSSEN, N. 2014. Incidental renal neoplasms: is there a need for routine screening? A Danish single-center epidemiological study. *APMIS,* 122**,** 708-14.

RAHMANI, M., DAVIS, E. M., CRABTREE, T. R., HABIBI, J. R., NGUYEN, T. K., DENT, P. & GRANT, S. 2007. The kinase inhibitor sorafenib induces cell death through a process involving induction of endoplasmic reticulum stress. *Mol Cell Biol,* 27**,** 5499-513.

RAO, A. & LAUER, R. 2015. Phase II study of sorafenib and bortezomib for first-line treatment of metastatic or unresectable renal cell carcinoma. *Oncologist,* 20**,** 370-1.

RAPPSILBER, J., MANN, M. & ISHIHAMA, Y. 2007. Protocol for micro-purification, enrichment, pre-fractionation and storage of peptides for proteomics using StageTips. *Nat Protoc,* 2**,** 1896-906.

RATNAYAKE, R., COVELL, D., RANSOM, T. T., GUSTAFSON, K. R. & BEUTLER, J. A. 2009. Englerin A, a selective inhibitor of renal cancer cell growth, from Phyllanthus engleri. *Org Lett,* 11**,** 57-60.

RAUZI, F., KIRKBY, N. S., EDIN, M. L., WHITEFORD, J., ZELDIN, D. C., MITCHELL, J. A. & WARNER, T. D. 2016. Aspirin inhibits the production of proangiogenic 15(S)-HETE by platelet cyclooxygenase-1. *FASEB J,* 30**,** 4256-4266.

REISMAN, D., GLAROS, S. & THOMPSON, E. A. 2009. The SWI/SNF complex and cancer. *Oncogene,* 28**,** 1653-68.

RICCIOTTI, E. & FITZGERALD, G. A. 2011. Prostaglandins and inflammation. *Arterioscler Thromb Vasc Biol,* 31**,** 986-1000.

RICHTER, J. M., SCHAEFER, M. & HILL, K. 2014. Riluzole activates TRPC5 channels independently of PLC activity. *Br J Pharmacol,* 171**,** 158-70.

RICKETTS, C. J., DE CUBAS, A. A., FAN, H., SMITH, C. C., LANG, M., REZNIK, E., BOWLBY, R., GIBB, E. A., AKBANI, R., BEROUKHIM, R., BOTTARO, D. P., CHOUEIRI, T. K., GIBBS, R. A., GODWIN, A. K., HAAKE, S., HAKIMI, A. A., HENSKE, E. P., HSIEH, J. J., HO, T. H., KANCHI, R. S., KRISHNAN, B., KWIATKOWSKI, D. J., LUI, W., MERINO, M. J., MILLS, G. B., MYERS, J., NICKERSON, M. L., REUTER, V. E., SCHMIDT, L. S., SHELLEY, C. S., SHEN, H., SHUCH, B., SIGNORETTI, S., SRINIVASAN, R., TAMBOLI, P., THOMAS, G., VINCENT, B. G., VOCKE, C. D., WHEELER, D. A., YANG, L., KIM, W. Y., ROBERTSON, A. G., CANCER GENOME ATLAS RESEARCH, N., SPELLMAN, P. T., RATHMELL, W. K. & LINEHAN, W. M. 2018. The Cancer Genome Atlas Comprehensive Molecular Characterization of Renal Cell Carcinoma. *Cell Rep,* 23**,** 3698.

RICKETTS, C. J., HILL, V. K. & LINEHAN, W. M. 2014. Tumor-specific hypermethylation of epigenetic biomarkers, including SFRP1, predicts for

poorer survival in patients from the TCGA Kidney Renal Clear Cell Carcinoma (KIRC) project. *PLoS One,* 9**,** e85621.

RINI, B., GODDARD, A., KNEZEVIC, D., MADDALA, T., ZHOU, M., AYDIN, H., CAMPBELL, S., ELSON, P., KOSCIELNY, S., LOPATIN, M., SVEDMAN, C., MARTINI, J. F., WILLIAMS, J. A., VERKARRE, V., RADULESCU, C., NEUZILLET, Y., HEMMERLE, I., TIMSIT, M. O., TSIATIS, A. C., BONHAM, M., LEBRET, T., MEJEAN, A. & ESCUDIER, B. 2015. A 16-gene assay to predict recurrence after surgery in localised renal cell carcinoma: development and validation studies. *Lancet Oncol*.

RINI, B. I., CAMPBELL, S. C. & ESCUDIER, B. 2009. Renal cell carcinoma. *Lancet,* 373**,** 1119-32.

RINI, B. I., ESCUDIER, B., MARTINI, J. F., MAGHELI, A., SVEDMAN, C., LOPATIN, M., KNEZEVIC, D., GODDARD, A. D., FEBBO, P. G., LI, R., LIN, X., VALOTA, O., STAEHLER, M., MOTZER, R. J. & RAVAUD, A. 2018. Validation of the 16-Gene Recurrence Score in Patients with Locoregional, High-Risk Renal Cell Carcinoma from a Phase III Trial of Adjuvant Sunitinib. *Clin Cancer Res,* 24**,** 4407-4415.

ROTHWELL, P. M., WILSON, M., ELWIN, C. E., NORRVING, B., ALGRA, A., WARLOW, C. P. & MEADE, T. W. 2010. Long-term effect of aspirin on colorectal cancer incidence and mortality: 20-year follow-up of five randomised trials. *Lancet,* 376**,** 1741-50.

ROUETTE, A., TROFIMOV, A., HABERL, D., BOUCHER, G., LAVALLEE, V. P., D'ANGELO, G., HEBERT, J., SAUVAGEAU, G., LEMIEUX, S. & PERREAULT, C. 2016. Expression of immunoproteasome genes is regulated by cell-intrinsic and -extrinsic factors in human cancers. *Sci Rep,* 6**,** 34019.

ROUTY, B., LE CHATELIER, E., DEROSA, L., DUONG, C. P. M., ALOU, M. T., DAILLERE, R., FLUCKIGER, A., MESSAOUDENE, M., RAUBER, C., ROBERTI, M. P., FIDELLE, M., FLAMENT, C., POIRIER-COLAME, V., OPOLON, P., KLEIN, C., IRIBARREN, K., MONDRAGON, L., JACQUELOT, N., QU, B., FERRERE, G., CLEMENSON, C., MEZQUITA, L., MASIP, J. R., NALTET, C., BROSSEAU, S., KADERBHAI, C., RICHARD, C., RIZVI, H., LEVENEZ, F., GALLERON, N., QUINQUIS, B., PONS, N., RYFFEL, B., MINARD-COLIN, V., GONIN, P., SORIA, J. C., DEUTSCH, E., LORIOT, Y., GHIRINGHELLI, F., ZALCMAN, G., GOLDWASSER, F., ESCUDIER, B., HELLMANN, M. D., EGGERMONT, A., RAOULT, D., ALBIGES, L., KROEMER, G. & ZITVOGEL, L. 2018. Gut microbiome influences efficacy of PD-1-based immunotherapy against epithelial tumors. *Science,* 359**,** 91-97.

RUBAIY, H. N., LUDLOW, M. J., BON, R. S. & BEECH, D. J. 2017a. Pico145 - powerful new tool for TRPC1/4/5 channels. *Channels (Austin)***,** 1-3.

RUBAIY, H. N., LUDLOW, M. J., HENROT, M., GAUNT, H. J., MITEVA, K., CHEUNG, S. Y., TANAHASHI, Y., HAMZAH, N., MUSIALOWSKI, K. E., BLYTHE, N. M., APPLEBY, H. L., BAILEY, M. A., MCKEOWN, L., TAYLOR, R., FOSTER, R., WALDMANN, H., NUSSBAUMER, P., CHRISTMANN, M., BON, R. S., MURAKI, K. & BEECH, D. J. 2017b. Picomolar, selective, and subtype-specific small-molecule inhibition of TRPC1/4/5 channels. *J Biol Chem,* 292**,** 8158-8173.

RYFFEL, B., WOERLY, G., GREINER, B., HAENDLER, B., MIHATSCH, M. J. & FOXWELL, B. M. 1991. Distribution of the cyclosporine binding protein cyclophilin in human tissues. *Immunology,* 72**,** 399-404.

SADA, K., TAKANO, T., YANAGI, S. & YAMAMURA, H. 2001. Structure and function of Syk protein-tyrosine kinase. *J Biochem,* 130**,** 177-86.

SALES, K. J., KATZ, A. A., HOWARD, B., SOETERS, R. P., MILLAR, R. P. & JABBOUR, H. N. 2002. Cyclooxygenase-1 is up-regulated in cervical carcinomas: Autocrine/paracrine regulation of cyclooxygenase-2, prostaglandin E receptors, and angiogenic factors by cyclooxygenase-1. *Cancer Research,* 62**,** 424-432.

SANDERS, E. & DIEHL, S. 2015. Analysis and interpretation of transcriptomic data obtained from extended Warburg effect genes in patients with clear cell renal cell carcinoma. *Oncoscience,* 2**,** 151-86.

SANKIN, A., HAKIMI, A. A., MIKKILINENI, N., OSTROVNAYA, I., SILK, M. T., LIANG, Y., MANO, R., CHEVINSKY, M., MOTZER, R. J., SOLOMON, S. B., CHENG, E. H., DURACK, J. C., COLEMAN, J. A., RUSSO, P. & HSIEH, J. J. 2014. The impact of genetic heterogeneity on biomarker development in kidney cancer assessed by multiregional sampling. *Cancer Med,* 3**,** 1485-92.

SARTI, M., SEVIGNANI, C., CALIN, G. A., AQEILAN, R., SHIMIZU, M., PENTIMALLI, F., PICCHIO, M. C., GODWIN, A., ROSENBERG, A., DRUSCO, A., NEGRINI, M. & CROCE, C. M. 2005. Adenoviral transduction of TESTIN gene into breast and uterine cancer cell lines promotes apoptosis and tumor reduction in vivo. *Clin Cancer Res,* 11**,** 806-13.

SATO, Y., YOSHIZATO, T., SHIRAISHI, Y., MAEKAWA, S., OKUNO, Y., KAMURA, T., SHIMAMURA, T., SATO-OTSUBO, A., NAGAE, G., SUZUKI, H., NAGATA, Y., YOSHIDA, K., KON, A., SUZUKI, Y., CHIBA, K., TANAKA, H., NIIDA, A., FUJIMOTO, A., TSUNODA, T., MORIKAWA, T., MAEDA, D., KUME, H., SUGANO, S., FUKAYAMA, M., ABURATANI, H., SANADA, M., MIYANO, S., HOMMA, Y. & OGAWA, S. 2013. Integrated molecular analysis of clear-cell renal cell carcinoma. *Nat Genet,* 45**,** 860-7.

SCELO, G., RIAZALHOSSEINI, Y., GREGER, L., LETOURNEAU, L., GONZALEZ-PORTA, M., WOZNIAK, M. B., BOURGEY, M., HARNDEN, P.,

EGEVAD, L., JACKSON, S. M., KARIMZADEH, M., ARSENEAULT, M., LEPAGE, P., HOW-KIT, A., DAUNAY, A., RENAULT, V., BLANCHE, H., TUBACHER, E., SEHMOUN, J., VIKSNA, J., CELMS, E., OPMANIS, M., ZARINS, A., VASUDEV, N. S., SEYWRIGHT, M., ABEDI-ARDEKANI, B., CARREIRA, C., SELBY, P. J., CARTLEDGE, J. J., BYRNES, G., ZAVADIL, J., SU, J., HOLCATOVA, I., BRISUDA, A., ZARIDZE, D., MOUKERIA, A., FORETOVA, L., NAVRATILOVA, M., MATES, D., JINGA, V., ARTEMOV, A., NEDOLUZHKO, A., MAZUR, A., RASTORGUEV, S., BOULYGINA, E., HEATH, S., GUT, M., BIHOREAU, M. T., LECHNER, D., FOGLIO, M., GUT, I. G., SKRYABIN, K., PROKHORTCHOUK, E., CAMBON-THOMSEN, A., RUNG, J., BOURQUE, G., BRENNAN, P., TOST, J., BANKS, R. E., BRAZMA, A. & LATHROP, G. M. 2014. Variation in genomic landscape of clear cell renal cell carcinoma across Europe. *Nat Commun,* 5**,** 5135.

SCHMID, H., COHEN, C. D., HENGER, A., IRRGANG, S., SCHLONDORFF, D. & KRETZLER, M. 2003. Validation of endogenous controls for gene expression analysis in microdissected human renal biopsies. *Kidney Int,* 64**,** 356-60.

SCHUETZ, A. N., YIN-GOEN, Q., AMIN, M. B., MORENO, C. S., COHEN, C., HORNSBY, C. D., YANG, W. L., PETROS, J. A., ISSA, M. M., PATTARAS, J. G., OGAN, K., MARSHALL, F. F. & YOUNG, A. N. 2005. Molecular classification of renal tumors by gene expression profiling. *J Mol Diagn,* 7**,** 206-18.

SCIACOVELLI, M., GUZZO, G., MORELLO, V., FREZZA, C., ZHENG, L., NANNINI, N., CALABRESE, F., LAUDIERO, G., ESPOSITO, F., LANDRISCINA, M., DEFILIPPI, P., BERNARDI, P. & RASOLA, A. 2013. The mitochondrial chaperone TRAP1 promotes neoplastic growth by inhibiting succinate dehydrogenase. *Cell Metab,* 17**,** 988-99.

SELIGER, B., MAEURER, M. J. & FERRONE, S. 1997. Tap Off - Tumors On. *Immunology Today,* 18**,** 292-299.

SHAH, S. A., POTTER, M. W., MCDADE, T. P., RICCIARDI, R., PERUGINI, R. A., ELLIOTT, P. J., ADAMS, J. & CALLERY, M. P. 2001. 26S proteasome inhibition induces apoptosis and limits growth of human pancreatic cancer. *J Cell Biochem,* 82**,** 110-22.

SHARMAN, J., HAWKINS, M., KOLIBABA, K., BOXER, M., KLEIN, L., WU, M., HU, J., ABELLA, S. & YASENCHAK, C. 2015. An open-label phase 2 trial of entospletinib (GS-9973), a selective Syk inhibitor, in chronic lymphocytic leukemia. *Blood*.

SHAW, G. 2016. The silent disease. *Nature,* 537**,** S98.

SHI, Z. G., LI, S. Q., LI, Z. J., ZHU, X. J., XU, P. & LIU, G. 2015. Expression of vimentin and survivin in clear cell renal cell carcinoma and correlation with p53. *Clin Transl Oncol,* 17**,** 65-73.

SHOEMAKER, R. H. 2006. The NCI60 human tumour cell line anticancer drug screen. *Nat Rev Cancer,* 6**,** 813-23.

SI, T., YANG, G., QIU, X., LUO, Y., LIU, B. & WANG, B. 2015. Expression of tumor necrosis factor receptor-associated protein 1 and its clinical significance in kidney cancer. *Int J Clin Exp Pathol,* 8**,** 13090-5.

SINGH RANGER, G. 2016. The role of aspirin in colorectal cancer chemoprevention. *Crit Rev Oncol Hematol,* 104**,** 87-90.

SLEIRE, L., FORDE-TISLEVOLL, H. E., NETLAND, I. A., LEISS, L., SKEIE, B. S. & ENGER, P. O. 2017. Drug repurposing in cancer. *Pharmacol Res,* 124**,** 74-91.

SMITH, C. J., ZHANG, Y., KOBOLDT, C. M., MUHAMMAD, J., ZWEIFEL, B. S., SHAFFER, A., TALLEY, J. J., MASFERRER, J. L., SEIBERT, K. & ISAKSON, P. C. 1998. Pharmacological analysis of cyclooxygenase-1 in inflammation. *Proc Natl Acad Sci U S A,* 95**,** 13313-8.

SMITH, D. M., CHANG, S. C., PARK, S., FINLEY, D., CHENG, Y. & GOLDBERG, A. L. 2007. Docking of the proteasomal ATPases' carboxyl termini in the 20S proteasome's alpha ring opens the gate for substrate entry. *Mol Cell,* 27**,** 731-44.

SMITTENAAR, C. R., PETERSEN, K. A., STEWART, K. & MOITT, N. 2016. Cancer incidence and mortality projections in the UK until 2035. *Br J Cancer,* 115**,** 1147-1155.

SMYTH, E. C., SCLAFANI, F. & CUNNINGHAM, D. 2014. Emerging molecular targets in oncology: clinical potential of MET/hepatocyte growth-factor inhibitors. *Onco Targets Ther,* 7**,** 1001-14.

SOURBIER, C., SCROGGINS, B. T., RATNAYAKE, R., PRINCE, T. L., LEE, S., LEE, M. J., NAGY, P. L., LEE, Y. H., TREPEL, J. B., BEUTLER, J. A., LINEHAN, W. M. & NECKERS, L. 2013. Englerin A stimulates PKCtheta to inhibit insulin signaling and to simultaneously activate HSF1: pharmacologically induced synthetic lethality. *Cancer Cell,* 23**,** 228-37.

SOYUPAK, B., ERDOGAN, S., ERGIN, M., SEYDAOGLU, G., KUZGUNBAY, B. & TANSUG, Z. 2005. CA9 expression as a prognostic factor in renal clear cell carcinoma. *Urol Int,* 74**,** 68-73.

STAKHOVSKYI, O., YAP, S. A., LEVERIDGE, M., LAWRENTSCHUK, N. & JEWETT, M. A. 2011. Small renal mass: what the urologist needs to know for treatment planning and assessment of treatment results. *AJR Am J Roentgenol,* 196**,** 1267-73.

STEPANENKO, A. A. & DMITRENKO, V. V. 2015. HEK293 in cell biology and cancer research: phenotype, karyotype, tumorigenicity, and stress-induced genome-phenotype evolution. *Gene,* 569**,** 182-90.

STERNBERG, C. N., DAVIS, I. D., MARDIAK, J., SZCZYLIK, C., LEE, E., WAGSTAFF, J., BARRIOS, C. H., SALMAN, P., GLADKOV, O. A., KAVINA, A., ZARBA, J. J., CHEN, M., MCCANN, L., PANDITE, L., ROYCHOWDHURY, D. F. & HAWKINS, R. E. 2010. Pazopanib in locally advanced or metastatic renal cell carcinoma: results of a randomized phase III trial. *J Clin Oncol,* 28**,** 1061-8.

STOREY, J. D. 2002. A direct approach to false discovery rates. *Journal of the Royal Statistical Society Series B-Statistical Methodology,* 64**,** 479-498.

SUKUMAR, P. & BEECH, D. J. 2010. Stimulation of TRPC5 cationic channels by low micromolar concentrations of lead ions (Pb2+). *Biochem Biophys Res Commun,* 393**,** 50-4.

SULZMAIER, F. J., LI, Z., NAKASHIGE, M. L., FASH, D. M., CHAIN, W. J. & RAMOS, J. W. 2012. Englerin a selectively induces necrosis in human renal cancer cells. *PLoS One,* 7**,** e48032.

SUN, C. Y., ZANG, Y. C., SAN, Y. X., SUN, W. & ZHANG, L. 2010. Proteomic analysis of clear cell renal cell carcinoma. Identification of potential tumor markers. *Saudi Med J,* 31**,** 525-32.

SUN, X. J., WEI, J., WU, X. Y., HU, M., WANG, L., WANG, H. H., ZHANG, Q. H., CHEN, S. J., HUANG, Q. H. & CHEN, Z. 2005. Identification and characterization of a novel human histone H3 lysine 36-specific methyltransferase. *J Biol Chem,* 280**,** 35261-71.

SUNWOO, J. B., CHEN, Z., DONG, G., YEH, N., CROWL BANCROFT, C., SAUSVILLE, E., ADAMS, J., ELLIOTT, P. & VAN WAES, C. 2001. Novel proteasome inhibitor PS-341 inhibits activation of nuclear factor-kappa B, cell survival, tumor growth, and angiogenesis in squamous cell carcinoma. *Clin Cancer Res,* 7**,** 1419-28.

TAJEDDINE, N., ZANOU, N., VAN SCHOOR, M., LEBACQ, J. & GAILLY, P. 2010. TRPC1: subcellular localization? *J Biol Chem,* 285**,** le1; author reply le2.

TANAKA, T., KUTOMI, G., KAJIWARA, T., KUKITA, K., KOCHIN, V., KANASEKI, T., TSUKAHARA, T., HIROHASHI, Y., TORIGOE, T., OKAMOTO, Y., HIRATA, K., SATO, N. & TAMURA, Y. 2017. Cancer-associated oxidoreductase ERO1-alpha promotes immune escape through up-regulation of PD-L1 in human breast cancer. *Oncotarget,* 8**,** 24706-24718.

TANIGUCHI, H., IWASA, S., YAMAZAKI, K., YOSHINO, T., KIRYU, C., NAKA, Y., LIEW, E. L. & SAKATA, Y. 2017. Phase 1 study of OCV-C02, a peptide vaccine consisting of two peptide epitopes for refractory metastatic colorectal cancer. *Cancer Sci,* 108**,** 1013-1021.

TANIGUCHI, T., KOBAYASHI, T., KONDO, J., TAKAHASHI, K., NAKAMURA, H., SUZUKI, J., NAGAI, K., YAMADA, T., NAKAMURA, S. & YAMAMURA, H. 1991. Molecular cloning of a porcine gene syk that encodes a 72-kDa protein-tyrosine kinase showing high susceptibility to proteolysis. *J Biol Chem,* 266**,** 15790-6.

TANNIR, N. M., FAN, A. C., LEE, R. J., CARTHON, B. C., ILIOPOULOS, O., MIER, J. W., PATEL, M. R., MERIC-BERNSTAM, F., DEMICHELE, A., VOSS, M. H., HARDING, J. J., SRINIVASAN, R., SHAPIRO, G., TELLI, M. L., MUNSTER, P. N., RICHARD D. CARVAJAL, R. D., JENKINS, Y., WHITING, S. H., BENDELL, J. C. & BAUER, T. M. 2018. Phase 1 study of glutaminase (GLS) inhibitor CB-839 combined with either everolimus (E) or cabozantinib (Cabo) in patients (pts) with clear cell (cc) and papillary (pap) metastatic renal cell cancer (mRCC). *Journal of Clinical Oncology,* 36**,** 603-603.

TATARELLI, C., LINNENBACH, A., MIMORI, K. & CROCE, C. M. 2000. Characterization of the human TESTIN gene localized in the FRA7G region at 7q31.2. *Genomics,* 68**,** 1-12.

TEW, K. D. 2016. Commentary on "Proteasome Inhibitors: A Novel Class of Potent and Effective Antitumor Agents". *Cancer Res,* 76**,** 4916-7.

THE UNIPROT CONSORTIUM 2017. UniProt: the universal protein knowledgebase. *Nucleic Acids Research,* 45**,** D158-D169.

THOMPSON, M. A., STUMPH, J., HENRICKSON, S. E., ROSENWALD, A., WANG, Q., OLSON, S., BRANDT, S. J., ROBERTS, J., ZHANG, X., SHYR, Y. & KINNEY, M. C. 2005. Differential gene expression in anaplastic lymphoma kinase-positive and anaplastic lymphoma kinase-negative anaplastic large cell lymphomas. *Hum Pathol,* 36**,** 494-504.

TOYAMA, T., IWASE, H., YAMASHITA, H., HARA, Y., OMOTO, Y., SUGIURA, H., ZHANG, Z. & FUJII, Y. 2003. Reduced expression of the Syk gene is correlated with poor prognosis in human breast cancer. *Cancer Lett,* 189**,** 97-102.

TSUJII, M., KAWANO, S., TSUJI, S., SAWAOKA, H., HORI, M. & DUBOIS, R. N. 1998. Cyclooxygenase regulates angiogenesis induced by colon cancer cells. *Cell,* 93**,** 705-716.

TURAJLIC, S., XU, H., LITCHFIELD, K., ROWAN, A., HORSWELL, S., CHAMBERS, T., O'BRIEN, T., LOPEZ, J. I., WATKINS, T. B. K., NICOL, D., STARES, M., CHALLACOMBE, B., HAZELL, S., CHANDRA, A., MITCHELL, T. J., AU, L., EICHLER-JONSSON, C., JABBAR, F., SOULTATI, A., CHOWDHURY, S., RUDMAN, S., LYNCH, J., FERNANDO, A., STAMP, G., NYE, E., STEWART, A., XING, W., SMITH, J. C., ESCUDERO, M., HUFFMAN, A., MATTHEWS, N., ELGAR, G., PHILLIMORE, B., COSTA, M., BEGUM, S., WARD, S., SALM, M., BOEING, S., FISHER, R., SPAIN, L., NAVAS, C., GRONROOS, E., HOBOR, S., SHARMA, S., AURANGZEB, I., LALL, S., POLSON, A., VARIA, M., HORSFIELD, C., FOTIADIS, N., PICKERING, L., SCHWARZ, R. F., SILVA, B., HERRERO, J., LUSCOMBE, N. M., JAMAL-HANJANI, M., ROSENTHAL, R., BIRKBAK, N. J., WILSON, G. A., PIPEK, O., RIBLI, D., KRZYSTANEK, M., CSABAI, I., SZALLASI, Z., GORE, M., MCGRANAHAN, N., VAN LOO, P., CAMPBELL, P., LARKIN, J., SWANTON, C. & CONSORTIUM, T. R. R. 2018. Deterministic Evolutionary Trajectories Influence Primary Tumor Growth: TRACERx Renal. *Cell,* 173**,** 595-610 e11.

TURIN, I., SCHIAVO, R., MAESTRI, M., LUINETTI, O., BELLO, B., PAULLI, M., DIONIGI, P., ROCCIO, M., SPINILLO, A., FERULLI, F., TANZI, M., MACCARIO, R., MONTAGNA, D. & PEDRAZZOLI, P. 2014. In Vitro Efficient Expansion of Tumor Cells Deriving from Different Types of Human Tumor Samples. *Medical Sciences,* 2**,** 70.

TURNER, M., MEE, P. J., COSTELLO, P. S., WILLIAMS, O., PRICE, A. A., DUDDY, L. P., FURLONG, M. T., GEAHLEN, R. L. & TYBULEWICZ, V. L. 1995. Perinatal lethality and blocked B-cell development in mice lacking the tyrosine kinase Syk. *Nature,* 378**,** 298-302.

TURNER, M., SCHWEIGHOFFER, E., COLUCCI, F., DI SANTO, J. P. & TYBULEWICZ, V. L. 2000. Tyrosine kinase SYK: essential functions for immunoreceptor signalling. *Immunol Today,* 21**,** 148-54.

TUVAL-KOCHEN, L., PAGLIN, S., KESHET, G., LERENTHAL, Y., NAKAR, C., GOLANI, T., TOREN, A., YAHALOM, J., PFEFFER, R. & LAWRENCE, Y. 2013. Eukaryotic initiation factor 2alpha--a downstream effector of mammalian target of rapamycin--modulates DNA repair and cancer response to treatment. *PLoS One,* 8**,** e77260.

UDAYAPPAN, U. K. & CASEY, P. J. 2017. c-Jun Contributes to Transcriptional Control of GNA12 Expression in Prostate Cancer Cells. *Molecules,* 22.

UDYAVAR, A. R., HOEKSEMA, M. D., CLARK, J. E., ZOU, Y., TANG, Z., LI, Z., LI, M., CHEN, H., STATNIKOV, A., SHYR, Y., LIEBLER, D. C., FIELD, J., EISENBERG, R., ESTRADA, L., MASSION, P. P. & QUARANTA, V. 2013. Co-expression network analysis identifies Spleen Tyrosine Kinase (SYK) as a candidate oncogenic driver in a subset of small-cell lung cancer. *BMC Syst Biol,* 7 Suppl 5**,** S1.

VALENTE, M. J., HENRIQUE, R., COSTA, V. L., JERONIMO, C., CARVALHO, F., BASTOS, M. L., DE PINHO, P. G. & CARVALHO, M. 2011. A rapid and simple procedure for the establishment of human normal and cancer renal primary cell cultures from surgical specimens. *PLoS One,* 6**,** e19337.

VANDER HEIDEN, M. G., CANTLEY, L. C. & THOMPSON, C. B. 2009. Understanding the Warburg effect: the metabolic requirements of cell proliferation. *Science,* 324**,** 1029-33.

VARELA, I., TARPEY, P., RAINE, K., HUANG, D., ONG, C. K., STEPHENS, P., DAVIES, H., JONES, D., LIN, M. L., TEAGUE, J., BIGNELL, G., BUTLER, A., CHO, J., DALGLIESH, G. L., GALAPPATHTHIGE, D., GREENMAN, C., HARDY, C., JIA, M., LATIMER, C., LAU, K. W., MARSHALL, J., MCLAREN, S., MENZIES, A., MUDIE, L., STEBBINGS, L., LARGAESPADA, D. A., WESSELS, L. F., RICHARD, S., KAHNOSKI, R. J., ANEMA, J., TUVESON, D. A., PEREZ-MANCERA, P. A., MUSTONEN, V., FISCHER, A., ADAMS, D. J., RUST, A., CHAN-ON, W., SUBIMERB, C., DYKEMA, K., FURGE, K., CAMPBELL, P. J., TEH, B. T., STRATTON, M. R. & FUTREAL, P. A. 2011. Exome sequencing identifies frequent mutation of the SWI/SNF complex gene PBRM1 in renal carcinoma. *Nature,* 469**,** 539-42.

VELICEASA, D., IVANOVIC, M., HOEPFNER, F. T., THUMBIKAT, P., VOLPERT, O. V. & SMITH, N. D. 2007. Transient potential receptor channel 4 controls thrombospondin-1 secretion and angiogenesis in renal cell carcinoma. *FEBS J,* 274**,** 6365-77.

VENABLES, J. P., KLINCK, R., KOH, C., GERVAIS-BIRD, J., BRAMARD, A., INKEL, L., DURAND, M., COUTURE, S., FROEHLICH, U., LAPOINTE, E., LUCIER, J. F., THIBAULT, P., RANCOURT, C., TREMBLAY, K., PRINOS, P., CHABOT, B. & ELELA, S. A. 2009. Cancer-associated regulation of alternative splicing. *Nat Struct Mol Biol,* 16**,** 670-6.

VENKATESAN, S. & SWANTON, C. 2016. Tumor Evolutionary Principles: How Intratumor Heterogeneity Influences Cancer Treatment and Outcome. *Am Soc Clin Oncol Educ Book,* 35**,** e141-9.

VOGEL, C. & MARCOTTE, E. M. 2012. Insights into the regulation of protein abundance from proteomic and transcriptomic analyses. *Nat Rev Genet,* 13**,** 227-32.

VOGELSTEIN, B., PAPADOPOULOS, N., VELCULESCU, V. E., ZHOU, S., DIAZ, L. A., JR. & KINZLER, K. W. 2013. Cancer genome landscapes. *Science,* 339**,** 1546-58.

VON RAHDEN, B. H. A., STEIN, H. J., PUHRINGER, F., KOCH, I., LANGER, R., PIONTEK, G., SIEWERT, J. R., HOFLER, H. & SARBIA, M. 2005. Coexpression of cyclooxygenases (COX-1, COX-2) and vascular endothelial growth factors (VEGF-A, VEGF-C) in esophageal adenocarcinoma. *Cancer Research,* 65**,** 5038-5044.

WAH, T. M. 2017. Image-guided ablation of renal cell carcinoma. *Clin Radiol,* 72**,** 636-644.

WAN, Y., KUROSAKI, T. & HUANG, X. Y. 1996. Tyrosine kinases in activation of the MAP kinase cascade by G-protein-coupled receptors. *Nature,* 380**,** 541-4.

WANG, D. & DUBOIS, R. N. 2006. Prostaglandins and cancer. *Gut,* 55**,** 115-22.

WANG, E. T., SANDBERG, R., LUO, S., KHREBTUKOVA, I., ZHANG, L., MAYR, C., KINGSMORE, S. F., SCHROTH, G. P. & BURGE, C. B. 2008. Alternative isoform regulation in human tissue transcriptomes. *Nature,* 456**,** 470-6.

WANG, J., ZHANG, P., ZHONG, J., TAN, M., GE, J., TAO, L., LI, Y., ZHU, Y., WU, L., QIU, J. & TONG, X. 2016a. The platelet isoform of phosphofructokinase contributes to metabolic reprogramming and maintains cell proliferation in clear cell renal cell carcinoma. *Oncotarget,* 7**,** 27142-57.

WANG, L., DEVARAJAN, E., HE, J., REDDY, S. P. & DAI, J. L. 2005. Transcription repressor activity of spleen tyrosine kinase mediates breast tumor suppression. *Cancer Res,* 65**,** 10289-97.

WANG, L., DUKE, L., ZHANG, P. S., ARLINGHAUS, R. B., SYMMANS, W. F., SAHIN, A., MENDEZ, R. & DAI, J. L. 2003. Alternative splicing disrupts a nuclear localization signal in spleen tyrosine kinase that is required for invasion suppression in breast cancer. *Cancer Res,* 63**,** 4724-30.

WANG, M., LI, X., ZHANG, J., YANG, Q., CHEN, W., JIN, W., HUANG, Y. R., YANG, R. & GAO, W. Q. 2017. AHNAK2 is a Novel Prognostic Marker and Oncogenic Protein for Clear Cell Renal Cell Carcinoma. *Theranostics,* 7**,** 1100-1113.

WANG, Y., GUO, X., BRAY, M. J., DING, Z. & ZHAO, Z. 2016b. An integrative genomics approach for identifying novel functional consequences of PBRM1 truncated mutations in clear cell renal cell carcinoma (ccRCC). *BMC Genomics,* 17 Suppl 7**,** 515.

WANG, Z., SUN, J., ZHAO, Y., GUO, W., LV, K. & ZHANG, Q. 2014. Lentivirus-mediated knockdown of tumor protein D52-like 2 inhibits glioma cell proliferation. *Cell Mol Biol (Noisy-le-grand),* 60**,** 39-44.

WARBURG, O. 1956. [Origin of cancer cells]. *Oncologia,* 9**,** 75-83.

WATROUS, J. D., HENGLIN, M., CLAGGETT, B., LEHMANN, K. A., LARSON, M. G., CHENG, S. & JAIN, M. 2017. Visualization, Quantification, and Alignment of Spectral Drift in Population Scale Untargeted Metabolomics Data. *Anal Chem,* 89**,** 1399-1404.

WATT, J. M. & BREYER-BRANDWIJK, M. G. 1927. MUFWEBA-BACHAZI—A NORTHERN RHODESIAN SUICIDE PLANT. *Bantu Studies,* 3**,** 395-400.

WEHENKEL, M., BAN, J. O., HO, Y. K., CARMONY, K. C., HONG, J. T. & KIM, K. B. 2012. A selective inhibitor of the immunoproteasome subunit LMP2 induces apoptosis in PC-3 cells and suppresses tumour growth in nude mice. *Br J Cancer,* 107**,** 53-62.

WEINBLATT, M. E., KAVANAUGH, A., BURGOS-VARGAS, R., DIKRANIAN, A. H., MEDRANO-RAMIREZ, G., MORALES-TORRES, J. L., MURPHY, F. T., MUSSER, T. K., STRANIERO, N., VICENTE-GONZALES, A. V. & GROSSBARD, E. 2008. Treatment of rheumatoid arthritis with a Syk kinase inhibitor: a twelve-week, randomized, placebo-controlled trial. *Arthritis Rheum,* 58**,** 3309-18.

WEISS, R. H. 2018. Metabolomics and Metabolic Reprogramming in Kidney Cancer. *Semin Nephrol,* 38**,** 175-182.

WILLIAMS, C. S., MANN, M. & DUBOIS, R. N. 1999. The role of cyclooxygenases in inflammation, cancer, and development. *Oncogene,* 18**,** 7908-16.

WILLIAMS, R. T., YU, A. L., DICCIANNI, M. B., THEODORAKIS, E. A. & BATOVA, A. 2013. Renal cancer-selective Englerin A induces multiple mechanisms of cell death and autophagy. *J Exp Clin Cancer Res,* 32**,** 57.

WIRTH, M. P. 1993. Immunotherapy for metastatic renal cell carcinoma. *Urol Clin North Am,* 20**,** 283-95.

WISNIEWSKI, J. R., ZOUGMAN, A., NAGARAJ, N. & MANN, M. 2009. Universal sample preparation method for proteome analysis. *Nat Methods,* 6**,** 359-62.

WRAGG, J. W., FINNITY, J. P., ANDERSON, J. A., FERGUSON, H. J., PORFIRI, E., BHATT, R. I., MURRAY, P. G., HEATH, V. L. & BICKNELL, R. 2016. MCAM and LAMA4 Are Highly Enriched in Tumor Blood Vessels of Renal Cell Carcinoma and Predict Patient Outcome. *Cancer Res,* 76**,** 2314-26.

WU, J., HE, Z., WANG, D. L. & SUN, F. L. 2016. Depletion of JMJD5 sensitizes tumor cells to microtubule-destabilizing agents by altering microtubule stability. *Cell Cycle,* 15**,** 2980-2991.

XIA, W., NAGASE, S., MONTIA, A. G., KALACHIKOV, S. M., KENIRY, M., SU, T., MEMEO, L., HIBSHOOSH, H. & PARSONS, R. 2008. BAF180 is a critical regulator of p21 induction and a tumor suppressor mutated in breast cancer. *Cancer Res,* 68**,** 1667-74.

XIONG, G., DENG, L., ZHU, J., RYCHAHOU, P. G. & XU, R. 2014. Prolyl-4-hydroxylase alpha subunit 2 promotes breast cancer progression and metastasis by regulating collagen deposition. *BMC Cancer,* 14**,** 1.

YAGI, S., SUZUKI, K., HASEGAWA, A., OKUMURA, K. & RA, C. 1994. Cloning of the cDNA for the deleted syk kinase homologous to ZAP-70 from human basophilic leukemia cell line (KU812). *Biochem Biophys Res Commun,* 200**,** 28-34.

YAGODA, A., ABI-RACHED, B. & PETRYLAK, D. 1995. Chemotherapy for advanced renal-cell carcinoma: 1983-1993. *Semin Oncol,* 22**,** 42-60.

YAGODA, A., PETRYLAK, D. & THOMPSON, S. 1993. Cytotoxic chemotherapy for advanced renal cell carcinoma. *Urol Clin North Am,* 20**,** 303-21.

YAMADA, T., TANIGUCHI, T., YANG, C., YASUE, S., SAITO, H. & YAMAMURA, H. 1993. Association with B-cell-antigen receptor with protein-tyrosine kinase p72syk and activation by engagement of membrane IgM. *Eur J Biochem,* 213**,** 455-9.

YANAGI, S., INATOME, R., DING, J., KITAGUCHI, H., TYBULEWICZ, V. L. & YAMAMURA, H. 2001a. Syk expression in endothelial cells and their morphologic defects in embryonic Syk-deficient mice. *Blood,* 98**,** 2869-71.

YANAGI, S., INATOME, R., TAKANO, T. & YAMAMURA, H. 2001b. Syk expression and novel function in a wide variety of tissues. *Biochem Biophys Res Commun,* 288**,** 495-8.

YANAGI, S., KUROSAKI, T. & YAMAMURA, H. 1995. The structure and function of nonreceptor tyrosine kinase p72syk expressed in hematopoietic cells. *Cell Signal,* 7**,** 185-93.

YANG, X., REN, H., YAO, L., CHEN, X. & HE, A. 2015. Role of EHD2 in migration and invasion of human breast cancer cells. *Tumour Biol,* 36**,** 3717-26.

YANG, Y. M., LEE, S., NAM, C. W., HA, J. H., JAYARAMAN, M., DHANASEKARAN, D. N., LEE, C. H., KWAK, M. K. & KIM, S. G. 2010. G(alpha)12/13 inhibition enhances the anticancer effect of bortezomib through PSMB5 downregulation. *Carcinogenesis,* 31**,** 1230-7.

YOO, J. Y., WANG, X. W., RISHI, A. K., LESSOR, T., XIA, X. M., GUSTAFSON, T. A. & HAMBURGER, A. W. 2000. Interaction of the PA2G4 (EBP1) protein with ErbB-3 and regulation of this binding by heregulin. *Br J Cancer,* 82**,** 683-90.

YOUNG, A. C., CRAVEN, R. A., COHEN, D., TAYLOR, C., BOOTH, C., HARNDEN, P., CAIRNS, D. A., ASTUTI, D., GREGORY, W., MAHER, E. R., KNOWLES, M. A., JOYCE, A., SELBY, P. J. & BANKS, R. E. 2009. Analysis of VHL Gene Alterations and their Relationship to Clinical Parameters in Sporadic Conventional Renal Cell Carcinoma. *Clin Cancer Res,* 15**,** 7582-7592.

YU, Z. H., ZHANG, Q., WANG, Y. D., CHEN, J., JIANG, Z. M., SHI, M., GUO, X., QIN, J., CUI, G. H., CAI, Z. M., GUI, Y. T. & LAI, Y. Q. 2013. Overexpression of cyclooxygenase-1 correlates with poor prognosis in renal cell carcinoma. *Asian Pac J Cancer Prev,* 14**,** 3729-34.

ZARAVINOS, A., PIERI, M., MOURMOURAS, N., ANASTASIADOU, N., ZOUVANI, I., DELAKAS, D. & DELTAS, C. 2014. Altered metabolic pathways in clear cell renal cell carcinoma: A meta-analysis and validation study focused on the deregulated genes and their associated networks. *Oncoscience,* 1**,** 117-31.

ZEA, A. H., RODRIGUEZ, P. C., ATKINS, M. B., HERNANDEZ, C., SIGNORETTI, S., ZABALETA, J., MCDERMOTT, D., QUICENO, D., YOUMANS, A., O'NEILL, A., MIER, J. & OCHOA, A. C. 2005. Arginase-producing myeloid suppressor cells in renal cell carcinoma patients: a mechanism of tumor evasion. *Cancer Res,* 65**,** 3044-8.

ZENG, B., YUAN, C., YANG, X., ATKIN, S. L. & XU, S. Z. 2013. TRPC channels and their splice variants are essential for promoting human ovarian cancer cell proliferation and tumorigenesis. *Curr Cancer Drug Targets,* 13**,** 103-16.

ZHANG, B., WANG, J., WANG, X., ZHU, J., LIU, Q., SHI, Z., CHAMBERS, M. C., ZIMMERMAN, L. J., SHADDOX, K. F., KIM, S., DAVIES, S. R., WANG, S., WANG, P., KINSINGER, C. R., RIVERS, R. C., RODRIGUEZ, H., TOWNSEND, R. R., ELLIS, M. J. C., CARR, S. A., TABB, D. L., COFFEY, R. J., SLEBOS, R. J. C., LIEBLER, D. C., CARR, S. A., GILLETTE, M. A., KLAUSER, K. R., KUHN, E., MANI, D. R., MERTINS, P., KETCHUM, K. A., PAULOVICH, A. G., WHITEAKER, J. R., EDWARDS, N. J., MCGARVEY, P. B., MADHAVAN, S., WANG, P., CHAN, D., PANDEY, A., SHIH, I.-M., ZHANG, H., ZHANG, Z., ZHU, H., WHITELEY, G. A., SKATES, S. J., WHITE, F. M., LEVINE, D. A., BOJA, E. S., KINSINGER, C. R., HILTKE, T., MESRI, M., RIVERS, R. C., RODRIGUEZ, H., SHAW, K. M., STEIN, S. E., FENYO, D., LIU, T., MCDERMOTT, J. E., PAYNE, S. H., RODLAND, K. D., SMITH, R. D., RUDNICK, P., SNYDER, M., ZHAO, Y., CHEN, X., RANSOHOFF, D. F., HOOFNAGLE, A. N., LIEBLER, D. C., SANDERS, M. E., SHI, Z., SLEBOS, R. J. C., TABB, D. L., ZHANG, B., ZIMMERMAN, L. J., WANG, Y., DAVIES, S. R., DING, L., ELLIS, M. J. C. & REID TOWNSEND, R. 2014. Proteogenomic characterization of human colon and rectal cancer. *Nature,* 513**,** 382-387.

ZHANG, H., LIU, T., ZHANG, Z., PAYNE, S. H., ZHANG, B., MCDERMOTT, J. E., ZHOU, J. Y., PETYUK, V. A., CHEN, L., RAY, D., SUN, S., YANG, F., CHEN, L., WANG, J., SHAH, P., CHA, S. W., AIYETAN, P., WOO, S., TIAN, Y., GRITSENKO, M. A., CLAUSS, T. R., CHOI, C., MONROE, M. E., THOMAS, S., NIE, S., WU, C., MOORE, R. J., YU, K. H., TABB, D. L., FENYO, D., BAFNA, V., WANG, Y., RODRIGUEZ, H., BOJA, E. S., HILTKE, T., RIVERS, R. C., SOKOLL, L., ZHU, H., SHIH, I. M., COPE, L., PANDEY, A., ZHANG, B., SNYDER, M. P., LEVINE, D. A., SMITH, R. D., CHAN, D. W., RODLAND, K. D. & INVESTIGATORS, C. 2016. Integrated Proteogenomic Characterization of Human High-Grade Serous Ovarian Cancer. *Cell*.

ZHANG, H., RAKHA, E. A., BALL, G. R., SPITERI, I., ALESKANDARANY, M., PAISH, E. C., POWE, D. G., MACMILLAN, R. D., CALDAS, C., ELLIS, I. O. & GREEN, A. R. 2010. The proteins FABP7 and OATP2 are associated with the basal phenotype and patient outcome in human breast cancer. *Breast Cancer Res Treat,* 121**,** 41-51.

ZHANG, J., BENAVENTE, C. A., MCEVOY, J., FLORES-OTERO, J., DING, L., CHEN, X., ULYANOV, A., WU, G., WILSON, M., WANG, J., BRENNAN, R., RUSCH, M., MANNING, A. L., MA, J., EASTON, J., SHURTLEFF, S., MULLIGHAN, C., POUNDS, S., MUKATIRA, S., GUPTA, P., NEALE, G., ZHAO, D., LU, C., FULTON, R. S., FULTON, L. L., HONG, X., DOOLING, D. J., OCHOA, K., NAEVE, C., DYSON, N. J., MARDIS, E. R., BAHRAMI, A., ELLISON, D., WILSON, R. K., DOWNING, J. R. & DYER, M. A. 2012. A novel

retinoblastoma therapy from genomic and epigenetic analyses. *Nature,* 481**,** 329-34.

ZHANG, J., WU, T., SIMON, J., TAKADA, M., SAITO, R., FAN, C., LIU, X. D., JONASCH, E., XIE, L., CHEN, X., YAO, X., TEH, B. T., TAN, P., ZHENG, X., LI, M., LAWRENCE, C., FAN, J., GENG, J., LIU, X., HU, L., WANG, J., LIAO, C., HONG, K., ZURLO, G., PARKER, J. S., AUMAN, J. T., PEROU, C. M., RATHMELL, W. K., KIM, W. Y., KIRSCHNER, M. W., KAELIN, W. G., JR., BALDWIN, A. S. & ZHANG, Q. 2018. VHL substrate transcription factor ZHX2 as an oncogenic driver in clear cell renal cell carcinoma. *Science,* 361**,** 290-295.

ZHENG, G., CHAUX, A., SHARMA, R., NETTO, G. & CATUREGLI, P. 2013. LMP2, a novel immunohistochemical marker to distinguish renal oncocytoma from the eosinophilic variant of chromophobe renal cell carcinoma. *Exp Mol Pathol,* 94**,** 29-32.

ZHOU, F., HU, J., MA, H., HARRISON, M. L. & GEAHLEN, R. L. 2006. Nucleocytoplasmic trafficking of the Syk protein tyrosine kinase. *Mol Cell Biol,* 26**,** 3478-91.

ZHOU, J., DENG, Z., CHEN, Y., GAO, Y., WU, D., ZHU, G., LI, L., SONG, W., WANG, X., WU, K. & HE, D. 2015. Overexpression of FABP7 promotes cell growth and predicts poor prognosis of clear cell renal cell carcinoma. *Urol Oncol,* 33**,** 113 e9-17.

ZIONCHECK, T. F., HARRISON, M. L. & GEAHLEN, R. L. 1986. Purification and characterization of a protein-tyrosine kinase from bovine thymus. *J Biol Chem,* 261**,** 15637-43.

ZIONCHECK, T. F., HARRISON, M. L., ISAACSON, C. C. & GEAHLEN, R. L. 1988. Generation of an active protein-tyrosine kinase from lymphocytes by proteolysis. *J Biol Chem,* 263**,** 19195-202.

ZISMAN, A., PANTUCK, A. J., DOREY, F., SAID, J. W., SHVARTS, O., QUINTANA, D., GITLITZ, B. J., DEKERNION, J. B., FIGLIN, R. A. & BELLDEGRUN, A. S. 2001. Improved prognostication of renal cell carcinoma using an integrated staging system. *J Clin Oncol,* 19**,** 1649-57.

ZOUGMAN, A., SELBY, P. J. & BANKS, R. E. 2014. Suspension trapping (STrap) sample preparation method for bottom-up proteomics analysis. *Proteomics,* 14**,** 1006-1000.

Appendix 1

Buffer formulations

Laemmli buffer - 60 mM Tris-HCL pH 6.8, 2% (w/v) SDS, 10% (v/v) glycerol, 5% (v/v) β-mercaptoethanol, 0.01% bromophenol blue

PBS - Made from tablets as per manufacturers instructions (Oxoid)

SBS Solution (with 1.5 mM Ca^{2+}) - 135 mM NaCl, 5mM KCl, 1.2mM MgCl, 8 mM glucose, 10 mM HEPES, 1.5mM $CaCl_2$ (pH 7.4)

Tris-glycine running buffer - 25 mM Tris pH 8.3, 192 mM glycine, 0.1% (w/v) SDS

Towbin's transfer buffer - 25 mM Tris pH 8.3, 192 mM glycine, 10% (v/v) methanol

Coomassie fix – 40% v/v methanol, 7% v/v acetic acid, 53% v/v H_2O

Coomassie Destain I – 25% v/v methanol, 10% v/v acetic acid, 65% v/v H_2O

Coomassie Destain II – 25% v/v methanol, 75% v/v H_2O

Modified RIPA buffer - 150mM NaCl, 50 mM Tris-HCl pH 7.4, 0.5% IGEPAL®CO-630, 0.2% sodium deoxycholate, protease inhibitor cocktail tablet

SDS lysis buffer solution - 5% SDS in 50 mM Tris-HCl, pH 7.6

Appendix 2

Suppliers and manufacturers

Abcam
332 Cambridge Science Park,
Cambridge,
CB4 0FW, UK

Anachem
Anachem House,
20 Charles Street,
Luton,
Bedfordshire,
LU2 0EB, UK

Applied Biosystems
7 Kingsland Grange,
Woolston,
Warrington,
Cheshire,
WA1 7SR, UK

Beckman Coulter (UK) Ltd.
Oakley Court,
Kingsmead Business Park,
High Wycombe,
HP11 1JU, UK

BD Biosciences
The Danby Building,
Edmund Halley Road,
Oxford Science Park,
Oxford,
OX4 4DQ, UK

Bio-Rad Laboratories Ltd
Bio-Rad House,
Maylands Avenue,
Hemel Hempstead,
Hertfordshire,
HP2 7 TD, UK

Corning Inc.
Riverfront Plaza,
Corning,
NY 14831, USA

Dako
Dakopatts Ltd,
16 Manor Courtyard,
Hughenden Avenue,
High Wycombe,
Buckinghamshire,
HP13 5AE, UK

GE Healthcare
Amersham Place,
Little Chalfont,
Buckinghamshire,
HP7 9NA, UK

Gibco
3 Fountain Drive,
Inchinnan Business Park,
Paisley,
PA4 9RF, UK

Invitrogen
PO BOX 2312,
9704 Ch Groningen
The Netherlands

Eastman Kodak Ltd.
Station Road,
Hemel Hempstead,
Hertfordshire,
HP1 1JU, UK

Mettler-Toledo, Inc.
1900 Polaris Parkway,
Columbus,
OH 43240, USA

Millipore
The Boulevard,
Blackmore Lane,
Watford,
WD1 8YG, UK

Nalge (Nunc) International
75 Panorama Creek Drive,
P.O. Box 20365,
Rochester,
NY, USA

Promega
Delta House,
Southampton Science Park,
Southampton,
SO16 7NS, UK

Qiagen Ltd.
Boundary Court,
Gatwick Road,
Crawley,
RH10 2AX, UK

R&D Systems (Europe) Ltd.
19 Barton Lane,
Abingdon,
OX14 3NB, UK

Roche
Roche Products Limited,
P.O. Box 8,
Welwyn Garden City,
Hertfordshire,
AL7 3AY, UK

Sigma-Aldrich
Fancy Road,
Poole,
Dorset
BH12 4QH, UK

Vector Labs (UK) Ltd.
3, Accent Park,
Bakewell Road,
Peterborough,
PE2 6XS, UK

VWR International
Hunter Boulevard
Magna Park
Lutterworth
Leicestershire
LE17 4XN, UK

Whatman Inc.
9 Bridewell Place,
Clifton,
NJ 07014, USA

Zeiss (UK) Ltd.
15-20 Woodfield Road,
Welwyn Garden City,
AL7 1LU, UK

Zymed
458 Carlton Court
S. San Francisco,
CA 94080, USA

Appendix 3

Proteins identified to be significantly upregulated compared to normal kidney in the proteomic study

Protein ID	Protein names	Gene names	% of tumour samples with expression
Q9H3K6	BolA-like protein 2	*BOLA2*	52
O15427	Monocarboxylate transporter 4	*SLC16A3*	52
P04839	Cytochrome b-245 heavy chain	*CYBB*	52
P02786	Transferrin receptor protein 1;Transferrin receptor protein 1, serum form	*TFRC*	52
Q13509	Tubulin beta-3 chain	*TUBB3*	52
P04233	HLA class II histocompatibility antigen gamma chain	*CD74*	52
Q15293	Reticulocalbin-1	*RCN1*	56
Q8IVF2	Protein AHNAK2	*AHNAK2*	56
Q8NBJ5	Procollagen galactosyltransferase 1	*COLGALT1*	60
Q14554	Protein disulfide-isomerase A5	*PDIA5*	60
P26447	Protein S100-A4	*S100A4*	60
E7ETU9	Procollagen-lysine,2-oxoglutarate 5-dioxygenase 2	*PLOD2*	60
O15540	Fatty acid-binding protein, brain	*FABP7*	60
P14317	Hematopoietic lineage cell-specific protein	*HCLS1*	64

Protein ID	Protein names	Gene names	% of tumour samples with expression
P13674	Prolyl 4-hydroxylase subunit alpha-1	*P4HA1*	68
Q6UVK1	Chondroitin sulfate proteoglycan 4	*CSPG4*	68
R4GMU1	GDH/6PGL endoplasmic bifunctional protein;Glucose 1-dehydrogenase;6-phosphogluconolactonase	*H6PD*	72
Q16666	Gamma-interferon-inducible protein 16	*IFI16*	72
P11166	Solute carrier family 2, facilitated glucose transporter member 1	*SLC2A1*	72
Q03518	Antigen peptide transporter 1	*TAP1*	72
O60568	Procollagen-lysine,2-oxoglutarate 5-dioxygenase 3	*PLOD3*	76
Q16790	Carbonic anhydrase 9	*CA9*	76
E9PHQ0	Protein diaphanous homolog 1	*DIAPH1*	80
Q96HE7	ERO1-like protein alpha	*ERO1L*	80
Q16363	Laminin subunit alpha-4	*LAMA4*	80
Q9UGI8	Testin	*TES*	84
Q9NRX3	NADH dehydrogenase [ubiquinone] 1 alpha subcomplex subunit 4-like 2	*NDUFA4L2*	84
P43121	Cell surface glycoprotein MUC18	*MCAM*	88
P13807	Glycogen [starch] synthase, muscle	*GYS1*	92
Q99541	Perilipin-2	*PLIN2*	92
Q9BUF5	Tubulin beta-6 chain	*TUBB6*	96
P09104	Gamma-enolase;Enolase	*ENO2*	96

Appendix 4

Comprehensive histopathological review of sections cut for proteomic study

Sample Number	Section number	Genetic group (based on four 'driver' mutations)	Histopathology review grade	Extent of necrosis	% viable tumour cells	Degree of inflammation	% fibrosis or exudate
031 T	1	*VHL* mutation only	2	0	70	0	30
031 T	2	*VHL* mutation only	3	2	60	1	40
031 T	3	*VHL* mutation only	3	0	60	1	40
128 T	1	No mutation group	4 and rhabdoid	0	70	0	30
128 T	2	No mutation group	4 and rhabdoid	0	70	0	30
128 T	3	No mutation group	4 and rhabdoid	0	70	0	30
231 T	1	*VHL* + *SETD2* mutation	2	0	70	0	30
231 T	2	*VHL* + *SETD2* mutation	2	0	70	0	30
231 T	3	*VHL* + *SETD2* mutation	2	0	70	0	30
233 T	1	No mutation group	2	0	70	1	30
233 T	2	No mutation group	2	0	70	1	30
233 T	3	No mutation group	2	0	70	1	30
255 T	1	*VHL* + *BAP1* mutation	2	0	60	2	60
255 T	2	*VHL* + *BAP1* mutation	2	0	60	0	60
255 T	3	*VHL* + *BAP1* mutation	2	0	60	0	60
340 T	1	*VHL* mutation only	2	0	75	0	25

Sample Number	Section number	Genetic group (based on four 'driver' mutations)	Histopathology review grade	Extent of necrosis	% viable tumour cells	Degree of inflammation	% fibrosis or exudate
340 T	2	*VHL* mutation only	2	0	70	0	30
340 T	3	*VHL* mutation only	2	0	70	0	30
344 T	1	*VHL* mutation only	2	0	80	0	20
344 T	2	*VHL* mutation only	2	0	75	0	25
344 T	3	*VHL* mutation only	2	0	75	0	25
357 T	1	*VHL* mutation only	2	1	50	2	50
357 T	2	*VHL* mutation only	2	0	40	2	60
357 T	3	*VHL* mutation only	2	2	50	2	50
364 T	1	*VHL* mutation only	2	0	75	0	25
364 T	2	*VHL* mutation only	2	0	75	0	25
364 T	3	*VHL* mutation only	2	0	75	0	25
370 T	1	*VHL* + *PBRM1* mutation	3	0	70	0	30
370 T	2	*VHL* + *PBRM1* mutation	3	0	70	0	30
370 T	3	*VHL* + *PBRM1* mutation	3	0	70	0	30
371 T	1	*VHL* + *SETD2* mutation	2	0	80	0	20
371 T	2	*VHL* + *SETD2* mutation	2	0	80	0	20
371 T	3	*VHL* + *SETD2* mutation	2	0	80	0	20
377 T	1	*VHL* + *PBRM1* mutation	3	0	80	0	20
377 T	2	*VHL* + *PBRM1* mutation	3	0	80	0	20

Sample Number	Section number	Genetic group (based on four 'driver' mutations)	Histopathology review grade	Extent of necrosis	% viable tumour cells	Degree of inflammation	% fibrosis or exudate
377 T	3	*VHL* + *PBRM1* mutation	3	0	80	0	20
382 T	1	*VHL* + *PBRM1* mutation	2	0	90	0	10
382 T	2	*VHL* + *PBRM1* mutation	2	0	90	0	10
382 T	3	*VHL* + *PBRM1* mutation	2	0	90	0	10
396 T	1	*PBRM1* mutation only	1	0	75	0	25
396 T	2	*PBRM1* mutation only	1	0	75	0	25
396 T	3	*PBRM1* mutation only	1	0	75	0	25
400 T	1	*VHL* mutation only	2	0	75	0	25
400 T	2	*VHL* mutation only	2	0	75	0	25
400 T	3	*VHL* mutation only	2	0	75	0	25
404 T	1	*VHL* + *PBRM1* mutation	1	0	90	0	10
404 T	2	*VHL* + *PBRM1* mutation	1	0	90	0	10
404 T	3	*VHL* + *PBRM1* mutation	1	0	90	0	10
409 T	1	No mutation group	3	0	70	1	30
409 T	2	No mutation group	3	0	70	1	30
409 T	3	No mutation group	3	0	60	1	40
413 T	1	*VHL* + *PBRM1* mutation	3	0	70	1	30
413 T	2	*VHL* + *PBRM1* mutation	3	0	70	1	30
413 T	3	*VHL* + *PBRM1* mutation	3	0	60	1	40

Sample Number	Section number	Genetic group (based on four 'driver' mutations)	Histopathology review grade	Extent of necrosis	% viable tumour cells	Degree of inflammation	% fibrosis or exudate
417 T	1	*VHL* mutation only	2	0	70	1	30
417 T	2	*VHL* mutation only	2	0	70	0	30
417 T	3	*VHL* mutation only	2	0	70	0	30
422 T	1	*VHL* mutation only	2	0	80	0	20
422 T	2	*VHL* mutation only	2	0	70	1	30
422 T	3	*VHL* mutation only	2	0	70	1	30
426 T	1	*VHL* mutation only	1	0	70	1	30
426 T	2	*VHL* mutation only	1	0	70	1	30
426 T	3	*VHL* mutation only	1	0	70	1	30
471 T	1	No mutation group	2	0	70	0	30
471 T	2	No mutation group	2	0	70	0	30
471 T	3	No mutation group	2	0	70	0	30
RS114563 T	1	*VHL* + *SETD2* mutation	2	0	70	0	30
RS114563 T	2	*VHL* + *SETD2* mutation	2	0	70	0	30
RS114563 T	3	*VHL* + *SETD2* mutation	2	0	70	0	30
RS114494 T	1	*VHL* + *BAP1* mutation	2	0	70	0	30
RS114494 T	2	*VHL* + *BAP1* mutation	2	0	70	0	30
RS114494 T	3	*VHL* + *BAP1* mutation	2	0	70	0	30
RS114585 T	1	*VHL* + *SETD2* mutation	2	0	70	0	30

Sample Number	Section number	Genetic group (based on four 'driver' mutations)	Histopathology review grade	Extent of necrosis	% viable tumour cells	Degree of inflammation	% fibrosis or exudate
RS114585 T	2	*VHL* + *SETD2* mutation	2	0	70	0	30
RS114585 T	3	*VHL* + *SETD2* mutation	2	0	70	0	30

Sample Number	Section number	Genetic group (based on four 'driver' mutations)	Cortex (%)	Medulla (%)	Degree of inflammation	% fibrosis or exudate
231 N	1	*VHL* + *SETD2* mutation	100	0	1	5
231 N	2	*VHL* + *SETD2* mutation	90	10	1	5
231 N	3	*VHL* + *SETD2* mutation	90	10	1	5
344 N	1	*VHL* mutation only	100	0	1	0
344 N	2	*VHL* mutation only	100	0	1	0
344 N	3	*VHL* mutation only	100	0	1	0
357 N	1	*VHL* mutation only	100	0	1	0
357 N	2	*VHL* mutation only	100	0	1	0
357 N	3	*VHL* mutation only	100	0	1	0
364 N	1	*VHL* mutation only	100	0	1	0
364 N	2	*VHL* mutation only	100	0	1	0
364 N	3	*VHL* mutation only	100	0	1	0
370 N	1	*VHL* + *PBRM1* mutation	100	0	1	0
370 N	2	*VHL* + *PBRM1* mutation	100	0	1	0

Sample Number	Section number	Genetic group (based on four 'driver' mutations)	Cortex (%)	Medulla (%)	Degree of inflammation	% fibrosis or exudate
370 N	3	*VHL* + *PBRM1* mutation	100	0	1	0
371 N	1	*VHL* + *SETD2* mutation	100	0	1	0
371 N	2	*VHL* + *SETD2* mutation	100	0	1	0
371 N	3	*VHL* + *SETD2* mutation	100	0	1	0
377 N	1	*VHL* + *PBRM1* mutation	100	0	0	0
377 N	2	*VHL* + *PBRM1* mutation	100	0	1	0
377 N	3	*VHL* + *PBRM1* mutation	100	0	1	0
382 N	1	*VHL* + *PBRM1* mutation	100	0	1	0
382 N	2	*VHL* + *PBRM1* mutation	100	0	1	0
382 N	3	*VHL* + *PBRM1* mutation	100	0	1	0
396 N	1	*PBRM1* mutation only	100	0	1	10
396 N	2	*PBRM1* mutation only	100	0	1	10
396 N	3	*PBRM1* mutation only	100	0	1	0
400 N	1	*VHL* mutation only	100	0	1	0
400 N	2	*VHL* mutation only	100	0	1	0
400 N	3	*VHL* mutation only	100	0	1	0
404 N	1	*VHL* + *PBRM1* mutation	100	0	1	0
404 N	2	*VHL* + *PBRM1* mutation	100	0	1	0
404 N	3	*VHL* + *PBRM1* mutation	100	0	1	0

Sample Number	Section number	Genetic group (based on four ‘driver’ mutations)	Cortex (%)	Medulla (%)	Degree of inflammation	% fibrosis or exudate
409 N	1	No mutation group	100	0	2	5
409 N	2	No mutation group	100	0	1	5
409 N	3	No mutation group	100	0	1	5
417 N	1	*VHL* mutation only	100	0	1	0
417 N	2	*VHL* mutation only	100	0	1	1
417 N	3	*VHL* mutation only	100	0	1	0
471 N	1	No mutation group	100	0	1	0
471 N	2	No mutation group	100	0	1	0
471 N	3	No mutation group	100	0	1	0